ORGANISATION EUROPÉENNE POUR LA RECHERCHE NUCLÉAIRE

CERN EUROPEAN ORGANIZATION FOR NUCLEAR RESEARCH

PROCEEDINGS OF THE INTERNATIONAL

CONFERENCE ON HYPERFRAGMENTS

St. Cergue, 28-30 March 1963.

Edited by

W.O. Lock

G E N E V A

1964

SCIENTIFIC ORGANIZING COMMITTEE :

Prof. E.H.S. Burhop   (CERN and University College, London)
Prof. R.H. Dalitz   (Chicago)
Prof. R. Levi Setti   (Chicago)
Dr. W.O. Lock   (CERN)
Dr. J. Sacton   (Brussels)
Dr. A. Zakrzewski   (Warsaw)

Organizing Secretary : Miss E.W.D. Steel (CERN)

CONTENTS

*   *   *

PREFACE

This volume contains the texts of all the invited talks
given at the Hyperfragment Conference except one, which the author
did not wish to publish. I am grateful to the speakers who kindly
provided me with the manuscripts of their talks.

I would also like to thank the following people who contri-
buted to the success of the Conference and to the production of the
Proceedings: Mr. E. Bissa, Mr. M.A. Roberts, Mr. P. de Vautibault
and Mr. R. Vannier for the technical arrangements at St. Cergue;
Mr. A. Bondi and the Scientific Information Service for the diagrams;
Dr. P. Zielinski for translating the talk of O.V. Lozhkin and
N.A. Perfilov from the original Russian text; my colleagues in the
Emulsion Group for assistance with the proof reading; and
Miss S. Greenstreet and Mrs. K. Wakley for their careful work
typing the stencils.

W.O. Lock,
Geneva, October, 1963.

I.   THE INTERACTIONS OF FREE HYPERONS

THE INTERACTIONS OF FREE HYPERONS

F.R. Stannard,

University College, London.

The short lifetimes of the hyperons make it exceedingly diffi-cult to accumulate data on scattering processes. It is well known that almost all our knowledge of hyperon-nucleon forces comes instead from studies of hyperfragments. In fact, I suspect the only reason I have been asked to give this short talk is to give delegates a sense of well-being at the start of the conference.

The following describes the experimental situation.

1. Λ interactions

Table 1

Reaction	No. of events	Cross-section for momentum range 400 to 1500 MeV/c	References
(A) $\Lambda^{0} + p \rightarrow \Lambda^{0} + p$	69	27 ± 5 mb	1), 2), 3), 4)
(B) $\Lambda^{0} + p \rightarrow \Sigma^{0} + p$	3	8.5 ± 4.9 mb	2)
(C) $\Lambda^{0} + p \rightarrow \Sigma^{+} + n$	2	30 ± 20 mb	1)

The cross-section for reaction (A) applies to scattering through angles greater than about 20° in the c.m.s. Within the wide limits allowed by the poor statistics, no change in the cross-section with energy has been detected.

The 72" hydrogen chamber group at Berkeley expect to publish the remaining two-thirds of their data for reaction (A) in the next few months, and have still to report on reaction (C).

The 80 cm hydrogen chamber of the Ecole Polytechnique was recently exposed to 10^6 stopped K^- mesons, and work is to start soon on scanning for Λ-particle interactions. Data from this film will be especially valuable as the momenta of the Λ particles will be small, about 200 MeV/c, and will more readily allow a comparison with theory.

The angular distribution for elastic scattering is almost isotropic, the forward-backward ratio being 27 : 34.

Σ interactions

i) In flight

Table 2

Reaction	No. of events	Cross-sections for momentum ranges:		References
		300 to 1500 MeV/c	< 200 MeV/c	
(D) $\Sigma^+ + p \to \Sigma^+ + p$	12	$38 \begin{array}{c} + \ 18 \ \text{mb} \\ - \ 14 \ \text{mb} \end{array}$	–	5), 6), 7)
(E) $\Sigma^- + p \to \Sigma^- + p$	8	$10 \begin{array}{c} + \ 6 \ \text{mb} \\ - \ 4 \ \text{mb} \end{array}$	–	5), 8)
(F) $\Sigma^- + p \to \Sigma^0 + n$ (G) $\Sigma^- + p \to \Lambda^0 + n$	5	–	170 ± 80 mb	8)

The angular distributions give forward to backward ratios of 5 : 7 and 8 : 0 for reactions (D) and (E), respectively.

Thirteen examples of Σ scatterings on complex nuclei have been observed in nuclear emulsion[9]. Based on a study of the other prongs emitted with the Σ particle in eight of these events, reactions (D) and (E) are found to have cross-sections in the ratio of 6 : 2.

ii) <u>At rest</u>

Σ^- hyperons at rest interact through reactions (F) and (G). The following ratio has been observed for Σ^- particles stopped in hydrogen[10]

$$\frac{\Sigma^0}{\Sigma^0 + \Lambda^0} = 0.33 \pm 0.05 .$$

In deuterium the ratio is[11]

$$\frac{\Sigma^0}{\Sigma^0 + \Lambda^0} = 0.037 \pm 0.022 .$$

The lack of reliable guidance from experiment has necessarily made theoretical work rather speculative.

One may begin from the standpoint of the Doublet Approximation[12] which groups the Λ and Σ particles into two doublets:

$$N_2 = \begin{pmatrix} \Sigma^+ \\ (\Lambda^0 - \Sigma^0)/\sqrt{2} \end{pmatrix} \qquad N_3 = \begin{pmatrix} (\Lambda^0 + \Sigma^0)/\sqrt{2} \\ \Sigma^- \end{pmatrix} .$$

Assuming that N_2 and N_3 are coupled with the same strength to the pion field, one may immediately relate the ΛN and ΣN cross-sections. In particular,

$$2[\sigma(A) + \sigma(B)] = [\sigma(D) + \sigma(E)] ,$$

where $\sigma(A)$ refers to the elastic cross-section for Λ energies above the threshold for Σ^0 production. Experimentally, the values of the left- and right-hand sides of the equation are found to be (57 ± 18) mb and (48 ± 17) mb, respectively.

The Global Symmetry hypothesis[13] is more restrictive, re- quiring the coupling of N_2 and N_3 to be the same as that of the nucleon doublet N_1. One may now relate the ΛN and ΣN cross-sections to the

NN cross-sections. At first sight this would appear to offer defini-
tive predictions for hyperon scattering as the NN scattering data can
be accurately reproduced by various potential models. However, the
hyperons are unaffected by the Pauli exclusion principle and so can
explore regions of the potential that play only minor roles in p-p
scattering, and are consequently not well understood.

de Swart and Dullemond[14] find cross-sections of about 30 mb
for reaction (A), 50 mb for (D), and 33 mb for (E) at momenta of about
600 MeV/c. They require a forward/backward ratio for reaction (A) of
1.5 : 1, which is not in very good agreement with experiment. They
successfully reproduce the strong forward peaking observed for (E),
but then also require a 2 : 1 forward peaking for reaction (D) which is
not indicated by the present data. Ferrari and Fonda[15], on the other
hand, show that if instead of using a Signell-Marshall potential, one
adopts the Gammel-Thaler potential, an essentially isotropic distribu-
tion is obtained for the latter reaction.

Global symmetry predicts that the ratio $\Sigma^\circ/(\Sigma^\circ + \Lambda^\circ)$ for Σ^-
interactions at rest in hydrogen should have a value of 0.40[14]. The
low value found for the ratio in deuterium can be explained in terms
of there being only a small energy release, about 0.9 MeV, in the pro-
cess producing the Σ° [16].

An alternative approach is that of Kovacs and Lichtenberg[17]
who calculate cross-sections for reaction (A) from potentials derived
from the binding energies of hyperfragments. The difficulty here is
that spin-orbit terms, while having little effect on the binding energies,
may be quite important in scattering processes. Cross-sections of
32 mb and 21 mb are obtained with and without spin-orbit corrections.

* * *

REFERENCES

1) F.S. Crawford, M. Cresti, M.L. Good, F.T. Schmitz, M.L. Stevenson and H.K. Ticho, Phys.Rev.Letters 2, 174 (1959).

2) G. Alexander, J.A. Anderson, F.S. Crawford, W. Laskar and L.J. Lloyd, Phys.Rev.Letters 7, 348 (1961).

3) B.A. Arbuzov, E.N. Kladnitskaya, V.N. Penev and R.N. Faustov, JETP 15, 676 (1962) (translation).

4) T.H. Groves, Phys.Rev. 129, 1372 (1963).

5) F.R. Stannard, Phys.Rev. 121, 1513 (1961).

6) F.C. Gilbert and R.S. White, Phys.Rev. 107, 1685 (1957).

7) B. Bhowmik, P.C. Jain and P.C. Mathur, Nuovo Cimento 25, 211 (1962).

8) L.W. Alvarez, Report to the Ninth International Conference on High-Energy Physics (1959), Kiev.

9) A.E. Fisk and D.J. Prowse, Rutherford Jubilee Conference, Manchester (1961), p. 185; and M. Blau, C.F. Carter and A. Perlmutter, Nuovo Cimento 27, 774 (1963).

10) R.R. Ross, Bull.Am.Phys.Soc. 3, 335 (1958).

11) O. Dahl, N. Horwitz, D. Miller and J. Murray, Phys.Rev.Letters 4, 77 (1960).

12) A. Pais, Phys.Rev. 110, 574 (1958); and Nuovo Cimento 18, 1003 (1960).

13) E.P. Wigner, Proc. Nat. Acad.Sci. U.S. 38, 449 (1952). J. Schwinger, Ann.Phys. 2, 407 (1957). M. Gell-Mann, Phys.Rev. 106, 1296 (1957).

14) J.J. de Swart and C. Dullemond, Ann.Phys. 16, 263 (1961); Ann.Phys. 19, 458 (1962); Nuovo Cimento 25, 1072 (1962).

15) F. Ferrari and L. Fonda, Phys.Rev. 114, 874 (1959).

16) T.B. Day, G.A. Snow and J. Sucher, Phys.Rev.Letters 2, 468 (1959).

17) J.S. Kovacs and D.B. Lichtenberg, Nuovo Cimento 13, 371 (1959).

*   *   *

II.   NUCLEAR EMULSION STUDIES

IDENTIFICATION METHODS FOR HYPERFRAGMENTS *)

R.G. Ammar,
Physics Department, Northwestern University,
Evanston, Ill., USA.

I. INTRODUCTION

Information relevant to the identification of hyperfragments may be classified into three general categories accordingly as it is derived from the configuration at production, from that at decay, or from information regarding charge and mass supplied by direct measurements on the tracks themselves. In order to obtain a unique identification for an event it is obviously necessary to impose a sufficient number of constraints to rule out all but one hypothesis regarding its interpretation. Thus, although the three categories will be discussed separately it should be borne in mind that information of more than one type is often used in the analysis of a single event.

For purposes of orientation as regards the energy released at production and decay, some typical reactions are given in Table 1, together with their corresponding energies. These values will, of course, be modulated by effects arising from the binding of the particles involved in any particular reaction, an appreciable effect for the π^- decays. Nevertheless, the relative magnitudes of these energies give some indication as to the type of problems which one might expect to encounter in the different processes.

In the ensuing discussion of the various methods of identification I shall confine my remarks primarily to hyperfragments produced in nuclear emulsion, as other talks have been scheduled which will deal with work performed in bubble chambers.

Table 1

Some characteristic reaction energies
in Λ production and decay

Reaction	Energy release (MeV)
$K^- + 2p \to \Lambda + p$	316.7
$K^- + n \to \Lambda + \pi^-$	178.4
$\Lambda + p \to n + p$	175.9
$\Lambda \to p + \pi^-$	37.6

II. PRODUCTION CONFIGURATION

Kinematic considerations at production have already been used
by many authors[1-7] as an auxiliary method in the identification of
hyperfragments produced by K^- and Σ^- capture in emulsion. In addition,
systematic investigations have been made relating to this production
process, establishing the fact that hypernuclei with charge $Z \gtrsim 3$ are
primarily from the light elements (C, N, O) of the emulsion[8-12].

The power of this method tends to increase with the mass
number A of the hyperfragment produced (for $A \lesssim 16$), since the per-
missible production reactions become simpler. It is therefore ideally
suited to augment the analysis of the π^- decays of hypernuclei with
$5 < A \lesssim 16$ where the information at decay is usually less complete than
for those with $A \lesssim 5$ (see Section III). In addition, a particularly
good illustration of the usefulness of this approach may be found in
the problem of identifying non-mesic decays where the large energy
release and the emission of neutrons makes a decay analysis by itself

rather unreliable. At present a systematic investigation of such decays of hypernuclei with $Z \gtrsim 3$ is under way in our laboratory using production kinematics as a tool[13,14]. To facilitate the analysis, only those hyperfragments produced in association with a charged π from K^- captures are considered. Thus events produced with a π^0 or with no pion and which are somewhat more difficult to analyse, are excluded from the sample. The production process under consideration is, however, not necessarily confined to the second of the reactions in Table 1 since an appreciable fraction ($\gtrsim 7\%$) of the charged pions are π^+ and cannot be produced in association with a Λ via K^- capture on a single nucleon.

Figure 1 shows a photomicrograph of an event analysed in this manner. The primary π^- is brought to rest after ~ 2.8 cm and the production reaction is most likely given by

$$K^- + C^{12} \rightarrow {}_\Lambda Be^9 + H^1 + H^1 + n + \pi^-$$
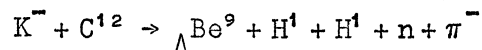
although one cannot rigorously rule out the possibility that some other isotope of $_\Lambda Be$ is produced with more than one neutron. The decay, however, is ambiguous and although consistent with that of $_\Lambda Be^9$, is also consistent with many other interpretations.

The dimensions of the stack (~ 10 cm $\times$ 15 cm $\times$ 10 cm) used in this work was designed primarily to stop pions from the decay reaction. Thus, because of the much larger energy release at production, $\sim 60\%$ of the pions could not be followed to rest in the stack. In such cases, ionization measurements on the pion can still yield much useful information in the analysis of the event.

III. DECAY CONFIGURATION

The analysis of the π^--mesic decays of hypernuclei with $A \leq 5$ is fairly straightforward and has been discussed, for example, in Refs. 15 and 16. For such events, the decay prongs are comparatively

well defined and the concept of coplanarity and colinearity of tracks is meaningful, in contrast to the case for $A > 5$, so that the application of momentum conservation is frequently sufficient to yield a unique interpretation. Even so, for short recoils, misidentification of events can take place as may be seen with reference to Fig. 2 showing a recoil range versus momentum, taken from Ref. 16. Such misidentification may introduce systematic errors in the measured binding[17] since, for example, $_\Lambda He^5$ has a higher binding than $_\Lambda He^4$ and if misinterpreted as the latter, will tend to increase the measured binding for $_\Lambda He^4$.

For the heavier hypernuclei, the problem of identification is somewhat more difficult. A large number of the decays (e.g. ~ 50% of the events presented in Ref. 5) consist of only a π^- and a stub, usually too short to permit a precise measurement of its range and direction. Thus the recoil can not usually be identified from momentum balance. Information bearing on the recoil identity can be obtained by observing whether it undergoes β decay with a half-life short compared with the sensitive time of the detector. Figure 3 shows an event interpreted as $_\Lambda B^{11} \rightarrow \pi^- + C^{11}$ in which a β is associated with the recoil. In exceptional cases the identity of the recoil may be inferred from its decay (e.g. a "hammer track" configuration). Such an event, interpreted as $_\Lambda Li^9 \rightarrow \pi^- + H^1 + Li^8$, is shown in Fig. 4. For this event the interpretation of the "hammer track" as B^8 can be ruled out by detailed considerations[5]. Examples of both types of events were already presented in Ref. 5.

Information regarding the $(\pi^- - r)$ decay mode of hypernuclei with $6 \leq A \leq 16$, already presented in Refs. 4 and 5, is summarized in Fig. 5. Not all the species shown in this figure are known to exist. Their decays are separated into two groups depending on whether or not a β is expected to be seen from the recoil. The $(\pi^- - r)$ mode is, however, not the only one which can give rise to this type of configuration. Table 2 presents a list of values for Q_0 (the energy release assuming zero binding for the Λ), as well as the expected energy release

Table 2

Characteristics of $(\pi^- - n - r)$ decays
for hypernuclei with mass number ≤ 16

| Hypernuclide | Q_0 (MeV) | $\tilde{Q}$ (MeV) | Recoil | | |
			Identity	Decay	Half-life (sec)
$_\Lambda H^4$	36.81	34.7	He^3		Stable
$_\Lambda He^7$	40.33	36.5	Li^6		Stable
$_\Lambda Li^8$	35.93	29.4	Be^7	K capture	4.6×10^6
$_\Lambda Li^9$	52.80	44.8	Be^8	$He^4 + He^4$	$< 2 \times 10^{-14}$
$(_\Lambda Li^{10})$	50.89	41.9	Be^9		Stable
$_\Lambda Be^9$	18.82	12.3	B^8	Hammer	0.8
$(_\Lambda Be^{11})$	37.35	27.9	B^{10}		Stable
$(_\Lambda Be^{12})$	48.27	37.8	B^{11}		Stable
$_\Lambda B^{11}$	33.02	23.1	C^{10}	β^+	19.1
$_\Lambda B^{12}$	34.82	24.4	C^{11}	β^+	1.2×10^3
$(_\Lambda B^{13})$	50.17	38.2	C^{12}		Stable
$(_\Lambda B^{14})$	50.23	36.7	C^{13}		Stable
$_\Lambda C^{13}$	19.34	8.5	N^{12}	β^+	0.012
$_\Lambda C^{14}$	34.57	21.4	N^{13}	β^+	606
$(_\Lambda C^{15})$	36.95	22.5	N^{14}		Stable
$(_\Lambda C^{16})$	46.57	31.1	N^{15}		Stable
$(_\Lambda N^{15})$	31.65	17.2	O^{14}	β^+	76.5
$(_\Lambda N^{16})$	34.04	18.5	O^{15}	β^+	124

The species in parenthesis have not been uniquely identified. In
calculating Q, B_Λ has been inferred from the trend of the B_Λ versus
A curve.

Q, for various $(\pi^- - n - r)$ decay modes. For the more massive species, these decays will present the same appearance as the $(\pi^- - r)$ events. In addition, so can more complex decay modes involving three charged particles. Some of these are shown in Table 3 which lists only those for which both heavy particles in the final state have $Z \geq 3$.

<div align="center">

Table 3

Complex decays of hypernuclei with mass
number ≤ 16 which may simulate the $(\pi^- - r)$ mode

</div>

| Decay	Q_o (MeV)	$\sim Q$ (MeV)
$_\Lambda B^{12} \rightarrow \pi^- + Li^6 + Li^6$	25.35	15.0
$(_\Lambda B^{13} \rightarrow \pi^- + Li^6 + Li^7)$	29.24	17.2
$(_\Lambda B^{14} \rightarrow \pi^- + Li^7 + Li^7)$	31.61	18.1
$_\Lambda C^{13} \rightarrow \pi^- + Li^6 + Be^7$	15.00	4.2
$_\Lambda C^{14} \rightarrow \pi^- + Li^7 + Be^7$	17.31	4.1
$(_\Lambda C^{15} \rightarrow \pi^- + Li^6 + Be^9)$	22.45	8.0
$(_\Lambda C^{16} \rightarrow \pi^- + Li^6 + Be^{10})$	28.04	12.5
$(_\Lambda C^{16} \rightarrow \pi^- + Li^7 + Be^9)$	28.48	13.0
$_\Lambda N^{14} \rightarrow \pi^- + Be^7 + Be^7$	18.67	7.0
$(_\Lambda N^{16} \rightarrow \pi^- + Li^6 + B^{10})$	18.82	3.3
$(_\Lambda N^{16} \rightarrow \pi^- + Be^7 + Be^9)$	17.84	2.3
$(_\Lambda O^{16} \rightarrow \pi^- + Li^6 + C^{10})$	17.80	2.3 β^+ expected

The species in parenthesis have not been uniquely identified. In calculating Q, B_Λ has been inferred from the trend of the B_Λ versus A curve.

Fortunately the energy carried by the π^- in the majority of the decays shown in these tables, tends to be on the low side and does not cause too much confusion with the $(\pi^- - r)$ decays of hypernuclei with $A \leq 16$, tending instead to simulate the decay of heavier ones.

If the hyperfragments are produced under conditions where the hypothesis of production in C, N, O is valid, then quite often only the conservation of charge and baryons need be invoked in order to rule out various competing interpretations from the decay, although at other times a more detailed analysis is necessary. Without such information at production, the problem of identification is very difficult indeed.

It should also be remarked that the presence of excited states in the recoil may contribute to the misidentification of events and thereby introduce systematic errors into the measured value of B_Λ.

As mentioned earlier, the non-mesic decay modes are not usually easy to identify. In some cases however, additional information regarding the decay tracks can be of considerable help in the analysis. Such an example is shown in Fig. 6 which is interpreted as the decay

$$_\Lambda Be^9 \rightarrow Li^8 + H^1$$
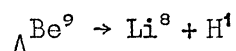
in which the "hammer track" identifies the recoil as Li^8, B^8 being ruled out by considering the maximum Z possible at production. The proton appears to scatter inelastically and it is not possible to obtain a good binding energy from the event.

IV. DIRECT MASS AND CHARGE DETERMINATION

As an aid to analysis, one can also perform profile measurements to determine the charge of tracks of interest (usually that of the hyperfragment). In addition it is sometimes possible to obtain the mass by making gap-length measurements. This is of particular importance for the non-mesic decay mode of $_\Lambda H^{3,4}$. These events consist

of the hyperfragment decaying into only one charged particle and may be confused with Σ^- capture or Σ^+ decay via the proton mode. However, for sufficiently long connecting tracks, it is possible to distinguish a factor of ~ 3 in mass and thereby separate the non-mesic $_\Lambda H^{3,4}$ from the background. Such an analysis is under way in our laboratory[13]. In doing this we require flat tracks with $\gtrsim$ 1 mm range and use the parameter η described by Ammar et al.[18].

Figure 7 shows a photomicrograph of an event which has been analysed in this manner. Mass measurement on the connecting track favours the interpretation that it is due to a particle of greater than baryonic mass. As seen from Table 4, the observed range of 4.2 mm for the secondary excludes the possibility that it comes from either of the two-body modes $_\Lambda H^4 \rightarrow H^3 + n$ or $_\Lambda H^3 \rightarrow H^2 + n$ which require a unique range of 3.5 mm and 7 mm, respectively. Mass determination

Table 4

Non-mesic decay modes of $_\Lambda H^3$ and $_\Lambda H^4$

$_\Lambda H^3$	$_\Lambda H^4$
$H^2 + n$ R_d = 7 mm	$H^3 + n$ R_t = 3.5 mm
$H^1 + 2n$	$H^2 + 2n$
----	$H^1 + 3n$

on the secondary also favours its interpretation as a particle of greater than baryonic mass. The event can therefore most likely be interpreted as

$$_\Lambda H^4 \rightarrow H^2 + 2n \, .$$
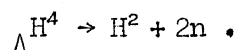
It should be emphasized, however, that events analysed in this manner are subject to far more uncertainty than those identified entirely by kinematic considerations, and as a result their significance rests more on a statistical basis than on an individual one.

Although the yield is low, it is hoped that by the accumulation of such events, normalized to the appropriate number of π^- decays of $_\Lambda H^{3,4}$, one can determine a precise value of the non-mesic to π^--mesic ratio for these hyperfragments directly.

* * *

REFERENCES

1) F.C. Gilbert, C.E. Violet and R.S. White, Phys.Rev. 103, 248 (1956).

2) B.P. Bannik, U.G. Guliamov, D.K. Kopylova, A.A. Nomofilov, M.I. Podgoreetskii, B.G. Rakhimbaev and M. Usranova, Sov.Phys. JETP 7, 198 (1958).

3) P.H. Fowler, Phil.Mag. 3, 1460 (1958).

4) P.E. Schlein and W.E. Slater, Nuovo Cimento 21, 213 (1961).

5) R.G. Ammar, L. Choy, W. Dunn, M. Holland, J.H. Roberts, E.N. Shipley, N. Crayton, D.H. Davis, R. Levi Setti, M. Raymund, O. Skjeggestad and G. Tomasini: "Binding energies of hypernuclei with mass number A > 5". Submitted to Nuovo Cimento.

6) D.J. Prowse, Physics Letters 1, 178 (1962).

7) B. Blowmik, Physics Letters 2, 220 (1962).

8) J. Schneps, W.F. Fry and M. Swami, Phys.Rev. 106, 1062 (1957).

9) J. Sacton, Kiev Conference (1959), reported by E.H.S. Burhop: UCRL-9354.

10) V. Gorge, W. Koch, W. Lindt, M. Nikolić, S. Subotic-Nicolić and H. Winzeler, Nucl.Phys. 21, 599 (1961).

11) O.E. Overseth, Bull.Am.Phys.Soc. 6, 39 (1961).

12) D. Abeledo, L. Choy, R.G. Ammar, N. Crayton, R. Levi Setti,
    M. Raymund and O. Skjeggestad, Nuovo Cimento <u>22</u>, 1171 (1961).

13) M.W. Holland, R.G. Ammar, A. Behkami and J.H. Roberts, Bull.Am.
    Phys.Soc. <u>8</u>, 349 (1963).

14) M.W. Holland: thesis, in course of preparation.

15) W.E. Slater, Suppl. Nuovo Cimento <u>10</u>, 1 (1958).

16) R. Ammar, R. Levi Setti, W.E. Slater, S. Limentani, P.E. Schlein
    and P.H. Steinberg, Nuovo Cimento <u>15</u>, 181 (1960).

17) N. Crayton, R. Levi Setti, M. Raymund, O. Skjeggestad, D. Abeledo,
    R.G. Ammar, J.H. Roberts and E.N. Shipley, Rev.Mod.Phys. <u>34</u>,
    186 (1962).

18) R.G. Ammar, N. Crayton, K.P. Jain, R. Levi Setti, J.E. Mott,
    P.E. Schlein, O. Skjeggestad and P.K. Srivastava, Phys.Rev.
    <u>120</u>, 1914 (1960).

*   *   *
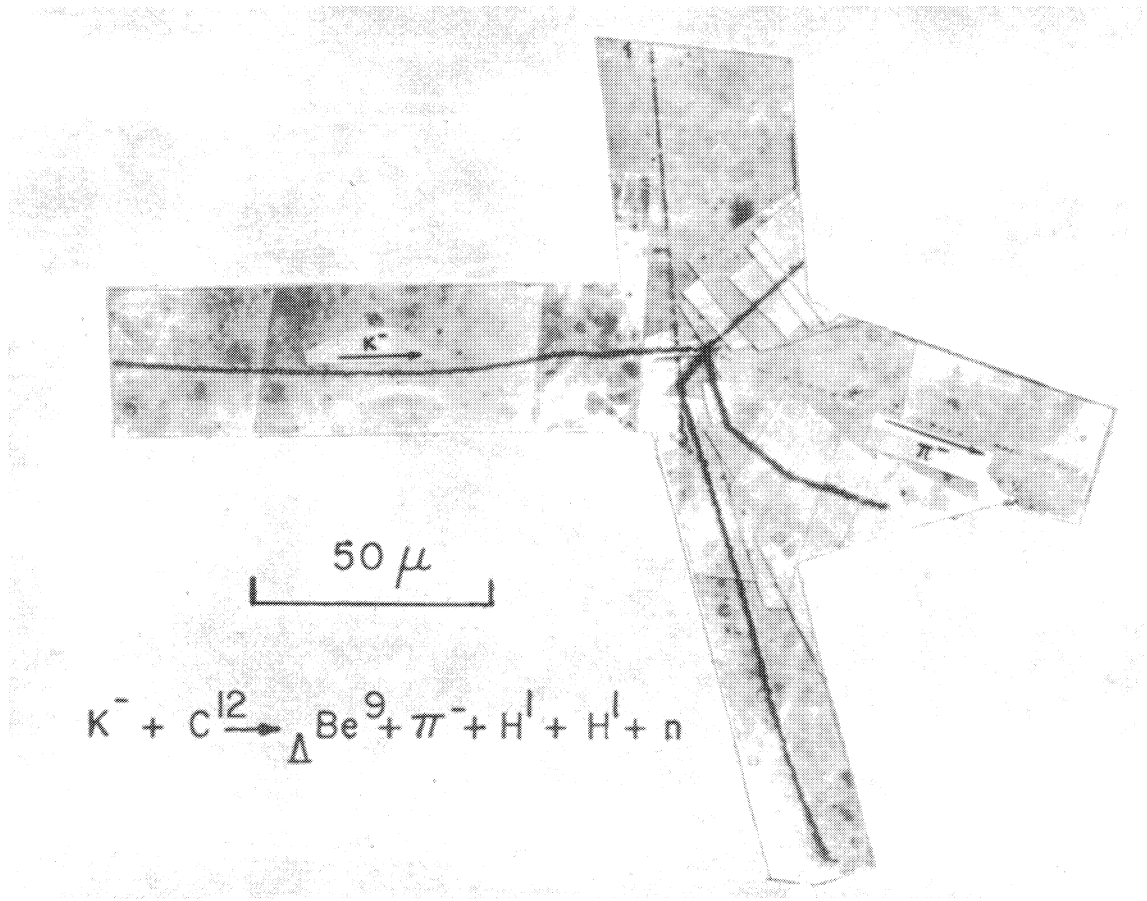
$$K^- + C^{12} \longrightarrow {_\Lambda}Be^9 + \pi^- + H^1 + H^1 + n$$

Fig. 1. - Photomicrograph of event interpreted as $K^- + C^{12} \to {_\Lambda}Be^9 + H^1 + H^1 + n + \pi^-$.
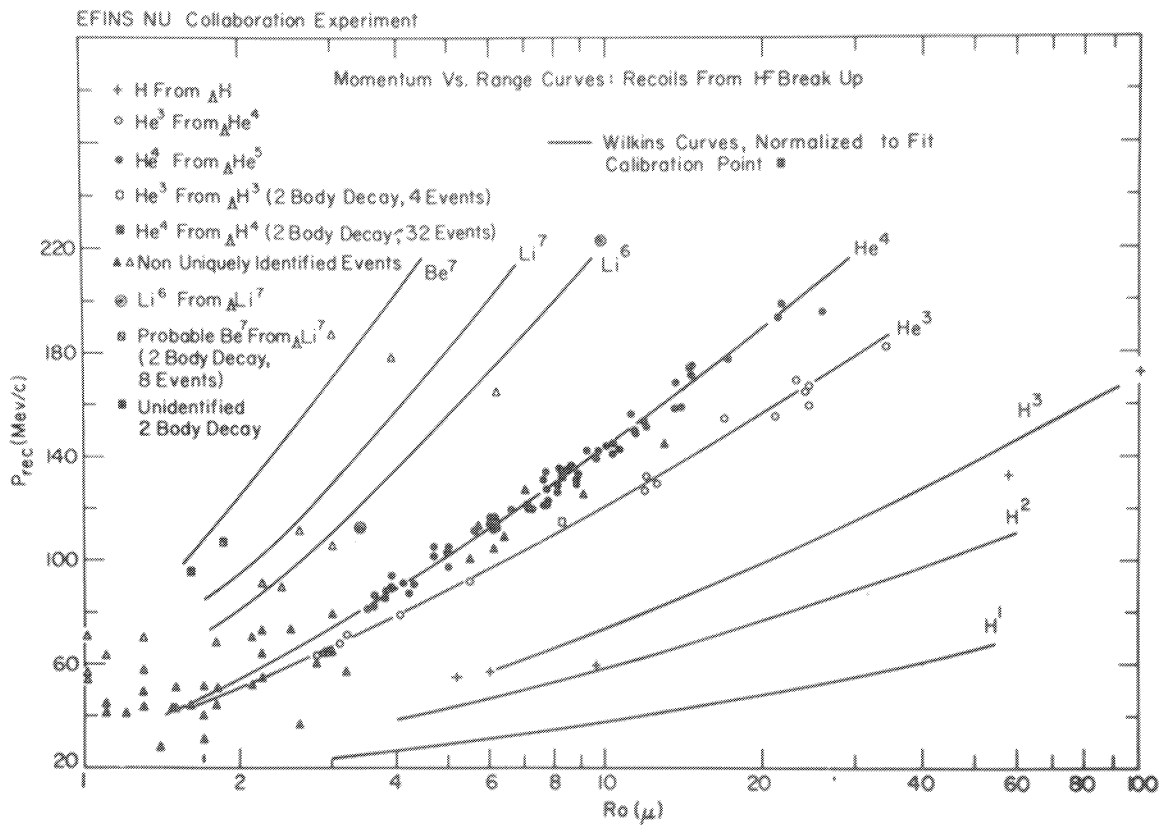
Fig. 2. - Range vs. momentum curves for recoils from hyperfragment decays.
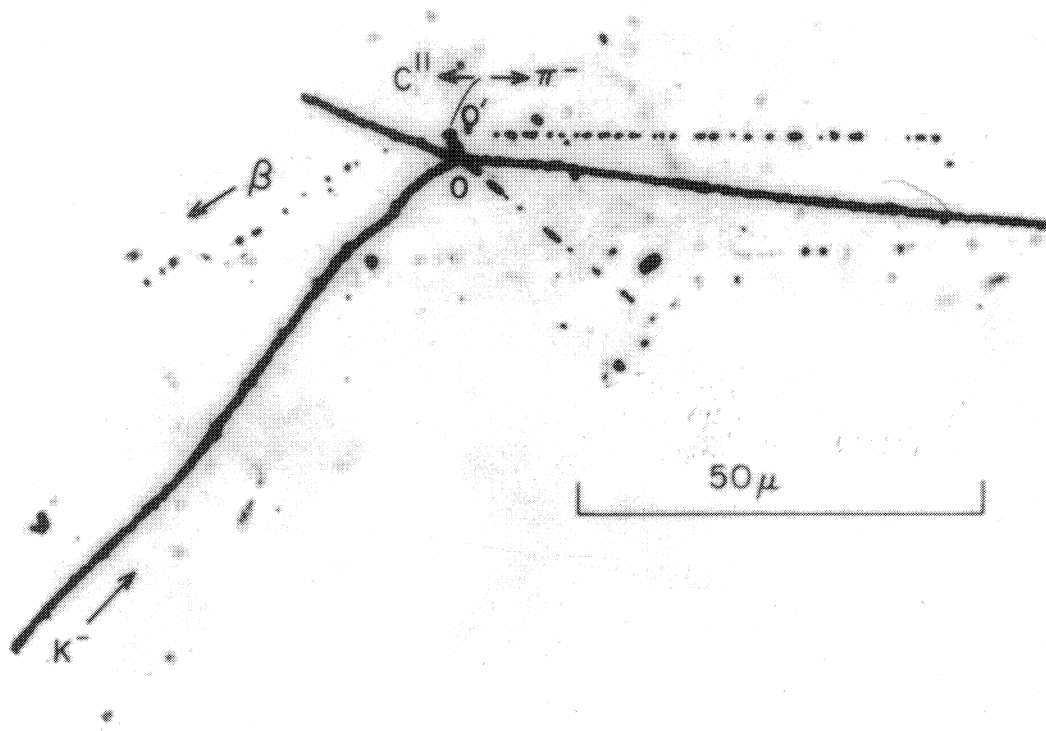
Fig. 3. – Photomicrograph of event interpreted as $_\Lambda B^{11} \to \pi^{\mp} C^{11}$.

Fig. 4. – Photomicrograph of event interpreted as $_\Lambda Li^9 \to \pi^- + H^1 + Li^8$.

$$_{\Lambda}Z^A \rightarrow (Z+1)^A + \pi^-$$

$$6 \leq A \leq 16$$

1) NO β EXPECTED TO BE SEEN

PION ENERGY (Mev)

RECOIL RANGE (μ)

PION RANGE (mm)

2) β EXPECTED

PION ENERGY (Mev)

RECOIL RANGE (μ)

PION RANGE (mm)
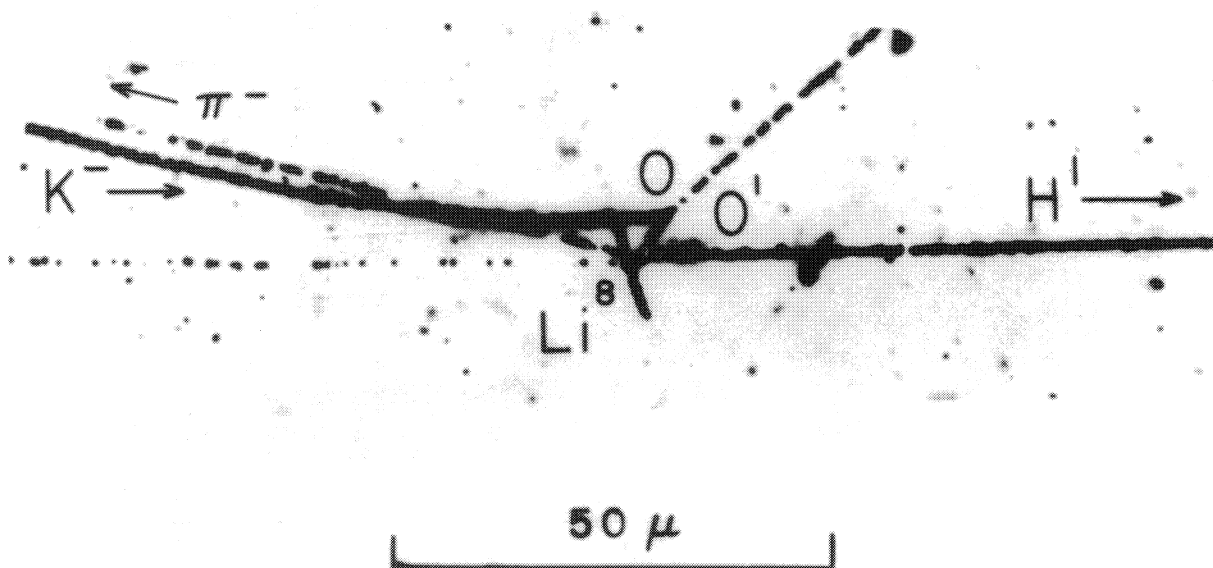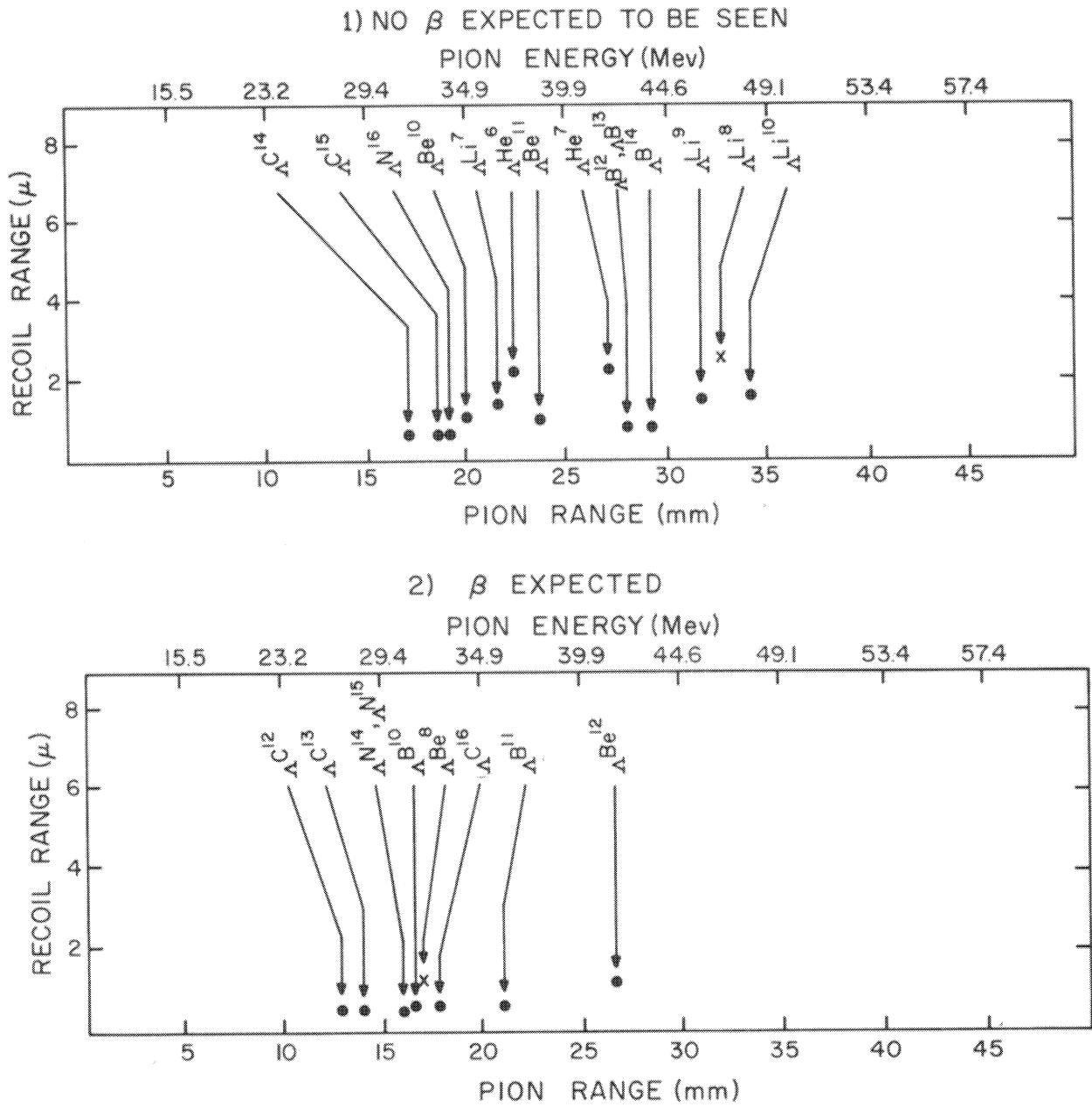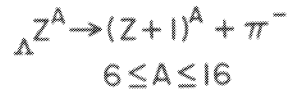
Fig. 5. - (π^- - r) Configurations displayed in two groups according as the lifetime for β decay of the recoil is long or short compared with the sensitive time of the emulsion. Several species shown have not been actually observed and for these the B_Λ used in calculating the energy release has been estimated from the trend of the B_Λ vs. A curve. Events denoted by x have recoils which decay into heavy particles.
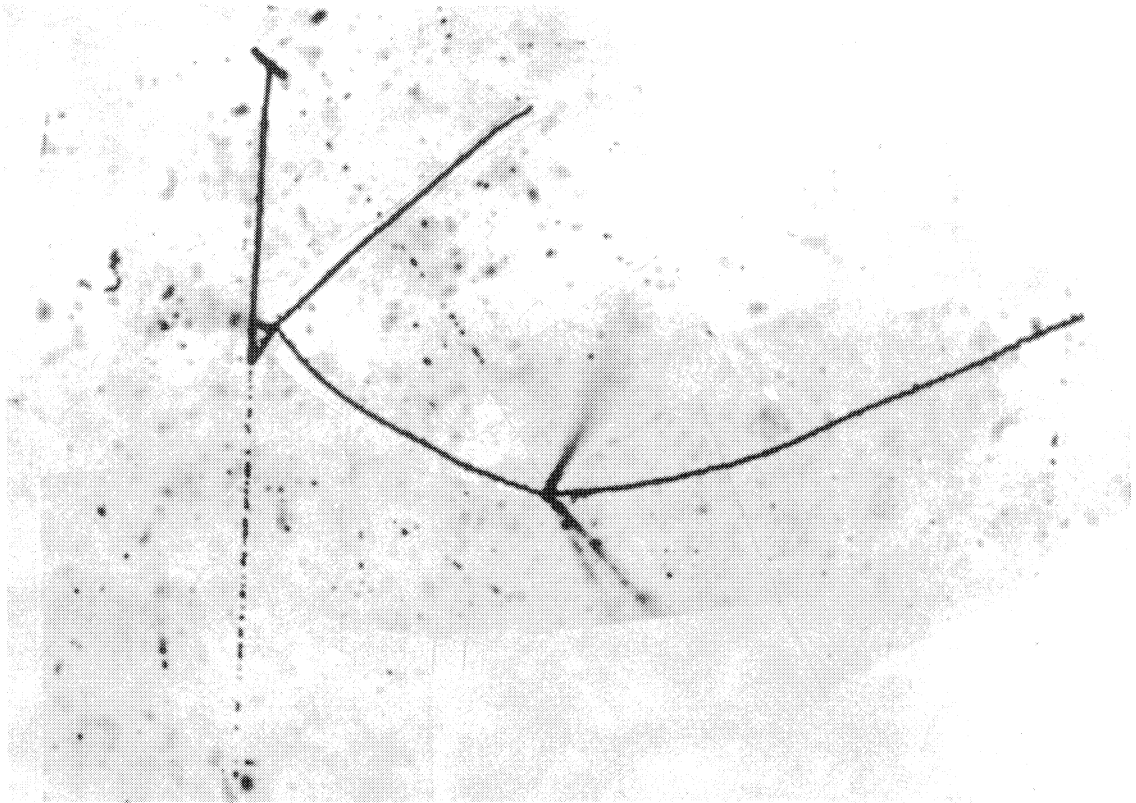
Fig. 6. – Photomicrograph of event interpreted as $_\Lambda Be^9 \to Li^8 + H^1$.

$$_\Lambda H^4 \longrightarrow H^2 + 2n$$

4·2 mm

1·9 mm
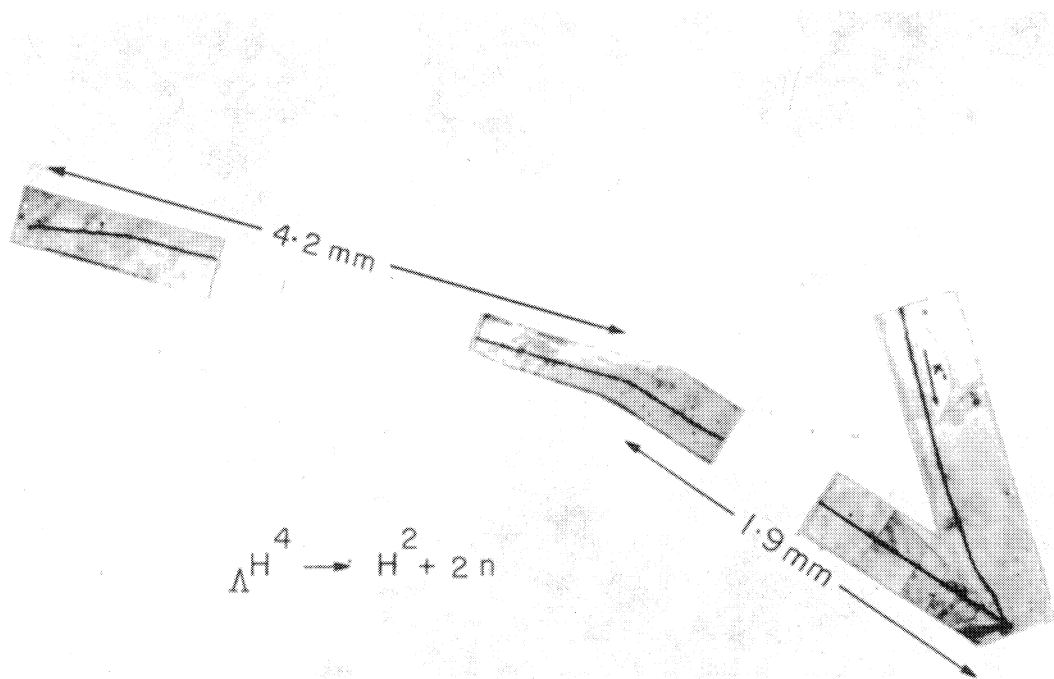
Fig. 7. – Photomicrograph of event interpreted as $_\Lambda H^4 \to H^2 + 2n$.

HYPERNUCLEI [*]

R. Levi-Setti,

Enrico Fermi Institute, University of Chicago.

I. BASIC DEFINITIONS AND NOMENCLATURE

Λ hypernucleus: a hyperon bound to a nuclear core

$$\left(\Lambda + H^2\right) \rightarrow {}_\Lambda H^3$$

$$\left(\Lambda + H^3\right) \rightarrow {}_\Lambda H^4 \text{ , etc.}$$
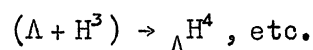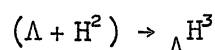
The nuclear core need not be a stable nucleus; examples of hypernuclei in which the core in its ground state is a nuclear resonant state are e.g. $\left(\Lambda + Be^8\right) \rightarrow {}_\Lambda Be^9$, where ordinary Be^8 would disintegrate $Be^{8*} \rightarrow 2He^4 + 0.1$ MeV. Occasionally the Λ-nucleon attraction provides sufficient binding to form hypernuclei out of a completely unbound core, e.g. $\left(\Lambda + Be^6\right) \rightarrow {}_\Lambda Be^7$ where ordinarily $Be^{6*} \rightarrow 2p + He^4 + 1.4$ MeV.

The Λ-binding energy B_Λ is defined as usual from

$$_\Lambda(A,Z) = (A-1,Z) + \Lambda - B_\Lambda \tag{1}$$

and can be measured, since $_\Lambda(A,Z) \rightarrow \Sigma_{ij}(A_i,Z_j) + Q$

$$B_\Lambda = Q_0 - Q, \text{ where } Q_0 = (A-1,Z) + \Lambda - \Sigma_{ij}(A_i,Z_j). \tag{2}$$

Hypernuclear disintegrations in which $\Lambda \rightarrow \begin{matrix} \pi^- + p \\ \pi^0 + n \end{matrix}$ are called __mesonic__ decays; those where $\Lambda + n,p \rightarrow n + n,p$ are called __non-mesonic__ decays. Common abbreviations for decay modes are

$(\pi - r)$ e.g. $_\Lambda H^3 \rightarrow \pi^- + He^3$, $_\Lambda Li^7 \rightarrow \pi^- + Be^7$, etc.,

$(\pi - p - r)$ e.g. $_\Lambda He^5 \rightarrow \pi^- + p + He^4$, etc.,

$(\pi - n - r)$ e.g. $_\Lambda H^4 \rightarrow \pi^- + n + He^3$, $_\Lambda Li^9 \rightarrow \pi^- + n + Be^8$, etc.

---
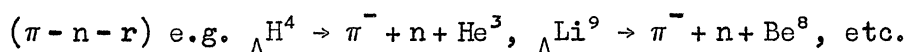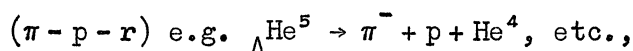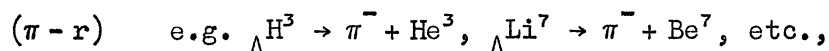
[*] This talk was also given at the 1963 Easter School for Emulsion Physicists.

Note that Q_0 for (π, p, r) decays is always $Q_\Lambda = 37.58$ MeV. B_Λ can be measured best from mesonic or mesic decays in view of the low energy release, usually in the range $25 - 55$ MeV. For non-mesic decays $Q \approx 176$ MeV $- B_\Lambda$.

II. OBSERVATION AND IDENTIFICATION OF HYPERNUCLEI

Although hyperfragments can originate any time a Λ is created within a nucleus, and therefore from reactions such as

$$\pi^- + p \to \Lambda + K^o, \quad p + p \to \Lambda + K^+ + p, \text{ etc.} \tag{3}$$
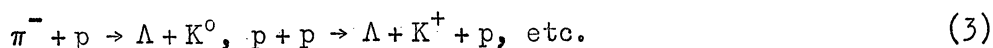
the most copious source of h.f. are K^- induced reactions in nuclear matter, where the elementary reactions are

$$K^- + n, p \to \Lambda + \pi^{-, o}. \tag{4}$$
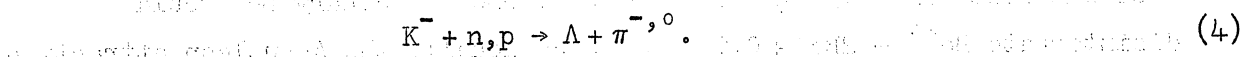
The reason is obvious; while reactions of type (3) have a high threshold and small cross-section, reactions of type (4) are exothermic and occur very frequently. The big step of creating strangeness is separated, in Eq. (4), from that of producing h.f.'s. Typical production rates of h.f.'s from K^- absorbed at rest in light nuclei are $\sim 2 - 5\%$. In the processes of production, survival and decay of a hyperfragment we find the means of observation and identification of particular hypernuclear species. It would be desirable, of course, to be able to compare the observables on the three steps simultaneously. This is, however, seldom possible.

1. Identification at production

Identification at production is particularly reliable in two-body reactions

$$K^- + He^4 \to \begin{array}{l} _\Lambda He^4 + \pi^- \\ _\Lambda H^4 + \pi^o \end{array}. \tag{5}$$

These reactions are obviously exclusive domain of the He bubble chamber. Similar reactions have been observed in nuclear emulsion, such as:

$$K^- + C^{12} \rightarrow {}_\Lambda B^{12} + \pi^0$$

$$\Sigma^- + C^{12} \rightarrow {}_\Lambda B^{12} + n .$$

(6)

Fig.1
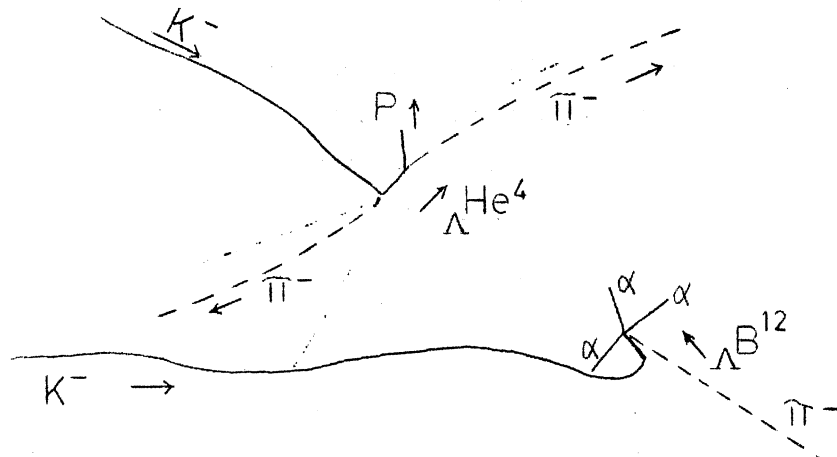
In this case, however, the uncertainty as to the target nucleus detracts from the evidence. The requirements of energy and momentum balance can only be checked approximately in Eq. (6), where the only observable of the production process is a very short ($\sim 4~\mu$m) h.f. track. Hopefully, reactions such as in lithium-loaded emulsion should yield an independent clear-cut identification at production

$$K^- + Li^7 \rightarrow \begin{array}{c} {}_\Lambda Li^7 + \pi^- \\ {}_\Lambda He^7 + \pi^0 \end{array} .$$

(7)

Occasionally it is possible to obtain a satisfactory energy, momentum, charge and mass balance of more complicated production reactions in nuclear emulsion. Very seldom, however, is such information independent from that supplied by the decay process. This method is in all cases a very powerful tool; very likely the only method to give a reliable identification of relatively heavy hypernuclei. As we shall see, some decay modes ($\pi - r$) of heavy hypernuclei become completely non-characteristic and a combined analysis of production and decay reaction is called for, e.g.

$$K^- + O^{16} \rightarrow {}_\Lambda C^{14} + 2H^1 + \pi^- ; \quad {}_\Lambda C^{14} \rightarrow \pi^- + N^{14} .$$

(8)
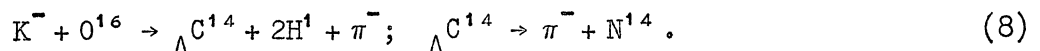
Related remark   The use of small emulsion stacks for h.f. work
                 prevents, in general, the observation of the
                 production pion in its entire range, and its sign
                 determination. On the other hand, at this stage
                 in h.f. work, this information is quite fundamental.

2. Identification during survival

Hyperfragments can be identified during their survival namely
from measurements on the h.f. track itself. If the h.f. comes to rest
and it has sufficient range, any of the conventional means of determining
mass and charge in emulsion apply. Thus, direct mass measurements can
occasionally identify $_\Lambda H^3$ and $_\Lambda H^4$ when several millimeters of track are
available. Z determinations usually require more than ~ 50 μm of h.f.
track to be reliable. Thickness measurements in various ways, as well
as gap-length measurements have been used. A direct determination of Z
often determines the identity of a h.f., when its decay offers certain
alternatives, e.g. for $_\Lambda H^4$, $_\Lambda He^4$, when in the $\pi - p - r$ mode of decay the
recoil has a very short range, insufficient for direct distinction from
range-momentum curves. Identification from h.f. decay is still the most
widely attained.

3. Identification at decay

A blind approach to this problem is that of feeding input data,
such as ranges and angles into a computer programmed to try all permutations
of prong identities until a good fit is obtained. Then, amongst the output
reactions, one chooses the one which yields the lowest momentum unbalance
ΔP. Although this procedure is necessary for the analysis of complicated
decays, it may often hide some relevant information. Thus, a few remarks
are in order.

$(\pi - r)$ events

The pion momentum uniquely determines the recoil momentum and
comparison with P - R curves immediately identifies the event. This is
true, of course, for recoils which are long enough to afford discrimination.

In order to improve the fit, collinearity may be imposed, when justified. The direction of the recoil is, in fact, seldom well-defined, in particular its dip angle. One can obtain a better recoil range estimate by measuring its projected range, and inferring its dip angle from the knowledge of the π direction.

Note   This is a procedure which should be used with caution. There is a point in measuring accurately ΔP and deviations from collinearity even for species as common and typical as $_\Lambda H^4 \to \pi^- + He^4$. In fact, if species such as $_\Lambda H^5$, $_\Lambda H^6$ should exist, their decays

$$_\Lambda H^5 \to \pi^- + n + He^4, \quad _\Lambda H^6 \to \pi^- + 2n + He^4 \tag{9}$$
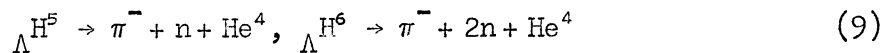
could very well simulate $_\Lambda H^4 \to \pi^- + He^4$, with some departure from collinearity. Furthermore, a decay

$$_\Lambda H^6 \to He^6 + \pi^- \tag{10}$$

would look like an anomalous $\pi - r$ decay of $_\Lambda H^4$, with a recoil somewhat shorter ($\sim 5.4\ \mu m$) than usual ($8.1\ \mu m$).

Some of the possible pitfalls in identifying $\pi - r$ events are worth mentioning. Even $_\Lambda H^3 \to \pi^- + He^3$ is not exempt from simulators. In fact,

$$_\Lambda Li^9 \to \pi^- + n + 2He^4 \tag{11}$$

can occur in a configuaration similar to $_\Lambda H^3$ $(\pi - r)$. In such a case, however, the h.f. track should tell the difference unless too short (as usually the case for $_\Lambda Li^9$). The real difficulties arise from $\pi - r$ decays of heavier species, when the discriminating power of the recoil range is lost (as well as the possibility of ascertaining collinearity!). The trouble begins very soon. We are very likely unable to tell the difference between

$$_\Lambda He^6 \to \pi^- + Li^6 \quad (\text{if it exists}),$$

and $\quad\quad\quad _\Lambda Li^7 \to \pi^- + Be^7. \tag{12}$
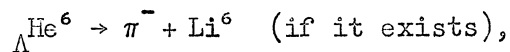
Both decays yield (or are expected to) π ranges of ~ 2.2 cm and recoil ranges in the neighbourhood of 2 μm. If $_\Lambda\text{He}^8$ should exist, its decay

$$_\Lambda\text{He}^8 \rightarrow \pi^- + n + \text{Li}^7 \tag{13}$$

would have an overwhelming chance of being confused with

$$_\Lambda\text{He}^7 \rightarrow \pi^- + \text{Li}^7 . \tag{14}$$

From $_\Lambda\text{Be}^{10}$ on, all recoils have
a range of 1 μm or less. On the
other hand, the π ranges from
many different species overlap.
The properties of the recoils
may then help, like their
β decay

See fig. 2

$$_\Lambda\text{B}^{11} \rightarrow \pi^- + \text{C}^{11}, \text{ recoil } \beta^+, \text{ range } \sim 2.07 \text{ cm}$$

$$_\Lambda\text{Be}^{10} \rightarrow \pi^- + \text{B}^{10}, \text{ recoil stable, } \pi \text{ range } \sim 2.0 \text{ cm}. \tag{15}$$
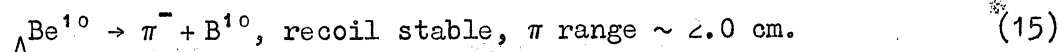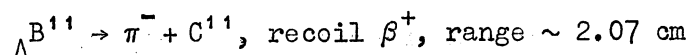
The failure to observe the decay
β will automatically involve
misidentification. Even when
the recoil is unstable like Li^8,
a pitfall is open. Take

See fig. 3

$$_\Lambda\text{Be}^8 \rightarrow \pi^- + \text{B}^8, \quad \text{B}^8 \rightarrow \beta^+ + \nu + \text{Be}^{8*}, \quad \text{Be}^{8*} \rightarrow 2\text{He}^4. \tag{16}$$
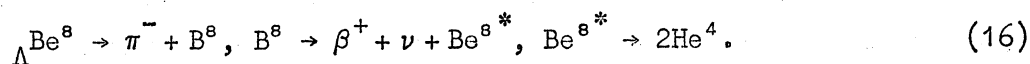
If the β^+ were overlooked, the event may be interpreted in a very complicated way, perhaps even as

$$_\Lambda\text{Li}^9 \rightarrow \pi^- + n + 2\text{He}^4 . \tag{17}$$

The same would hold for a hypothetical decay

$$_\Lambda\text{He}^8 \rightarrow \pi^- + \text{Li}^8 . \tag{18}$$

All this is further complicated by the possibility that heavy recoils
be emitted in excited states, or that the hypernucleus decays from an
isomeric state. For these reasons, identifications based on $\pi - r$ events
of heavy h.f. should always be taken with great caution and in general
are <u>not</u> as clear-cut as those based on other all-charged decay modes.
The importance of a combined analysis <u>production-decay</u> vertices for these
events cannot be stressed any further.

$(\pi - p - r)$ events

After checking for consistency with coplanarity, it is, in
general, useful to impose coplanarity by inferring the recoil direction
from that of the resultant
momentum $\vec{P}_{\pi p} = \vec{P}_{\pi} + \vec{P}_{p}$. Next it
is useful to plot $|\vec{P}_{\pi p}|$ versus
the corrected recoil range R_{rec}.
Range momentum curves can be
constructed experimentally in this
way for various isotopes. Errors
and anomalies can easily be
spotted. Below certain recoil
ranges it becomes impossible to
discriminate among neighbouring
isotopes. Thus, below ~ 3 μm,
it becomes meaningless to accept

See fig. 4

a discrimination between He^3 and He^4. Problem cases of this type are
frequently encountered for all species, $_{\Lambda}$H^3, $_{\Lambda}$H^4, $_{\Lambda}$He^4, $_{\Lambda}$He^5, $_{\Lambda}$Li^7, etc.
For the lighter species, however, a good fraction of the events yield
recoils in the sensitive region. For the heavier species, <u>problem cases</u>
become the rule because the recoil ranges, usually very short, become
increasingly insensitive to the momentum $\vec{P}_{\pi p}$. Obviously in this region,
one cannot even assess that the decay is indeed of the $\pi - p - r$ type,
nor that neutrons are emitted. Analysis in conjunction with the production
kinematics becomes once more crucial. In discussing $\pi - p - r$ events of
even the lighter hypernuclei, one should bear in mind that the recoil
co-ordinates in the P-R plot have considerable spread. In certain regions

of the plot, in particular when an abundant species $(_\Lambda He^5)$ is next to a less abundant one $(_\Lambda He^4)$ some overlap of the distributions will always occur, so that some contamination of one species with another may be present. With increased statistics one can attempt to purify a collection of events of a given species by imposing a progressively increasing range cut-off on the recoil in order to accept events only in a region of the $(P-R)$ plots where no overlap can occur.

Remark   A procedure as outlined above is the only method to eliminate from a sample of a given species possible contaminations. Such contaminations introduce systematic biases in the determination of, for example, binding energies. The addition of small or large samples of identified h.f. to the world statistics becomes a worthless proposition if only B_Λ's or worse, $\bar{B}_\Lambda$'s are given. The raw data are instead needed in order to attempt an elimination of the intrinsic, systematic errors due to contamination.

Again, some features of the recoil may help, when the recoil itself is too short. For example, in the decay

Fig. 5

$$_\Lambda Li^9 \to \pi^- + p + Li^8, \quad Li^8 \to \beta^- + \bar{\nu} + Be^{8\ *}, \quad Be^{8\ *} \to 2He^4 ; \qquad (19)$$
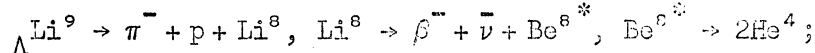
watch out, however, for the very similar decay

$$_\Lambda B^9 \to \pi^- + p + B^8, \quad B^8 \to \beta^+ + \nu + Be^{8\ *}, \quad Be^{8\ *} \to 2He^4 . \qquad (20)$$
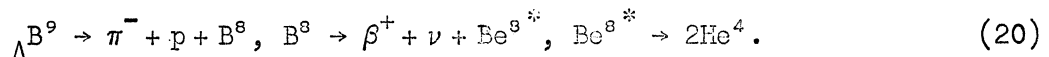
Incidentally, the range energy curves obtained from h.f. recoil in nuclear emulsion are quite certainly the best available in the approximate range $2-40$ μm.

$(\pi - n - r)$ and complex decays

These events are best analysed with computer programmes. However, the following example illustrates some auxiliary method to improve the over-all reliability in the identification of a certain class of events.

The decay

$$_\Lambda Li^9 \rightarrow \pi^- + n + 2He^4 \qquad (21)$$
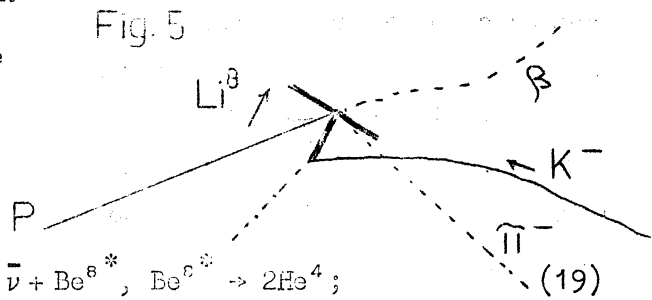
may easily be confused with

$$_\Lambda Li^8 \rightarrow \pi^- + 2He^4 \qquad (22)$$

when the neutron momentum is $|\vec{P}_n| \leq 40$ MeV/c. The ΔP distribution for three-body charged decays, in fact, extends up to this approximate value, due to measurement errors. If the energy release Q is plotted against the missing momentum P_n (or ΔP), a separation between $_\Lambda Li^8$ and $_\Lambda Li^9$ can be achieved on an entire body of events, and some statistical method may be used to cut off a possible contamination of $_\Lambda Li^8$ events amongst $_\Lambda Li^9$.

See fig.6

A general comment is required concerning all decays involving neutron emission, when considering B_Λ. Such events will yield <u>systematically</u> underestimates of B_Λ. In fact, while the momentum unbalance ΔP, due to exp. errors is neglected in decays involving only charged particles, ΔP will contribute to the estimate of the neutron momentum, as

$$(P_n)_{exp} = (P_n)_{true} + \frac{(\Delta P)^2}{3(P_n)_{true}}. \qquad (23)$$

Thus, the neutron energy will be overestimated, and so will Q, giving a corresponding underestimate of B_Λ. Of course, this effect will be felt at small ($P_n \approx \Delta P$) neutron momenta and is in general small. However, since average B_Λ's for some species, or even individual decay modes, have errors (statistical) smaller than 0.1 MeV, even an effect of this kind should not be neglected. Whenever possible, it may be best to base binding energy estimates on decay modes involving charged particles only.

4. Identification on the basis of B_Λ

This is the last remedy, resort to which is obviously very dangerous. It is difficult, of course, to assess the extent to which it is practiced. To some extent it is always used, if nothing else, when one rejects an identification leading to a negative B_Λ. It should be realized, however, that an identity, giving a B_Λ in agreement with a known value is by no means an identification. Pitfalls may be wide open when a species is "expected" to have a certain B_Λ, and an event is attributed to that species on this basis. This is particularly the case with $(\pi - r)$ events, where the interpolated B_Λ is the only basis on which to predict the configuration. The only situation in which this approach seems justified is encountered in the determination of branching ratios between various decay modes of a certain species, e.g. the separation between the $(\pi - p - r)$ decays of $_\Lambda H^3$ and $_\Lambda H^4$, when the recoil is invisible. Careless use of this method will, on the other hand, produce non-Gaussian distributions of B_Λ, will cut off interesting tails, and will hide possible splittings in B_Λ due to excited initial or final states.

5. Experiments with known target nuclei

Some have been mentioned previously. It may be that even accurate B_Λ estimates may be obtained from the measurement of the π range following

$$K^- + (A, Z) \rightarrow {}_\Lambda(A, Z) + \pi^- + Q \tag{24}$$

where $Q = B_\Lambda - B_n + 176$ MeV, and B_n is the binding of the last neutron in (A, Z). This approach carries the identification at production to its logical extreme, that of producing particular h.f. species. It may be valuable for $A \gtrsim 8 - 10$. It offers the advantage that techniques other than nuclear emulsion may be used advantageously, such as bubble chambers, spark chambers, etc.

III. INFORMATION DERIVED FROM HYPERNUCLEAR PROPERTIES

What does one learn from the study of hypernuclei, study which is based so far on a sample of perhaps 2000 mesic decays analysed in nuclear emulsion and several hundreds in the He bubble chamber? Several basic answers have been given to properties of the strong and weak interaction of the Λ hyperon with nucleons, as well as to intrinsic questions regarding strange particles properly.

A brief summary of the main results is the following.

1. Strong Λ - n interaction

a)   The Λ-nucleon interaction is charge symmetric as substantiated by the well-established existence of hypernuclear charge multiplets. Such multiplets correspond to those for the nuclear cores since the Λ has isospin T = 0.

b)   The Λ-nucleon interaction is strong with coupling constant of the order of unity. This follows from an analysis of the Λ-binding energies for light hypernuclei. A measure of this strength is given (following Dalitz) by the volume integral of a Λ-nucleon central potential of appropriate shape for a particular spin state S. In these terms one can compare the Λ - n to the n - n interaction, e.g.

$$^3S_1 \quad \text{n - p volume integral } U \approx 1400 \text{ MeV f}^3$$

$$^1S_0 \quad \Lambda \text{ - p volume integral } U \approx 380 \text{ MeV f}^3 .$$

Since the range of Λ-nucleon force is much shorter (at least two π exchange) than that of the n -n force, the over-all Λ - n binding is weaker than the corresponding nucleon-nucleon binding, even though the interactions have comparable strengths[1]. Alternatively, the interaction can be described in terms of singlet and triplet scattering lengths. (See Dalitz, following lecture.)

c)   The Λ-nucleon interaction is strongly spin-dependent. This
follows from an analysis of both the Λ-binding energies and the direct
determination of the spin of several hypernuclei ($_\Lambda H^3$, $_\Lambda H^4$, $_\Lambda Li^8$).
Indirect information stems also from the measurement of hypernuclear
lifetimes. The $^1S_0$ Λ-n interaction is more attractive than that in the
$^3S_1$ state, opposite to the nucleon-nucleon case[2].

For the sake of illustration, recall that the Fermi scattering
lengths are, for:

n - p Λ - p (See Dalitz, next lecture).

$a_s = -2.34 \times 10^{-12}$ cm $a_s \approx -2.4 \times 10^{-13}$ cm

$a_t = 0.52 \times 10^{-12}$ cm $a_t \approx -0.6 \times 10^{-13}$ cm

Fig. 7
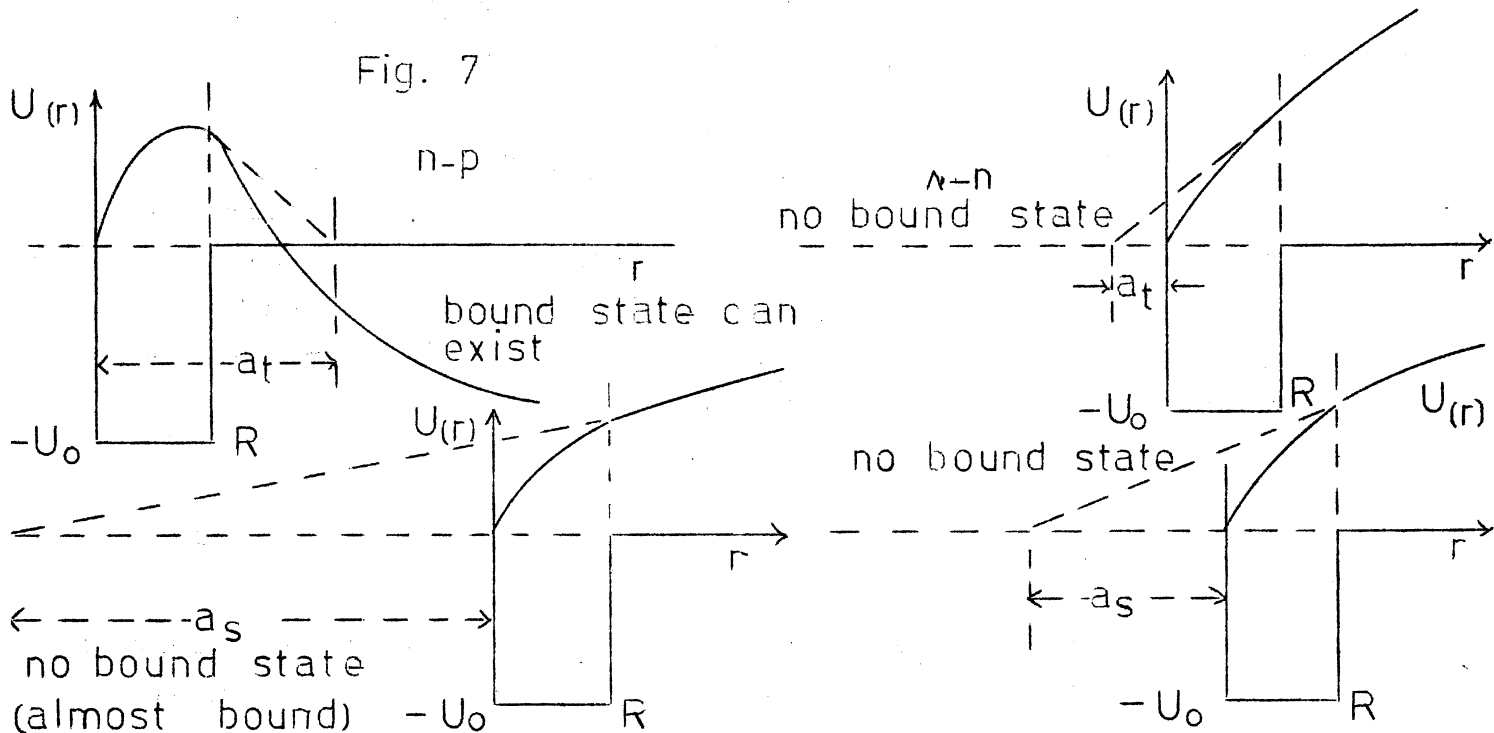
d)   The well-depth experienced by a Λ particle in nuclear matter
is $\approx$ 30 MeV. This result stems from the determination of B_Λ for heavy
hypernuclei as well as from theoretical calculations.

e)   The K^- is a pseudoscalar particle. This follows the study of
the reaction $K^- + He^4 \rightarrow {}_\Lambda H^4 + \pi^0$ in the He bubble chamber, knowing that
$J(_\Lambda H^4) = 0$.

2. Weak $\Lambda - n$ interaction

a)   Several checks of the validity of the $|\Delta T| = \frac{1}{2}$ rule in Λ-pionic decay modes have been given from the study of branching ratios in the decay modes of some light hypernuclei. Perhaps the most significant result is the determination of the ratio p_0/s_0 between the p- and s-wave amplitudes in Λ-decay via the π^0 mode obtained by the He bubble chamber group. The prediction of the $|\Delta T| = \frac{1}{2}$ rule, that $p_0/s_0 = p/s$ seems well satisfied.

b)   Information on the strength of the weak interaction leading to $\Lambda + n \rightarrow n + n$. This is obtained from the branching ratios non-mesic/mesic for the decay modes of individual hypernuclear species. Very little is known on this subject. One would like to know whether, for instance, this interaction is spin-dependent or not.

3. Nuclear physics

A variety of final state interaction effects can be found in hypernuclear decays. Typical examples $_{\Lambda}\text{He}^5 \rightarrow \pi^- + \text{Li}^{5*}$; $\text{Li}^{5*} \rightarrow p + \text{He}^4$ ($P_{3/2}$ resonance dominant) $_{\Lambda}\text{Li}^8 \rightarrow \pi^- + \text{Be}^{8*}$; $\text{Be}^{8*} \rightarrow \pi^- + 2\text{He}^4$ (0^+, 2^+ intermediate states present). These properties, as we shall see, may be very useful for specific purposes, like spin determination. Occasionally, new information on low energy nuclear physics problems may be gained as a by-product.

We will now try to justify some of the above results by presenting the evidence in some detail.

IV. Λ BINDING ENERGIES

The enclosed tabulation contains up-to-date averages of B_{Λ} for established species. When relevant, $\bar{B}_{\Lambda}$ are given separately for the most abundant decay modes of the same species. Several features are exhibited by a plot of B_{Λ} versus mass number A.

See fig.8

These are:

i) the presence of _charge multiplets_ reflecting the isospin structure of the core nuclei;

ii) an over-all _monotonic increase_ of B_Λ as a function of A;

iii) a _discrete structure_ within the multiplets which is to be attributed to _spin-dependent_ effects.

$_\Lambda H^3$ is the lightest hypernucleus known. It is attributed T = 0 since there is no evidence for the other members of a T = 1 state, $_\Lambda n^3$ and $_\Lambda He^3$. Its B_Λ is very small, (0.31 ± 0.15) MeV and the B_Λ distribution for this species is rather broad, somewhat more than expected from range-straggling alone.

See fig.9

$_\Lambda H^4$, $_\Lambda He^4$ are mirror hypernuclei (T = $\frac{1}{2}$) and have very similar $\overline{B}_\Lambda$'s (2.14 ± 0.08) MeV and (2.47 ± 0.09) MeV respectively as required from charge symmetry. One may comment that these values, due to the small errors, are almost in disagreement. The $\overline{B}_\Lambda$ determination of $_\Lambda H^4$ requires some more detailed investigation. As can be seen from Table 1, $\pi - r$ events yield for $\overline{B}_\Lambda$ the value (2.40 ± 0.12) MeV, very close to $_\Lambda He^4$. n events give a very low $\overline{B}_\Lambda$, (1.75 ± 0.1_) MeV and perhaps should not be included in the average for the reasons discussed above. Finally, ($\pi - p - r$) events for which $\overline{B}_\Lambda$ = (2.00 ± 0.14) MeV could contain a contamination of $_\Lambda H^3$ which would lower $\overline{B}_\Lambda$. On the other hand, $_\Lambda He^4$ could well contain a contamination of $_\Lambda He^5$, which would increase $\overline{B}_\Lambda$, in the sense of emphasizing a difference between $_\Lambda H^4$ and $_\Lambda He^4$ which may not be real at all. The one way to improve the situation here is not a mere increase in statistics, but a more severe selection of the events as pointed out in the section on identification problems.

The B_Λ distribution for the $\pi - r$ decays of $_\Lambda H^4$ is somewhat skew at the higher end. This could be due on one side to the inclusion of events in which the long pion (4 cm) may have lost energy in undetected interactions. On the other hand, a contamination of still hypothetical decays:

$$_\Lambda H^5 \rightarrow \pi^- + n + He^4, \quad _\Lambda H^6 \rightarrow \pi^- + 2n + He^4 \tag{25}$$
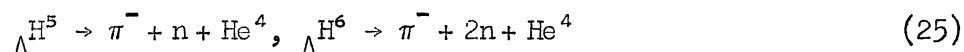
cannot be ruled out and should perhaps be kept in mind.

$_\Lambda He^5$. It is the most abundant hypernucleus. It decays essentially by the $\pi - p - r$ mode only. Its $\overline{B}_\Lambda$, (3.10 ± 0.05) MeV, is the best known and the B_Λ distribution is the closer to a Gaussian than any of the others.

($_\Lambda He^6$, $_\Lambda Li^6$). No clear cut evidence for the existence of these hypernuclei has been reported, nor the large number of $_\Lambda He^5$ giving decays also compatible with

$$_\Lambda He^6 \rightarrow \pi^- + p + n + He^4 \tag{26}$$

is a valid argument to support the existence of $_\Lambda He^6$. The decay

$$_\Lambda He^6 \rightarrow \pi^- + H^3 + H^3, \quad Q_0 = 26.44 \text{ MeV} \tag{27}$$
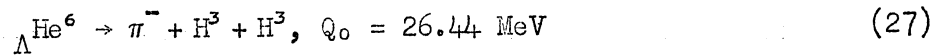
would provide good evidence.

See fig.10

$_\Lambda He^7$, $_\Lambda Li^7$, $_\Lambda Be^7$. $_\Lambda Li^7$ has T = 0 while $_\Lambda He^7$ and $_\Lambda Be^7$ are members of a T = 1 state. The B_Λ for $_\Lambda Li^7$ is well-established, (5.52 ± 0.12) MeV from decays other than $\pi - r$. Only two examples of $_\Lambda Be^7$ are known, yielding $\bar{B}_\Lambda = (4.9 \pm 0.5)$ MeV while for $_\Lambda He^7$ an average of 14 B_Λ values would give $\bar{B}_\Lambda = (3.96 \pm 0.24)$ MeV.

See fig.11

Two effects are present here. On one side, the $\bar{B}_\Lambda$ of $_\Lambda\text{Li}^7$ is higher than either of the $\bar{B}_\Lambda$ of $_\Lambda\text{He}^7$ or $_\Lambda\text{Be}^7$, and this can be understood in terms of the spin dependence of the Λ-nucleon interaction. On the other side, the $\bar{B}_\Lambda$'s for $_\Lambda\text{He}^7$ and $_\Lambda\text{Be}^7$ which should be identical, are indeed in disagreement. A suggestion made by Danysz and Pniewski[3], is the following. $_\Lambda\text{He}^7$ may decay from an isomeric state (He^6 has a level at 1.6 MeV in the continuum) and the observed B_Λ distribution may contain, in fact, two groups of B_Λ's. That this should be the case is substantiated by the very existence of $_\Lambda\text{Be}^7$. In fact, the condition for the stability of $_\Lambda\text{Be}^7$ against break up

$$_\Lambda\text{Be}^7 \rightarrow 2p + _\Lambda\text{He}^5 , \tag{28}$$

is that its B_Λ be greater than 4.5 MeV. Thus even with only two $_\Lambda\text{Be}^7$ events, we know that $B_\Lambda(_\Lambda\text{Be}^7)$ must exceed 4.5 MeV. From charge symmetry one would then expect that the ground state $_\Lambda\text{He}^7$ should have B_Λ also > 4.5 MeV. Thus, considerable interest is attached to an increase in the statistics of $_\Lambda\text{He}^7$ events. At present it is difficult to detect a splitting in the B_Λ distribution. The reasons to expect such splitting are, however, plausible, as will be further illustrated by Dalitz (these lectures).

$_\Lambda\text{Li}^8$, $_\Lambda\text{Be}^8$. Another well-established pair of mirror hypernuclei. Their $\bar{B}_\Lambda$'s are in very close agreement.

See fig.12

$_\Lambda Li^9$, $_\Lambda Be^9$, (B^9). The binding energy of $_\Lambda Li^9$ $(T = 1)$ is about 1.5 MeV greater than that of $_\Lambda Be^9$ $(T = 0)$. This is of course a point of great interest because if this difference is to be attributed to spin dependence only, it may be incompatible with the results from the mass 7 hypernuclei. Unfortunately the B_Λ distribution for $_\Lambda Li^9$ is not one of the most satisfactory. $_\Lambda B^9$ has never been reported. Its decay $(\pi - p - r)$ could be confused, as remarked before, with that of $_\Lambda Li^9$. This misidentification would not, however, affect the observed large difference in B_Λ between the $T = 0$ and $T = 1$ states. For heavier species, the plot shows how <u>little</u> is known. The spread σ of the B_Λ distributions is shown as a function of Q in the following plot. The over-all monotonic increase of B_Λ versus A can be understood in a rather simple way. The Λ particle, not obeying the Pauli principle in a single Λ hypernucleus, occupies the lowest s state. Thus, no saturation effects are expected until the Λ will reach the bottom of the potential well, for a very heavy hypernucleus.

See fig. 13

As the radius R of the region of interaction increases, with increasing A, the Λ will progressively "sink" to a lower energy state in the well. This can be seen as follows. Consider for simplicity the Λ in a square potential well of depth $U(r) = - D_\Lambda$, radius R.

Fig. 14
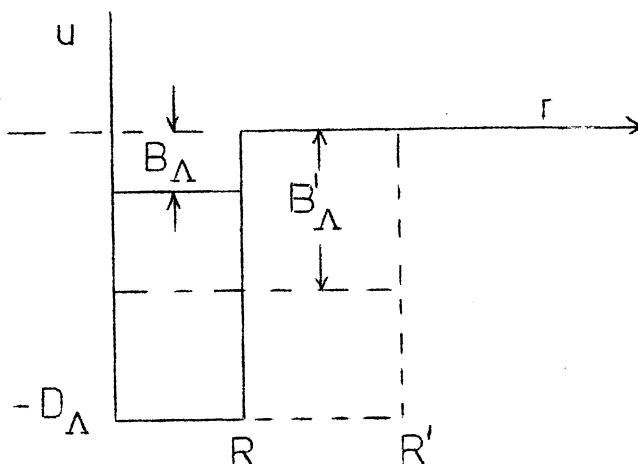
The standard solution of the Schrödinger equation for this problem, after matching the wave functions at the boundary R is:

$$K \cot KR = -\gamma, \text{ or } \sqrt{\frac{2M}{\hbar^2}(D_\Lambda - B_\Lambda)} \cot \sqrt{\frac{2M}{\hbar^2}(D_\Lambda - B_\Lambda)} R = -\sqrt{\frac{2M}{\hbar^2}B_\Lambda} \qquad (29)$$

$$\cot \sqrt{\frac{2M}{\hbar^2}(D_\Lambda - B_\Lambda)} R = -\sqrt{\frac{B_\Lambda}{D_\Lambda - B_\Lambda}} . \qquad (30)$$

One can now find approximate solutions for convenient asymptotic cases. Take for example $B_\Lambda \approx D_\Lambda$, then

$$\sqrt{\frac{2M}{\hbar^2}(D_\Lambda - B_\Lambda)} R \approx \pi; \quad B_\Lambda \approx D_\Lambda - \frac{\pi^2 \hbar^2}{2M_\Lambda r_0^2 A^{2/3}} . \qquad (31)$$

Equation (31) expresses explicitly how B_Λ depends on A for heavy hypernuclei. This equation suggests a method for the determination of D_Λ. In fact, a plot of B_Λ versus $A^{-2/3}$ for heavy hypernuclei should be, in the zeroth approximation, a linear plot. Extrapolation to $A \to \infty$ will give a value for D_Λ. This has indeed been accomplished at least partially from the knowledge of an upper limit of B_Λ for hypernuclei in the mass range $60 < A < 100$. The result[4] is that $D_\Lambda \lesssim 30$ MeV. The upper limit of B_Λ for $60 < A < 100$ hypernuclei was obtained from the upper limit in the energy release of mesic and non-mesic disintegrations of "spallation hyperfragments".

See fig.15

An attempt is being made at present to obtain a _lower_ limit of B_Λ for bromine hypernuclei following the measurement of the energy release in the reaction at rest

$$K^- + Br^{79} \rightarrow {}_\Lambda Br^{79} + \pi^- \,, \tag{32}$$
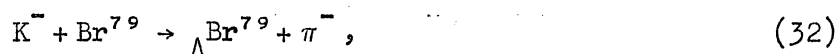
if such a reaction is found to occur to the ground state or some low lying state of ${}_\Lambda Br^{79}$. This study is made in a large CF_3Br bubble chamber where K^- mesons have been brought to rest. Even when B_Λ for heavy hypernuclei is known more accurately, the crude linear extrapolation to D_Λ will have to be improved, making use of a better approximation of Eq. (31). This will take into account a more realistic shape for the potential and indications are (Dalitz) that the correct functional dependence of B_Λ versus $A^{-2/3}$ is not linear but possesses some curvature (the slope increases slightly with A).

V. THE SPINS OF Λ HYPERNUCLEI

Spin assignments have been obtained so far for $_\Lambda H^3$, $_\Lambda H^4$, and $_\Lambda Li^8$. The spin of species with spinless core, such as $_\Lambda He^5$ can be inferred as being equal to the Λ spin, $J = \frac{1}{2}$. We can distinguish several approaches to this problem.

i) Determination by direct methods. It implies the production or selection of an aligned sample of hypernuclei. It is based on the study of angular correlations of the decay products with respect to some axis of quantization.

ii) Determination from branching ratios of different decay modes. Conservation of angular momentum may favour certain final states over others.

iii) More indirect approaches, e.g. based on hypernuclear lifetimes. These are, however, not independent of (ii).

Take, for example, $_\Lambda H^4$. A direct spin determination has been obtained by the He bubble chamber group from a study of the sequence of reactions

$$K^- + He^4 \rightarrow {_\Lambda H^4} + \pi^0 \; ; \quad {_\Lambda H^4} \rightarrow \pi^- + He^4 . \tag{33}$$
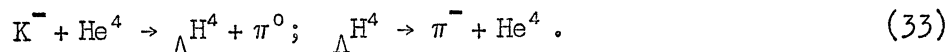
All particles in these reactions are spinless except possibly $_\Lambda H^4$ which can have at the most $J = 0$ or 1. If $_\Lambda H^4$ has $J = 0$, the decay $_\Lambda H^4 \rightarrow \pi^- + He^4$ is then necessarily isotropic. Note that in such a case, since the orbital angular momentum ℓ in the initial state must equal the orbital angular momentum L in the final state, the observation of Eq. (33) implies that the intrinsic parity $\omega_K = \omega_\pi = -1$ or $(\omega_\Lambda = +1$ by convention) that the K is _pseudoscalar_. Consider now the case of $J = 1$, and K^- capture from an s-orbital (there are good arguments in favour of this assumption)[5]. Then $L = 1$ in the final state which implies that $\omega_K = +1$, a _scalar_ K meson. As to the angular distribution in the decay of $_\Lambda H^4$, take the direction of $_\Lambda H^4$ as the axis Z of quantization. Only the projection $J_Z = m(_\Lambda H^4) = 0$ is allowed in the final state.

This, in turn, implies that in the rest system of π, He^4, $\ell_\pi = 1$, $m_\pi = 0$. Then the angular distribution is characterized by the spherical harmonic $Y_1^0(\Theta)$ only and $P(\Theta) \propto \cos^2\Theta$. The exp. distribution found by Block et al.[6]

Fig. 16
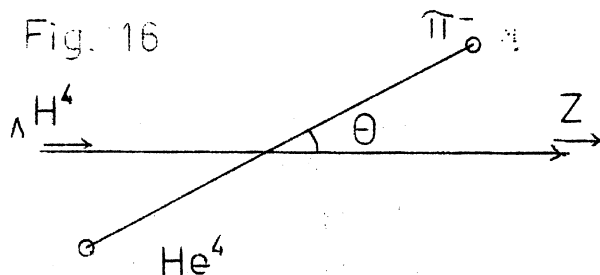
is isotropic, strongly suggesting that $J(_\Lambda H^4) = 0$ and that the K is pseudoscalar. Prior to this direct determination, $J = 0$ for $_\Lambda H^4$ had already been assigned as a result of an emulsion experiment.

Fig. 17
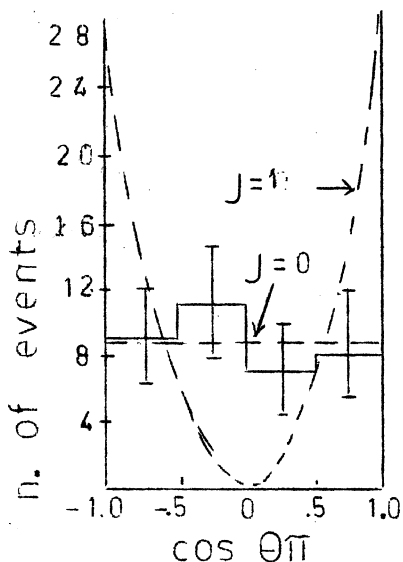
The spin assignment in question follows:

a) the original argument given by Dalitz[7] and also Dalitz and Liu[8] which relates the branching ratio $R_4 = \dfrac{\pi^- + He^4}{\text{all modes}}$ to the spin J and to the p/s ratio in Λ decay;

b) an exp. determination of R_4 in nuclear emulsion[9];

c) the accurate determination of the p/s ratio in Λ decay by Beall et al.[10] and by Cronin et al.[11].

The argument in its essence is the following: the decay $\Lambda \to \pi^- + p$ violates parity conservation and can proceed through both

s- and p-wave pion emission (see Dalitz, following lecture). Since the decay $_\Lambda H^4 \to \pi^- + He^4$ involves spinless particles in the final state, the spin J of $_\Lambda H^4$ equals the orbital angular momentum L in the final state.

See fig. 18

Thus, if $J(_\Lambda H^4) = 0$, the $\pi - r$ decay will be favoured if s-wave pion emission predominates in Λ decay, being forbidden for zero s-wave amplitude. Conversely, $J(_\Lambda H^4) = 1$, the $\pi - r$ decay is forbidden for zero p-wave amplitude and enhanced otherwise.

The experimental value of R_4 found in emulsion is 0.67 ± 0.06. This combined with the value $\dfrac{p^2}{(s)^2 + (p)^2} = 0.11 ± 0.03$, and on the basis of the curves calculated by Dalitz and Liu, clearly determines $J(_\Lambda H^4) = 0$. A more recent determination of R_4 has recently been reported by the He bubble chamber group. Their value, 0.68 ± 0.04, is in substantial agreement with that mentioned above.

By an entirely ~imilar reasoning $J = \frac{1}{2}$ has been assigned to $_\Lambda H^3$ [12]).

Both angular correlation among the decay products and branching ratios among different final states have enabled a determination of the spin of $_\Lambda Li^8$. This is the first hypernucleus of the nuclear p-shell for

which such information is available. The ground state of Li^7 has $J = 3/2$ while the first excited state of 0.475 MeV has $J = 1/2$. The Λ can couple to form $_\Lambda Li^8$ to either of these states so that a priori the spin of $_\Lambda Li^8$ could be 0^-, 1^- or 2^-. The solution of the problem hinges on evidence that the dominant decay

$$_\Lambda Li^8 \rightarrow \pi^- + 2He^4 \qquad\qquad (34)$$
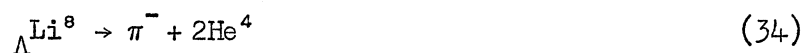
indeed proceeds through intermediate Be^{8*} states

$$_\Lambda Li^8 \rightarrow \pi^- + Be^{8*}; \quad Be^{8*} \rightarrow 2He^4 . \qquad\qquad (35)$$
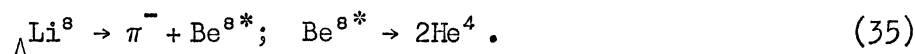
The information on the spin is derived from:

i) the existence of transitions to discrete Be^{8*} states and a comparison of the observed with the predicted partial rates for particular final states[13];

ii) the study of the angular correlation between the π^- direction and the $2He^4$ direction in their centre of mass.

Values of E_{rel} and $\cos \Theta$ have been calculated for about 43 events[14]. A plot of E_{rel} shows a remarkable grouping of events for E_{rel} values of ~ 0.1 MeV, ~ 3 MeV and ~ 17 MeV corresponding to all known levels of Be^{8*}.

A very small continuum background seems to contribute. The theoretical predictions by Dalitz are based on the following assumptions (simplified here).

a) The Λ-decay interaction is dominantly s interaction and therefore has odd parity. Thus, any transition via π^- emission to a final state of _even_ parity [like the 0^+, 2^+ (T = 0), 2^+ (T = 1) levels detected here] requires ℓ_π = odd. Very likely only ℓ_π = 1 contributes significantly.

b) The continuum in the E_{rel} distributions is neglected.

c) The calculations are based on appropriate intermediate-complying nuclear wave functions.

The predictions and the expt. results can be summarized as follows.

		Theory	Expt.
If J = 2⁻	i)	Very small transition rate to Be^{8*} (2^+, 3.0 MeV) or $P(\Theta) \approx \sin^2\Theta$ for (2^+) events	Very large
	ii)	Ratio $\dfrac{2^+,(T=1) \text{ at } 17 \text{ MeV}}{2^+,(T=0) \quad 3 \text{ MeV}} \sim 4.5$	4/32
If J = 1⁻	i)	$\dfrac{2^+(T=0)\ 3.0 \text{ MeV}}{0^+(T=0)\ 0.09 \text{ MeV}} \to 2.7 - 6.4$	32/5
	ii)	$\dfrac{2^+(T=1)\ 17 \text{ MeV}}{2^+(T=0)\ 3 \text{ MeV}} \sim 0$	4/32
	iii)	$P(\Theta) \approx 1 + 3\cos^2\Theta$ for (2^+) events	Consistent

Fig. 20

$$—P(\Theta)\propto 1+3\cos^2\Theta$$
$$--P(\Theta)\propto \sin^2\Theta$$
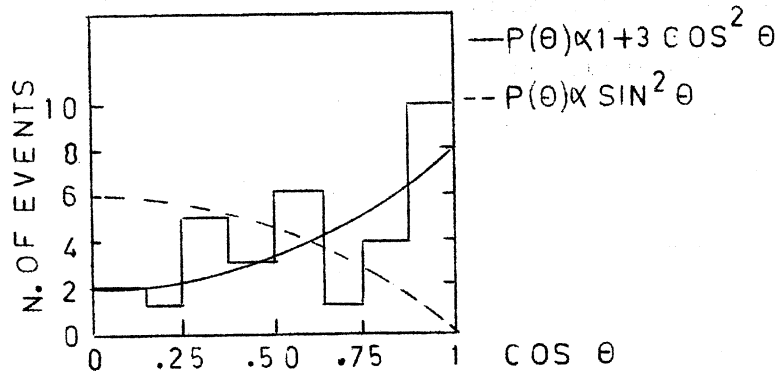
	Theory	Expt.
If $J = 0^-$	Transitions to 0^+, 2^+ states forbidden by angular momentum conservation	Both observed

In conclusion the over-all evidence favours $J = 1$ for $_\Lambda Li^8$. This shows that even in the p-shell hypernuclei, as well as in the s-shell ones like $_\Lambda H^3$, $_\Lambda H^4$,

$$J(HF) = |(J_i - \tfrac{1}{2})|$$

where J_i = spin of the core in its ground state. Purely as an exercise, a calculation of the angular correlation in $_\Lambda Li^8$ decay, assuming $\ell_\pi = 1$ is appended. This is valid for transitions to the 2^+, 3.0 MeV state of Be^{8*}.

As mentioned previously, the study of hypernuclear lifetimes provides us with another check on the spin assignments. Lifetime estimates of some significance are available for $_\Lambda H^3$ and $_\Lambda H^4$. For $_\Lambda He$ hypernuclei some data have been collected; for heavier hypernuclei no information is available at all. Dalitz and Rajasekharan[15] have shown that if $_\Lambda H^3$ has spin $J = \tfrac{1}{2}$, the total decay rate is enhanced considerably. A similar situation occurs if $J(_\Lambda H^4) = 0$. This can be understood qualitatively as due to the fact that if $J(_\Lambda H^3) = \tfrac{1}{2}$ and $J(_\Lambda H^4) = 0$, the s-channel decay is enhanced by both the Pauli principle, since it leads predominantly to allowed spin configurations, and by the energetic $(\pi^- + He^3)$ and $(\pi^- + He^4)$ final states respectively. A good estimate of the $_\Lambda H^3$ lifetime is available from the He bubble chamber group experiment[16]. An estimate of the lifetime of $_\Lambda H^4$ has been reported by Crayton et al.[17] from an emulsion experiment.

A comparison of the theoretical expectation with the experimental data is given in the following table.

$\tau\left(_\Lambda H^3\right)$ $J = \frac{1}{2}$ $J = \frac{3}{2}$

Theory $(1.79 \pm 0.10) \times 10^{-10} \sec$ $(2.40 \pm 0.03) \times 10^{-10} \sec$

$\left(\tau_\Lambda = 2.35 \times 10^{-10} \sec\right)$

Exp. $\left(1.05^{+\ 0.20}_{-\ 0.18}\right) \times 10^{-10} \sec$ (36 events of which 29 in flight)

$\tau\left(_\Lambda H^4\right)$ $J = 0$ $J = 1$

Theory $1.5 \times 10^{-10} \sec$ $> 2.7 \times 10^{-10} \sec$

Exp. $\left(1.2^{+\ 0.6}_{-\ 0.3}\right) \times 10^{-10} \sec$ (52 $\pi - r$ events of which 9 in flight)

The predicted enhancement of the total decay rate for the $\Lambda - n$ anti-parallel spin orientation has been observed. As a matter of fact the enhancements seem to be even greater than expected at least for $_\Lambda H^3$, and this may have to be explained.

Examples of $_\Lambda H^4$ decays in emulsion by the $\pi - r$ mode are shown:

Fig. 21
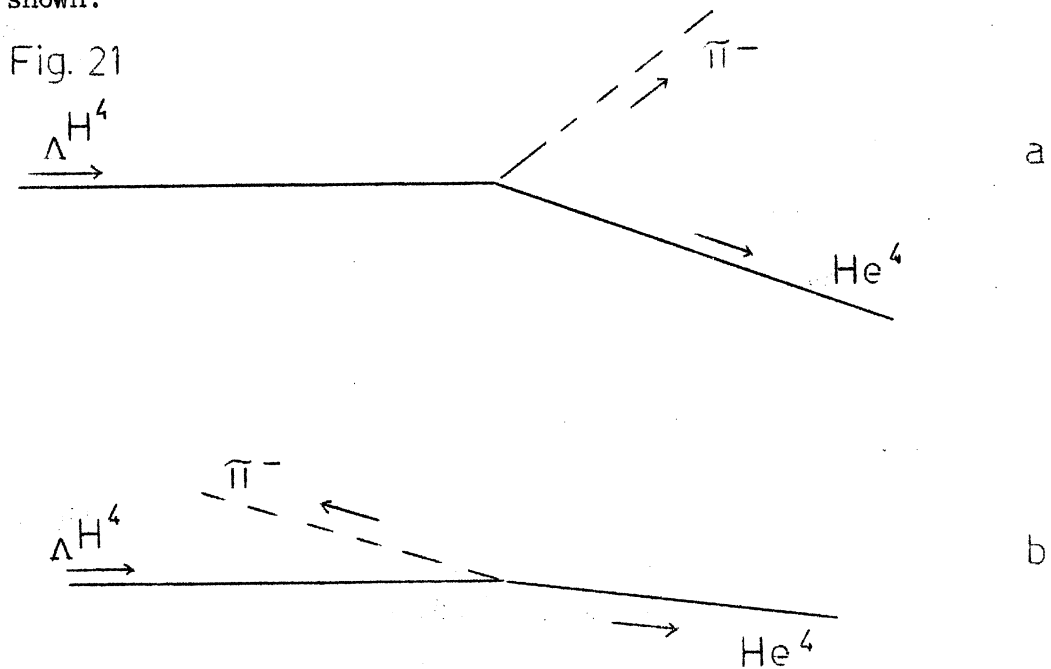
In a recent study by Ammar et al.[18] out of 99 π^- mesic decay of $_\Lambda He^{4,5}$ five were found to occur in flight. This yields

$$\tau(_\Lambda He^{4,5}) = (1.2^{+\,1.0}_{-\,0.4}) \times 10^{-10} \text{ sec.}$$

A result in substantial agreement[19] based on 51 $_\Lambda He$ events of which only four in flight, is again

$$\tau(_\Lambda He^{4,5}) = (1.4^{+\,1.8}_{-\,0.5}) \times 10^{-10} \text{ sec.}$$

* * *

REFERENCES

1. R.H. Dalitz and B.W. Downs, Phys.Rev. 111, 967 (1958).

2. R.H. Dalitz, The nuclear interaction of the hyperons, Bangalore Lectures, EFINS 62-9.

3. M. Danysz and J. Pniewski, Phys.Letters 1, 142 (1962).

4. D.H. Davis, R. Levi-Setti, M. Raymund, O. Skjeggestad, G. Tomasini, J. Lemonne, P. Renard and J. Sacton, Phys.Rev.Letters 9, 464 (1962).

5. T.B. Day and G.A. Snow, Phys.Rev.Letters 2, 59 (1959).

6. M.M. Block, L. Lendinara and L. Monari, Int.Conf.on High-Energy Phys., CERN 1962, p. 371.

7. R.H. Dalitz, Phys.Rev. 112, 605 (1958).

8. R.H. Dalitz and L. Liu, Phys.Rev. 116, 1312 (1959).

9. R.G. Ammar, R. Levi-Setti, W.E. Slater, S. Limentani, P.E. Schlein and P.M. Steinberg, Nuovo Cimento 19, 20 (1961).

10. E.F. Beall, B. Cork, D. Keefe, P.G. Murphy and W.A. Wenzel, Phys.Rev. Letters 8, 75 (1962).

11. J.W. Cronin, Bull.Am.Phys.Soc. 7, 68 (1962).

12. M.M. Block, C. Meltzer, S. Ratti, L. Grimellini, T. Kikuchi, L. Lendinara and L. Monari, Int.Conf.on High-Energy Phys., CERN 1962, p. 458; R.G. Ammar et al. NUPHYS 62104 - in press.

13. R.H. Dalitz, Nucl.Phys. 41, 78 (1963).

14. D.H. Davis, R. Levi-Setti and M. Raymund, Nucl.Phys. - in press,
    EFINS 62-48.

15. R.H. Dalitz and G. Rajasekharan, Phys.Letters 1, 58 (1962).

16. M.M. Block, C. Meltzer, S. Ratti, L. Grimellini, T. Kikuchi,
    L. Lendinara and L. Monari, Int.Conf.on High-Energy Phys.,
    CERN 1962, p. 458 and Hyperfragment Conference 1963.

17. N. Crayton, D.H. Davis, R. Levi-Setti, M. Raymund, O. Skjeggestad,
    G. Tomasini, R.G. Ammar, L. Choy, W. Dunn, M. Holland, J.H. Roberts
    and E.N. Shipley, Int.Conf.on High-Energy Phys., CERN 1962, p. 460.

18. R.G. Ammar et al., Phys.Letters - in press - NUPHYS 62105.

19. Y.W. Kang, N. Kwak, J. Schneps and P.A. Smith, Hyperfragment
    Conference 1963.

* * *

APPENDIX

Angular correlation in the decay $_\Lambda \text{Li}^8 \to \pi^- + \text{Be}^8$
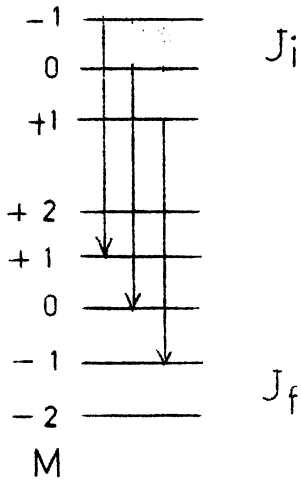
$$_\Lambda \text{Li}^8 \to \pi^- + \text{Be}^8$$

$$J \to 1 \quad 0 \quad 2$$

Fig. 22   Fig. 23

Take $\ell_\pi = 1$

$$\omega(\Theta) = \sum_{\ell_p \ell_q} | C(\ell_p, m_p, \ell_q, m_q | J, m) \, Y_{\ell_p}^{m_p}(\hat{p}) \, Y_{\ell_q}^{m_q}(\hat{q}) |^2$$

$$\cos \Theta_p = 1 \quad \cos \Theta_q = \cos \Theta$$

$$Y_{\ell_p}^{m_p}(1) = 0 \quad Y_{\ell_p}^{o}(1) = 1$$
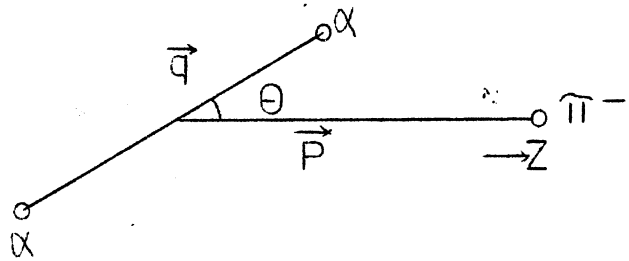
$$\omega(\Theta) \sim \sum_{\ell_p \ell_q} |C(\ell_p,0,\ell_q,m_q|j,m) \; Y_{\ell_q}^{m_q}(\cos \Theta)|^2$$

$$\ell_p = 1, \quad \ell_q = 2, \quad j = 1, \quad \Delta m_j = 0$$

$$\omega(\Theta) \sim \Sigma |<1,0,2,M|1,M> \; Y_2^M (\cos \Theta)|^2$$

$$M = m = m_q$$

$$M = m_p + m_q$$

$$\omega(\Theta) \sim |<1,0,2,1|1,1> \; Y_2^1|^2 + |<1,0,2,0|1,0>|Y_2^0|^2 + |<1,0,2,-1|1,-1> \; Y_2^{-1}|^2$$

$$<1,0,2,1|1,1> = \left[\frac{(j+M)(j+M+9)}{(2j+1)(2j+2)} \right]^{1/2} = \sqrt{1/2} \quad \begin{array}{c} J = j+1 \\ {}_2 \quad {}_1 \end{array}$$

$$<1,0,2,0|1,0> = \left[\frac{(j-M+1)(j+M+1)}{(2j+1)(2j+2)} \right]^{1/2} = \sqrt{2/3}$$

$$<1,0,2,-1|1,-1> = \left[\frac{(j-M)(j-M+1)}{(2j+1)(2j+2)} \right]^{1/2} = \sqrt{1/2}$$

$$Y_2^0 = \sqrt{\frac{5}{16\pi}} \; (3 \cos^2 \Theta - 1)$$

$$Y_2^{\pm1} = \mp \sqrt{\frac{15}{8\pi}} \sin \Theta \cos \Theta \; e^{\pm i\varphi}$$

$$Y_2^{\pm2} = \sqrt{\frac{15}{32\pi}} \sin^2 \Theta \; e^{\pm 2i\varphi}$$

$$\omega(\Theta) = 2 \frac{1}{2} \frac{15}{8} \sin^2\Theta \cos^2\Theta + \frac{2}{3} \frac{5}{16} (9 \cos^4\Theta - 6 \cos^2\Theta + 1) =$$

$$\frac{15}{8} \sin^2\Theta \cos^2\Theta + \frac{15}{8} \cos^4\Theta - \frac{30}{24} \cos^2\Theta + \frac{5}{24} = \frac{5}{24} (1 + 3 \cos^2\Theta) .$$

Case $2 \to 2$

$$\omega(\Theta) = 2 \left| <1,0,2,2|2,2> Y_2^2 \right|^2 + 2 \left| <1,0,2,1|2,1> Y_2^1 \right|^2$$
$$+ \left| <1,0,2,0|2,0> Y_2^0 \right|^2 \to \sim \sin^2\Theta .$$

*   *   *

Table 1

Binding energies from uniquely identified mesonic decays[†]
March, 1963

Identity	Decay mode	$\bar{B}_\Lambda$ (MeV)	σ_{av}[*] (MeV)	σ (MeV)	No. of events
$_\Lambda H^3$	$\pi - r$	0.38	0.24	1.05 ± 0.16	20
	all other	0.27	0.19	0.80 ± 0.15	18
	total	0.31	0.15	-	38
$_\Lambda H^4$	$\pi - r$	2.40	0.12	0.99 ± 0.10	62
	n	1.75	0.18	0.82 ± 0.13	20
	all other	2.00	0.14	0.71 ± 0.10	27
	total	2.14	0.08	-	109
$_\Lambda He^4$	all	2.47	0.09	0.61 ± 0.008	48
$_\Lambda He^5$	all	3.10	0.05	0.57 ± 0.04	147
$_\Lambda He^7$	all	3.96	-	0.9 ± 0.2	14
$_\Lambda Li^9$	$\pi - r$	5.51	-	1.0 ± 0.3	9
	all other	5.52	0.12	0.45 ± 0.08	16
$_\Lambda Li^8$	all	6.65	0.15	1.06 ± 0.12	44
$_\Lambda Li^9$	$\pi - r$	6.9	0.8	inferred	1
	all other	8.01	0.29	-	9
$_\Lambda Be^7$	all	4.9	0.5	inferred	2
$_\Lambda Be^8$	all	6.35	0.30	inferred	4
$_\Lambda Be^9$	all	6.50	0.16	0.30 ± 0.06	10
$_\Lambda Be^{10}$	$\pi - r$	9.48	-	1.0 ± 0.4	4
	all other	8.36	0.6	inferred	1
$_\Lambda B^{10}$	$\pi - r$	10.0	-	1.0 ± 0.3	6
$_\Lambda B^{11}$	$\pi - r$	10.0	-	0.6 ± 0.2	4
	all other	9.9	0.6	inferred	1
$_\Lambda B^{12}$	all	10.50	0.18	0.6 ± 0.15	8
$_\Lambda C^{13}$	$\pi - r$	10.6	0.4	inferred	2
$_\Lambda C^{14}$	$\pi - r$	13.2	0.7	inferred	1
$_\Lambda N^{14}$	$\pi - r$	11.7	0.5	inferred	1

[*] Possible systematic errors (± 0.2 MeV) have not been included.

[†] Computed from the data contained in the enclosed references.

REFERENCES to Table 1

R.G. Ammar, R. Levi-Setti, W.E. Slater, S. Limentani, P.E. Schlein
and P.H. Steinberg, Nuovo Cimento 15, 181 (1960).

R.G. Ammar, R. Levi-Setti, W.E. Slater, S. Limentani, P.E. Schlein
and P.H. Steinberg, Nuovo Cimento 19, 20 (1961).

P.E. Schlein and W.E. Slater, Nuovo Cimento 21, 213 (1961).

R. Levi-Setti, W.E. Slater and V.L. Telegdi, Nuovo Cimento 10, 68 (1958);
contains previous literature.

S. Mora and I. Ortalli, Nuovo Cimento 12, 635 (1959).

G.C. Deka, Nuovo Cimento 14, 1217 (1959).

S. Lokanathan, D.K. Robinson and S.J. St. Lorant, Proc.Roy.Soc.(London)
A254, 470 (1960).

J. Sacton, Nuovo Cimento 15, 110 (1960).

J. Tietge, Nucl.Phys. 20, 227 (1960).

M. Taher-Zadeh, Nuovo Cimento 17, 980 (1960).

M.M. Nikolić, Nucl.Phys. 21, 595 (1961).

Y. Prakash, P.H. Steinberg, D.A. Chandler and R.J. Prem, Nuovo Cimento
21, 235 (1961).

M.J. Beniston and D.H. Davis, Phil.Mag. 7, 2119 (1962) and private
communication.

N. Crayton, R. Levi-Setti, M. Raymund, O. Skjeggestad, D. Abeledo,
R.G. Ammar, J.H. Roberts and E.N. Shipley, Rev.Mod.Phys. 34, 186 (1962).

W. Gajewski, J. Pniewski, T. Pniewski and S. Popov (to be published),
quoted in J. Pniewski and M. Danysz, Phys.Letters 1, 142 (1962);
1 $_\Lambda$He^7 event.

A.A. Varfolomev, R.I. Gerasimova and L.A. Karpova, Soviet Phys.Doklady
1, 579 (1956), DAN 110, 758 (1956); 1 $_\Lambda$He^7 event.

S.J. St. Lorant, private communication, 1 $_\Lambda$Be^7 event.

R.G. Ammar, M. Holland, J.H. Roberts and E.N. Shipley, Nuovo Cimento
27, 769 (1963); 1 $_\Lambda$Be^7 event.

D.J. Prowse, Bull.Am.Phys.Soc. II, $\underline{7}$, 297 (1962), and private communication June 1962;   1 $_\Lambda N^{14}$ event.

A.Z. Ismail, I. Kenyon, A. Key, S. Lokanathan and Y. Prakash, Nuovo Cimento $\underline{27}$, 1228 (1963);   3 $_\Lambda He^{7}$, 1 $_\Lambda Li^{7}$, 1 $_\Lambda Li^{8}$ and 2 $_\Lambda B^{12}$ events.

R.G. Ammar, L. Choy, W. Dunn, M. Holland, J.H. Roberts, E.N. Shipley, N. Crayton, D.H. Davis, R. Levi-Setti, M. Raymund, O. Skjeggestad and G. Tomasini, Nuovo Cimento $\underline{27}$, 1078 (1963).

D.H. Davis, R. Levi-Setti and M. Raymund, Nucl.Phys. $\underline{41}$, 73 (1963).

* * *
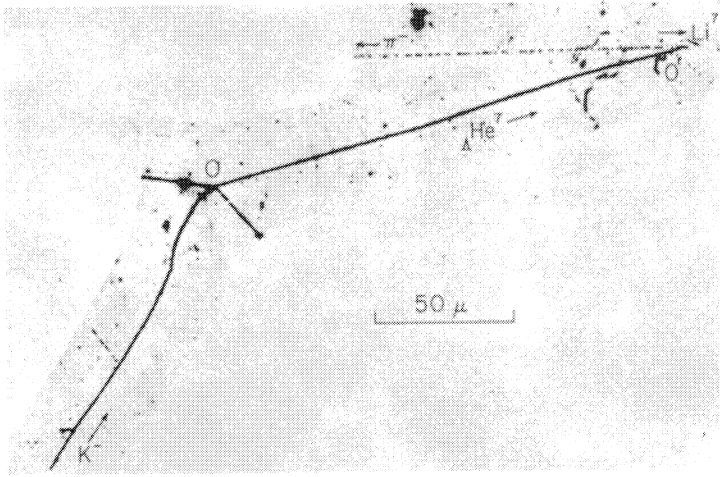
Fig. 2.   Example of $_{\Lambda}\mathrm{He}^7 \to \mathrm{Li}^7 + \pi^-$
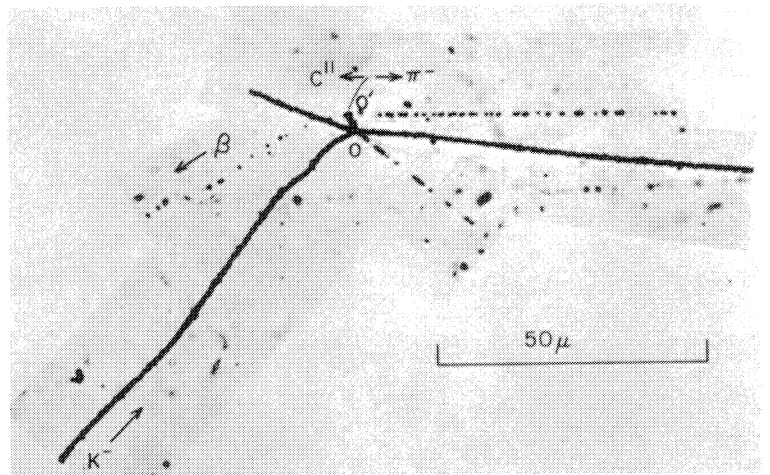
Fig. 3.   Example of $_{\Lambda}\mathrm{B}^{11} \to \bar{\pi} + \mathrm{C}^{11} + \beta^+$
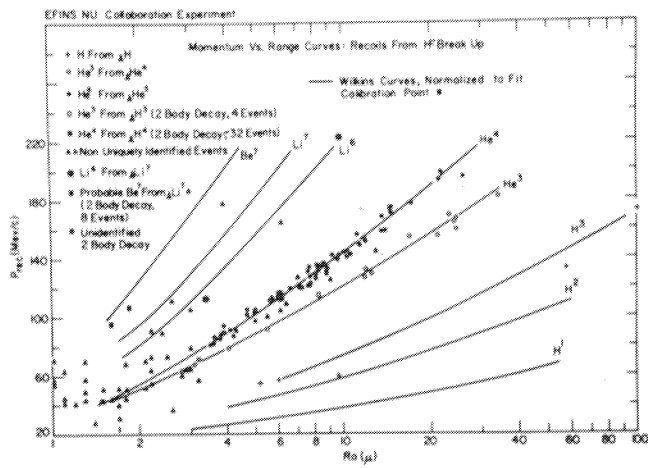
Fig. 4.   Plot of recoil momentum against range.
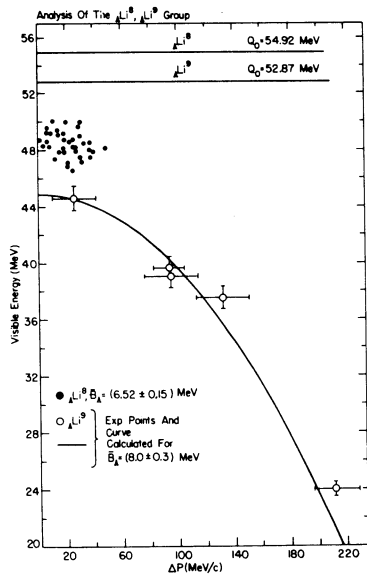
Fig. 6. Energy release Q versus missing momentum (Δ P) for Li^8 and Li^9 events.
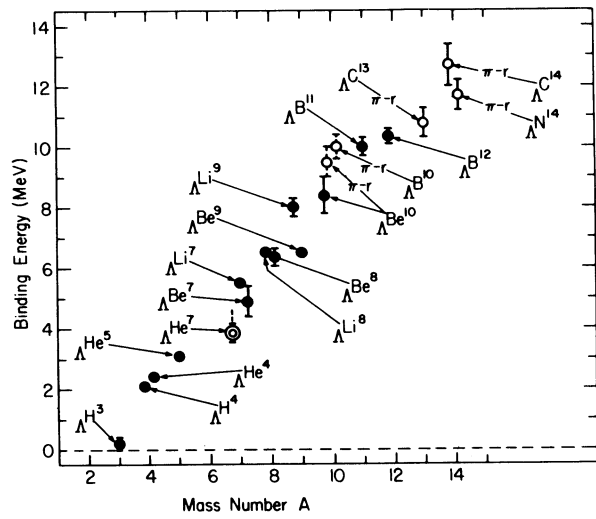
Fig. 8. Binding energy versus Mass Number.
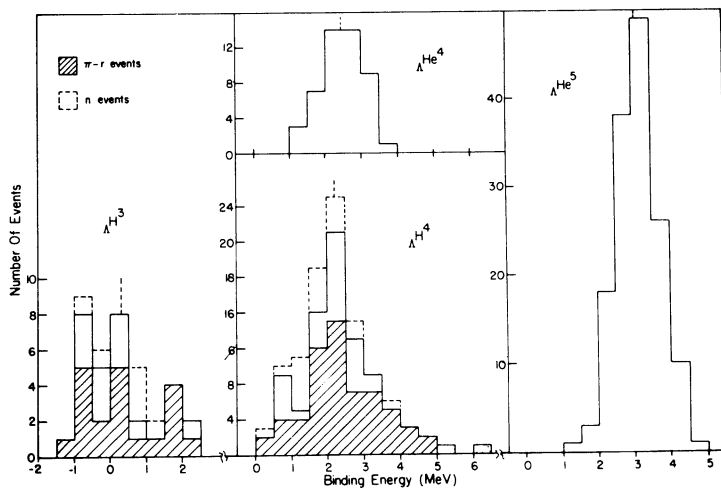
Fig. 9. Binding energies of $_\Lambda H^3$, $_\Lambda He^4$, $_\Lambda H^4$ and $_\Lambda He^5$.
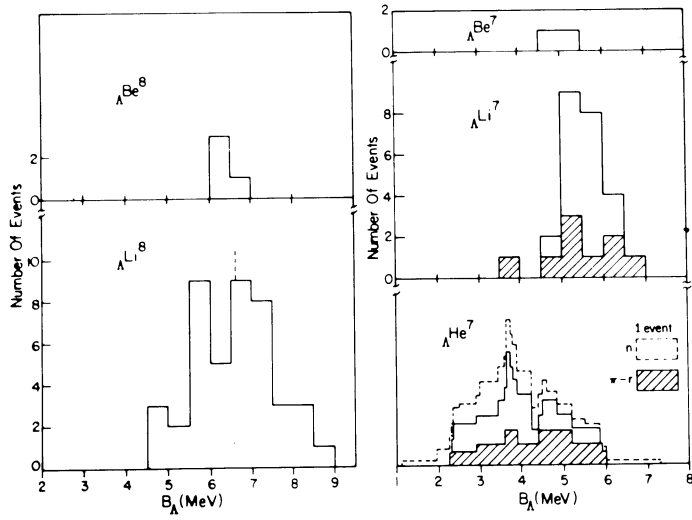
Fig. 10. Binding energies of $_\Lambda Be^7$, $_\Lambda Li^7$, $_\Lambda He^7$, $_\Lambda Be^8$ and $_\Lambda Li^8$
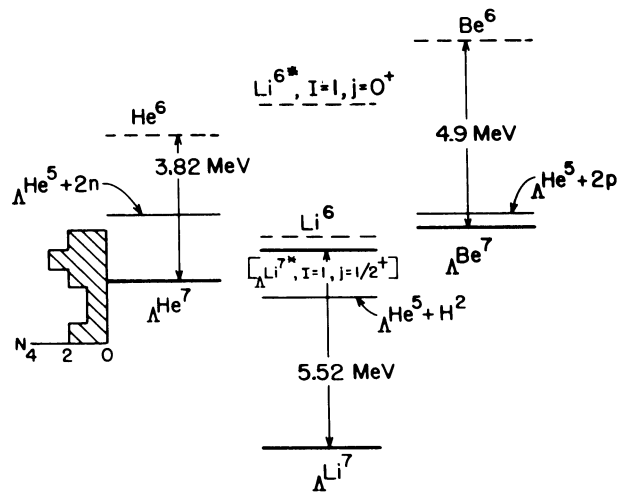
Fig. 11. Energy level diagram.
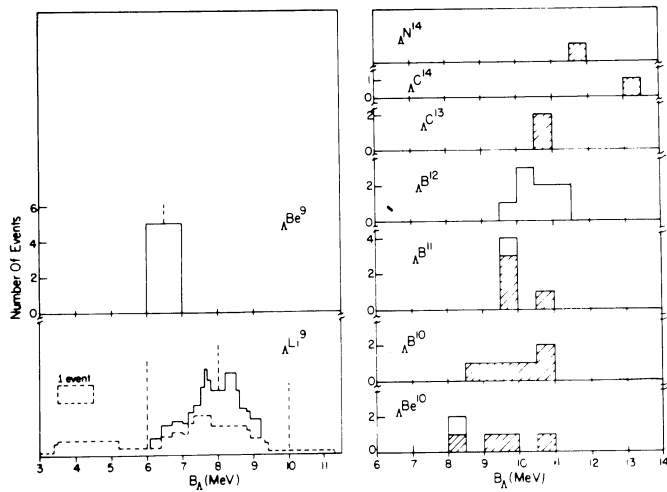
Fig. 12. Binding energies of Li, Be, B, C, and H hypernuclei.
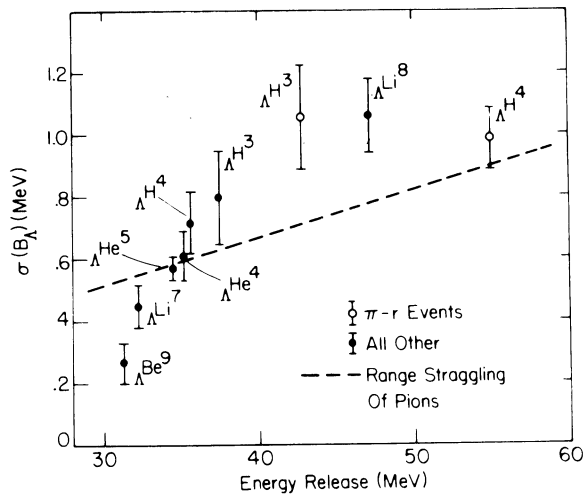
Fig. 13. Spread σ of B_Λ distributions as a function of the energy release Q.
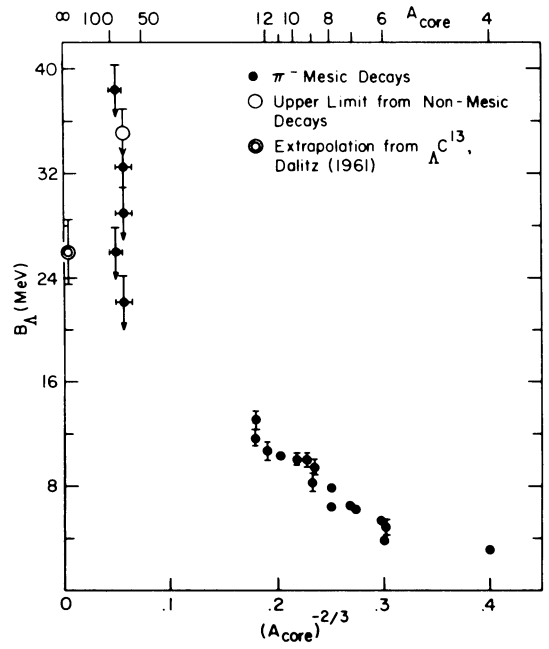
Fig. 15. B_Λ versus $A^{-2/3}$.
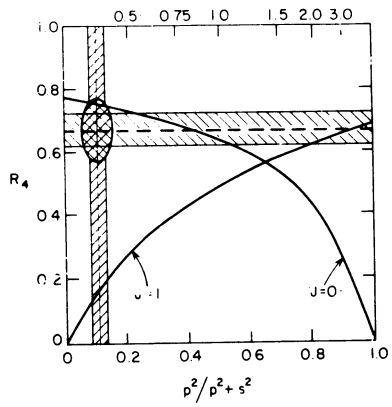
Fig. 18. The branching ratio $R = (He^4 + \pi^-)/(all\ \pi^-\ modes)$ for $_\Lambda H^4$ decay is compared with the calculated ratios for $_\Lambda H^4$ spin $J = 0$ and $J = 1$, and with the measured value $p^2/(p^2 + s^2) = 0.11 \pm 0.03$.
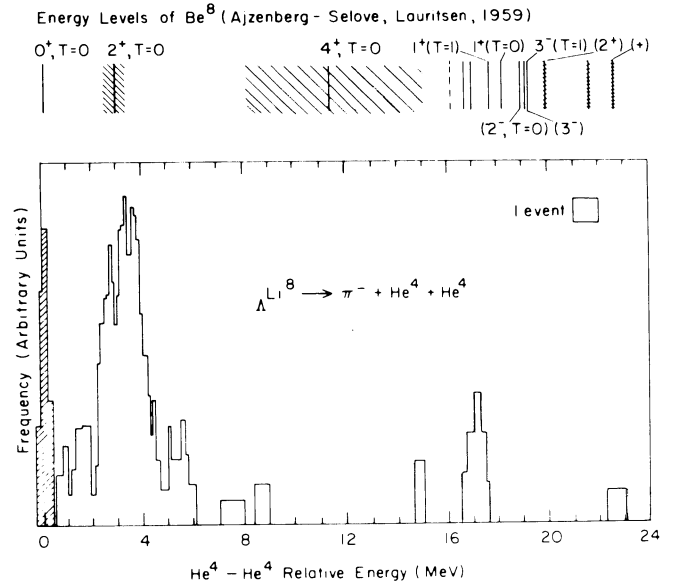
Fig. 19. Plot of $He^4 - He^4$ relative energy for $Li^8 \to \pi^- + He^4 + He^4$.

NON-MESONIC DECAY MODES

J. Sacton,
Institut de Physique,
Université de Bruxelles, Belgium.

The decay of a Λ^0 hyperon bound to a nuclear fragment does not always proceed by the emission of a pion; it is well known that with increasing mass of the nuclear core the non-mesonic mode rapidly begins to be the dominant decay process. The non-mesonic decay of hypernuclei is considered to be the result of the stimulated decay of the Λ^0 hyperon in the presence of nucleons. As suggested by Cheston and Primakoff[1], the decay proceeds through an intermediate step involving a virtual pion which is subsequently re-absorbed by a neighbouring nucleon.

The reactions are as follows:

$$\Lambda^0 + p \rightarrow (p + \pi^-) + p \rightarrow p + n \tag{1}$$

$$\rightarrow (n + \pi^0) + p \rightarrow n + p \tag{2}$$

$$\Lambda^0 + n \rightarrow (n + \pi^0) + n \rightarrow n + n \tag{3}$$
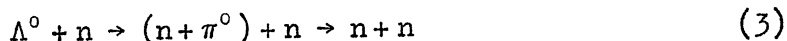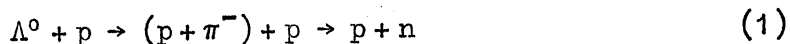
the energy release being of the order of 180 MeV $(m_{\Lambda^0} - m_n)$.

These stimulation processes have been analysed in some detail by different authors[2-5] and, in particular, their matrix elements have been estimated taking account of the contributions from the interactions involving either one or more exchange pions, or a K meson, and including the possibility of the existence of the Λ in a virtual Σ state when in the presence of nucleons. It is not within my competence to discuss here these studies; I will restrict myself to trying to give a summary of what has been done from the experimental point of view. You will easily see that the situation is particularly

confused due to the experimental difficulties one meets in the study of the non-mesonic decays.

Two problems have been particularly investigated.

i) The variation of Q, the non-mesonic to mesonic
   decay ratio as a function of the HF charge

Ruderman and Karplus[2] have shown that the ratio Q is very sensitive to the angular momentum of the pion emitted in the free Λ decay. The study of the variation of Q with the HF charge has been used as a means to determine the spin of the Λ^0 hyperon. However, extensive studies of the free Λ^0 hyperon have now provided definite information concerning the spin of the Λ^0 hyperon. More recently, it was pointed out by Dalitz and Liu[5] that the determination of Q could give us with good accuracy the value of the ratio p/s of the p- and s-channel amplitudes of the decay of the free Λ^0 hyperon. Recent experiments carried out by Beall et al.[6], and Cronin et al.[7], have clearly established that the s interaction is dominant. The results of Cronin et al. indicate that $p/s = 0.36^{+0.5}_{-0.8}$. Dalitz and Rajasekharan[8] have suggested that definite predictions of the lifetimes of light hyperfragments would require a better knowledge of the interaction $\Lambda + n \rightarrow n + n$.

ii) The ratio of proton to neutron stimulation

This could provide useful information concerning the Λ^0-nucleon interaction[4].

The detailed study of both these problems involves the detection of all hyperfragment decay modes and the elaboration of an unbiased charge distribution. It is, however, well known that the experimental study of the non-mesonic decays presents great difficulties, both in the classification of the events as definite hyperfragments and in the subsequent interpretation of their identity from decay kinematics. The energy release in such a decay is ~ 175 MeV, so that in the case of

light hyperfragments this will normally lead to a more or less complete break-up of the nuclear core followed by the emission of fragments and of neutrons. The absence among the decay products of an easily identified particle like the π^- meson in the mesonic decays, makes the kinematic analysis extremely difficult and leads, in general, to confusion with other phenomena such as slow pions, K^- or Σ^- captures, collision of moderately energetic particles, etc. Moreover, typical decay modes, such as those involving only one charged particle, are practically undetectable because they are overwhelmed by scatterings. These difficulties have led to the use of selection criteria which were not always perfectly adapted to the problem. In particular, any selection criteria on the decay characteristics must undoubtedly lead to biased statistics. This was clearly pointed out by Zakrzewski and St. Lorant[9] in their review analysis of work published in 1962. In some cases the use of measurements of the track of the hyperfragments has been of great importance. However, these measurements are only useful on long-range hyperfragments which are very rare especially in K^- meson absorptions at rest, the richest source of hyperfragments actually used, and also the only one for which the contamination due to other events is rather easily eliminated by applying some selection criteria on the parent star.

The kinematic analysis of non-mesonic decays proceeds generally as follows. The computer runs each possible combination of the decay products under each of the assumptions:

a) no neutral particles

b) a π meson

c) a neutron

d) two neutrons (not in all cases).

The machine is instructed to derive B_Λ. The B_Λ values are compared with those obtained for mesonic hyperfragments, taking into account the large errors.

That this type of analysis is insufficient was clearly demonstrated by Silverstein[10] who compared, for "uniquely" identified events, the energy distributions of both the neutrons and the protons resulting from the decays and found them completely different, the neutrons being shifted systematically to higher energy. Such a shift is due to a systematic underestimate of the number of neutrons involved in the decays leading to an overestimate of the energy imparted to each of them.

Another proof of the weakness of this type of analysis is obtained from the comparison of the range distribution of both the non-mesonic and mesonic hyperfragments of a given charge identified in the same experiment. In most cases it was found that the range distribution of the non-mesonic hyperfragments was more concentrated in the region of shorter ranges (background of heavy hyperfragments).

Keeping all these restrictions in mind we will now try to look at the experimental results.

1. NM/M as a function of Z

Most of the information comes from Silverstein[10], Sacton[11], Gorge et al.[12], and more recently from Bhowmik[13] and Block[14]. The hyperfragments are produced in K^- absorptions at rest except in Silverstein's experiment where the hyperfragments are produced in high-energy π^- interactions.

The problem here is to get a true idea of the charge distribution of the hyperfragments, both mesonic and non-mesonic. The charge distribution of M hyperfragments produced in K^- absorption at rest has been determined with large statistics by Abeledo et al.[15] and is as follows: Z = 1, 26%; Z = 2, 45%; Z = 3, 22%, and Z > 3, 7%.

Concerning the non-mesonic decays, the statistics are not only poorer but also less homogeneous: 131 events have been collected in three different laboratories using different selection criteria (Brussels, 55; Delhi, 54; Bern, 22). The charge distribution of these hyperfragments is established as follows.

i) Uniquely identified events

These are events for which only one interpretation leads to an acceptable value for the Λ° hyperon binding energy.

Table 1

Z =	2	3	4	≥ 5
Brussels	6	4	6	10
Bern	5	7	7	12
Bombay	17	-	3	-
Total	28	11	16	22

Large discrepancies are observed between these results. (In the Bombay experiment the emission of two neutrons was not considered.)

ii) Non-uniquely identified events

For the remaining events for which the charge is not uniquely determined, a rather similar analysis was used by all the authors to get a true idea of the charge distribution; for such events, all the possible interpretations were assumed to be equally probable and normalized in each case to unity. Combining all these events, one obtains the following distribution:

Table 2

Z =	2	3	4	≥ 5
Brussels	8	7	8	22
Bern	5.5	8.6	7.4	13.5
Bombay	21	5.7	4.7	0.6
Total 112	34.5	21.3	20.1	36.1

Note: I have excluded the DC events which are probably very heavy hyperfragments.

Using the results of Abeledo et al.[15] for the M hyperfragments, one obtains for the non-mesonic to mesonic decay ratio the values given in Table 3. These values must be taken with great care.

Table 3

Z	2	3	≥ 3
Q	1.4	~3	~50

Indeed, I would remind you that almost all the decays into a single charged particle have not been recorded so that the values quoted here are surely underestimated.

In the case of hyperhelium, another approach has been made by Schlein[16] in 4.5 GeV/c π^- meson interactions, and led to the value Q = 1.5 ± 0.4. The theoretical values to which these results are to be compared are as follows:

Table 4

Z	1		2		> 2
$\ell = 0$	0.55	0.3 (H^3) 0.8 (H^4)	0.9	0.85 (He^4) 1.0 (He^5)	40
$\ell = 1$	9.0	4.5 (H^3) 13.6 (H^4)	16	14 (He^4) 17 (He^5)	680

It is concluded that the ratio p/s is definitely smaller than 1 in agreement with the information obtained by Cronin and Overseth[7] for free Λ hyperons. It is, however, too early to get any information of the type asked of the experimentalists by Dalitz and Rajasekharan[8].

ii) n/p ratio in stimulated decay

The other point I should like to discuss is the question of the stimulated decay of the Λ^0 hyperon. My task in this case is considerably reduced due to the fact that a careful and critical re-examination of the published work was made recently by Zakrzewski and St. Lorant[9]. Several attempts have been made to study this problem. All of them are based on the examination of the energy spectrum of fast protons emitted from non-mesonically decaying hyperfragments. Most of the remarks and criticisms which I have put forward previously must be kept in mind in the analysis of the experimental results.

The method of analysis first proposed by Baldo-Ceolin et al.[17] is based on the following assumptions:

i) the one-nucleon stimulated decays are dominant;

ii) the nucleons emitted as a result of these processes and, in particular, the proton resulting from reaction (1) have a momentum above a certain cut-off which has to be determined;

iii) the nucleons do not lose so much energy by collisions that all memory of their origins disappears.

The bottle-neck in this type of analysis is the estimate of the cut-off energy at which the two processes merge. This is made from consideration of the energy distribution of all charged particles emitted in the non-mesonic decay stars. A typical such distribution appears to consist of two energy groupings: one contains the protons of energy less than 30 MeV; the other constitutes the tail of the distribution extending to ~ 140 MeV. The low-energy part is interpreted as being due to the break-up of the residual nucleus following the emission of the two fast nucleons from the stimulation process. The fast protons are attributed to the initial stimulation process by protons. The total energy release in a stimulated decay (180 MeV) is shared equally between the two nucleons resulting from the reaction (in the Λ-n rest frame). Outside the nucleus, the energy is slightly reduced due to binding energy of Λ and nucleon. Assuming that the effect of

the Fermi momentum of the stimulating nucleons is to introduce a symmetrical spread around a mean value, the cut-off can be obtained experimentally from the energy distribution of all charged particles. In this way, Baldo-Ceolin et al.[17] and Silverstein[10] have obtained 30 and 40 MeV (240 MeV/c and 275 MeV/c), respectively. All the events containing a proton of energy greater than this limit are attributed to a proton-stimulated process.

It is very difficult, for the reasons given before, to study the n/p ratio for a particular species of hyperfragment, so that in the beginning no attempts were made to separate the hyperfragments according to their charges. The results of different experiments lead to n/p ranging from 1 to 2. Selection criteria and scanning losses seem, however, to play an important role in these results.

Moreover, Zakrzewski and St. Lorant[9] have suggested that in some cases the sample of events could be artificially enriched in very heavy hyperfragments for which it is to be expected that the criteria used to study the stimulation processes could be less reliable. This is especially true for the hyperfragments produced in high-energy interactions and for very short-range hyperfragments ($< 2\mu$) produced in K^- absorption at rest.

The stimulation processes have recently been studied by Bhowmik et al.[13]. The hyperfragments were produced by stopping K^- and Σ^-. The results of this work are:

$$\text{for He} \quad : \quad \frac{p}{n} = 15/4 = 3.8$$

$$\text{for } Z \gtrsim 3 \quad : \quad \frac{p}{n} = 10/4 = 2.5 \ .$$

The result is to be compared to that of Block et al.[14] for helium hyperfragments:

$$\sim 5 = \frac{p}{n} \quad \left(_\Lambda He^4 \ 2p \ 1n\right) .$$

It seems that for helium, p/n is clearly > 1, which following Ferrari and Fonda implies that the stimulated decay takes place when the hyperon is in the Λ state.

It is to be noted that the p/n ratio could be drastically dependent on nucleon structure or on diffferent distributions of p and n inside the nucleus.

As a conclusion, I should say that practically everything remains yet to be studied. Even if many competing processes are likely to contribute to the production of HF, it seems that valuable experimental information could be obtained with rather clean statistics selected on the basis of the production rather than on the decay processes. At the present time, it seems that K^- absorptions at rest are best suited for such a study, even if most of the hyperfragments with $Z \geq 3$ are of such short range that no measurements are possible on the tracks themselves.

* * *

REFERENCES

1) W. Cheston and H. Primakoff, Phys.Rev. 92, 1537 (1953).

2) M. Ruderman and R. Karplus, Phys.Rev. 102, 247 (1956).

3) D.B. Lichtenberg and M. Ross, Phys.Rev. 103, 1131 (1956).

4) F. Ferrari and L. Fonda, Nuovo Cimento 7, 320 (1957).

5) R.H. Dalitz, Phys.Rev. 112, 605 (1958).
   R.H. Dalitz, Rev.Mod.Phys. 31, 823 (1959).
   R.H. Dalitz and L. Liu, Phys.Rev. 116, 1312 (1959).

6) E.F. Beall, B. Cork, D. Keefe, P.G. Murphy and W.A. Wenzel, Phys.Rev. Letters 7, 285 (1961).

7) J.W. Cronin and O.E. Overseth, 1962 International Conference on High-Energy Physics at CERN, p. 453.

8) R.H. Dalitz and G. Rajasekharan, Physics Letters 1, 58 (1962).

9) J. Zakrzewski and S.J. St. Lorant, Nuovo Cimento 25, 693 (1962).

10) E.M. Silverstein, Suppl. Nuovo Cimento 10, 41 (1958).

11) J. Sacton, thesis, Bulletin de l'Université de Bruxelles and Nuovo Cimento 18, 266 (1960).

12) V. Gorge, W. Koch, W. Lindt, M. Nikolić, S. Subotic-Nikolić and H. Winzeler, Nucl.Phys. 21, 599 (1960).

13) B. Bhowmik, P. Goyal and N.K. Yamdagni, Physics Letters 3, 13 (1962), and preprint 1963.

14) M.M. Block, R. Gessaroli, S. Ratti, L. Grimellini, T. Kikuchi and E. Harth, preprint 1962.

15) D. Abeledo, L. Choy, R.G. Ammar, N. Crayton, R. Levi Setti, M. Raymund and O. Skjeggestad, Nuovo Cimento 22, 1171 (1961).

16) P.E. Schlein, Phys.Rev.Letters 2, 220 (1959).

17) M. Baldo-Ceolin, C. Dilworth, W.F. Fry, W.D.B. Greening, H. Huzita, S. Limentani and A.E. Sichirollo, Nuovo Cimento 7, 328 (1958).

*　　*　　*

III. BUBBLE CHAMBER STUDIES

HYPERFRAGMENT STUDIES IN THE HELIUM BUBBLE CHAMBER[*]

M.M. Block, R. Gessaroli[†], J. Kopelman, S. Ratti[††] and M. Schneeberger,
Northwestern University, Evanston, Ill., USA.

L. Grimellini, T. Kikuchi[+], L. Lendinara and L. Monari,
University of Bologna, Bologna, Italy.

W. Becker and E. Harth,
Syracuse University, Syracuse, N.Y., USA.

I. INTRODUCTION

The $K^- + He^4$ reactions which are capable of producing hyper-fragments are

$$K^- + He^4 \rightarrow {}_\Lambda He^4 + \pi^- \qquad (a)$$

$$\rightarrow {}_\Lambda H^4 + \pi^0 \qquad (b)$$

$$\rightarrow {}_\Lambda H^3 + \pi^- + p \qquad (c)$$

$$\rightarrow {}_\Lambda H^3 + \pi^0 + n \qquad (d)$$

$$\rightarrow {}_\Lambda H^3 + n \qquad (e) .$$
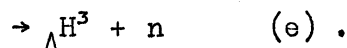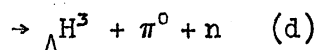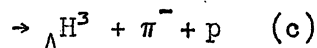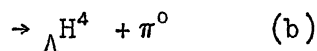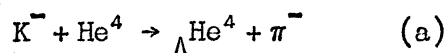
We have not observed any cases of (e). For experimental reasons, we have confined our attention exclusively to reactions (a) - (c). Our studies were performed using the helium bubble chamber, $20 \times 10 \times 12.5 \text{ cm}^3$, operated in a magnetic field of 14 kgauss. The spatial resolution is such that tracks of 0.5 mm range can be measured to an accuracy of ~ 0.1 mm.

Figure 1 shows the signature for the reactions $K^- + He^4 \rightarrow \pi^- + {}_\Lambda He^4$, ${}_\Lambda He^4 \rightarrow \pi^0 + He^4$. The hyperfragment range is 0.53 mm, the production pion momentum is 256 MeV/c and, of course, the two tracks are co-linear. The decay recoil has too low an energy to produce a visible bubble, so that we

see "nothing" at the decay. This is by far the most typical type of $_\Lambda$He^4 event. Figure 2 shows the signature for the reaction $K^- + He^4 \rightarrow \pi^0 + _\Lambda H^4$, $_\Lambda H^4 \rightarrow \pi^- + He^4$. The $_\Lambda H^4$ range is 2.2 mm, and the decay pion momentum is 137 MeV/c. The recoil α particle has too low an energy to be visible. We have limited our acceptance to only those $_\Lambda H^4$ that undergo π^- decay (either two-body or multi-body decays). This allows us to have a sample of $_\Lambda H^4$ in which background corrections are minor. We have accepted $_\Lambda H^3$ events only in the case where the $_\Lambda H^3$ undergoes π^- decay. The signature for (c) is shown in Fig. 3.

The distinct advantages of the helium bubble chamber for studying light hyperfragments are the following:

i) All hyperfragments are completely identified by production kinematics. The magnetic field allows us to make momentum and charge measurements. Conservation laws of charge, baryons, etc., allow complete and certain identification.

ii) Hyperfragments are produced copiously in an exposure to stopping K^- mesons. Approximately 3% of all K^- stars produce hypernuclei.

iii) The hypernuclei are produced in a very symmetric nucleus, i.e. He^4 has spin zero and isotopic spin zero. This allows us to employ general symmetry arguments, such as conservation of angular momentum, parity, and isospin, for the analysis of the production reactions. In particular, isospin conservation leads to a 2 : 1 branching ratio for reactions (a) to (b), as well as for (c) to (d).

The motivation for these studies was twofold; first, the determination of the relative K-Λ parity, and second, the systematic description of the properties of the light hypernuclei.

II. K-Λ PARITY AND SPIN OF $_\Lambda H^3$, $_\Lambda H^4$, $_\Lambda He^4$

If we assume that the spin of $_\Lambda He^4$ (or $_\Lambda H^4$) is zero, then it is easily shown that the conservation of parity requires that the reactions (a) and (b) be forbidden if the K^- is scalar, and be allowed if

the K^- is pseudoscalar (with respect to the Λ^0, conventionally assumed to be scalar), independent of what atomic state from which the K^- is absorbed. If we adopt the argument of Day and Snow[1] that the K^- is absorbed from an s-state Bohr orbital, then we can make an argument which immediately tells us about both the spin of the $_\Lambda He^4$ (or $_\Lambda H^4$) and the K parity. This is as follows. Consider reaction (b), where we look at only those decays where $_\Lambda H^4 \to \pi^- + He^4$. If our quantum axis is taken as the $_\Lambda H^4$ direction, and total $J = 0$, then $J_z = 0 = S_z$, where S_z is the z component of the spin of the $_\Lambda H^4$. Thus, the wave function for the two-body decay $_\Lambda H^4 \to \pi^- + He^4$ is $P_1^0(\cos \vartheta)$ or $P_0^0(\cos \vartheta)$, depending on whether the $_\Lambda H^4$ has a spin of 1 or 0, respectively. Table 1 summarizes the results.

Table 1

	K parity	Spin of $_\Lambda H^4$	Angular distribution
case (a)	pseudoscalar	0	isotropic
(b)	scalar	1	$\cos^2 \vartheta$
(c)	pseudoscalar	1	forbidden
(d)	scalar	0	forbidden

To date, 347 cases of reaction (a) and 154 cases of (b) have been identified in an exposure of our bubble chamber to a stopping K^- beam from the Berkeley Bevatron. Of the 154 cases of (b), 96 cases are the two-body mode $_\Lambda H^4 \to \pi^- + He^4$. The angular distribution of these decay pions is shown in Fig. 4. The data obviously correspond to case (a) of Table 1, indicating that the K^- is pseudoscalar and the spin of $_\Lambda H^4$ is zero. Since $_\Lambda H^4$ and $_\Lambda He^4$ are isotopic doublets, this also indicates that the spin of $_\Lambda He^4$ is zero. The evidence strongly favours the antiparallel Λ-nucleon spin orientation as the more strongly bound state. Thus, we would expect that the spin of $_\Lambda H^3$ would therefore be $S = \frac{1}{2}$, and not $S = \frac{3}{2}$.

Dalitz and Liu[2] have outlined methods of determining the spin of $_\Lambda H^4$ and $_\Lambda H^3$ from a study of π^- decay branching ratios, using the ratios

$$R_4 = \frac{_\Lambda H^4 \to \pi^- + He^4}{_\Lambda H^4 \to \text{all } \pi^-} \quad \text{and} \quad R_3 = \frac{_\Lambda H^3 \to \pi^- + He^3}{_\Lambda H^3 \to \text{all } \pi^-},$$

respectively. The argument for $_\Lambda H^4$ is as follows.

i) An impulse model of the hyperfragment decay is assumed, using the parameters of the free Λ^0 decay.

ii) For the decay $_\Lambda H^4 \to \pi^- + _\Lambda He^4$, the rate of decay is proportional to s^2, if $S = 0$, because both the pion and He^4 are spin zero particles. The amplitudes of the free Λ^0 decay are s and p, corresponding to the $\ell = 0$ and $\ell = 1$ channels, respectively. Conversely, the rate of two-body decay is proportional to p^2 if $S = 1$. Since the ratio $p^2 / p^2 + s^2 = 0.12 \pm 0.03$, as measured by Beall et al.[3], we expect R_4 to be large if $S = 0$ and small if $S = 1$. Similar arguments pertain to $_\Lambda H^3$.

We have plotted R_4 for 148 $_\Lambda H^4$ in Fig. 5. Also shown there is the theoretical curve of Dalitz and Liu[2]. Our value, $R_4 = 0.68 \pm 0.04$, along with the experimental values of $p^2 / p^2 + s^2$, is shown in Fig. 5. It is clear that the data strongly indicate $S = 0$. We have measured $R_3 = 0.39 \pm 0.07$ for 44 cases of $_\Lambda H^3$. The data are shown in Fig. 6, along with the theoretical results of Dalitz and Liu using a binding energy of $_\Lambda H^3$, $\epsilon = 0.21$ MeV. The measured value is $\epsilon = 0.21 \pm 0.20$ MeV[4]. Since the calculated result is proportional to $\sqrt{\epsilon}$, it is clear that the theoretical uncertainty is quite large. However, the data strongly favour $S = \frac{1}{2}$. It is amusing perhaps to reverse the argument, assume $S = \frac{1}{2}$, the measured value of R_3, and the theoretical structure, and then deduce the binding energy. This leads us to a redetermination of ϵ, albeit indirect, of $\epsilon = 0.16 \pm 0.06$ MeV. The results for R_4 and R_3 are in agreement with emulsion results[5,6] of lower statistical weight.

In summary, all methods of spin determination of $_\Lambda\text{H}^3$ and $_\Lambda\text{H}^4(_\Lambda\text{He}^4)$ agree that the antiparallel Λ-nucleon spin state is more strongly bound. Thus, we must conclude that the ground state spin of $_\Lambda\text{H}^3$ is $\frac{1}{2}$, and that the spins of $_\Lambda\text{He}^4$ and $_\Lambda\text{H}^4$ are zero.

If it were not for the possibility of an excited state for $_\Lambda\text{H}^4(_\Lambda\text{He}^4)$, the parity argument for the K^- would be unassailable. However, the possibility has been advanced that what really happens is that the hyperfragment is produced in an excited spin 1 state, which rapidly γ-decays to the ground state of spin zero, and that what we observe is the spin zero ground state. Dalitz and Downs[7] have estimated that if such an excited state exists, its binding energy is $\lesssim 0.1$ MeV, whereas the ground state is bound by ~ 2 MeV. This large a difference in binding energies should lead to a measurable difference in the rate of production of hypernuclei in reactions (a) and (b), i.e. the rate should be very low if the excited state is formed, because of the low binding. The ratio

$$R = \frac{(_\Lambda\text{He}^4 + \pi^-)}{(_\Lambda\text{He}^4 + \pi^-) + (\Lambda^0 + \text{He}^3 + \pi^-)}$$

should be proportional to $\sqrt{\epsilon}$, where ϵ is the binding energy of the type of $_\Lambda\text{He}^4$ produced. In particular, the ratios R should differ by a factor of ~ 4.5 for the ground and excited states. Originally, Dalitz and Downs calculated the ratio R using an impulse model and the reaction chain,

$$K^- + \text{He}^4 \rightarrow \pi^- + \Lambda^0 + \text{He}^3 \rightarrow \pi^- + _\Lambda\text{He}^4 .$$
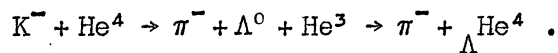
Their result was R = 22%. More recently, the Helium Bubble Chamber Group[8] has demonstrated strong evidence for the formation of Y_1^* as an intermediate state. Thus, one must calculate the reaction chain

$$K^- + \text{He}^4 \rightarrow Y_1^{*-} + \text{He}^3 \rightarrow \pi^- + \Lambda^0 + \text{He}^3 \rightarrow \pi^- + _\Lambda\text{He}^4 .$$
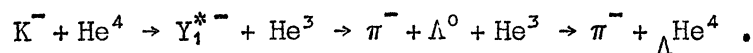
M.M. Block[9] has calculated the ratio R assuming an intermediate Y* state. The calculation uses an impulse model, and is quite sensitive to the spin

and parity assignment of the Y_1^*. The predictions, along with our experimental result R = 0.20 ± 0.02, are summarized in Table 2.

Table 2

Model	R(ϵ = 2.2 MeV)	R(ϵ = 0.10 MeV)
Simple impulse model	0.23	$\lesssim$ 0.05
Y_1^* $S_{1/2}$	0.23	$\lesssim$ 0.05
Y_1^* $p_{3/2}$	0.14	$\lesssim$ 0.05
Y_1^* $p_{1/2}$	0.07	$\lesssim$ 0.05
Experiment	0.20 ± 0.02	

Recently, two groups[10,11] have determined the spin of the Y_1^* to be S = 3/2, and Shafer et al.[11] have preliminary evidence favouring $p_{3/2}$. Our experimental data strongly favour the assignment $p_{3/2}$, and at the same time indicate that the hyperfragment was produced via the ground state and not the excited state. Thus, the conclusion is reinforced that the K^- is pseudoscalar.

III. LIFETIME OF $_\Lambda H^3$

The $_\Lambda H^3$'s have a mean length before decay of ~ 0.5 cm which is a convenient and accurately measured distance in the helium chamber. Of the 69 $_\Lambda H^3$, 36 satisfied our selection criteria:

a) decay length longer than 0.5 mm;

b) decay occurring further than 1 cm from chamber boundaries;

c) χ^2 from kinematics fitting programmes were acceptably small.

These criteria were used to eliminate possible biases, and to provide accurate measurements.

A maximum likelihood function of these 36 events (seven decayed at rest), is shown in Fig. 7. The lifetime obtained was $\tau_3 = 1.05^{+0.20}_{-0.18} \times 10^{-10}$ sec, a value considerably smaller than the free Λ^0 lifetime, $\tau_\Lambda = 2.36 \pm 0.06 \times 10^{-10}$ sec [12]. Dalitz and Rajasekharan[13] have made estimates of τ_3 for various assumptions of the spin of $_\Lambda H^3$. They find $\tau_3(S = \frac{1}{2}) = 1.79 \pm 0.10 \times 10^{-10}$ sec, and $\tau_3(S = \frac{3}{2}) = 2.40 \pm 0.03 \times 10^{-10}$ sec. The calculations both seem in disagreement with experiment, but the experimental value is in much less disagreement with the assignment $S = \frac{1}{2}$.

IV. MEASUREMENT OF $p_0^2/p_0^2 + s_0^2$ RATIO FOR $\Lambda^0 \to n + \pi^0$

The impulse model predicts that the dominant decay modes of the $_\Lambda He^4$ hypernucleus are

$$_\Lambda He^4 \to \pi^0 + n + He^3 \tag{1}$$

$$\text{and} \quad _\Lambda He^4 \to \pi^- + p + H^3 . \tag{2}$$

Further, the final state interactions between He^3 and n will often cause reaction (1) to appear as

$$_\Lambda He^4 \to \pi^0 + He^4 , \tag{3}$$

i.e. a bound state of $n - He^3$ which enhances the reaction rate. The corresponding reaction (2) between p and H^3 does <u>not</u> lead to a bound state and hence is not enhanced. We assume spin 0 for $_\Lambda He^4$; since the π^0 and He^4 are also spin zero, reaction (3) can only go via the s-wave channel of Λ^0 decay ($\Lambda^0 \to \pi^0 + n$). Thus the ratio

$$R_0 = \frac{_\Lambda He^4 \to \text{all } \pi^0 \text{ modes}}{_\Lambda He^4 \to \text{all } \pi^- \text{ modes}}$$

will depend sensitively on the ratio $p_0^2/p_0^2 + s_0^2$, where p_0 and s_0 are the amplitudes of the p and s channels, respectively, for the free decay $\Lambda^0 \to n + \pi^0$. In particular, assuming the experimental value

$p^2/p^2 + s^2 = 0.12 \pm 0.03$ for the charged decay mode $(\Lambda^0 \rightarrow \pi^- + p)$, and

$p^2 + s^2 = 2(p_0^2 + s_0^2)$, along with the formula derived by Dalitz and Liu[2],

$$R_0 = \frac{1.96\ s_0^2 + 0.35\ p_0^2}{0.40\ s^2 + 0.32\ p^2}, \qquad (4)$$

we obtain the expression

$$R_0 = 2.51 - 2.06\ p_0^2 / p_0^2 + s_0^2. \qquad (5)$$

Table 3 is a summary of the decay modes (corrected for background and geometrical detection efficiency) of a sample of 317 observed $_\Lambda He^4$. From Table 3 we obtain $R_0 = 2.49 \pm 0.34$. Figure 8 shows the result of Eq. (5) and our experimental determination. We obtain $p_0^2 / p_0^2 + s_0^2 = 0.01\,^{+0.17}_{-0.01}$, a value in good agreement with the value of 0.12 ± 0.03 predicted by the $\Delta I = \frac{1}{2}$ law. This result is in agreement with the asymmetry parameter ratio $\alpha_0/\alpha_- = 1.10 \pm 0.27$ of Cork et al.[14]. However, it should be pointed out that their experiment yielded two solutions for $p_0^2 / p_0^2 + s_0^2$, whereas this experiment also selects the proper solution.

Table 3

Decay mode distribution for 317 $_\Lambda He^4$ decays

Decay mode	π^0 modes	π^- modes				Non-mesic modes		π^+ modes		
Topological description	nothing	π^-	π^-p	π^-pp	π^-ppp	p	pp	π^+	π^+p	π^+p or pp
Observed	199	4	58	11	0	10	32	0	2	1
	199	73				42		2(+ 1)		
Background corrections	132	73				33		2(+ 1)		
Geometrical corrections	251	101				52		3(+ 1)		

V. DECAY MODES OF $_\Lambda He^4$

Table 3 summarizes the decay modes for 317 $_\Lambda He^4$. We observe that R_N = (non-mesonic modes / π^- modes) is given by R_N = 0.52 ± 0.10. Further, R_0 = 2.49 ± 0.34. We also note a quite high ratio of π^+/π^- decays, i.e. $\approx$ 3%. The two π^+ decays definitely identified both had the π^+ stopping in the chamber, undergoing the characteristic $\pi^+ \to \mu^+ \to e^+$ decay chain. The uncertain event had too short a decay track to rule out the "proton" hypothesis. The mean π^+ momentum is very low ($\approx$ 65 MeV/c), which is to be contrasted with a typical π^- decay, which has a momentum $\sim$ 90 MeV/c.

Ferrari and Fonda[15] have noted that the basic force between Λ^0 and nucleons could be due to an intermediate Σ state as shown in Fig. 9a. Deloff et al.[16] have calculated the formation of π^+, using as a model the decay of the intermediate Σ, as shown in Fig. 9b. They find that the ratio of π^+/π^- can be as high as several percent, and further, that the π^+ decay momentum would be quite low for the decay $_\Lambda He^4 \to \pi^+ + n + H^3$.

The non-mesonic events broke up into two categories, i.e. 10 "p" and 32 "pp" events. It was estimated that of the 10 "p" events, 4 were really $_\Lambda He^4 \to \pi^0 + He^3 + n$, where the He^3 recoil produced a visible track. Either the direct four-fermion interaction

$$\Lambda^0 + p \to p + n \qquad (6)$$

or the reabsorption of a virtual pion by a nucleon,

$$\Lambda + N \to (N + \pi) + N \to N + N \qquad (7)$$
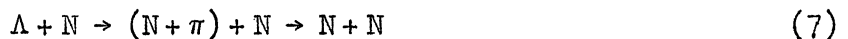
can be responsible for the non-mesic decay of the $_\Lambda He^4$ hypernucleus.

The direct four-fermion interaction, however, forbids in principle

$$\Lambda + n \to n + n \ ,$$
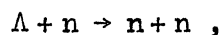
because of the absence of neutral currents in the Fermi interaction (it can still be permitted in practice by absorption and emission of virtual pions).

On the other hand, the $(\Lambda^0 p)$ interactions

$$\Lambda^0 + p \rightarrow (p + \pi^-) + p \rightarrow p + n \qquad (8a)$$

$$\Lambda^0 + p \rightarrow (n + \pi^0) + p \rightarrow n + p \qquad (8b)$$

or the $(\Lambda^0 n)$ interactions,

$$\Lambda^0 + n \rightarrow (p + \pi^-) + n \rightarrow n + n \qquad (9a)$$

$$\Lambda^0 + n \rightarrow (n + \pi^0) + n \rightarrow n + n \qquad (9b)$$

can occur.

It is clear that if the non-mesonic decay occurs via either (6) or (8), it involves the emission of a fast proton (≈ 400 MeV/c) due to the rather large energy release in the interaction, while if the decay goes via reactions (9a) or (9b), there are two fast neutrons, and visible protons can come only from the evaporation process in the residual nucleus. If the proton had a momentum of $\gtrsim 250$ MeV/c, we arbitrarily decided to call the event de-excitation off a proton. All of the "p" events had a momentum less than 250 MeV/c. Of the 32 "pp" events, only 6 had both protons < 250 MeV/c. Thus, an estimate of the ratio of non-mesonic de-excitation off the proton to that off the neutron is

$$\frac{\Lambda - p}{\Lambda - n} = 2.2 \pm 0.8 \ .$$

Since $_\Lambda\text{He}^4$ has twice as many protons as neutrons, the ratio **per pair** is 1.1 ± 0.4. The number is too crude, however, to be more than an indication that the basic de-excitation mechanism for non-mesonic decay is about the same with either the proton or neutron.

VI. NON-MESONIC DECAYS OF $_\Lambda\text{H}^4$

If we accept charge independence in the production of $_\Lambda\text{H}^4$ and $_\Lambda\text{He}^4$, we observe that the number of $_\Lambda\text{H}^4$ produced is one-half the number of $_\Lambda\text{He}^4$ produced. Although we observe only $_\Lambda\text{H}^4 \rightarrow \pi^-$, we can, using the production argument, find out how many $_\Lambda\text{H}^4$ decayed via either π^0

modes or non-mesonic decays. Further, if we assume the $\Delta I = \frac{1}{2}$ law for the decay of $_\Lambda H^4$ and $_\Lambda He^4$, then the ratio we obtained for $_\Lambda He^4$, i.e.

$$R_0 = \frac{_\Lambda He^4 \to \pi^0}{_\Lambda He^4 \to \pi^-} = 2.49 \, ,$$

is related to the same ratio for $_\Lambda H^4$, i.e.

$$R_0 \left(_\Lambda He^4 \right) \times R_0 \left(_\Lambda H^4 \right) = \frac{1}{4} \, ,$$

as shown by Dalitz and Liu[2]. Thus

$$R_0 \left(_\Lambda H^4 \right) \equiv \frac{_\Lambda H^4 \to \pi^0}{_\Lambda H^4 \to \pi^-} = 0.10 \, .$$

Putting these numbers together, after using a restricted sample where all events have been measured, and allowing for corrections for detection efficiency, background, etc., we find that we predict (from the $_\Lambda He^4$ rate) that 163 ± 10 $_\Lambda H^4$ were produced, compared to 120 ± 11 $_\Lambda H^4 \to \pi^-$. Thus, 132 ± 12 $_\Lambda H^4$ decayed either via π^- or π^0 modes. The remainder, attributed to non-mesonic decays, is therefore 31 ± 15. Thus, the ratio of (non-mesonic)/(π^- mesic) for $_\Lambda H^4$ is found to be $26 \pm 13\%$.

* * *

REFERENCES

1) T. Day and G. Snow, Phys.Rev.Letters 2, 59 (1959).

2) R. Dalitz and L. Liu, Phys.Rev. 116, 1312 (1959).

3) E.F. Beall, B. Cork, D. Keefe, P.G. Murphy and W.A. Wentzel,
   Phys.Rev.Letters 7, 285 (1961);
   J.W. Cronin, Bull.Am.Phys.Soc. 7, 68 (1962).

4) N. Crayton, R. Levi Setti, M. Raymond, O. Skjeggestad, D. Abeledo,
   R. Ammar, J. Roberts and E. Shipley, Phys.Rev. (to be published).

5) R. Ammar, R. Levi Setti, W. Slater, S. Limentani, P. Schlein and
   P. Steinberg, Nuovo Cimento 19, 20 (1961).

6) R. Ammar, W. Dunn and M. Holland, Nuovo Cimento 26, 840 (1962).

7) R. Dalitz and B. Downs, Phys.Rev. 111, 967 (1958).

8) J. Auman, M.M. Block, R. Gessaroli, J. Kopelman, S. Ratti,
    L. Grimellini, T. Kikuchi, L. Lendinara, L. Monari and E. Harth,
    Proc. of the International Conference on High-Energy Physics,
    CERN (1962), p. 330.

9) M.M. Block, paper submitted to this conference (1963).

10) L. Bertanza, V. Brisson, P. Connolly, E. Hart, I. Mittra, G. Moneti,
    R. Rau, N. Samios, I. Skillicorn, S. Yamamoto, M. Goldberg,
    J. Leitner, S. Lichtman and J. Westgard, Phys.Rev.Letters 10,
    176 (1963).

11) J. Shafer, J. Murray and D. Huwe, Phys.Rev.Letters 10, 179 (1963).

12) M.M. Block, R. Gessaroli, S. Ratti, L. Grimellini, T. Kikuchi,
    L. Lendinara, L. Monari, E. Harth, W. Becker, W.M. Bugg, H. Cohn,
    Phys.Rev. (in press).

13) R.H. Dalitz and G. Rajasekharan, EFINS Report 62-14 (1962).

14) B. Cork, L. Kerth, W. Wentzel, J. Cronin and R. Cool, Phys.Rev. 120,
    1000 (1960).

15) F. Ferrari and L. Fonda, Nuovo Cimento 9, 842 (1958).

16) A. Deloff, J. Szymanski, J. Wrzecienko, "Bulletin de l'Académie
    Polonaise des Sciences", Series des Sciences Mathématiques,
    Astronomiques et Physique 7, 521 (1959).

*   *   *
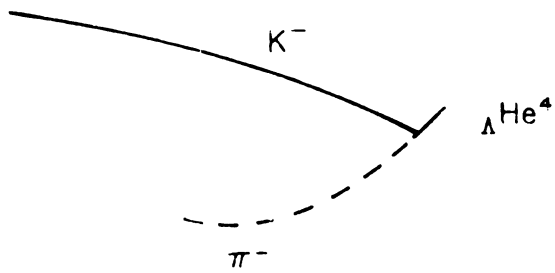
Fig. 1. Schematic Drawing of Reaction $K^- + He^4 \to \pi^-$
$+ {}_\Lambda He^4$, ${}_\Lambda He^4 \to \pi^0 + He^4$.
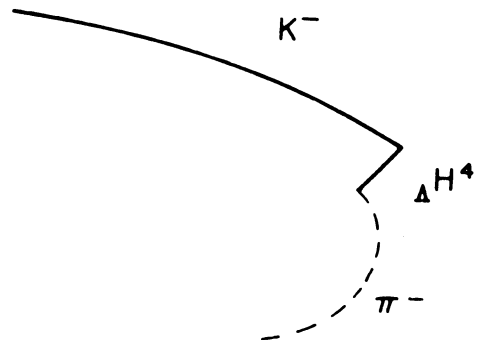
Fig. 2. Schematic Drawing of Reaction $K^- + He^4 \to \pi^0$
$+ {}_\Lambda H^4$, ${}_\Lambda H^4 \to \pi^- + He^4$.
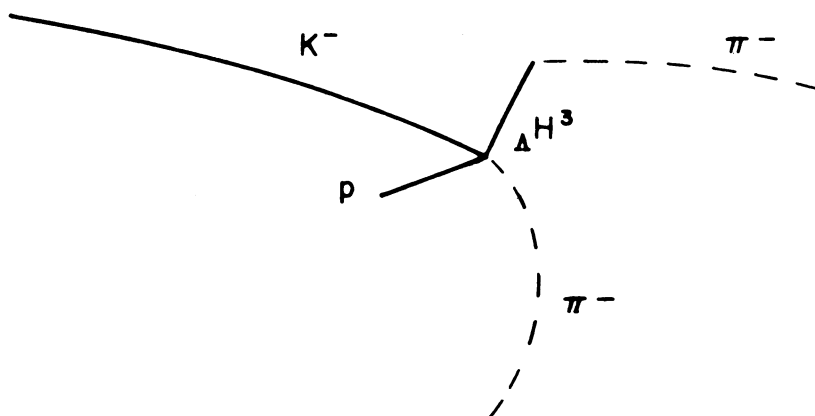
Fig. 3. - Schematic Drawing of Reaction $K^- + He^4 \to p + \pi^- + {}_\Lambda H^3$, ${}_\Lambda H^3 \to \pi^- + He^3$.
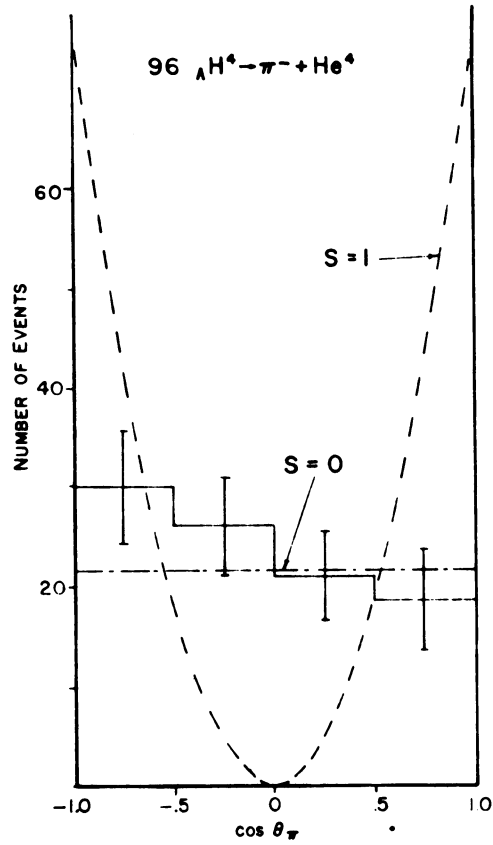
Fig. 4. - The Angular Distribution of the π^- from 96 Decays
$_\Lambda H^4 \to \pi^- + He^4$, for Hyperfragments Produced in the
Capture Reaction $K^- + He^4 \to \pi^0 + _\Lambda H^4$.
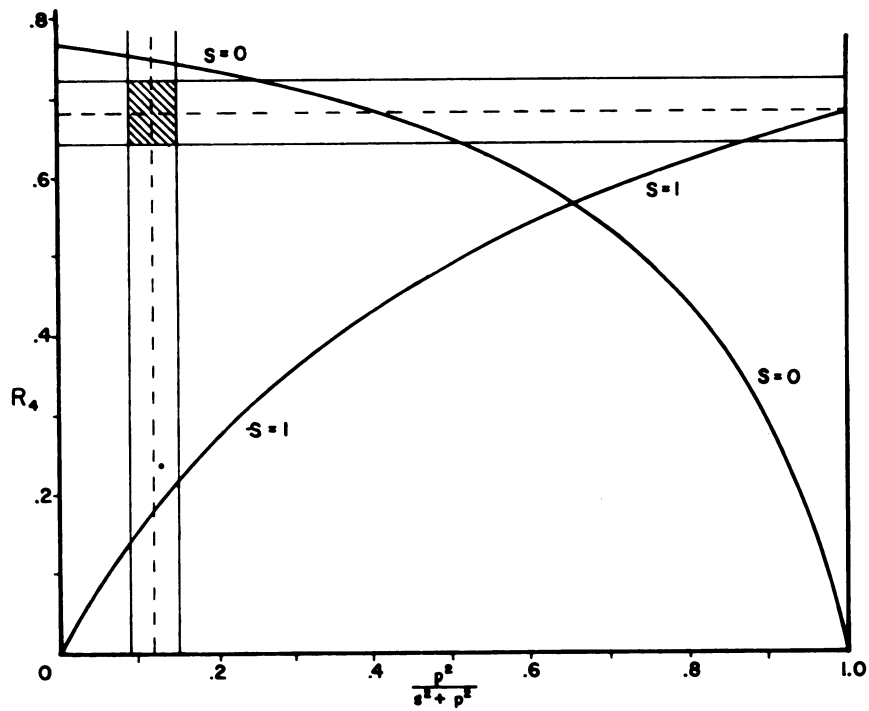
Fig. 5. - R_4, the Ratio of $_\Lambda H^4 \to \pi^- + He^4$ to $_\Lambda H^4 \to$ all
π^- modes, as a function of $p^2/p^2 + s^2$. The
Theoretical Curves are the Calculated R_4 of
Dalitz and Liu for S = O and S = 1.
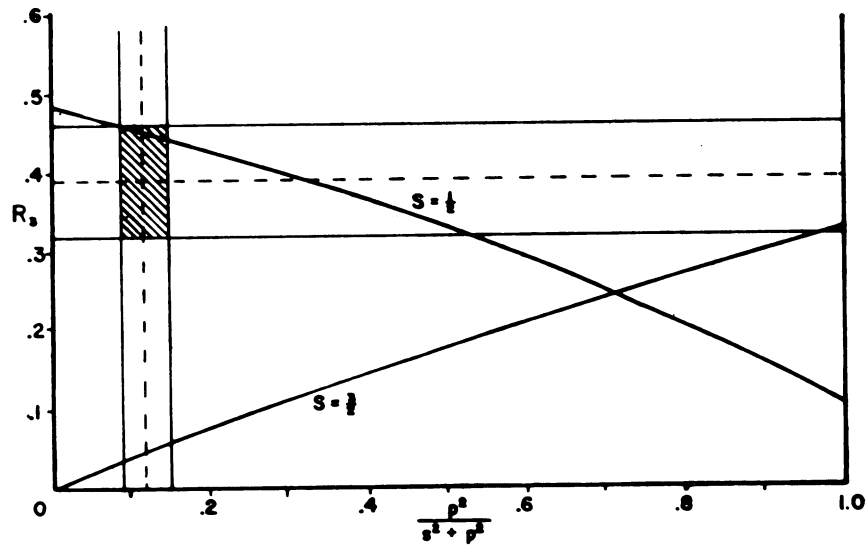
Fig. 6. - R_3, the Ratio of $_\Lambda H^3 \to \pi^- + He^3$ to $_\Lambda H^3 \to$ all π^- modes as a Function of $p^2/p^2 + s^2$. The Theoretical Curves are the Calculated R_3 of Dalitz and Liu for $S = 1/2$ and $S = 3/2$.

$\tau = (1.05^{+20}_{-18}) \times 10^{-10}$ sec

$_\Lambda H^3$ LIFETIME

36 EVENTS - 29 IN FLIGHT
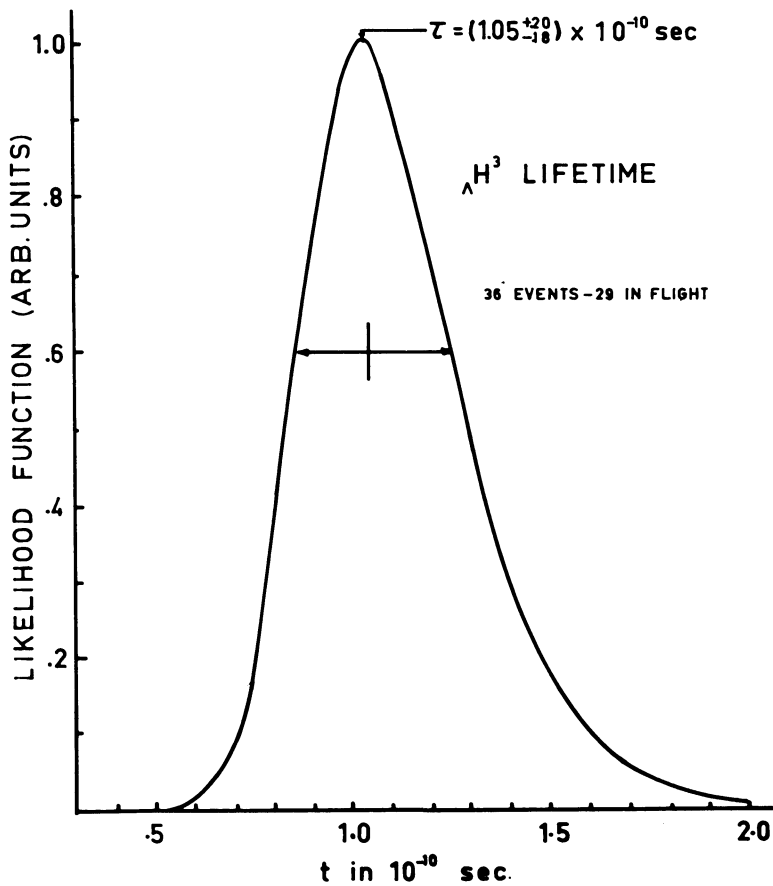
Fig. 7. - The Likelihood Function in Arbitrary Units, for 36 $_\Lambda H^3$ Decays, as a Function of the $_\Lambda H^3$ Lifetime.
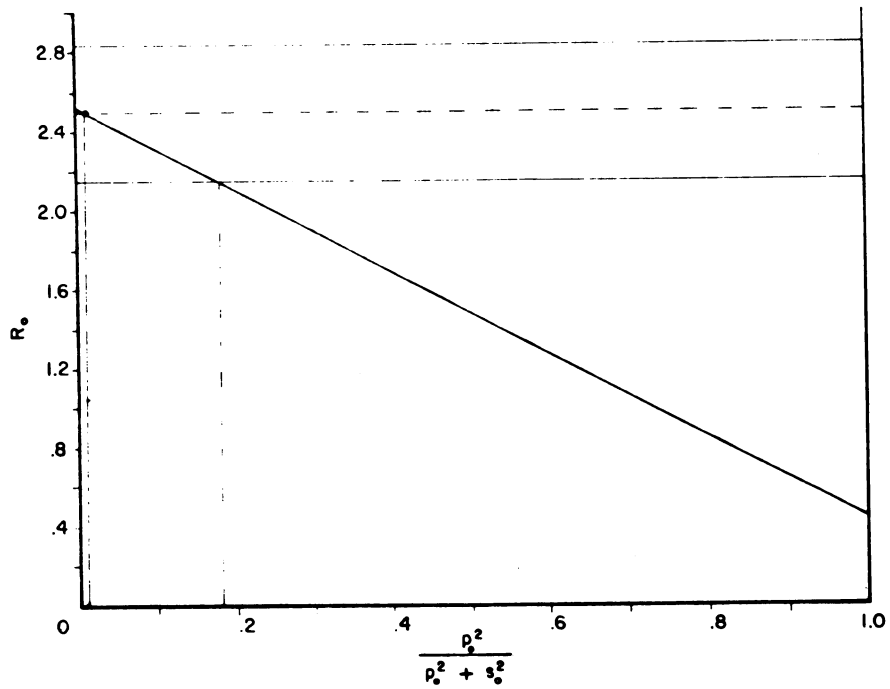
Fig. 8. - R_o, the Ratio of $_\Lambda He^4 \to$ all π^0 modes to $_\Lambda He^4 \to$ all π^- modes, as a Function of $p_o^2/p_o^2 + s_o^2$.

(a)   (b)
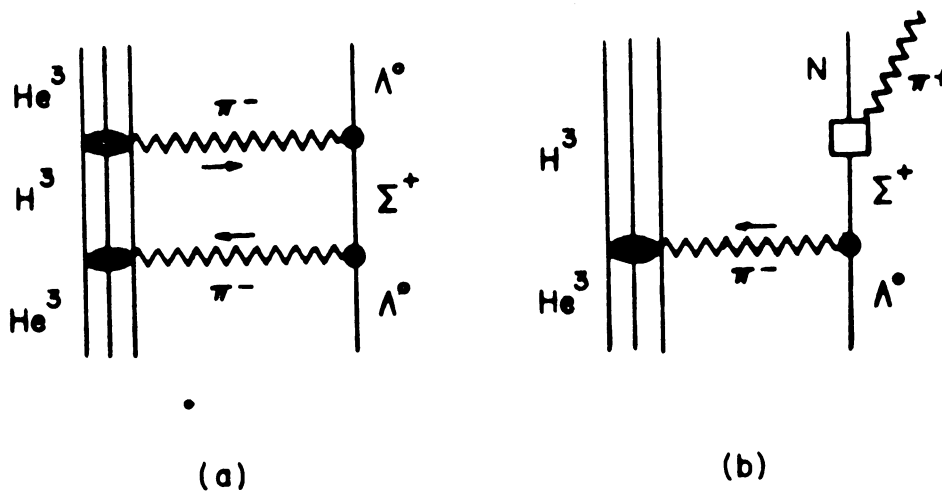
Fig. 9. - Feymman Diagrams of Intermediate States.

A METHOD FOR DETERMINING THE SPIN AND PARITY OF THE Y_1^* [†]

M.M. Block,
Northwestern University, Evanston, Ill., USA.

The helium bubble chamber group[1] has presented evidence for the presence of the mass 1385 MeV Y_1^* state in the absorption at rest of K^- mesons in He^4. They find that the reaction channel

$$K^- + He^4 \rightarrow \pi^- + \Lambda^0 + He^3 \tag{1}$$

is dominated by

$$K^- + He^4 \rightarrow Y_1^{*-} + He^3, \quad Y_1^{*-} \rightarrow \Lambda^0 + \pi^- . \tag{2}$$
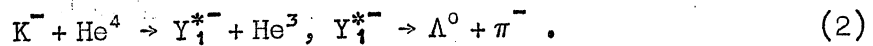
Also, this group[2] has reported a large yield of helium hypernuclei from the reaction

$$K^- + He^4 \rightarrow \pi^- + {}_\Lambda He^4 . \tag{3}$$

Dalitz and Downs[3] have successfully analysed hypernuclear states by considering, for example, that ${}_\Lambda He^4$ is a bound state of a real He^3 core, surrounded by a loosely bound (~ 2.2 MeV) Λ^0. This implies that the hypernuclei in Eq. (3) are created by the strong final state interactions causing binding between the Λ^0 and He^3 from reaction (1). Since the Y^* mechanism dominates (2), this implies that hypernuclear formation in (3) is due to the reaction chain

$$K^- + He^4 \rightarrow Y_1^{*-} + He^3 \rightarrow \pi^- + {}_\Lambda He^4 . \tag{4}$$
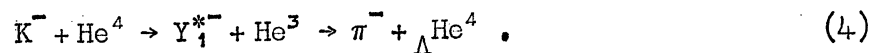
This note will investigate the rate of hyperfragment production in (4) as a function of three level assignments for Y_1^*, i.e. $s_{1/2}$, $p_{1/2}$ and $p_{3/2}$.

It is convenient to introduce the ratio

$$R = (\pi^- + _\Lambda He^4)/(\pi^- + _\Lambda He^4) + (\pi^- + \Lambda^\circ + He^3) ,$$

where the symbols represent the rates of the indicated reactions. The dependence of R on the Y* spin and parity can be most clearly qualitatively seen as follows. We adopt the co-ordinate system sketched in Fig. 1, and make the following assumptions:

a) only a pure Y* state is found in reaction (1);

b) the K⁻ is absorbed from an s-state atomic orbit[4];

c) the K⁻ is pseudoscalar[2].

Since the total angular momentum J = 0, and parity is conserved in (2), it is readily seen that ℓ = L, independent of the Y* spin or parity. If we let J_Y be the spin of the Y*, then $\vec{J}_Y = \vec{\ell} + \vec{\frac{1}{2}}$. For the level assignment $s_{1/2}$, we then have ℓ = 0, L = 0, and $J_Y = \frac{1}{2}$; for $p_{1/2}$, ℓ = 1, L = 1, $J_Y = \frac{1}{2}$; and for $p_{3/2}$, ℓ = 1, L = 1, $J_Y = \frac{3}{2}$. Thus, there is only one possible state produced in reaction (2), and it is uniquely determined by the Y* quantum numbers. A convenient axis of quantization is the normal to the production plane of (1), since $\vec{p}_\pi + \vec{p}_\Lambda + \vec{p}_3 = 0$. If we rewrite the wave function of the system, not in terms of J_Y, L, and s_3, but rather in terms of ℓ, L and $\vec{S} \equiv \vec{s}_\Lambda + \vec{s}_3$, we obtain

$$\chi = a_0 \cos \phi | S = 0, \, S_z = 0 > + \, a_1 \sin \phi | S = 1, \, S_z = 0 > \qquad (4)$$

where ϕ is the angle between $\vec{p}_{\Lambda\pi}$ and $\vec{p}_3$. The relative Λ-π momentum is given by $\vec{p}_{\Lambda\pi} = m_\pi \vec{p}_\Lambda - m_\Lambda \vec{p}_\pi / m_\Lambda + m_\pi$, and the spinors $| S = 0, \, S_3 = 0 >$ and $| S = 1, \, S_3 = 0 >$ refer to the total spin S of the system, i.e. S = 0 or 1. For $s_{1/2}$, we have a_1 = 0; for $p_{1/2}$, $|a_0|^2 = |a_1|^2$; for $p_{3/2}$, $|a_0|^2 = 4|a_1|^2$. The corresponding angular distributions are shown in Table 1. Although the angular distributions for $s_{1/2}$ and $p_{1/2}$ are the same, they yield very different hyperfragment production rates. The spin of $_\Lambda He^4$ has been shown to be zero[2]. Hence, only those states with S = 0 can form hypernuclei. The probability for S = 0 is also

Table 1

Hyperfragment production rate R, as a function of
the Y* state, for capture of a pseudoscalar K^-
meson in an s-state orbit.

Y* level	Spin	Parity	Angular distribution	Probability of S = 0	R (hypernuclear rate), in %
$s_{1/2}$	$1/2$	-	isotropic	1	23
$p_{1/2}$	$1/2$	+	isotropic	$1/3$	7
$p_{3/2}$	$3/2$	+	$1 + 3 \cos^2 \phi$	$2/3$	14

shown in Table 1. It is clear that, all other factors being equal,
the $s_{1/2}$ state will yield the most hypernuclei. A detailed quantita-
tive estimate is made below.

We will calculate the rate for the continuum reaction

$$K^- + He^4 \rightarrow Y_1^{*-} + He^3 \rightarrow \pi^- + \Lambda^0 + He^3 , \qquad (5)$$
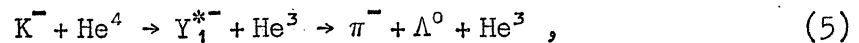
using the impulse model. The final state wave function is taken to be

$$v_{\vec{k}}(\vec{r}_\Lambda - \vec{r}_3)e^{i\vec{p}_\pi} \cdot \left(\vec{r}_\pi - \frac{m_3 \vec{r}_\Lambda + m_3 \vec{r}_3}{m_3 + m_\Lambda} \right) ,$$

i.e. a plane wave pion and a continuum $\Lambda^0 - He^3$ wave function $v_{\vec{k}}$, labelled
by its internal momentum $\vec{k}$. The co-ordinate system and coupling scheme
used is illustrated in Fig. 2, where

$$\vec{k} = \frac{m_3 \vec{p}_\Lambda - m_\Lambda \vec{p}_3}{m_\Lambda + m_3} .$$

The wave function for $_\Lambda He^4$ is taken as a gaussian, that is

$$\phi\, He^4 = N_1\, \exp - \left(\beta \sum_{i,j} (\vec{r}_i - \vec{r}_j)^2 \right)$$

where β is fitted to the charge radius deduced from the Hofstadter[5] electron scattering experiments. The initial wave function for our process, $u(r)$, is thus the decomposition of the He^4 wave function into the relative motion of nucleon 1 (which is later transformed into a Λ) and the centre-of-mass of the He^3-like core. Thus

$$u(r) = N \exp - \left(\alpha(\vec{r}_1 - \vec{r}_3)^2 \right),$$

where N is the normalization factor. In units where $\hbar = c = 1$, we find that $\sqrt{\alpha} = 89$ MeV/c. Let T be defined as the transition operator for the elementary reaction $K^- + N \rightarrow Y^*$, operating on the final state wave function. Since the appropriate impulse operator also includes the contact interaction terms $\delta(\vec{r}_\pi - \vec{r}_\Lambda) \, \delta(\vec{r}_\Lambda - \vec{r}_1)$, the matrix element for the transition of reaction (5) is given by

$$M = \int \left[T v_{\vec{k}}(r) \right]^* e^{-i\vec{p}\cdot\vec{r}} \, u(r) \, d\vec{r} , \qquad (6)$$

where

$$\vec{p} \equiv \frac{m_3}{m_\Lambda + m_3} \, \vec{p}_\pi .$$

If a pure Y^* state is formed, the transition operator T in the $p_{\Lambda\pi}, p_3$ language (see Fig. 1) is completely specified. It is in

cases (a) and (b): $\quad T = A_0 p_{\Lambda\pi} \cdot p_3 + A_1 (p_{\Lambda\pi} \times p_3) \cdot \sigma_\Lambda ,$

if $p_{3/2}$ or $p_{1/2}$;

case (c) $\qquad : \quad T = B_0 ,$

if $s_{1/2} ,$

with $A_0 = a_0/(p_{\Lambda\pi}^2/2\mu - p_{\Lambda\pi}^{*2}/2\mu) + i\Gamma/2, \quad A_1 = a_1/(p_{\Lambda\pi}^2/2\mu - p_{\Lambda\pi}^{*2}/2\mu) + i\Gamma/2,$

and $B_0 = b_0/(p_{\Lambda\pi}^2/2\mu - p_{\Lambda\pi}^{*2}/2\mu) + i\ \Gamma/2$, i.e. the coefficients are given by Breit-Wigner resonance amplitudes, with $p_{\Lambda\pi}^{*2}/2\mu$ being the resonant energy ($\mu = m_\Lambda m_\pi/m_\Lambda + m_\pi$), and $\Gamma/2$ being the level half-width. We assume the a's and b's are constants, and for $p_{3/2}$, $|a_0|^2 = 4|a_1|^2$, and for $p_{1/2}$, $|a_0|^2 = |a_1|^2$.

In order to discuss hypernuclear formation, we must use the co-ordinate scheme of Fig. 2. We carry out this co-ordinate change by transforming the transition operator T to the $\vec{k}, \vec{p}_\pi$ language by noting that

$$\vec{p}_{\pi\Lambda} = - \frac{m_\pi}{m_\Lambda + m_k} \vec{k} + \left[1 - \frac{m_\pi m_3}{(m_\pi + m_\Lambda)(m_3 + m_\Lambda)} \right] \vec{p}_\pi \tag{7a}$$

and

$$\vec{p}_3 = -\vec{k} - \frac{m_3}{m_3 + m_\Lambda} \vec{p}_\pi . \tag{7b}$$

Since m_π is small, we simplify our relations (7a), (7b) to be

$$\vec{p}_{\pi\Lambda} = \vec{p}_\pi \tag{8a}$$

$$\vec{p}_3 = -\vec{k} - \frac{m_3}{m_3 + m_\Lambda} \vec{p}_\pi . \tag{8b}$$

Using Eqs. (8a) and (8b) we obtain the transformed T operator,

cases (a) and (b): $T = -A_0 \left[\frac{m_3}{m_3 + m_\Lambda} p_\pi^2 + \vec{p}_\pi \cdot \vec{k} \right] - A_1 \left[\vec{p}_\pi \times \vec{k} \right] \cdot \vec{\sigma}_\Lambda$,

for $p_{3/2}$ or $p_{1/2}$, where $\vec{k}$ represents the gradient operator on the relative co-ordinate $\vec{r}_\Lambda - \vec{r}_3$;

case (c)   : $T = B_0$,

for $s_{1/2}$.

Using partial integration, it can be readily shown that the matrix element of (6) is given by

$$M = -A_0 p_\pi \int v_{\vec{k}}^*(r) e^{-i\vec{p}\cdot\vec{r}} \cos\Theta \frac{d}{idr} u(r) d\vec{r}$$

$$-A_0 p_\pi \int v_{\vec{k}}^*(r) e^{-i\vec{p}\cdot\vec{r}} \sin\Theta \frac{d}{idr} u(r) d\vec{r} \ , \tag{9}$$

where Θ is the angle between $\vec{p}_\pi$ and $\vec{r}$ for the $p_{1/2}$ and $p_{3/2}$ cases. For $s_{1/2}$ we obtain

$$M = B_0 \int v_{\vec{k}}^*(r) e^{-i\vec{p}\cdot\vec{r}} u(r) d\vec{r} \ . \tag{10}$$

To evaluate Eqs. (9) and (10), we employ closure. We calculate the total transition rate which is proportional to

$$\iint |M|^2 d\vec{k} \, d\vec{p}_\pi$$

by allowing $\vec{k}$ to range from zero to infinity (ignoring momentum conservation) and replacing the integration over p_π by its maximum value, i.e. the value of p_π corresponding to $K^- + He^4 \to \pi^- + {}_\Lambda He^4$. This procedure in general tends to overestimate the rate, an effect which can reasonably be neglected if the allowed region of integration is dominated by the final state interactions. Thus we use the relation

$$\frac{1}{(2\pi)^3} v_{\vec{k}}^*(r) v_{\vec{k}}(\vec{r}') d\vec{k} = \delta(\vec{r}-\vec{r}') - v_B^*(\vec{r}) v_B^*(\vec{r}') ,$$

where v_B is the bound state <u>singlet</u> hyperfragment wave function. We thus obtain

$$R = \frac{\left| \int v_B(r) e^{-i\vec{p}\cdot\vec{r}} \cos \frac{du}{dr}(r) d\vec{r} \right|^2}{\left[1 + 2\frac{|a_1|^2}{|a_0|^2} \right] < q^2 >} \tag{11}$$

for $p_{1/2}$, and $p_{3/2}$, where $<q^2>$

$$<q^2> \equiv \int u*(r) \frac{d^2}{dr^2} u(r)d\vec{r} = 3\alpha.$$

In a similar way, for $s_{1/2}$,

$$R = |I|^2 , \qquad (12)$$

where

$$I = \int v_B^*(r) e^{-i\vec{p}\cdot\vec{r}} u(r)d\vec{r} . \qquad (13)$$

Dalitz and Downs[3]) have numerically evaluated I as a function of p, using the gaussian wave function for $u(r)$ and a numerical solution of the Schroedinger equation for v_B, i.e.

$$I(p) = N \int v_B^*(\vec{r}) e^{-i\vec{p}\cdot\vec{r}} e^{-\alpha r^2} d\vec{r} . \qquad (14)$$

Letting

$$J(p) \equiv \int v_B^*(r) e^{-i\vec{p}\cdot\vec{r}} \cos\Theta \frac{d}{dr} u(r)d\vec{r} , \qquad (15)$$

we note that

$$J(p) = \frac{2\alpha}{i} \frac{dI}{dp} . \qquad (16)$$

Table 1 gives the numerical evaluation of the three cases. We observe the large difference between the rates for $s_{1/2}$ and $p_{1/2}$, in spite of their identical angular distribution.

Angular distributions can be markedly changed from these predictions by a small admixture of background terms, e.g. terms arising from the strong $\Lambda^0 - He^3$ interactions. This is clear because interference terms, etc., arise from the amplitudes, whereas rates go as the square of amplitudes and hence are rather insensitive to small admixtures

of contamination terms. Thus, one should expect to have much greater confidence in the predictive powers of a rate calculation than in angular distributions. The large difference predicted between the three cases of Y* level assignments should provide us with a valuable tool for assigning these quantum numbers.

In order to check the sensitivity of the calculation to the assumption of p-state capture, the following transition operators were used:

cases (a) and (b): $T = A_0 \vec{p}_{\pi\Lambda} \cdot \emptyset(0) + A_1 \left[\nabla\emptyset(0) \times p_{\pi\Lambda} \right] \cdot \sigma_\Lambda$

$$+ C_0 p_3^2 \vec{p}_{\pi\Lambda} \cdot \nabla\emptyset(0) + C_1 p_3^2 \left[\nabla\emptyset(0) \times \vec{p}_{\pi\Lambda} \right] \cdot \vec{\sigma}_\Lambda$$

$$(17)$$

where $\nabla\emptyset(0)$ is the gradient of the $K^- - He^4$ atomic wave function, evaluated at the origin. It is now assumed that the C terms will be neglectable, since they correspond to $L = 2$ recoil terms and are probably suppressed by the angular momentum barrier. Therefore,

$$T \rightarrow A_0 \vec{p}_{\pi\Lambda} \cdot \nabla\emptyset(0) + A_1 \left[\nabla\emptyset(0) \times \vec{p}_{\pi\Lambda} \right] \cdot \vec{\sigma}_\Lambda \, , \qquad (18)$$

where again the A's are resonant amplitudes. The corresponding operator for $s_{1/2}$ is given by

$$\text{case (c)} \; : \quad T \rightarrow B_0 \, p_3 \cdot \nabla\emptyset(0) \, . \qquad (19)$$

The rates for hyperfragment production are given by

$$R = \frac{|I|^2}{1 + 2 \frac{|a_1|^2}{|a_0|^2}} \qquad (20)$$

where $\quad |a_0|^2 = |a_1|^2 \quad$ for $p_{1/2}$,

and $\quad |a_0|^2 = 4|a_1|^2 \quad$ for $p_{3/2}$,

and $\quad R = \frac{|J|^2}{<q>^2} \quad$ for $s_{1/2}$. $\qquad (21)$

Table 2 summarizes these rates, which are approximately equal to those of s-state capture.

Table 2

Hyperfragment production rate for pseudoscalar K capture
in p-wave and scalar K capture in s-wave states

Y* level	Spin	Parity	R (hypernuclear rate in %) for p-wave capture, pseudoscalar K	R (hypernuclear rate in %) for s-wave capture, scalar K
$s_{1/2}$	$\frac{1}{2}$	−	21	$\lesssim 5$
$p_{1/2}$	$\frac{1}{2}$	+	7.5	$\lesssim 5$
$p_{3/2}$	$\frac{3}{2}$	+	15	$\lesssim 5$

We further test the hypothesis that the K^- is __scalar__, and is captured in an s-state. This would require that the hyperfragment be produced in a spin 1 excited state, and decay into the spin zero ground state. Dalitz and Downs[3] have estimated that if such an excited state is found, its binding energy is $\lesssim 0.1$ MeV.

The matrix elements for the transition are given by

$$T = A_1 \vec{p}_{\Lambda\pi} \cdot \vec{\sigma}_\Lambda \text{ for } p_{1/2} \text{ and } p_{3/2} , \qquad (22)$$

and

$$T = B_1 \vec{p}_3 \cdot \vec{\sigma}_\Lambda \text{ for } s_{1/2} . \qquad (23)$$

The corresponding rates are given by

$$R = |I'|^2 \text{ for } p_{1/2} \text{ and } p_{3/2} , \qquad (24)$$

and by

$$R = |J'|^2 < q^2 > . \qquad (25)$$

The primes refer to the hyperfragment wave function corresponding to 0.1 MeV binding energy.

For our purposes, it is sufficiently accurate to assume that both I and J are proportional to $E^{1/2}$, where E is the binding energy. This proportionality comes from the normalization of the hypernuclear wave function, which for sufficiently small E, satisfies the above. These numerical results are indicated in Table 2. In summarizing, we see from Tables 1 and 2 that hypernuclear production is severely limited if the K is scalar, whereas the rates are insensitive to whether pseudoscalar K is captured from either an s or a p orbit.

*

The author would like to acknowledge stimulating discussions with Dr. M. Peshkin of the Argonne National Laboratory, and with Dr. L. Brown, Dr. P. Singer, and Dr. W. Wada of Northwestern University.

* * *

REFERENCES

1) M.M. Block, E.B. Brucker, R. Gessaroli, T. Kikuchi, A. Kovacs, C.M. Meltzer, R. Kraemer, M. Nussbaum, A. Pevsner, P. Schlein, R. Strand, H.O. Cohn, E.M. Harth, J. Leitner, L. Lendinara, L. Monari and G. Puppi, Nuovo Cimento 20, 724 (1961).

J. Auman, M.M. Block, R. Gessaroli, J. Kopelman, S. Ratti, L. Grimellini, T. Kikuchi, L. Lendinara, L. Monari and E. Harth, Proc. of the 1962 International Conference on High-Energy Physics at CERN, p. 330.

2) M.M. Block, L. Lendinara and L. Monari, Proc. of the 1962 International Conference on High-Energy Physics at CERN, p. 371.

3) R.H. Dalitz and B.W. Downs, Phys.Rev. 111, 967 (1958).

4) T.B. Day and G.A. Snow, Phys.Rev.Letters 5, 112 (1960).

5) R. Hofstadter, Rev.Mod.Phys. 28, 214 (1956).

$\vec{P}_{\Lambda\overline{\Pi}}$

ℓ

$\vec{r}_{\overline{\Pi}}$

ϕ

$\vec{r}_\Lambda$

$\vec{P}_3$

L

$\vec{r}_3$

Fig 1

$\vec{r}_\Lambda$

$\vec{k}$

ℓ'

ϕ

$\vec{r}_3$

$\vec{P}_{\overline{\Pi}}$

L'

$\vec{r}_{\overline{\Pi}}$
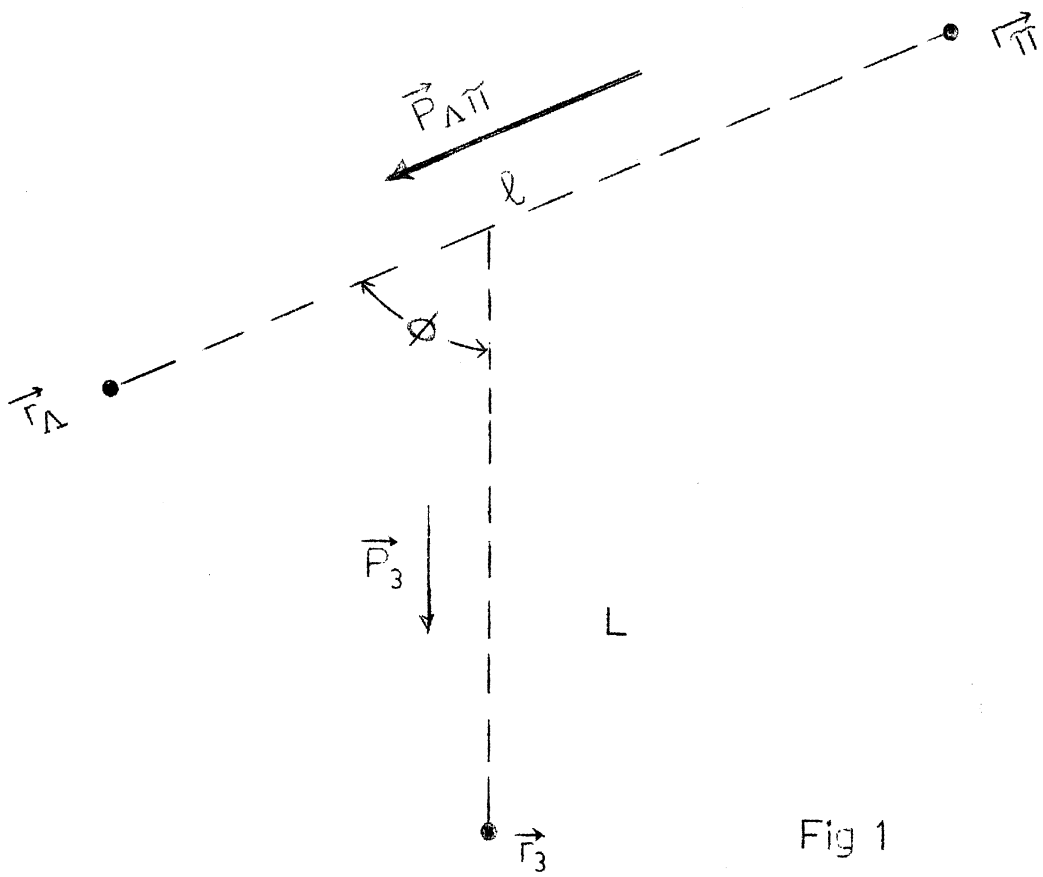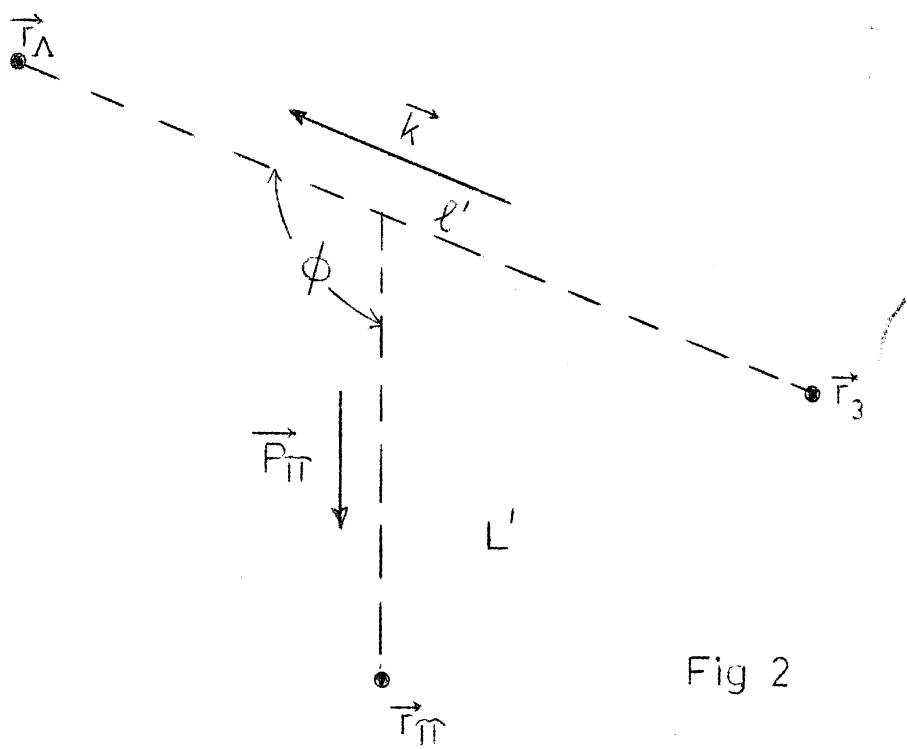
Fig 2

LIFETIME MEASUREMENTS OF $_\Lambda$H^3 AND $_\Lambda$H^4

L. Fortney[*],
Department of Physics, University of Wisconsin,
Madison, Wisconsin.

(Presented by W.F. Fry)

Hyperfragments were produced by K$^-$ mesons at rest in the Berkeley 30" heavy liquid bubble chamber of Professor W. Powell. The chamber was filled with a mixture of propane and freon. The separated K$^-$ beam from the Berkeley bevatron gave about five stopping K$^-$ mesons per picture. About 90,000 pictures were scanned for hyperfragments. Hydrogen hyperfragments which are produced with a momentum greater than 75 MeV/c per nucleon, travel more than 0.75 mm in the liquid before coming to rest. This length of track can generally be observed if it is not obscured by other tracks or steep in the chamber.

The two-body mesonic decays

$$_\Lambda H^3 \rightarrow He^3 + \pi^- + \sim 42 \text{ MeV}$$

$$_\Lambda H^4 \rightarrow He^4 + \pi^- + \sim 55 \text{ MeV}$$
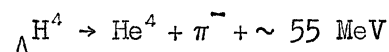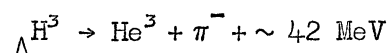
can generally be identified by kinematics, both when in flight and at rest. The lifetime measurements are restricted to these two-decay modes. For analysis considerations, the mesonic hyperfragments were separated into two classifications:

i) hydrogen hyperfragments which decay in flight with more than 80 MeV/c per nucleon, at the time of decay, can yield a visible nuclear recoil (He^3 or He^4) of length greater than 0.75 mm; these events are called two-prong decays;

ii) hyperfragments which decay either in flight or at rest and
do not have a visible recoil are called one-prong events. Only
those events are accepted where the angle between the pion
direction and the hyperfragment is less than 85°, in order to
eliminate Σ^- decays in flight from the sample.

Each event of class (i) was subject to a three constraint
kinematic fitting programme under the hypotheses that the event was

a) a $_\Lambda H^3$ two-body decay,

b) a $_\Lambda H^4$ two-body decay,

c) or a free Λ decay from the K^- origin with the Λ vertex
superimposed on a nuclear track. This category also
includes three-body decays, since they will fit a free
Λ decay in some cases.

The accepted two-body events were required to fit (a) or (b)
with a $\chi^2 \leq 10$ and to not fit (c) ($\chi^2 \geq 10$). The sample of group (a)
is subject to some contamination of three-body decays which have only
one visible nuclear track. This contamination is probably small.

Five $_\Lambda H^3$ and five $_\Lambda H^4$ decays were found by this method of
analysis. The maximum likelihood method using this sample of decays in
flight only give

$$\tau_\Lambda H^3 = 0.70^{+0.9}_{-0.3} \times 10^{-10} \text{ sec}$$

$$\tau_\Lambda H^4 \geq 1.9 \times 10^{-10} \text{ sec}.$$

Events of type (ii) were analysed by assuming that the events
with P_π (lab) greater than 130 MeV/c and less than about 150 MeV/c are
$_\Lambda H^4$ two-body decays; and events with P_π (lab) greater than 110 MeV/c
and less than 130 MeV/c are $_\Lambda H^3$ two-body decays. Background studies show
that other phenomena leading to pions of these momenta are unimportant.

This method yielded five $_\Lambda H^3$ decays at rest and four in flight decays.

Ten $_\Lambda H^4$ decays at rest and three $_\Lambda H^4$ decays in flight were found. A maximum likelihood method of analysis for these one-prong events yields the following lifetimes

$$\tau_{\Lambda H^3} = 0.6^{+0.4}_{-0.3} \times 10^{-10} \text{ sec}$$

$$\tau_{\Lambda H^4} = 2.0^{+2.0}_{-1.0} \times 10^{-10} \text{ sec}.$$

A third method of analysis was used to combine the in-flight decays of class (i) with the decays at rest and in flight of class (ii). Assuming that there are equal numbers of decays at rest with pions backward, with respect to the hyperfragment, as there are forward, the maximum likelihood method for the four $_\Lambda H^3$ two-body decays in flight, and five at rest, yield

$$\tau_{\Lambda H^3} = 0.63^{+0.5}_{-0.3} \times 10^{-10} \text{ sec}.$$

The four $_\Lambda H^4$ events in flight and the ten at rest yield a lifetime of

$$\tau_{\Lambda H^4} = 2.4^{+1.9}_{-0.9} \times 10^{-10} \text{ sec}.$$

The good agreement of these three largely independent methods of determining the mean life of $_\Lambda H^3$ suggests that the background of three-body decays in the two-body sample, is small.

IV. PRODUCTION OF HYPERFRAGMENTS

HYPERFRAGMENT PRODUCTION

J. Zakrzewski,
Institute of Experimental Physics,
University of Warsaw, Warsaw.

I. INTRODUCTION

1. General

In this talk we shall make a brief survey of the experimental results on hyperfragment production. Most of these results have come from work with nuclear emulsion, although interesting studies have also been made with the use of bubble chambers[1,2]. Nuclear emulsion is in this field of research an important experimental technique because of the very high spatial resolution of which it is capable. It can resolve events separated by distances of the order of $0.5\ \mu$ or even less and record observable tracks of charged particles of very low energy. On the other hand, the complex composition of nuclear emulsion bears significantly on the experimental results. We shall pay particular attention to this problem in the following.

In the remaining part of this section we shall outline the general conditions in which hyperfragments can be produced. Section II will be devoted to the discussion of those aspects of nuclear emulsion technique that are relevant to the observation of hyperfragment production. Finally, in Section III, we shall discuss the main experimental results obtained, mostly in recent work in which a systematic approach to this problem has been made.

2. Conditions of hyperfragment production

The formation of a hyperfragment[*] requires the binding in a nuclear fragment of a Λ° hyperon, i.e. a particle with a negative strangeness

---

[*] Only the production of ordinary hyperfragments, i.e. nuclear structures containing one bound Λ° hyperon, is discussed in this lecture. The observation of a double hyperfragment, i.e. a structure containing two bound Λ° hyperons, has been the subject of a separate talk[3].

(S = - 1). In practice, this condition is realized by the bombardment
of atomic nuclei with particles having such properties that their
strong interactions can lead to the appearance of negative strangeness
(S = - 1) inside the struck nuclei. A Λ° hyperon produced at some stage
of such an interaction can be emitted from the struck nucleus, free or
bound in a light nuclear fragment, or else it can become trapped in a
residual nucleus, i.e. the heaviest "splinter" of all the disintegration
products of the reaction.

A negative strangeness can appear inside the atomic nucleus as
a result of the interaction of:

i) a non-strarge particle (e.g. a π meson or a nucleon) with energy
above the threshold for associated production of strange particles;

ii) a strange particle with a negative strangeness (e.g. a K^- meson or
a Σ^- hyperon) interacting at rest or in flight.

Experimental results show that the cross-section for hyper-
fragment production in processes of type (ii) is about an order of
magnitude higher than that of processes of type (i). As a result,
exhaustive studies of hyperfragment production under various experimental
conditions became possible only with the advent of separated beams of K^-
mesons of both high intensities and purities and of various energies.

II. EXPERIMENTAL CONDITIONS

1. Nuclear emulsion as a target

In studying the production of hyperfragments, nuclear emulsion
constitutes at the same time a "target" and a "detector". The atomic
composition of the target must therefore be taken into account in any
interpretation of the experimental results since a hyperfragment may
originate from the interaction of an incident particle with any complex

nucleus of the main emulsion constituents[*]: C, N, O, Br or Ag (we neglect here the less abundant elements S and I).

In connection with the presence in nuclear emulsion of two distinct groups of complex nuclei, i.e. "light" nuclei with mass number $A \leq 16$ (C, N, O) and "heavy" nuclei with $A \gg 16$ (Br, Ag), we introduce the following phenomenological definitions. We shall refer to a hypernucleus as "light" or "heavy" if its mass number is $A \leq 16$ or $A > 16$, respectively. These definitions correspond to the fact that the most massive hypernucleus that can be produced in emulsion from known interactions of incident particles with light nuclei has a mass number $A = 16$. It will follow in practice that the atomic number of a "light" or a "heavy" hypernucleus is $Z \leq 8$ or $Z > 8$, respectively.

2. Nuclear emulsion as a detector

A hyperfragment is observed in emulsion as a double star resulting from the registration of the interaction of an incident particle with an emulsion nucleus and of the decay of the produced hyperfragment. The smallest separation between the centres of these two stars (i.e. the shortest range of a hyperfragment) that can be observed under ordinary experimental conditions is $1 \pm 0.5\,\mu$. If the centres of the two stars cannot be resolved (i.e. the hyperfragment decays practically at the point of its production) then we speak of the formation of a "cryptofragment". It is clear that the difference between a "hyperfragment" and a "crypto-fragment" is of purely phenomenological nature. Different methods must be applied for investigation of cryptofragments as the basic criterion of hyperfragment selection, i.e. the observation of a double star, is missing in this case.

Recently the Amsterdam group[5] have used a new method to detect and to measure the very closely spaced double stars. The x and y coordinates of the grains of the prongs near the centre of a star were

---

[*] Most of the results available at present come from nuclear emulsion of normal composition. Emulsion loaded with various elements may be used in order to study hyperfragment production from other nuclei and some efforts have been made already in this direction[4].

determined with a special apparatus and straight lines were then
fitted to them. The intersection of these lines defined a centre of
the star. By this method it was possible to determine the distance
between the two centres with an error of about 0.07 μ (or even less),
the smallest separation observed being about 0.25 μ[5].

3. Identification of hyperfragments

Methods of hyperfragment identification have been fully
discussed at the conference[6,7]. In this talk we are only concerned
with the problem of how to select a possibly unbiased sample of all
the hyperfragments produced in a given interaction, keeping in mind
the fact that the ranges of most of the observed hyperfragments are
too short, i.e. less than about 20 μ, to assist in their identification.

Mesonic hyperfragments[*] are readily identified as such and
their identity can often be uniquely established from the kinematical
analysis of their production and decay processes. The unique identification
of non-mesonic hyperfragments is, however, rare because their decays
usually involve the emission of neutrons and nuclear fragments of low
energy (i.e. short range). Attempts were made to identify individual
events by assuming the emission of a single neutral particle and by
permuting charged particle identities in the kinematic analysis computer
programme. This procedure may often lead to serious misinterpretations as
some of the decay configurations of non-mesonic heavy hyperfragments may
resemble, and be interpreted as, the decay of much lighter hypernuclei.
This is illustrated in Fig. 1, which shows range distributions of Li^8
fragments, mesonic $_\Lambda Li$ hyperfragments and so-called non-mesonic "$_\Lambda Li$"
events[8]. The difference in their range distributions is apparent. The
effects of this and other similar misinterpretations are far reaching and
have led to many conclusions which should be questioned[8,9].

Most of the non-mesonic hyperfragments must, therefore, remain
individually unidentified and some sort of statistical approach is required
to identify such events. This approach should be based solely on

---

[*] It is customary to use the term "mesonic" only for those hyperfragments
whose decay involves the emission of charged π mesons.

consideration of the characteristics of the production process and
on the observed hyperfragment range distribution[8,9]. In this manner
it should be possible:

i) to make a statistical division of all the hyperfragments into
two classes of light and heavy ones; and

ii) to estimate independently the experimental losses and biases
for these classes.

4. Biases

There are other phenomena caused by the interactions of charged
particles emitted from the primary disintegrations whose appearance in
emulsion is often very similar to that of hyperfragment decay in that
they also lead to the formation of double stars. The following phenomena
are to be taken into account:

i) interactions in flight of secondary charged particles (including
single scattering events);

ii) captures at rest of negative particles, e.g. π^- and K^- mesons, and
Σ^- hyperons;

iii) decay of unstable ordinary fragments, e.g. Li^8, Li^9, B^8, and C^{12};

iv) decay of unstable elementary particles, e.g. Σ^+ hyperons.

Some of these events may simulate, by their configuration,
the decay of non-mesonic hyperfragments*). If the length of the connecting
tracks is too small (say, less than about 20 μ) then, in general, such
events cannot be individually identified. Statistical arguments must,
therefore, be used to estimate the contamination of the selected sample
of double stars, chosen for a given range cut-off, with these background
phenomena. It is clear that such an analysis must be carried out separately

---

*) The confusion with background phenomena, mainly single scattering events,
is particularly pronounced for those types of non-mesonic hyperfragment
decay which lead to the emission of a single charged particle (one-
pronged decay).

for each experiment as the contribution from various background phenomena
may differ for various experimental conditions[*].

III. GENERAL FEATURES OF PROCESSES IN WHICH HYPERFRAGMENTS ARE PRODUCED

1. Introduction

Table 1 lists the particles of various energies that have
been used to produce hyperfragments in nuclear emulsion. It also gives
the observed fractions of interactions yielding hyperfragments and the
non-mesonic to mesonic decay ratios taken from published work. The
compilation of data from various experiments is made difficult by the fact
that often different criteria of selection of non-mesonic hyperfragments
were adopted and different corrections were introduced by various authors;
sometimes these conditions were not clearly specified in the publications.

Table 1

Production of hyperfragments

Particle	Energy	Fraction of interactions yielding HF (%)	Non-mesonic to mesonic HF decay ratio
π^- mesons	3.0 GeV	0.090 ± 0.012	-
π^- mesons	4.5 GeV	0.18 ± 0.03	5.0 ± 1.3
π^- mesons	17.2 GeV	0.3 ± 0.05	~ 6.3
Protons	3.0 GeV	0.096 ± 0.019	-
Protons	6.0 GeV	0.07	-
Protons	25.0 GeV	0.3 ± 0.05 (~0.5)	~ 5.9
K^- mesons	Rest	4.7 ± 0.3	3.2 ± 0.8
K^- mesons	85 MeV (mean)	3.9 ± 0.8	7.5 ± 5.6
K^- mesons	225 MeV	6.3 ± 2.5	-
K^- mesons	450 MeV	5.3 ± 0.3	11.5 ± 2.1
K^- mesons	750 MeV	2.4 ± 0.4	-
K^- mesons	900 MeV	4.2 ± 0.2	15.5 ± 2.4
K^- mesons	1.07 GeV	4.1 ± 0.2	13.3 ± 1.1
K^- mesons	1.85 GeV	2.1 ± 0.2	-
Σ^- hyperons	Rest	2.5 ± 0.8	5.2 ± 2.0

[*] For instance, it appears that the contamination with background phenomena
of a sample of short range heavy hyperfragments resulting from the inter-
actions of energetic K^- mesons is much smaller[10] than in the case of
π^- mesons[11].

2. Fractions of interactions yielding hyperfragments

Table 1 shows that:

i) the observation frequency of hyperfragments is much lower for the interactions of π^- mesons and protons $(0.1 - 0.5\%)$ than for those of K^- mesons and Σ^- hyperons $(2 - 5\%)$;

ii) there appears to be a tendency for this frequency to increase with the energy of the incident π mesons and protons: such an increase could be explained if with the increase of the incident particle energy, most of the Λ^0 production occurred in secondary collisions inside the struck nuclei, in particular those of π mesons on nucleons[12];

iii) in the case of K^- mesons, the observation frequency seems to stay near 5% for both interactions at rest and in flight at least up to 450 MeV;

iv) for Σ^- hyperons the fraction of captures at rest giving rise to hyperfragments is less than that for K^- mesons: this may be ascribed to the fact that the nuclear absorption of Σ^- hyperons is more peripheral than that of K^- mesons[13].

The fractions of interactions leading to the binding of Λ^0 hyperons in emulsion nuclei may actually be higher than the values given in Table 1 because of the formation of cryptofragments.

Several estimates of the frequency of crptofragment formation in the capture at rest of K^- mesons were made from an analysis of the total balance of strangeness in such interactions. With the use of nuclear emulsion, Davis et al.[14] found for this frequency $(30 \pm 7)\%$ (upper limit), Cester et al.[15] $(0 - 15)\%$ and Filipkowski et al.[16] $(13^{+22}_{-24})\%$.

Recently Knight et al.[17] have performed an experiment in which K^- mesons were stopped in the 30" Berkeley heavy liquid bubble chamber in a 50%-50% mixture by volume of CF_3Br and C_3H_8. The result was that $(22.5 \pm 1.7)\%$ of the interactions did not emit a strange particle and so presumably involved the trapping of a Λ^0 hyperon. This observation, together with that of Davis et al., led to the conclusion that the

frequency of Λ° trapping in light and heavy nuclei of the emulsion is $(18.5 \pm 3.5)\%$ and $(51 \pm 14)\%$[17], respectively.

Cryptofragment formation from the capture at rest of Σ^- hyperons in emulsion was investigated by Sacton et al.[13]. From a study of the energy released in capture stars, they estimated that the frequency of cryptofragment formation is $(9 \pm 3)\%$.

Theoretical estimates of the probability of Λ° trapping in heavy emulsion nuclei, following the absorption at rest of K^- mesons and Σ^- hyperons calculated by Martin[18], are in agreement with the emulsion results quoted above.

3. Non-mesonic to mesonic decay ratio

It is seen from Table 1 that the non-mesonic to mesonic decay ratio increases markedly when we pass from hyperfragments produced by K^- meson capture at rest (~ 3) to those produced by K^- mesons interacting in flight (~ 12).

This ratio strongly varies with the range of hyperfragments originating from the interactions of energetic K^- mesons. This is illustrated in Table 2 in which the combined results obtained in the study of hyperfragment production from the interactions of 1.3 and 1.5 GeV/c K^- mesons were used[19].

Table 2

The variation of the non-mesonic to mesonic decay ratio for hyperfragments produced in the interactions of 1.3 and 1.5 GeV/c K^- mesons

HF range in μm	0 - 10	10 - 100	> 100
Non-mesonic to mesonic decay ratio	~ 100	~ 3.5	~ 1

From these results it is clear that short-range hyperfragments originating from the interactions of energetic particles (in particular K^- mesons) are much heavier than those produced from the capture of K^- mesons at rest. In fact, detailed analysis shows[8,10,19-21] that most of the short-range hyperfragments produced in the interactions of energetic particles are residual spallation products of heavy nucleus disintegrations containing a trapped Λ^0 hyperon. When such heavy spallation hyperfragments receive sufficient momenta in the interaction they yield, visible tracks in emulsion and thus their decay can be distinguished from the primary disintegrations. In the case of K^- mesons interacting at rest, the momenta transferred to the heavy residual nuclei are, in general, too low so that heavy cryptofragments are formed instead of resolvable double stars.

4. Range distribution of hyperfragments

A typical range distribution of hyperfragments[19] produced in the interactions of energetic particles is shown in Fig. 2. It is seen that the range distributions of mesonic and non-mesonic hyperfragments are strikingly different. The range distribution of non-mesonic hyperfragments exhibits a maximum between 2 and 5 μ and then sharply decreases. On the other hand, the distribution in range of the mesonic hyperfragments shows no such feature. Combining this observation with the previous one concerning the variation of the non-mesonic to mesonic decay ratio with range (see Table 2), one can divide all the hyperfragments into three categories in a natural manner: those with ranges less than 10 μ, between 10 and, say, 100 μ, and greater than 100 μ, respectively. The hyperfragments of range less than 10 μ are in the main the residual spallation products of the heavy emulsion nuclei containing trapped Λ^0 hyperons which received sufficient momentum to record visible tracks in emulsion. Those of range greater than about 100 μ are mainly very light (A < 5) hyperfragments as indicated by their low non-mesonic to mesonic decay ratio. The events from the range region of ~ 10 to ~ 100 μ are probably a mixture of very light (A < 5) and medium light (A $\geq$ 5) hyperfragments and perhaps some heavy hyperfragments from the tail of their range distribution. In fact, if one

knew the identities of the light mesonic hyperfragments and the non-
mesonic to mesonic ratio as a function of Z, then using the range distri-
bution of such identified mesonic hyperfragments, one could construct
the range distribution of the corresponding non-mesonic hyperfragments.
By this indirect method, it would be possible to establish statistically
the composition of the sample of non-mesonic hyperfragments of intermediate
range, apart from any direct methods of establishing their identity.

In connection with the shape of the range distribution of
hyperfragments (Fig. 2), the following remark should be made. From
considerations presented in Section II.2 it follows that the short-
range end of this distribution may be biased against the detection of
very closely spaced double stars (i.e. hyperfragments of ranges less
than about 1 μ). The Amsterdam group demonstrated by the application
of their method (see Section II.3), that such a loss may indeed exist.
For instance, they found nine double-centred events among 179 stars
which on first inspection did not appear to be double-centred[5]. The
range distribution in 0.25 μ intervals of a sample of double stars measured
by their method is shown in Fig. 3.

The Warsaw group[22] have attempted to determine what is the
minimum momentum transfer to a heavy hypernucleus that leads to a separa-
tion between the two centres which can be recognized under normal
conditions. For this purpose observations were made on the scattering
in Ilford K2 emulsion of argon ions. Figure 4 shows the preliminary
results of this work, i.e. the relation between the momentum imparted to
the struck emulsion nucleus (determined from the kinematics) and its
observed range in emulsion defined as the distance between the point of
scattering and the tangent to the last grain of the recoil track. It is
seen that the experimental points lie in two regions, I and II. Region II
corresponds to the scattering on light nuclei, C, N, O, whereas region I
corresponds to the scattering on heavy nuclei, Br, Ag. It is seen that
the struck heavy nuclei start recording visible tracks in the emulsion
when the momenta imparted to them are $\gtrsim$ 0.5 GeV/c. Now heavy spallation
hyperfragments observed in the interactions of particles with momentum up

to several GeV/c possess mass numbers between A = 40 and A = 100. This observation may help to understand the reason for the high average momentum of the order of 1 GeV/c found for the spallation hyperfragments when the incident K⁻ momentum was only 0.8 GeV/c [23]. If the argument given above is correct the spallation heavy hyperfragments of low momentum would not be observed.

5. The nuclei from which hyperfragments originate

The range distribution of hyperfragments changes with the increase of incident particle momentum. In Table 3 the fractions of hyperfragments of range less than 5 μ are shown for several values of the momentum of the incident particles. There is an increase of this fraction when we pass from K interactions at rest to those at 0.8 GeV/c; then we observe a slow decrease with increasing momentum of the incident particles. Such a variation is presumably a reflection of the complex composition of our target, i.e. nuclear emulsion.

Table 3

The variation of the fraction of non-mesonic
hyperfragments of range less than 5 μm
with the incident particle momentum

Particle and momentum (in GeV/c)	K⁻ at rest	K⁻ 0.3	K⁻ 0.8	K⁻ 1.5	K⁻ 2.3	π⁻ 4.5	π⁻ 17	p 25
Fraction of HF of ranges < 5 μm (%)	~ 63	~ 60	~ 88	~ 71	~ 64	~ 27	$\lesssim$ 25	$\lesssim$ 8

Indeed, most of the mesonic hyperfragments produced as a result of the capture of K^- mesons at rest come from the light nuclei of the emulsion and this effect becomes more marked as the atomic number, Z, of the hyperfragment increases[24]. This is illustrated in Table 4. Similar studies have not been made for the non-mesonic hyperfragments. However, using the non-mesonic to mesonic decay ratio given in Ref. 24 and assuming that the same proportions of production by light nuclei are applicable to those hyperfragments which decay non-mesonically, one can estimate that the majority ($\gtrsim 80\%$) of non-mesonic hyperfragments must have originated from light nuclei as well.

Table 4

Proportion of hyperfragment
production in light nuclei

Atomic number Z of mesonic HF	1	2	3	≥ 4
Lower limit for the proportion of light nucleus production (%)	57	73	84	94

On the other hand, most of the hyperfragments produced from interactions of particles in flight come from the heavy nuclei of the emulsion. This is illustrated in Table 5 which shows the proportion of hyperfragment production in heavy nuclei for several reactions.

Table 5

Proportion of hyperfragment
production in heavy nuclei

Particle and momentum (GeV/c)	K^- at rest	K^- 0.8	K^- 1.5	K^- 2.3	π^- 4.5
Proportion of heavy nucleus production (%)	> 13	> 63	> 82	> 84	$\gtrsim 90$

Thus, the explanation is that with the increase of the
incident particle momentum, heavy cryptofragments start recording
visible tracks in the emulsion and so the observed yield of short-range
non-mesonic hyperfragments increases. However, as the incident particle
momentum is further increased, the heavy spallation hyperfragments will,
on average, be of slightly lower mass. This conclusion follows from
the observation of the mean prong number, $\bar{N}_h$, of the hyperfragment
parent stars. The increase of $\bar{N}_h$ with the incident particle momentum
is clearly seen from Table 6 and indicates that the residual hypernuclei
will have correspondingly lower masses.

Table 6

Mean prong number $\bar{N}_h$ of the
hyperfragment parent stars

Particle and momentum (GeV/c)	K^- 0.8	K^- 1.3	K^- 1.5	K^- 2.3
$\bar{N}_h$	6.3	7.7	8.7	11.2

Therefore, if the average momentum transfer does not decrease the fact
that the heavy spallation hyperfragments have lower masses implies that
they will have larger range; the number of events with range less than
5 μ will decrease. It should be added that an increase in the mean range
of the heavy hyperfragments might also be due to an increase in the
momentum imparted to the struck nucleus.

The mesonic hyperfragments resulting from the interactions of
K^- mesons in flight are, in general, of longer ranges than those coming
from the K^- meson captures at rest. This observation is illustrated in
Fig. 5, which shows: a) range distribution of the mesonic hyperfragments
from the interactions of K^- mesons of 800 MeV/c momentum; and b) range
distribution of the mesonic hyperfragments from the interaction of K^- mesons
at rest.

The average size of a star with a hyperfragment is in general larger than that of a single star. For illustration, the results obtained by the Brussels and Warsaw groups in the study of hyperfragment production by 800 MeV/c K⁻ mesons[23] are presented in Fig. 6. It shows the distributions of heavy prong number N_h for stars containing hyperfragments of range $\leq 5 \mu$, i.e. heavy spallation hyperfragments (class I: $\bar{N}_h = 6.3 \pm 0.3$) and of range $\geq 5 \mu$ (class II: $\bar{N}_h = 5.3 \pm 0.5$) and for single stars with one or more short tracks of range $\leq 5 \mu$ (class III: $\bar{N}_h = 4.8 \pm 0.2$) and without such short tracks (class IV: $\bar{N}_h = 4.9 \pm 0.2$). These short tracks in single stars can be attributed to recoiling heavy residual nuclei: consequently both the events of class I and of class III must have originated from heavy emulsion nuclei. The range distribution of recoils in single stars (class III) is almost identical with that of heavy hyperfragments (class I) [see Ref. 23 for discussion].

6. Charge distribution of mesonic hyperfragments

It has been shown above that for the captures of K⁻ mesons at rest, the hyperfragments observed come predominantly from light nuclei whereas for the interactions of particles in flight they come from heavy nuclei. It is interesting, therefore, that the observed charge distributions of mesonic hyperfragments are similar in both cases.

Table 7[*])

Charge distribution of
mesonic hyperfragments

Atomic number Z of mesonic hyperfragment	1	2	3	4
K⁻ at rest, 192 events, %	33.8 ± 4.2	42.7 ± 4.9	15.6 ± 2.9	5.2 ± 1.7
K⁻ at 0.8 GeV/c, 73 events, %	39.7 ± 7.4	42.5 ± 7.6	13.7 ± 4.3	4.1 ± 2.4
π⁻ at 4.5 GeV/c, 65 events, %	33.8 ± 7.2	53.9 ± 9.1	7.7 ± 3.5	4.5 ± 2.7

*) Only events with uniquely determined Z have been used.

Table 7 shows the charge distribution of mesonic hyperfragments resulting from K^- captures at rest[24] and from the interactions of 0.8 GeV/c K^- [25] and 4.5 GeV/c π^- mesons[26]. It is not clear whether this similarity is a real effect or a fluctuation due to poor statistics and different scanning biases which may affect both samples of events; this problem is certainly worth investigating.

Knowing the non-mesonic to mesonic ratio for the various hypernuclear species, the Chicago group[24] estimated the hyperfragment emission probabilities for K^- meson captures at rest (defined as the ratio of the number of hyperfragments to the number of bound plus unbound Λ^0 hyperons produced) for the light hyperfragments. These estimates are given in Table 8. The emission probability is seen to increase with the mass of the hypernucleus (see Section III.8).

Table 8

Average probability of mesonic
hyperfragment emission from
interactions of K^- mesons at rest

Hypernuclide	$_\Lambda H^3$	$_\Lambda H^4$	$_\Lambda He^4$	$_\Lambda He^5$	$_\Lambda Li, _\Lambda Be, _\Lambda B, _\Lambda C$
Average emission probability $\times 10^2$	0.14 ± 0.06	0.43 ± 0.15	0.45 ± 0.10	1.4 ± 0.3	3.4 ± 1.0

7. Angular and energy correlations

Hyperfragments originating from the interactions of particles in flight are preferentially ejected in the forward direction with respect to that of the incident particles. This observation is illustrated with the results from the Brussels-Warsaw work[23]. Figure 7 shows the angular distributions of hyperfragments and of recoils in single stars with respect to the line of flight of the incident K^- mesons. The short-range hyperfragments ($\leq 5\mu$) are seen to be strongly peaked in the forward direction, their forward to backward ratio being $F/B = 3.3 \pm 0.7$. The angular

distribution of long-range hyperfragments ($> 5 \mu$) is more isotropic ($F/B = 1.8 \pm 0.6$); and similarly so is that of recoils observed in single K^- stars ($F/B = 1.5 \pm 0.3$)[*].

For ordinary fragments emitted from high-energy nuclear reactions, a marked anisotropy of their direction of emission is also observed. It is seen that their forward collimation increases with the energy of the emitted fragments, i.e. with their ranges. This is shown in Table 9 for Li^8 fragments emitted from 4.5 GeV/c π^- meson interactions[27]. A similar increase in the forward collimation with energy has also been observed for light identified hyperfragments[28].

Table 9

Forward to backward ratios for Li^8 fragments
from interactions of 4.5 GeV/c π^- mesons

Range of Li^8 (μ)	< 101	$101 - 134$	$134 - 232$
F/B ratio	1.03 ± 0.2	1.6 ± 0.2	2.5 ± 0.4

The values of the over-all forward to backward ratios for light hyperfragments are, in general, slightly lower than those for heavy ones; the same is true also for ordinary light fragments and recoils[29]; this is illustrated in Table 10.

There are some indications that both the angular and energy distributions of ordinary fragments and light hyperfragments are similar[25,28,30], but certainly more work is needed to clarify the situation in this respect. Of course one should compare respective distributions only for those ordinary fragments and hyperfragments which at least possess the same atomic number Z. The easiest approach

---

*) The low value of this F/B ratio might be due to a strong bias against the detection in single K^- stars of short recoils projected in the forward direction. However, no reason for such a bias could be found.

Table 10

Forward to backward ratios for light
fragments and hyperfragments and for
recoils and heavy hyperfragments

Incident particle and energy (GeV)	Protons			K^- mesons		
	1.0	2.0	3.0	0.45	0.9	1.07
Light fragments Recoils [†)	1.5 ± 0.2 3.1 ± 0.6	1.8 ± 0.3 1.8 ± 0.3	1.8 ± 0.3 2.3 ± 0.4	- 	- 	-
Light hyperfragments Heavy hyperfragments	 -	 -	 -	1.8 ± 0.6 3.3 ± 0.7	1.4 ± 0.3 2.4 ± 0.2	2.2 ± 0.5 3.2 ± 0.4

consists of investigating $_\Lambda$Li mesonic hyperfragments and Li^8 fragments;
both types of events can be identified by their decay characteristics and
any experimental biases will be considerably reduced in this case[*].

In fact, such a comparison has been performed by the Chicago
group[24] in a detailed study of the capture of K^- mesons at rest. The
results show that range distributions of both $_\Lambda$Li and $_\Lambda$He hyperfragments
are respectively very similar to those of ordinary Li^8 and He nuclei.
In Fig. 8 the normalized range distributions of $_\Lambda$Li and Li^8 events are
displayed as an illustration[**].

---

[*] One can extend this type of investigation to other types of fragments
by using, for instance, less sensitive types of emulsion exposed to
the same beam of particles to which normal emulsions have been exposed.
Then one can study the emission of hyperfragments in the normal emulsion,
and that of ordinary fragments in the less sensitive emulsions where it
is much easier to identify the charges of fragments from observations
on their tracks.

[**] It has been shown that the lower limit of the proportion of Li^8
production in light nuclei is 75%; see also Table 4.

[†] Particles and light fragments were observed in addition to a recoil
in a primary disintegration.

Hyperfragments originating from interactions of K^- mesons at rest are emitted preferentially in the opposite direction to that of accompanying π mesons or fast protons; an angular correlation of the same type is also observed for Li^8 fragments[24]. A possible reason for this observation is discussed in Section III.8.

8. Models of hyperfragment production

i) Hyperfragments produced in the capture at rest of K^- mesons and Σ^- hyperons

Two models for the production of hyperfragments following K^- meson captures at rest in emulsion nuclei have been proposed[24].

In the first, the "trapped Λ^0 hyperon" model, it is suggested that the Λ^0 hyperon, either created directly in the initial K^- meson interaction or as a result of Σ hyperon conversion, becomes trapped in the potential well of the excited struck nucleus and is subsequently emitted as a hyperfragment in the ensuing de-excitation stage. This model accounts satisfactorily for the observed preponderance of hyperfragment emission from the light nuclei of the emulsion following K^- meson captures at rest. The small amount of excitation energy available, less than 100 MeV, is sufficient to cause a complete break-up of a light nucleus, as a result of which a Λ^0 hyperon may sometimes remain in one of the disintegration products to form a recognizable hyperfragment. However, a **multiply**-charged hyperfragment would rarely receive sufficient energy to surmount the Coulomb barrier of a bromine or silver nucleus. Thus, when a Λ^0 hyperon is trapped in a heavy nucleus, it will remain there after the completion of the de-excitation phase to form a cryptofragment. On this model it is to be expected that a similarity should exist between the energy spectra of hyperfragments and those of corresponding ordinary fragments emitted from K^- captures at rest.

The angular correlations between the direction of the hyper-fragment emission and that of a fast proton or a π meson is also accounted for by this model since the prompt emission of a fast proton or a π meson

will impart to the residual nucleus a momentum of around 200 MeV/c
and the resulting hyperfragment emission direction is that expected
from a moving nucleus.

In the second, the "prompt hyperfragment" model, it is
suggested that the K^- meson interacts with a cluster of nucleons
to produce a hyperfragment directly. There are several examples
in which this model seems operative, notably the observation of
$_\Lambda He^4$ and $_\Lambda H^4$ production in a helium bubble chamber:

$$K^- + He^4 \rightarrow {}_\Lambda He^4 + \pi^- ,$$

$$\rightarrow {}_\Lambda H^4 + \pi^0 ,$$
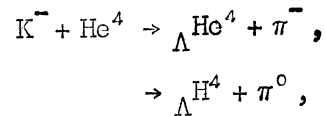
and in emulsion the production of $_\Lambda B^{12}$ both from K^- meson and Σ^- hyperon
captures on carbon [*] :

$$K^- + C^{12} \rightarrow {}_\Lambda B^{12} + \pi^0 ,$$

$$\Sigma^- + C^{12} \rightarrow {}_\Lambda B^{12} + n .$$
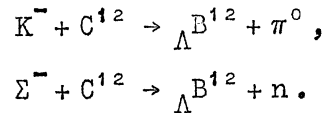
However, whilst this model cannot be excluded in such cases, several
features of the observed results suggest that this is not the dominant
process in hyperfragment production. First, the angular correlations
between the hyperfragment direction and those of π mesons and fast
protons are not so marked as might be expected from considerations of
the model. Secondly, the observed similarities of the spectra of
hyperfragments and of stable nuclei are not easily understood. Finally,
there is the objection that a K^- meson interaction with a large aggregate
of nucleons has to be a rather frequent process.

---

*) Recently an event has been observed[31] which is interpreted as the
production of a $_\Lambda C^{14}$ hyperfragment in the capture at rest of a Σ^-
hyperon on N^{14} nucleus:

$$\Sigma^- + N^{14} \rightarrow {}_\Lambda C^{14} + n ,$$

$$_\Lambda C^{14} \rightarrow {}_\Lambda N^{14} + \pi^- .$$
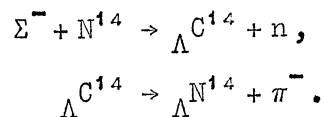
ii) Hyperfragments produced in the interactions in flight

A so-called "recoil" model was originally proposed for hyperfragment production by 0.8 GeV/c K⁻ meson interactions in flight[10,20,21]; recently it has been shown to be operative for other high-energy interactions as well[8].

In this model it is assumed that a high-energy particle on entering a heavy nucleus initiates a nuclear cascade as a result of which fast mesons and baryons are ejected. A fast hyperfragment may occasionally be ejected at this stage but from the experimental data it appears that such emission is infrequent. Often a Λ^0 hyperon produced in the initial phase at sufficiently low energy, or degraded to a low energy in subsequent cascade collisions, remains in the highly excited nucleus. In the ensuing evaporation phase, nucleons or clusters of nucleons are emitted. Sometimes these clusters may contain the Λ^0 hyperon forming a light hyperfragment. However, in the majority of cases of hyperfragment formation the Λ^0 hyperon is not evaporated but remains within the residual nucleus forming a heavy spallation hyperfragment. In collisions of this kind the average recoil momentum may be of the order of the incident momentum which in this case allows it to produce an observable track in the emulsion. Since it contains a trapped Λ^0 hyperon, it subsequently decays leading to the formation of a double star with a short interconnecting track. In this model, the forward collimation of short-range heavy hyperfragments is to be explained as a result of the development of a nuclear cascade which eventually leads to the Λ^0 trapping within a residual nucleus[*]. Light hyperfragments of longer range are expected to have a smaller forward to backward ratio if they are mainly evaporated from a slowly moving nucleus. The similarity of the energy distributions of light hyperfragments to those predicted by evaporation theory has been, in fact, demonstrated before[28]. Several investigations that have been performed recently also suggest that the emission of light hypernuclei from heavy emulsion nuclei occurs mostly during the evaporation process[25].

---

[*] Detailed discussion of this problem is given in Ref. 23.

This "recoil" model is equivalent to the "trapped Λ^0 hyperon" model discussed above in that both are based on the assumption that Λ^0 hyperons are capable of becoming trapped in the residual excited nuclei, their fate being then determined by the subsequent nuclear de-excitation processes developing in these nuclei.

ACKNOWLEDGEMENTS

* * *

REFERENCES

1. M.M. Block, report at this Conference, p. 63.

2. W.F. Fry, report at this Conference, p. 85.

3. J. Pniewski, report at this Conference, p. 117.

4. See, for example, R. Levi-Setti and W.E. Slater, Nuovo Cimento 14, 895 (1959).

5. S.J. Bosgra and W. Hoogland, preprint (1963).

6. R. Levi-Setti, report at this Conference, p. 17.

7. R.G. Ammar, report at this Conference, p. 7.

8. J. Zakrzewski, D.H. Davis and O. Skjeggestad, Nuovo Cimento 27, 652 (1963).

9. J. Zakrzewski and S.J. St. Lorant, Nuovo Cimento 25, 693 (1962).

10. B.D. Jones, B. Sanjeevaiah, J. Zakrzewski, M. Csejthey-Barth, J.P. Lagnaux, J. Sacton, M.J. Beniston, E.H.S. Burhop and D.H. Davis, Phys.Rev. 127, 236 (1962).

11. E.M. Silverstein, Nuovo Cimento Suppl. 10, 111 (1958); see also Ref. 8.

12. I.R. Kenyon et al., preprint No. 87/62 (1962).

13. J. Sacton, M.J. Beniston, D.H. Davis, B.D. Jones, B. Sanjeevaiah and J. Zakrzewski, Nuovo Cimento 23, 702 (1962).

14. D.H. Davis, M. Csejthey-Barth, J. Sacton, B.D. Jones, B. Sanjeevaiah and J. Zakrzewski, Nuovo Cimento 22, 275 (1961).

15. R. Cester, G. Ciocchetti, A. Debenedetti, A. Marzari-Chiesa, G. Rinaudo, C. Deney, K. Gottstein and W. Püschel, Nuovo Cimento 22, 1069 (1961).

16. A. Filipkowski, E. Marquit, E. Skrzypczak and A. Wroblewski, Nuovo Cimento 25, 1 (1962).

17. W. Knight, F.R. Stannard, F. Oppenheimer, B. Rickey and R. Wilson, preprint (1963) [contributed paper to the International Hyper-fragment Conference, March 1963].

18. A.D. Martin, Nuovo Cimento 27, 1359 (1963).

19. E.R. Fletcher, J. Lemonne, P. Renard, J. Sacton, D. O'Sullivan, T.P. Shaw, A. Thompson, P. Allen, Sr. A. Heeran, A. Montwill, J.E. Allen, M.J. Beniston, D.A. Garbutt, R.C. Kumar, P.V. March, J. Pniewski and J. Zakrzewski, Phys.Letters 3, 280 (1963).

20. N.A. Nickols, S.B. Curtis and D.J. Prowse, Phys.Letters 1, 327 (1962). I.R. Kenyon, preprint (1962).

21. I.R. Kenyon, preprint (1962).

22. M. Danysz and J. Zakrzewski, to be published shortly.

23. P. Renard et al., to be published shortly.

24. D. Abeledo, L. Choy, R.G. Ammar, N. Crayton, R. Levi-Setti, M. Raymund and O. Skjeggestad, Nuovo Cimento 22, 1171 (1961).

25. A.Z.M. Ismail et al., report No. 101/62 (1962).

26. W.E. Slater, Nuovo Cimento Suppl. 10, 1 (1958). G.C. Deka, Nuovo Cimento 14, 1217 (1959). S. Lokanathan, D.K. Robinson and S.J. St. Lorent, Proc.Roy.Soc. A 254, 470 (1960).

27. G.C. Deka, D. Evans, D.J. Prowse and M. Baldo-Ceolin, Nucl.Phys. 23, 657 (1961).

28. O. Skjeggestad, Archiv for Mathematik og Naturviolenskab B 54, No. 7 (1959).

29. E.W. Baker and S. Katcoff, Phys.Rev. <u>123</u>, 641 (1961).

30. P. Cüer, report at this Conference, p. 123.

31. B. Bhowmik, Phys.Letters <u>2</u>, 220 (1962).

*   *   *

CAPTIONS TO FIGURES DRAWN ON STENCIL

Fig. 1   Range comparison of:
a) Li^8, 191 events R < 100 μ, 81 events R > 100 μ;
b) mesonic $_\Lambda$Li hyperfragments, 6 events;
c) non-mesonic "$_\Lambda$Li" events, 16 events.

Fig. 2   Range distribution of mesonic and non-mesonic hyperfragments produced by K^- mesons of 1.3 and 1.5 GeV/c momentum.

Fig. 3   Distribution of the distance between the two centres of 54 double centred stars which are between 0.25 and 1.5 μ apart.

Fig. 5   a) Range distribution of the mesonic hyperfragments from the interactions of K^- mesons of 800 MeV/c momentum.
b) Range distribution of the mesonic hyperfragments from the interaction of K^- mesons at rest.

*   *   *

Fig.1

81 events →

n. of events

range (μm)

Fig.2

Mesonic HF

A 1.3 GeV/c

B 1.5 GeV/c

Non mesonic HF

n. of events

Hyperfragment range in microns

Fig. 3

Distance centres in μ

Fig. 5

Hyperfragment range in microns

Hyperfragment range in microns
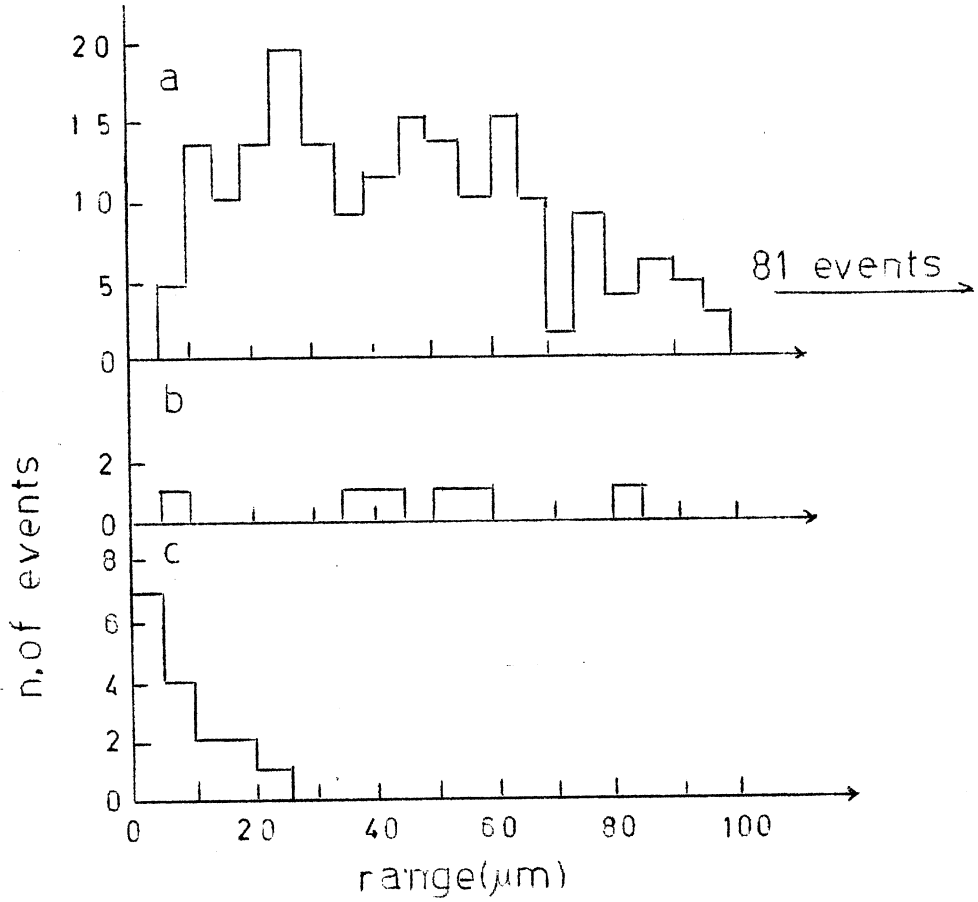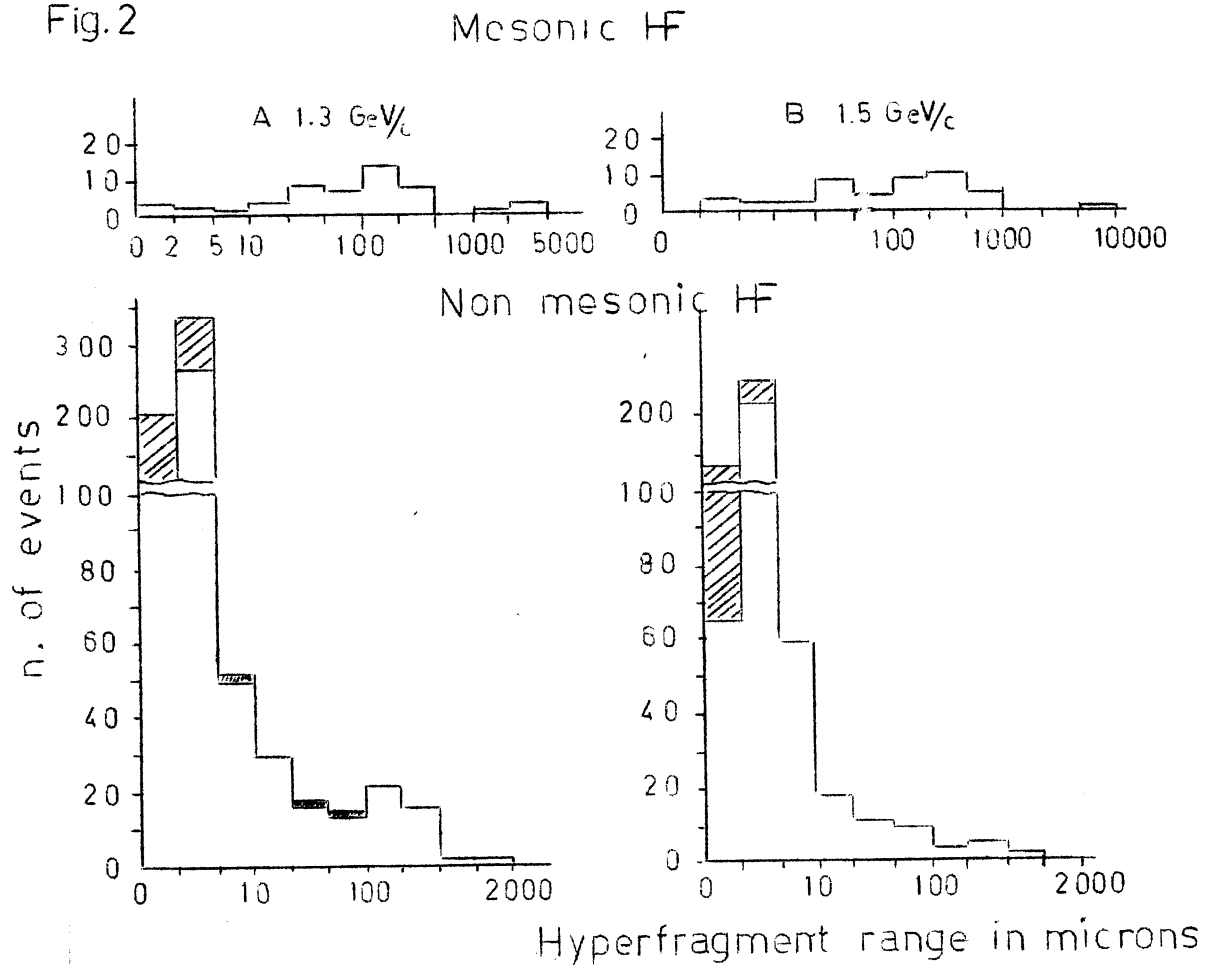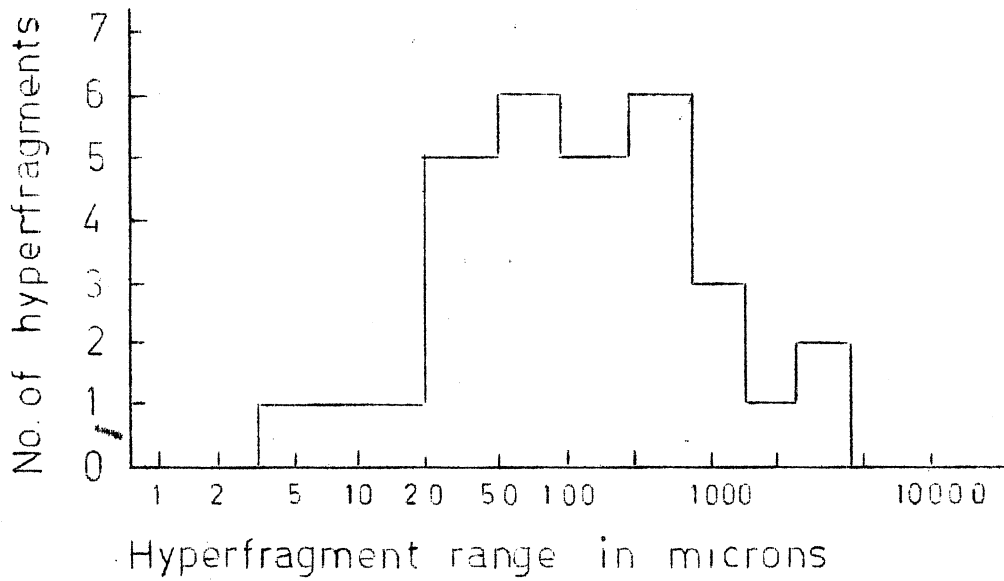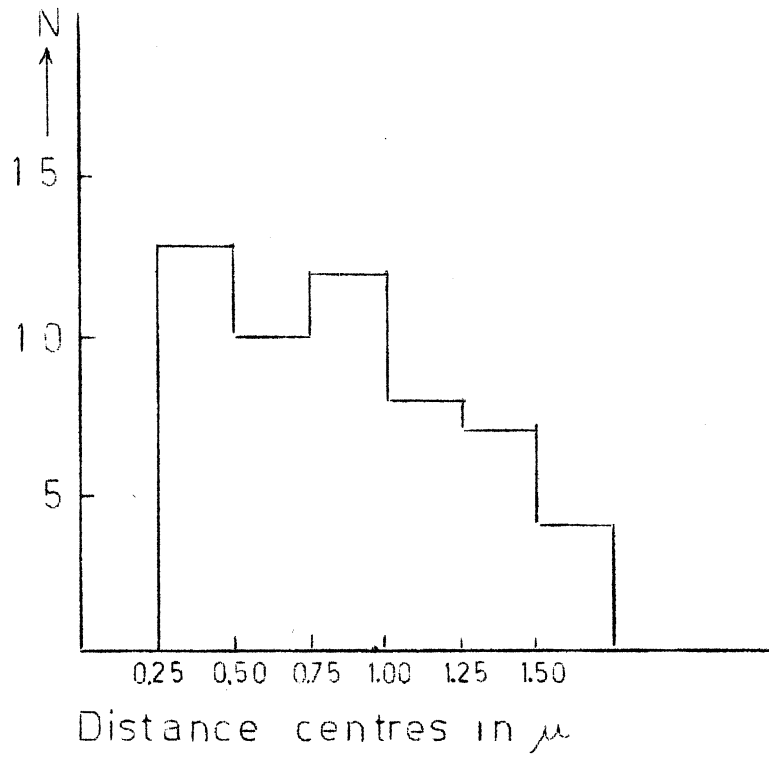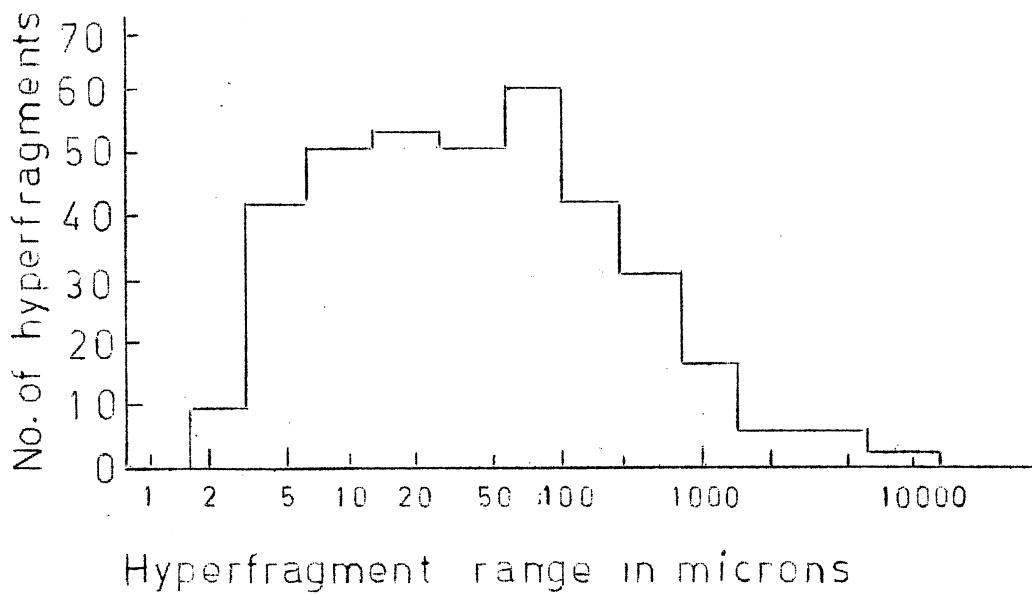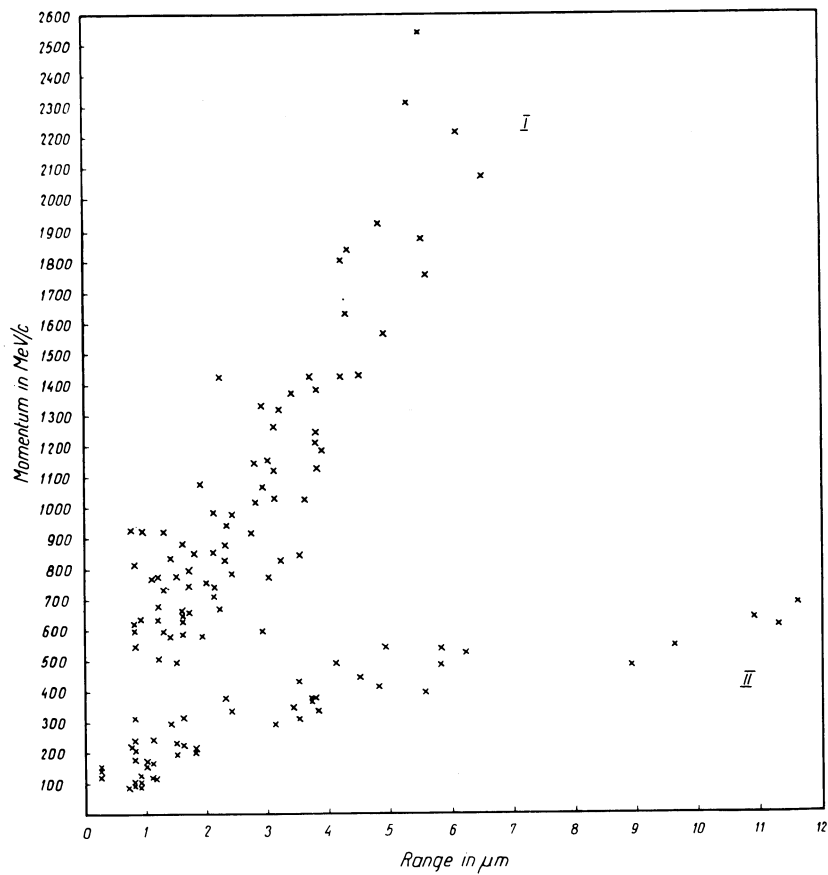
Fig. 4. - Relation between the transverse momentum, p_T, imparted to the struck emulsion nucleus and its observed range, R, in emulsion.
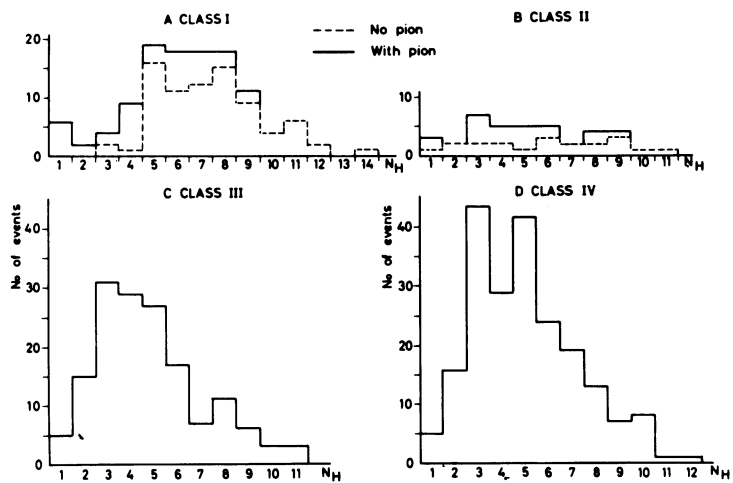
Fig. 6. - Distribution of the heavy prong number, N_h, for stars containing a hyperfragment and for single stars.
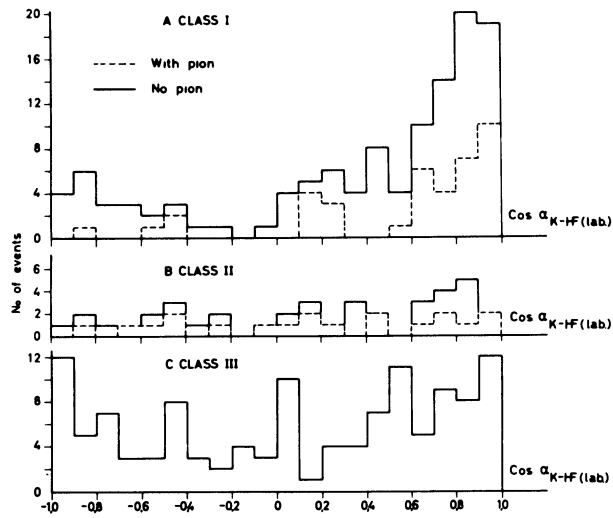
Fig. 7.   Angular distributions of the hyperfragments and
recoils with respect to the line of flight of the inci-
dent K^- mesons.
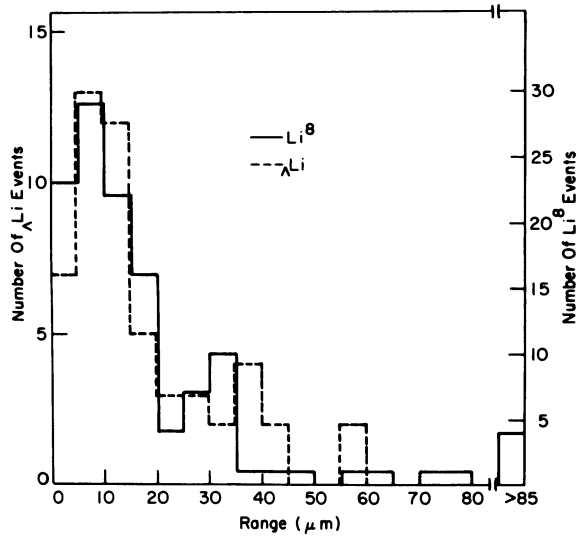
Fig. 8.   Range distribution for $_\Lambda Li$ and Li^8 events,
normalized to the same area.

HEAVY HYPERFRAGMENTS

D.H. Davis,

Physics Department, University College, London.

It has been shown that the bulk of the hyperfragments produced by the interactions of fast K^- mesons with emulsion nuclei are the residual spallation products of silver and bromine and possess mass values in the range A = 50 to A = 100 [1,2]. Thus one is able to obtain a sample, by a selection using a range criterion alone, typically R ≤ 5 μm, which consists almost entirely of these heavy hyperfragments. That they are indeed heavy is effectively demonstrated by Fig. 1 which shows the range distribution of the secondary particles from their non-mesonic disintegrations. The sharp fall-off of tracks of lengths less than 32 μm (corresponding to an α partial energy of 7 MeV) is attributed to the Coulomb barrier effect present in the decay of a heavy hypernucleus.

With such a sample of heavy hypernuclei it is possible to estimate their B_Λ values, the non-mesonic to π^--mesonic ratio and the neutron to proton stimulation ratio.

The upper limit of their B_Λ has been deduced from the observed energy releases in both their non-mesonic and mesonic disintegrations [3].

Figure 2 shows the visible energy release distribution for 470 non-mesonic disintegrations of these 'spallation hypernuclei'. The visible energy release in a decay has been computed as the sum of the kinetic and binding (8 MeV/particle) energies of the emitted charged particles, all of which were assumed to be protons. The available energy in decays of this kind is $M_\Lambda - M_n - B_\Lambda + B_n = (184 - B_\Lambda)$. Therefore the observation of total energy releases close to 150 MeV allows us to put an upper limit of about 35 MeV on the B_Λ of this sample.

Details of 17 π^--mesonic decays[3-5], which are attributed to the same class of hypernuclei, are set out in Table 1.

These are assumed to be heavy using the same considerations which have been applied to the sample which decay non-mesonically. However, it should be borne in mind that for no individual event is the identity ascertained. The estimates quoted for B_Λ are upper limits since the emission of a neutron or the excitation of the final recoil nucleus will escape detection.

Figure 3 shows the B_Λ versus $A_{core}^{-2/3}$ distribution obtained by the EFINS - Brussels group[3]*)[A], the low mass points being from a recent compilation by Ammar et al.[6]. The masses of the spallation hypernuclei have been roughly estimated from the number of charged particles emitted in the primary interaction, bearing in mind that no distinction can be made between either silver (A = 108) or bromine (A = 80) as the target nucleus. However, as can be seen, this uncertainty on the $A_{core}^{-2/3}$ plot is not too serious and thus it is suggested by extrapolation to infinite A from these results, that D_Λ, the Λ-nucleus potential well depth, cannot much exceed 30 MeV.

In order to obtain a lower limit for B_Λ for this type of hypernucleus an attempt[7] has been made to study the reaction

$$K^- + Br \rightarrow {_\Lambda}Br + \pi^- \tag{1}$$

by stopping K^- mesons in the Ecole Polytechnique heavy liquid bubble chamber containing pure freon (CF_3 Br) and looking at the high-energy end of the resulting π^- meson spectrum. The highest energy π^- meson which can result from a K^- meson capture at rest in freon would be that in reaction (1) and would correspond to the production of ${_\Lambda}$Br in its ground state. At the present time no π^- meson has been found of sufficient energy that it could only be attributed to reaction (1).

---

*) The new values for the upper limit of B_Λ are in very good agreement with those found in Ref. 3.

A compilation[8] yields the value 3800/17 for the non-mesonic to π^--mesonic ratio in the decay of heavy spallation hyper-fragments. This figure may be somewhat low if an appreciable number of non-mesonic disintegrations involve the emission of neutrons only and thereby pass unnoticed.

The neutron to proton stimulation ratio for the weak Λ-hyperon interaction in these heavy hypernuclei has been estimated, using Monte Carlo calculations, as $\sim 1.6 - 2$ [9] and 4 [10]. However, the n/p stimulation ratio obtained by this procedure would be an overestimate if the multinucleon stimulation of the Λ-hyperon was significant.

※　※　※

REFERENCES

1) B.D. Jones, B. Sanjeevaiah, J. Zakrzewski, M. Csejthey-Barth, J.P. Lagnaux, J. Sacton, M.J. Beniston, E.H.S. Burhop and D.H. Davis, Phys.Rev. 127, 236 (1962).

2) E. Fletcher, J. Lemonne, P. Renard, J. Sacton, D. O'Sullivan, T.P. Shah, A. Thompson, P. Allen, Sr. M. Heeran, A. Montwill, J.E. Allen, M.J. Beniston, D.A. Garbutt, R.C. Kumar, P.V. March, T. Pniewski and J. Zakrzewski, Phys.Letters 3, 280 (1963).

3) D.H. Davis, R. Levi-Setti, M. Raymund, O. Skjeggestad, G. Tomasini, J. Lemonne, P. Renard and J. Sacton, Phys.Rev.Letters 9, 464 (1962).

4) K⁻ European Collaboration (to be published).

5) J. Cuevas, J. Diaz, D. Harmsen, W. Just, H. Kramer, H. Spitzer, M.W. Teucher and E. Lohrmann, Nuovo Cimento 27, 1500 (1963).

6) R.G. Ammar, L. Choy, W. Dunn, M. Holland, J.H. Roberts, E.N. Shipley, N. Crayton, D.H. Davis, R. Levi-Setti, M. Raymund, O. Skjeggestad and G. Tomasini, Nuovo Cimento 27, 1078 (1963).

7) Brussels, EFINS, Oslo and U.C.L. emulsion groups.

8) EFINS, Hamburg, K⁻ European Collaboration and Oxford results.

9) J.P. Lagnaux, private communication 1963.

10) M.J. Beniston, private communication 1963.

Table 1

Details of π^--mesonic 'spallation hyperfragment' decays

Event No.	Origin	HF range (μm)	HF decay products Identity	HF decay products K.E. (MeV)	Assumed decay mode	Upper limit of B_Λ (MeV)
EFINS 1	RK⁻	~1	π^- (p)	6.4 / 5.2	$\pi - p - r$	26.0
EFINS 2	"	~1	π^-	7.1	$\pi - r$	38.5
EFINS 3	800 MeV/c K⁻	2	π^- (p)	0.9 / 4.1	$\pi - p - r$	32.6
Bx 1	1.5 GeV/c K⁻	4.4	π^-	16.6	$\pi - r$	29.0
Bx 2	"	2.6	π^- (p)	7.1 / 7.4	$\pi - p - r$	23.1
Bx 46/1608	"	3.7	π^-	18.5	$\pi - r$	27.1
Wars. 188/188	"	5.4	π^- (p)	10.5 / 3.0	$\pi - p - r$	24.1
West. 95/98	"	2.0	π^- (p)	4.5 / 1.3	$\pi - p - r$	31.8
UCD 65/15	1.3 GeV/c K⁻	4.0	π^- (p)	1.8 / 7.1	$\pi - p - r$	28.7
UCL 76/2	"	1.9	π^-	13.5	$\pi - r$	32.1
UCL 71/444	"	1.5	π^-	15.9	$\pi - r$	29.7
UCL T61/23/11	RK⁻	0.8	π^-	7.8	$\pi - r$	36.8
DIAS 51/1435	1.3 GeV/c K⁻	0.8	π^- (p)	4.0 / 5.7	$\pi - p - r$	27.9
Ha. 1	1.5 GeV/c K⁻	3.6	π^-	24.5	$\pi - r$	21.1
Ha. 2	"	4.4	π^-	18.0	$\pi - r$	27.6
Ha. 3	"	5.1	π^-	17.3	$\pi - r$	28.3
Ha. 4	"	12.5	π^-	15.5	$\pi - r$	30.1

Fig. 1. Range distribution of the secondary particles from non-mesonic decays of hyperfragments with $R \leqslant 5\mu$m.
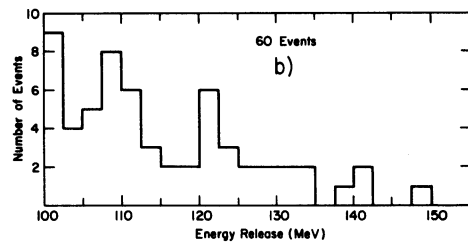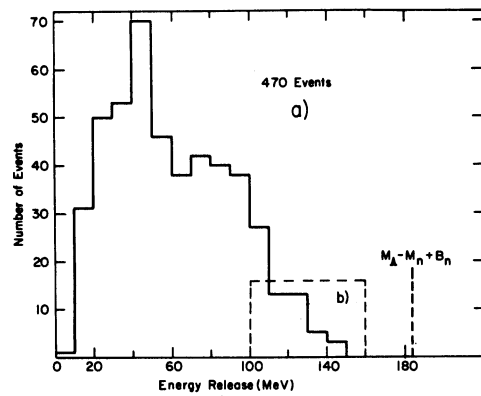
Fig. 2. The visible energy release for 470 non-mesonic disintegrations of "spallation hypernuclei".
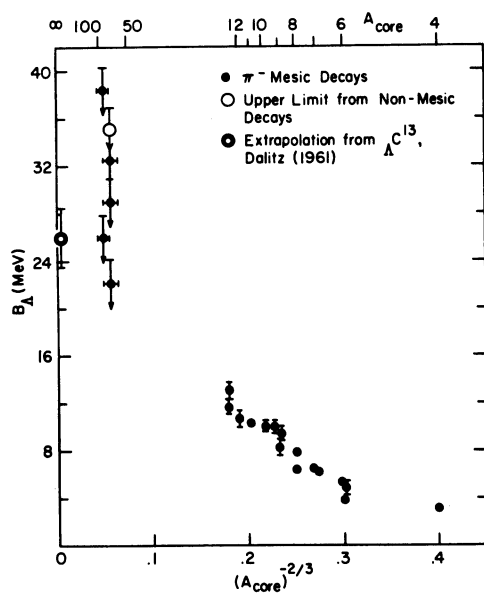
Fig. 3. - B_Λ versus $A_{core}^{-2/3}$ distribution obtained by EFINS-Bruxelles group.

A DOUBLE HYPERFRAGMENT EVENT

J. Pniewski,
Institute of Experimental Physics,
University of Warsaw, Poland.

This is a report on the work done by the European K^- collaboration[1] concerning the production and decay of a double hyperfragment. The event was found in a systematic search by the collaborating groups for events of double strangeness in a stack of Ilford K.5 nuclear emulsion exposed to the 1.3 and 1.5 GeV/c K^- beam at CERN. Altogether some 50,000 interactions of K^- mesons were observed, and among them several double strangeness events were recognized. In one case, the production of a Ξ^- hyperon on an emulsion nucleus according to the reaction

$$K^- + n = \Xi^- + K^0$$
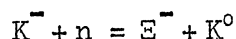
was observed.

The Ξ^- hyperon comes to rest and is absorbed by a light nucleus of the emulsion — most likely by carbon 12. In this capture a double hyperfragment is produced. It could be recognized by the mesonic cascade decay. The most likely interpretations of the double hyperfragment are those in terms of either $_{\Lambda\Lambda}Be^{10}$ or $_{\Lambda\Lambda}Be^{11}$. A photomicrograph and explanatory schematic drawing of the event are given in Fig. 1.

The four stars were interpreted as follows:

star A - interaction of a 1.5 GeV/c K^- meson with the production of a Ξ^- hyperon (track 1);

star B - capture of the Ξ^- hyperon with the production of a double hyperfragment (track 6);

star C - decay of the double hyperfragment with the emission of a π^- meson (track 7) and an ordinary hyperfragment (track 9);

star D - decay of the ordinary hyperfragment with the emission of
a π^- meson (track 10).

The π^- mesons gave capture stars observed in other pellicles.
The ranges of both the double hyperfragment and the ordinary hyperfrag-
ment resulting from its decay are very short and therefore the analysis
of the event presents serious difficulties. In particular, the most
important feature of the analysis was the demonstration that one of the
two π^- meson tracks originated in star C and the other in star D. One
could discard all interpretations other than the production and subse-
quent mesonic cascade decay of a double hyperfragment. The probability
of a chance coincidence of a background star (star D) has been estimated
to be less than 10^{-10} per each interacting K^-; on the other hand, the
probability of the production of a slow Ξ^- hyperon followed by the dis-
cussed sequence of events seems to be reasonable in our experimental
conditions. One may notice that the production of a double hyperfrag-
ment in a Ξ^- capture star is energetically favoured and that the competing
reactions of the type

$$C^{12} + \Xi^- = {}_\Lambda B^{12} + \Lambda^0, \quad \text{or} \quad C^{12} + \Xi^- = B^{11} + 2\Lambda^0$$
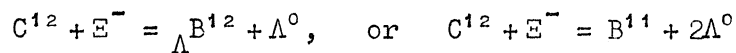
do not suppress the production of a double hyperfragment.

For the identification of the event, at first the ordinary
hyperfragment was analysed only by kinematical considerations concerning
its decay products (star D). The possible identities and decay schemes
of the double hyperfragment were assigned from a study of both the pro-
duction and decay processes (stars B and C). In particular, the
Coulomb barrier argument was used to establish the fact that the Ξ^-
hyperon capture occurred on a light nucleus of the emulsion. The final
results of this analysis are summarized in the table.

From a comparison of the binding energy $B_{\Lambda\Lambda}$ of the two Λ^0
hyperons in double hyperfragments with B_Λ for ordinary hyperfragments,
one can expect to obtain information not only on the strength of the
$\Lambda^0 - \Lambda^0$ interaction but also on the spin-dependent part of the B_Λ in or-
dinary hyperfragments[2]. The value of $\Delta B_{\Lambda\Lambda} = B_\Lambda({}_{\Lambda\Lambda}Z^A) - B_\Lambda({}_\Lambda Z^{A-1})$

presented in column 6 of the table is the net contribution of the Λ^0-Λ^0 interaction and the reduction due to the spin-dependent part of the Λ^0-core interaction, provided that core distortion effects may be neglected. In the case of $_{\Lambda\Lambda}Be^{10}$, when the spin of the core is zero, $\Delta B_{\Lambda\Lambda}$ gives the contribution of the Λ^0-Λ^0 interaction only. On the other hand, in the case of $_{\Lambda\Lambda}Be^{11}$ the spin of the core differs from zero and the spin-dependent part of the Λ^0-core interaction must be taken into account. In this case, using the recent data of Λ^0-binding energies for ordinary hyperfragments, one can evaluate the pure contribution of the Λ^0-Λ^0 interaction to be approximately 1 MeV higher than $\Delta B_{\Lambda\Lambda}$.

From all the interpretations presented in the table, those in terms of lithium are less probable as they require the assumption that in star B an additional invisible prong exists. One of the three other interpretations in terms of beryllium involves the emission of a neutron in the decay of the double hyperfragment. On purely experimental grounds there is no reason to exclude this decay mode. If a neutron is really emitted in the decay of the double hyperfragment, then one can obtain less information from the present event concerning the Λ^0-Λ^0 interaction.

For two other decay schemes of beryllium double hyperfragments:

$$\left.\begin{array}{l} _{\Lambda\Lambda}Be^{10} \rightarrow {_\Lambda}Be^9 + H^1 + \pi^- \\ _\Lambda Be^9 \rightarrow 2Be^4 + H^1 + \pi^- \end{array}\right\} \Delta B_{\Lambda\Lambda} = 4.5 \pm 0.4 \text{ MeV}$$

$$\left.\begin{array}{l} _{\Lambda\Lambda}Be^{11} \rightarrow {_\Lambda}Be^{10} + H^1 + \pi^- \\ _\Lambda Be^{10} \rightarrow 2He^4 + H^2 + \pi^- \end{array}\right\} \Delta B_{\Lambda\Lambda} = 3.2 \pm 0.6 \text{ MeV}$$
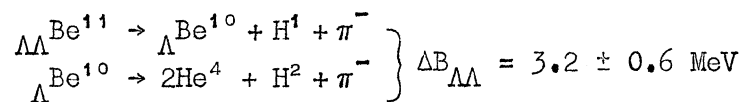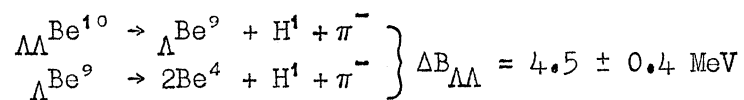
the values of $\Delta B_{\Lambda\Lambda}$ are well determined and give the same sign and approximately the same quantitative estimate of the strength of the Λ^0-Λ^0 interaction, provided that the spin-dependent part of the Λ^0-core interaction in $_{\Lambda\Lambda}Be^{11}$ is taken into account.

* * *

REFERENCES

1) M. Danysz, K. Garbowska, J. Pniewski, T. Pniewski, J. Zakrzewski,
   E.R. Fletcher, J. Lemonne, P. Renard, J. Sacton, W.T. Toner,
   D. O'Sullivan, T.P. Shah, A. Thompson, P. Allen, Sr. M. Heeran,
   A. Montwill, J.E. Allen, M.J. Beniston, D.H. Davis, D.A. Garbutt,
   V.A. Bull, R.C. Kumar and P.V. March, Phys.Rev.Letters 11,
   29 (1963); also

   "The identification of a double hyperfragment", to be published in
   Nuclear Physics.

2) R.H. Dalitz, lecture given at the Hyperfragment Conference,
   St. Cergue (1963), p. 147.

*　　*　　*

Results of the analysis

Star C		Star D			
Decay mode of the double HF	Binding energy of a Λ^0 hyperon in the double HF $B_\Lambda(_{\Lambda\Lambda}Z)$ (MeV)	Decay mode of the resulting ordinary HF	Binding energy of a Λ^0 hyperon in the ordinary HF $B_\Lambda(_\Lambda Z)$ (MeV)	Binding energy of the 2 Λ^0 hyperons in the double HF $B_{\Lambda\Lambda}(_{\Lambda\Lambda}Z^A) = B_\Lambda(_{\Lambda\Lambda}Z^A) + B_\Lambda(_\Lambda Z^{A-1})$ (MeV)	$\Delta B_{\Lambda\Lambda} = B_\Lambda(_{\Lambda\Lambda}Z^A) - B_\Lambda(_\Lambda Z^{A-1})$ (MeV)
$_{\Lambda\Lambda}Be^{10} \to {}_\Lambda Be^9 + H^1 + \pi^-$	11.0 ± 0.4	$_\Lambda Be^9 \to 2He^4 + H^1 + \pi^-$	7.2 ± 0.6	17.5 ± 0.4	4.5 ± 0.4
$_{\Lambda\Lambda}Be^{11} \to {}_\Lambda Be^9 + H^1 + n + \pi^-$	$< 7.6 \pm 0.7$	$_\Lambda Be^9 \to 2He^4 + H^1 + \pi^-$	7.2 ± 0.6	$< 16.0 \pm 0.4$	$< -0.3 \pm 1.0$
$_{\Lambda\Lambda}Be^{11} \to {}_\Lambda Be^{10} + H^1 + \pi^-$	11.1 ± 0.4	$_\Lambda Be^{10} \to 2He^4 + H^2 + \pi^-$	7.5 ± 0.6	19.0 ± 0.6	3.2 ± 0.6
$_{\Lambda\Lambda}Li^8 \to {}_\Lambda Li^7 + H^1 + \pi^-$	10.8 ± 0.4	$_\Lambda Li^7 \to He^4 + H^2 + H^1 + \pi^-$	6.5 ± 0.6	16.3 ± 0.4	5.3 ± 0.4
$_{\Lambda\Lambda}Li^9 \to {}_\Lambda Li^8 + H^1 + \pi^-$	10.9 ± 0.4	$_\Lambda Li^8 \to He^4 + H^3 + H^1 + \pi^-$	5.4 ± 0.6	17.4 ± 0.4	4.4 ± 0.4
$_{\Lambda\Lambda}Li^{10} \to {}_\Lambda Li^8 + H^1 + n + \pi^-$	$< 7.5 \pm 0.5$	$_\Lambda Li^8 \to He^4 + H^3 + H^1 + \pi^-$	5.4 ± 0.6	$< 15.5 \pm 0.4$	$< -0.5 \pm 0.6$

Note : For calculation of $\Delta B_{\Lambda\Lambda}$ given in column 6, the best known values of $B_\Lambda(_\Lambda Z)$ have been used.

All references are given in Ref. 1).
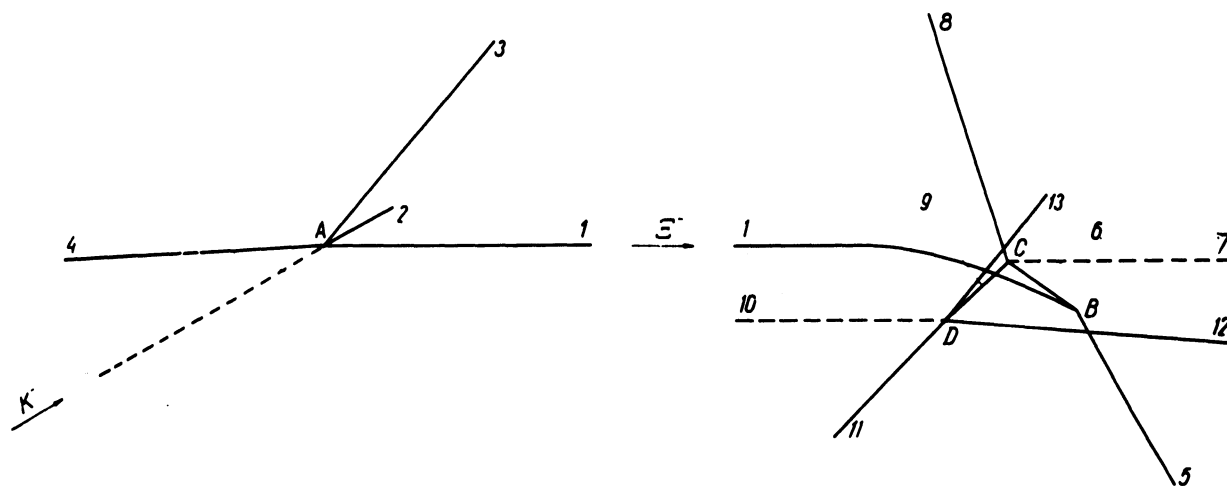
A schematic drawing of the event. A Ξ^- hyperon produced by a 1,5 GeV/c K$^-$ meson comes to rest and is absorbed by a light nucleus /C,N,O/ of the emulsion. In this capture a double hyperfragment is produced, which is identified from the mesonic cascade decay.

V. ORDINARY FRAGMENTS

EMISSION OF LIGHT FRAGMENTS FROM THE DISINTEGRATION OF HEAVY NUCLEI IN PHOTOGRAPHIC EMULSION CAUSED BY HIGH-ENERGY PARTICLES; FIRST COMPARISON WITH HYPERFRAGMENT EMISSION.

P. Cüer,

Département de Physique Corpusculaire,
Centre de Recherches Nucléaires, Strasbourg-Cronenbourg.

In high-energy physics, fragmentation is the best means of liaison between nuclear physicists and the physicists studying strange particles. The former excite the nucleus to higher and higher energies in order to obtain, after fragments, unstable hyperfragments which they would like to be able to consider as convenient indicators of fragmentation, whereas the strange particle physicists view these hyperfragments simply as a means of studying the hyperon-nucleon, or even hyperon-hyperon, forces.

Fragmentation is a very complicated history of the disintegration of a nucleus. In principle, a fragment consists entirely of nucleonic matter ejected from a nucleus in a state of excitation or broken. Therefore, every case must be studied with the utmost care, if possible on a given nucleus with a given projectile at a given energy.

In this preliminary study, which is mainly to clear up a little the clouds surrounding the comparison between the emission of fragments and of hyperfragments, we confine ourselves to examples of fragments well identified by us. For convenience, the comparisons which follow were made for fragments with charge 3, 4 and 5, especially Li^8, Be^8, and B^8. Since the proportion of Li^9 and of B^8 amongst the fragments is only a few per cent, we have studied in particular the emission of Li^8 and Be^8, which allows us to connect our results with the work carried out at a lower energy, especially by the groups of Perfilov and Lozhkin in Leningrad, and of Pniewski in Warsaw (energy range several hundred MeV to 9 GeV). The global comparisons were made, in this first

stage, with the emission of all hyperfragments of charge 3 and 4. In the absence of standardization between the different schools which investigate fragments and hyperfragments, which would be most desirable, the fragments and hyperfragments tabulated are those obtained by our own group during the last two years.

These results were obtained by Drs. H. Braun and G. Baumann of our Laboratory from a study of emulsion stacks exposed at CERN, thanks to the courtesy of Drs. Lock and Combe, either stacks exposed especially for the Strasbourg Group or CERN co-operation stacks (for example, for the π^- mesons of 17.2 GeV/c) or stacks exposed with Hamburg for the K^- of 1.5 GeV/c, thanks to the kindness of Professor Teucher of Hamburg and of Dr. Winzeler of Bern.

As an initial indication for the classification of these phenomenological comparisons one can choose the evaporation characteristics without evident prejudice of the fundamental mechanism. This choice is based, however, on previous results and also on the general tendency of most of the results obtained. The chosen fragments of Li^8 and Be^8, as well as the hyperfragments, are related to heavy nuclei disintegrations so that all comparisons are statistically valid. The presentation of the results is given in the order in which they were obtained, namely as incident particle protons of 24 GeV, π^- mesons of 17.2 GeV, protons of 14 GeV, K^- of 1.5 GeV, and some results from stopping π^- mesons.

The emission of fragments of charge greater than 2 is a nuclear phenomenon which is important at these incident high energies because in this field we obtain a ratio of $Li^8 / Li^6 + Li^7$ of the order of some per cent and the proportion of stars containing Li^8 also of the order of 1 to 2%. It is therefore probable that several fragments of $Z \geq 3$ are emitted during the course of only one inelastic interaction of a high-energy particle with a nucleus of silver or bromine. The relative proportion of hyperfragments is an important fraction, in general, of the emission of Li^8, mainly in the case of K^- when their

production becomes a quantitatively comparable phenomenon, even greater for slow K^- than the emission of ordinary fragments.

In order to facilitate these quantitative experimental comparisons with the classical nuclear theory, the energy spectra have been measured as well as the angular distribution which could give a preliminary indication of the emission mechanism.

The identification of Li^8, thanks to hammer tracks, is immediate; those of Be^8 were made from the two α particles emitted with a small calculable correlation angle; this identification is evidently only possible for the ground state. The comparison is therefore only applicable to the fundamental levels of fragments and hyperfragments. It seems, in any case, in agreement with other studies, that until now one can only observe a very small production (if any) of excited states.

If the fragmentation theory was definitely known, that of hyperfragmentation would certainly be facilitated. However, actually nuclear physicists and particle physicists count on each other, to some extent, the one hoping to find indications in the hyperfragmentation, and the particle physicist trying to invoke the more or less known mechanisms of fragmentation which they have a strong tendency to consider as certain.

Our experimental results are not decisive enough to choose between the 7 or 8 mechanisms which are proposed to explain and to calculate the characteristics of fragmentation of an excited nucleus by high-energy particles. Sometimes the production of nuclear hot points is invoked, sometimes an almost complete mechanical dissociation of the nucleus with the help of fission phenomena, which are due to the secondary interactions of the cascade. Several mechanisms seem to play a part. We believe that the hypothesis of the pick-up or the coalesence of similar particles, which are close together and of high energy, is worth investigation as well as the simultaneous interaction of particles near each other on the same nucleon or group of nucleons for which a theory has still to be developed.

With the statistics which we have at present, a certain number
of results, in the chosen phenomenological terminology, seem to be
definitely established. The parameters for the evaporation curves
give the best fit to the results with a temperature, T, of 8 to 10 MeV,
a potential barrier of 5 to 10 MeV, and a velocity for the centre of
gravity of about 0.01 c.

These parameters are evidently not critical except for T and
have been empirically adjusted. This adjustment is not very sensitive
to the velocity of the centre of mass, and therefore to the inelasticity
factor. This is favourable for the important presentation of the angu-
lar distributions in the C-system which do not vary much from those in
laboratory system.

It is evidently quantitatively possible to invoke several
temperatures during the same process in order to explain the global
aspect of the experimental results. On the other hand, the graphs of
the fragmentationd stribution as a function of the number of star
prongs of different energies confirms that which was already reported
by other experimentalists, that the correlation of the emission of
fragments and hyperfragments is not directly with the "shower" but
with the cascade.

The two extreme interpretations whi h have been invoked,
that is, pure evaporation at low energies or secondary interactions
provoked by the cascade, are both compatible with most of the results.
Nevertheless, some important nuclear remarks are necessary: the
temperature seems too high (greater than the binding of a nucleon) to
indicate a normal mechanism of evaporation from a thermodynamic equili-
brium which is due to the many secondary interactions. The fragment
does not seem to arise from a primary interaction because the angular
distribution of most of the fragments or hyperfragments does not re-
flect it, except for those of high-energy or those emitted from a
light nucleus.

As many experimental results (for emission from heavy nuclei) seemed phenomenologically compatible with some kind of evaporation mechanism, we have looked to see if this morphology of the presentation of results was too gross and too global, and if it did not contain, in fact, several different mechanisms.

With this in mind, we used some recent results obtained in our laboratory on the interactions of slow π^- mesons with light nuclei; in particular, those which have interested us for a long time, because of their possible temporary sub-structures, namely C^{12}, N^{14} and O^{16} giving Li^8. If we study carefully a certain number of favourable reactions, then by a detailed study of the energy and momentum balances we can determine the detailed mechanism of the interaction, and especially the transition via (Be^{10}) and (B^{12}) giving us, respectively, d or α by transition to ground state Li^8. In this precise case we evidently know that the evaporation theory is badly applicable or not at all applicable. The excited levels are not numerous enough, and the number of nucleons is too small. The energy distribution of the Li^8 fragments is, however, compatible with the evaporation curve with parameters which seem reasonable for this excitation energy and no barrier for these recoil fragments of Li^8.

A certain reserve should therefore be shown towards the presentation of the results in the form of evaporation, and the parameters which may differentiate between the different mechanisms which occur remain to be determined.

We think that the detailed and comparative study of nuclear balances with the identification of the initial nucleus (loaded emulsions), all the other conditions remaining identical between the fragments and the hyperfragments of the same nature, would soon enable us to give a more concrete reply on the exact mechanism of their production. But already it seems well established that there is no basic difference between the production of fragments and of hyperfragments.

Table 1

Number of Li^8 or Li^9 fragments emitted
per star for different primary particles of varying energy

Incident particle energy		Frequency of emission of fragments of Li^8 or Li^9	Authors and Laboratory
Protons	5.7 GeV	0.013 ± 0.001 $n_h \gtrsim 5$	Goldsack et al. (1957) [Birmingham]
	9 GeV	0.0188 ± 0.0018 $n_h > 8$	Gajewski et al. (1962) [Warsaw]
		0.015 ± 0.0016 all n_h	
	14 GeV	0.015 ± 0.003 all n_h	Strasbourg
	25 GeV	0.015 ± 0.002 all n_h	Warsaw and Strasbourg (1962)
	28 GeV	0.014 ± 0.002 $n_h \gtrsim 7$	Milwaukee (1962)
π^-	at rest	0.0019 ~ 0.002	Alumkal and Barkow (1960) [Milwaukee] Strasbourg
	4.5 GeV	0.0046 ± 0.0010 $7 \lesssim n_h \lesssim 17$	Skjeggestad (1959) [Oslo]
	4.5 GeV	0.031 ± 0.011 $n_h > 17$	
	17.2 GeV/c	0.015 ± 0.002 all n_h	Strasbourg
K^-	1.5 GeV/c	~ 0.01 all n_h	Strasbourg

<u>Editorial note</u>

The figures show data on fragment and hyperfragment emission from stars caused by protons of 25 GeV (Figs. 1 to 8), π^- mesons of 17.2 GeV/c (Fig.s 9 and 10), protons of 14 GeV (Figs. 11 and 12), K^- mesons of 1.5 GeV/c (Figs. 13 and 14), and π^- mesons at rest (Fig. 19). Figures 15, 16 and 17 show data on the size of the stars which emit fragments or hyperfragments for different primary particles. Figure 18 shows the spatial distribution of pairs of fragments.

* * *

PROTONS ~ 25 GeV
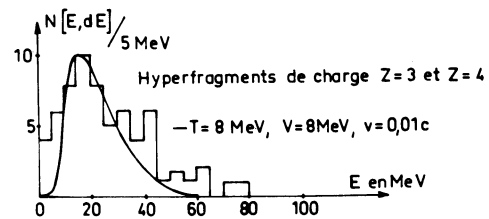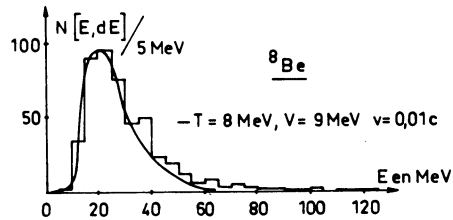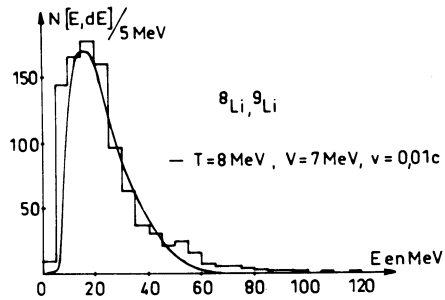
Fig. 1. - Energy spectrum of

    a) Li^8, Li^9 fragments

    b) Be^8 fragments

    c) hyperfragments of charge Z = 3 and 4

SPECTRE DE L'ENERGIE DES FRAGMENTS ^8Li, ^9Li

Fig. 2. - Energy spectrum of Li^8 and Li^9 fragments in the centre of mass system with v = 0.01c.

SPECTRE DE L'ENERGIE DES FRAGMENTS ^{8}Li,^{9}Li

$N[E,dE]/5\,MeV$

PROTONS 25 GeV

$7 < N_h \leqslant 17$

— $T = 8$ MeV ; $V = 7$MeV; $v = 0.01$c

100
80
60
40
20

0 20 40 60 80 100 E en MeV

$N[E,dE]/5\,MeV$

$N_h > 17$

$T = 11$ MeV; $V = 7$MeV; $v = 0.01$c

30
20
10

0 20 40 60 80 100 120 E en MeV
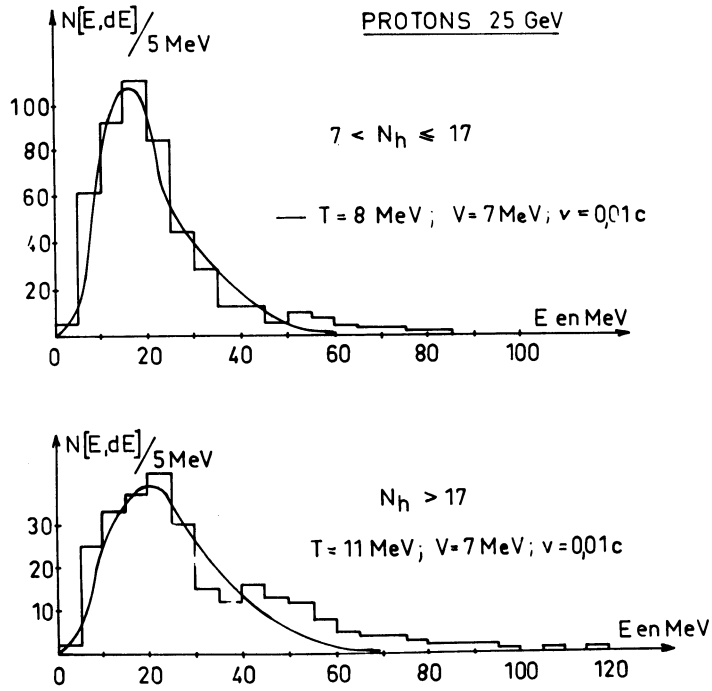
Fig. 3. - Energy spectrum of Li^8 and Li^9 fragments for

    a) $7 < n_h \leq 17$

    b) $n_h > 17$.

SPECTRE DE L'ÉNERGIE DES FRAGMENTS ^{8}Li,^{9}Li

PROTONS $\sim$ 25 GeV

$N[E,dE]/5\,MeV$

     ---: Arrière.
     ——: Avant.

100

50

0 10 20 30 40 50 60 70 80 90 100 E en MeV
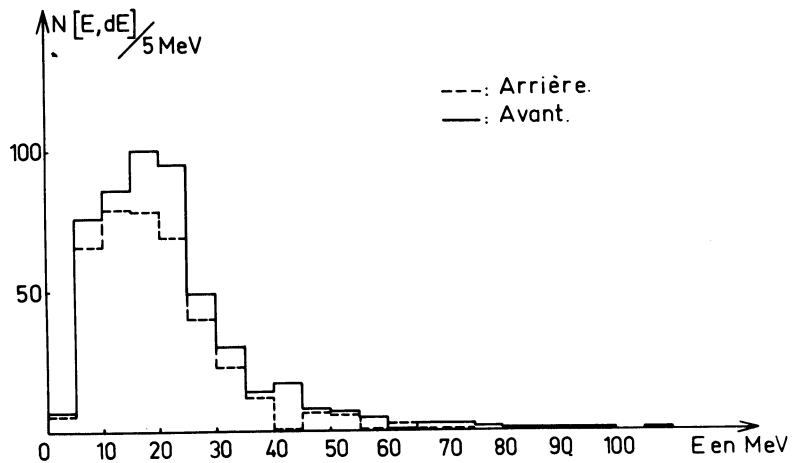
Fig. 4. - Energy spectrum of Li^8 and Li^9 fragments divided in two groups : forward emission and backward emission.

EMISSIONS DES FRAGMENTS ^{8}Li,^{9}Li DANS LES ETOILES

AVEC $N_h < 7$

PROTONS 25 GeV

DISTRIBUTION ANGULAIRE

—— avant correction

---- apres correction

θ° Laboratoire

SPECTRE DE L'ENERGIE

$N[E,dE]/5\,MeV$

E en MeV
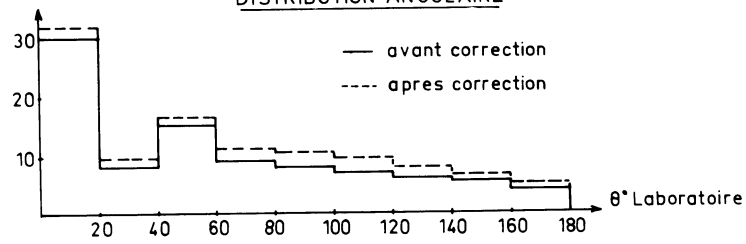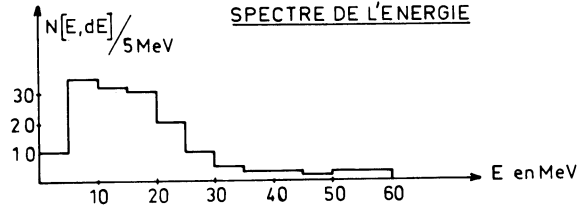
Fig. 5. - Energy and angular distribution of Li^8 and Li^9 fragments for $n_h < 7$ (corrected for scanning loss)
Θ = space angle between the direction of the incident proton and that of the fragment.

DISTRIBUTION ANGULAIRE

$E \leqslant 40\,MeV$

PROTONS 25 GeV

$\dfrac{dN}{d\omega}$

—— avant correction

--- après   "

^{8}Li,^{9}Li

θ° Laboratoire

$\dfrac{dN}{d\omega}$

^{8}Be

θ° Laboratoire
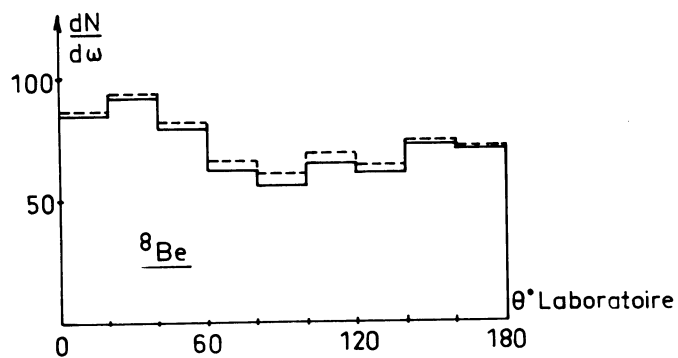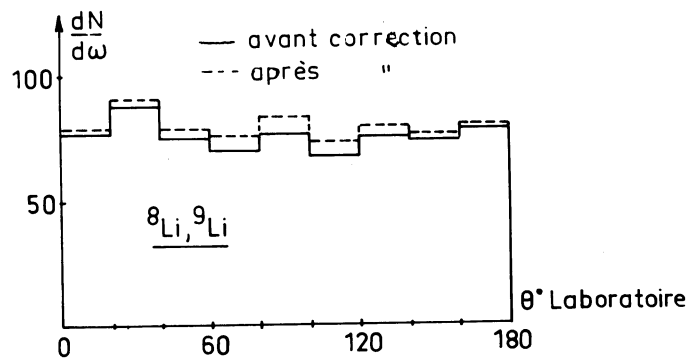
Fig. 6. - Angular distribution of fragments
a) Li^8, Li^9, E(Li^8, Li^9) $\leq$ 40 MeV
b) Be^8 E(Be^8) $\leq$ 40 MeV

DISTRIBUTION ANGULAIRE

CENTRE DE MASSE

$V_{c.d.m.} = 0,01\ c$

$E \leqslant 40\ MeV$

PROTONS 25 GeV
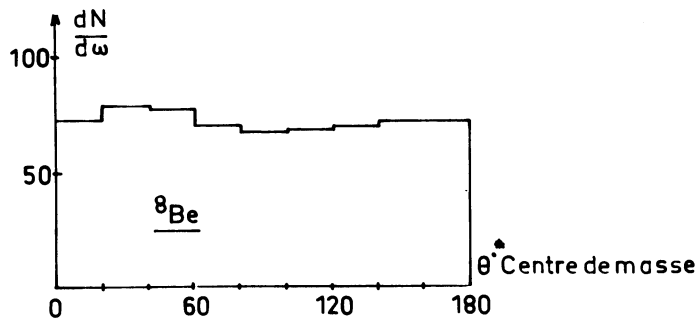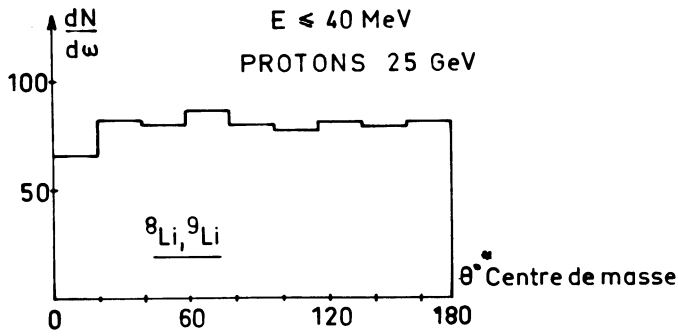
Fig. 7. - Angular distribution of fragments in the centre of mass system with v = 0.01 c.

a) Li^8, Li^9 $E(Li^8, Li^9) \leq 40\ MeV$

b) Be^8 $E(Be^8)$ $\leq 40\ MeV$

DISTRIBUTION ANGULAIRE

$E > 40\ MeV$

PROTONS 25 GeV

— avant correction

--- après   "
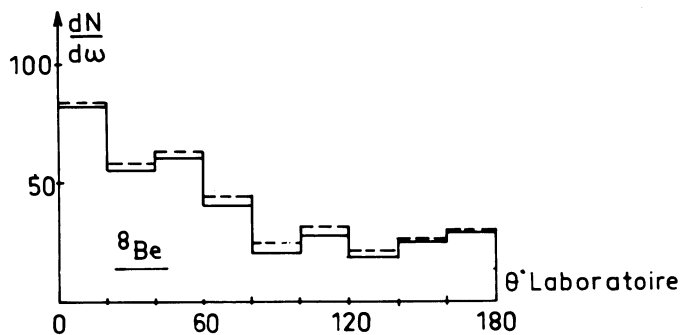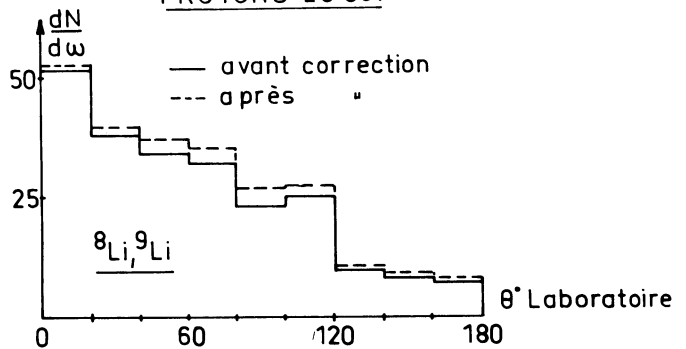
Fig. 8. - Angular distribution of fragments

a) Li^8, Li^9 $E(Li^8, Li^9) \geq 40\ MeV$

b) Be^8 $E(Be^8)$ $\geq 40\ MeV$

SPECTRE DE L'ENERGIE

$P_{\pi^-} \sim 17,2$ GeV/c

$N[E,dE]/5$ MeV

$^{8}Li, ^{9}Li$

— T = 8 MeV , V = 7 MeV , v = 0,01 c

E en MeV

$N[E,dE]/5$ MeV

Hyperfragments de charge Z = 3 et Z = 4

— T = 8 MeV, V = 8 MeV, v = 0,01 c

E en MeV
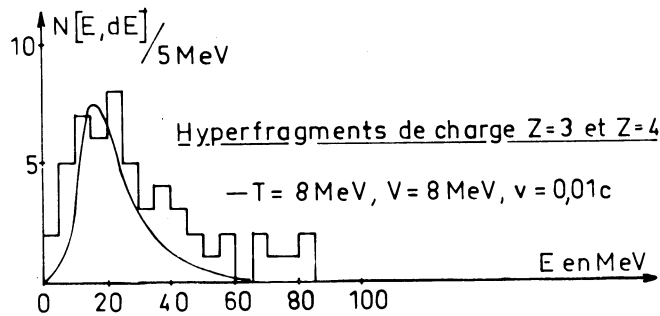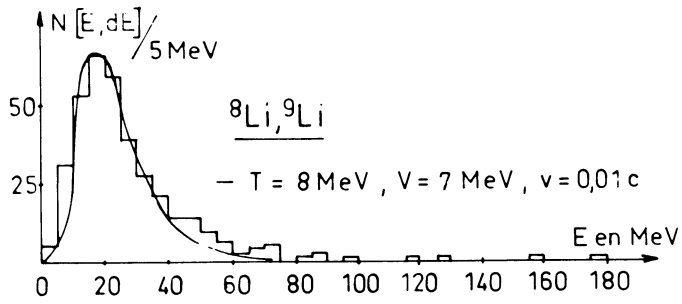
Fig. 9. –   Energy spectrum of
a) Li^{8}, Li^{9} fragments
b)   hyperfragments of charge Z = 3 and Z = 4

DISTRIBUTION ANGULAIRE

$P_{\pi^-} \sim 17,2$ GeV/c

$\frac{dN}{d\omega}$ $^{8}Li,^{9}Li$ E ≤ 40 MeV   —— avant correction
---- après   "

θ° Laboratoire

$\frac{dN}{d\omega}$ $^{8}Li,^{9}Li$ E > 40 MeV

θ° Laboratoire

$\frac{dN}{d\omega}$

Hyperfragments
(Toutes charges)

θ° Laboratoire
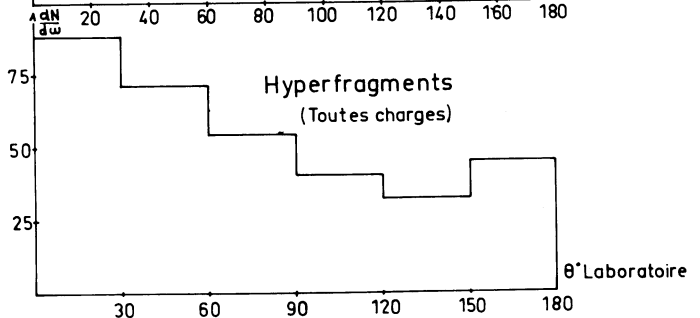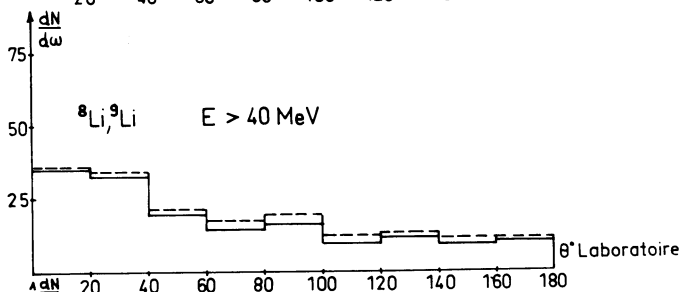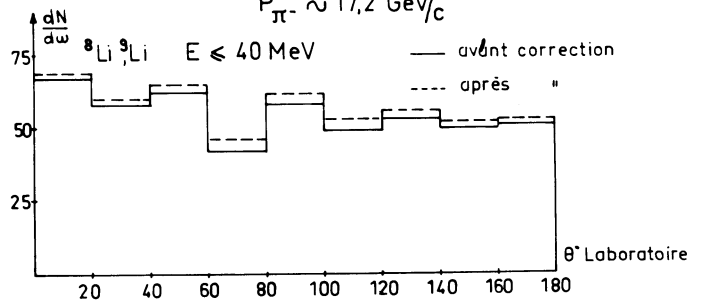
Fig. 10. –   Angular distribution of
a) Li^{8}, Li^{9} fragments $E(Li^{8}, Li^{9}) \leq 40$ MeV
b) Li^{8}, Li^{9} fragments $E(Li^{8}, Li^{9}) > 40$ MeV
c)   hyperfragments (all charges)

SPECTRE DE L'ENERGIE DES FRAGMENTS ^{8}Li,^{9}Li

Protons 14 GeV

Nb. d'événements

23

20

10

— T = 8 MeV , V = 7 MeV, v = 0,01c

0   20   40   60   80   E MeV
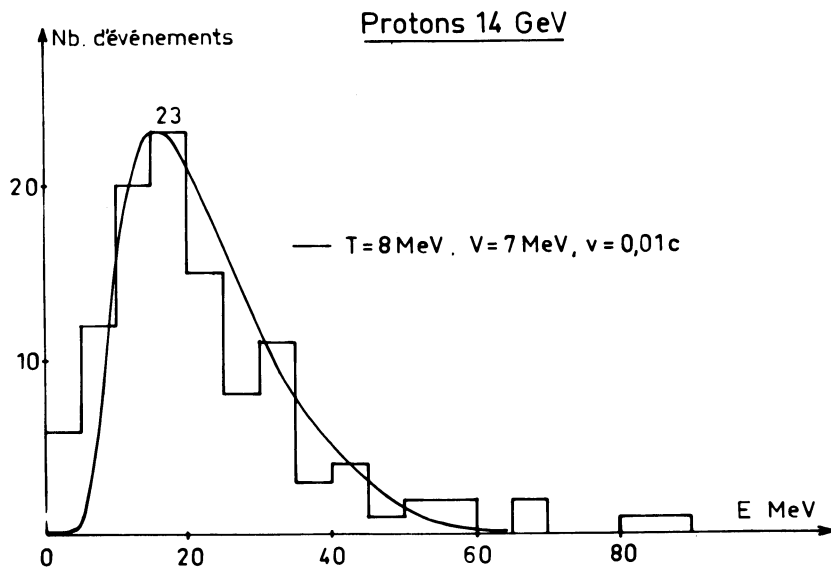
Fig. 11. - Energy spectrum of Li^8, Li^9 fragments.

DISTRIBUTION ANGULAIRE

FRAGMENTS ^{8}Li,^{9}Li

E$_{protons}$ $\sim$ 14 GeV
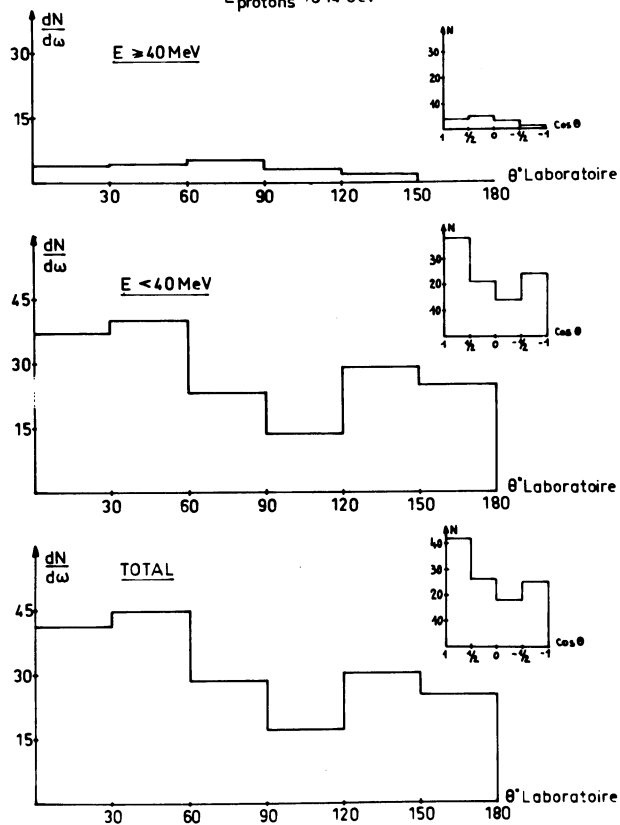
$\frac{dN}{d\omega}$

30

15

E $\geqslant$ 40 MeV

30   60   90   120   150   180 θ°Laboratoire

N

30
20
40

1   ½   0   -½   -1   Cos θ

$\frac{dN}{d\omega}$

45

30

15

E < 40 MeV

30   60   90   120   150   180 θ°Laboratoire

N

30
20
40

1   ½   0   -½   -1   Cos θ

$\frac{dN}{d\omega}$

45

30

15

TOTAL

30   60   90   120   150   180 θ°Laboratoire

N

40
30
20
40

1   ½   0   -½   -1   Cos θ

Fig. 12. - Angular distribution of fragments

a) Li^8, Li^9 E(Li^8, Li^9) $\geq$ 40 MeV

b) Li^8, Li^9 . E(Li^8, Li^9) < 40 MeV

c) Li^8, Li^9 Total

SPECTRE DE L'ENERGIE

$$P_{K^-} \sim 1{,}5 \text{ GeV}\!/\!_c$$

$$^8\text{Li}, \,^9\text{Li}$$

$$T = 8\,\text{MeV}; \quad V = 7\,\text{MeV}; \quad v = 0{,}01\,c$$

Hyperfragments de charge Z = 3 et Z = 4

$$T = 8\,\text{MeV}; \quad V = 8\,\text{MeV}; \quad v = 0{,}01\,c$$
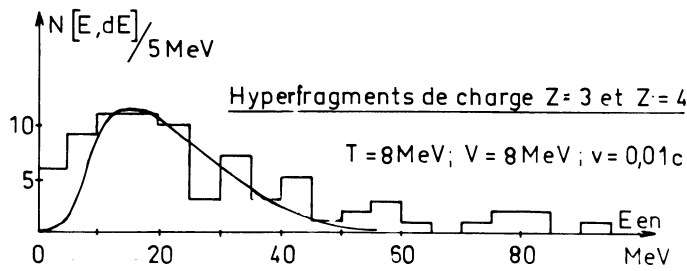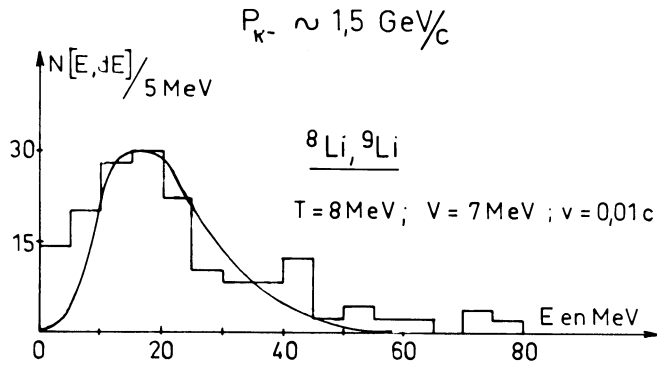
Fig. 13.- Energy spectrum

   a) of Li^8, Li^9 fragments

   b) hyperfragments of charge Z = 3 and Z = 4

DISTRIBUTION ANGULAIRE

$$P_{K^-} \sim 1{,}5 \text{ GeV}\!/\!_c$$

FRAGMENTS $^8\text{Li},^9\text{Li}$ E > 40 MeV

FRAGMENTS $^8\text{Li},^9\text{Li}$ E ⩽ 40 MeV

HYPERFRAGMENTS MESIQUES   R > 5 μ

HYPERFRAGMENTS NON MESIQUES   R > 5 μ
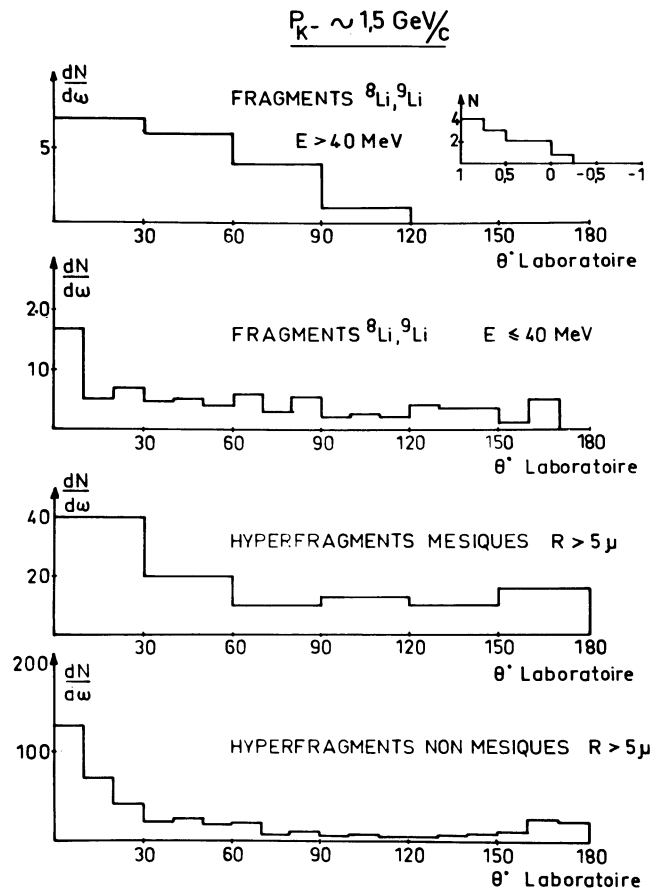
Fig. 14.- Angular distribution of

   a) Li^8, Li^9 fragments $E(\text{Li}^8, \text{Li}^9) > 40$ MeV

   b) Li^8, Li^9 fragments $E(\text{Li}^8, \text{Li}^9) \leqslant 40$ MeV

   c) mesonic hyperfragments with R > 5 μ

   d) non-mesonic hyperfragments with R > 5 μ

DISTRIBUTION DU NOMBRE DE BRANCHES DE L'ETOILE-MERE

$$N_h = N_b + N_g$$

Nb. d'étoiles

PROTONS 25 GeV

— $^8Li, ^9Li$ $E(^8Li) \leqslant 40\,MeV$

---- $^8Li, ^9Li$ $E(^8Li) > 40\,MeV$

Hyperfragments

N_h

Nb. d'étoiles

$P_{\pi^-} \sim 17,2\ GeV/c$

— $^8Li, ^9Li$

········ Hyperfragments

N_h
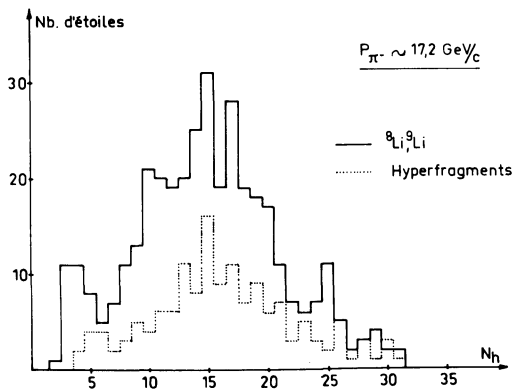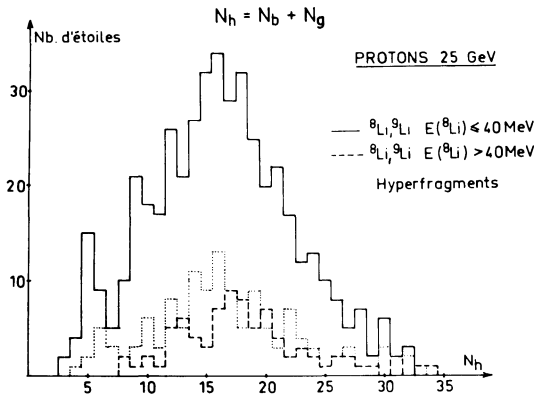
Fig. 15. - Distribution of the number of heavy prongs n_h
for the stars emitting Li^8, or Li^9 fragments
or hyperfragments for
a) protons of 25 GeV as primary particles
b) π^- mesons of 17.2 GeV/c as primary particles.

DISTRIBUTION DU NOMBRE DE BRANCHES

$$P_{K^-} \sim 1,5\ GeV/c$$

$$N_h = N_b + N_g$$

Nb. d'étoiles

$^8Li, ^9Li$

N_h

Nb. d'étoiles avec hyperfragments de parcours < 5 μ

N_h

Nb. d'étoiles avec hyperfragments non mésiques de parcours > 5 μ

N_h

Nb. d'étoiles avec hyperfragments mésiques

N_h
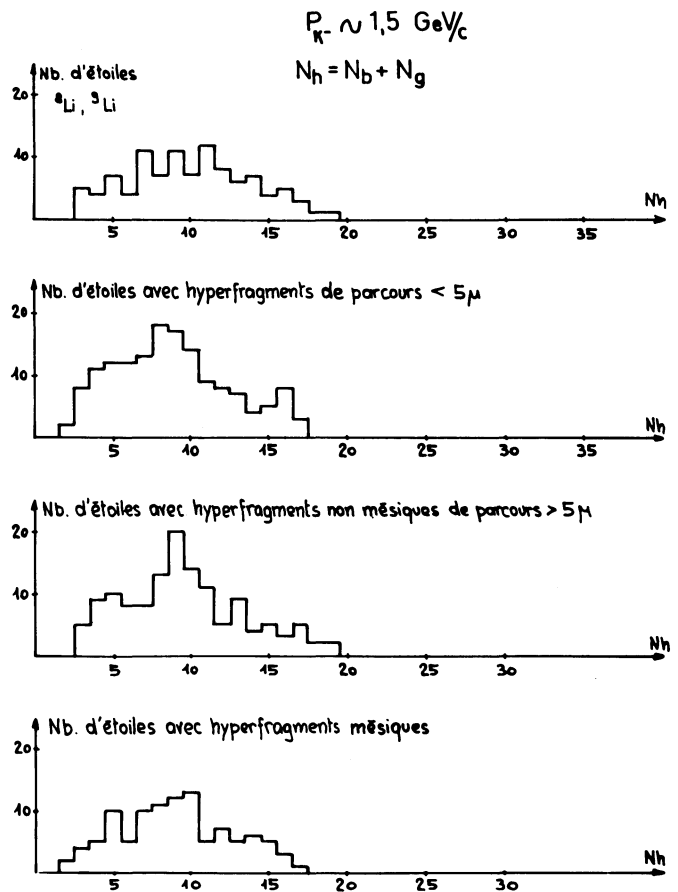
Fig. 16. - Distribution of the number of heavy
prongs n_h of the parent stars produced
by K^- mesons of 1.5 GeV/c for the
emission of
a) Li^8 or Li^9 fragments
b) hyperfragments of range < 5 μ
c) hyperfragments of range > 5 μ
d) mesonic-hyperfragments.

DISTRIBUTION DU NOMBRE DE BRANCHES

N_S

Nb. d'étoiles
^8Li, ^9Li

—— E < 40 MeV

---- E ⩾ 40 MeV

K^- 1,5 GeV/c

Nb. d'étoiles
^8Li, ^9Li

Protons 14 GeV

Nb. d'étoiles
^8Li, ^9Li
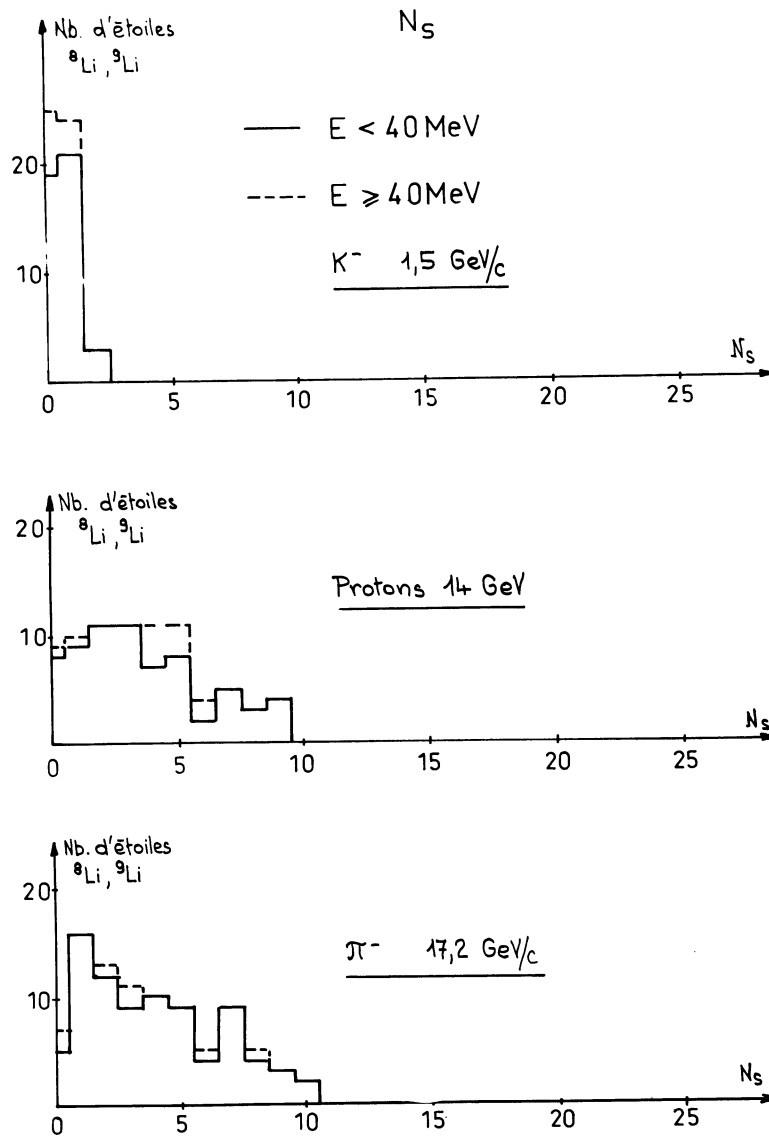
π^- 17,2 GeV/c

Fig. 17. - Distribution of the number of shower particles n_s of the parent stars

    a) Interactions of K^- mesons of 1.5 GeV/c

    b) Interactions of protons of 14 GeV

    c) Interactions of π^- mesons of 17.2 GeV/c.

DISTRIBUTION SPATIALE DES PAIRES DE FRAGMENTS

Z = 3

—— Marteaux doubles (13) Strasbourg $\begin{cases} 25 \text{ GeV protons} \\ 17,2 \text{ GeV}/c \ \pi^- \end{cases}$

----- " " (7) Varsovie 9 GeV protons

·········· " " (4) Milwaukee 28 GeV protons

Courbe approximative de Léningrad pour toutes
les paires de fragments

9 GeV protons
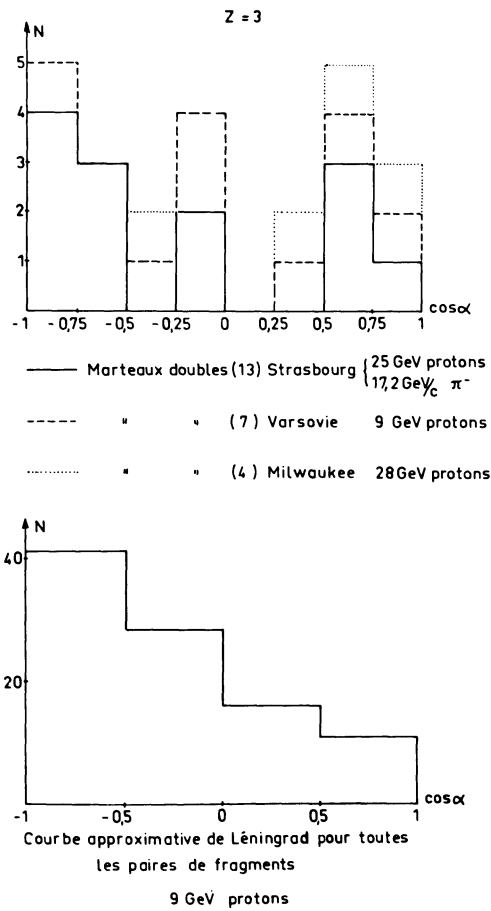
Fig. 18. - Spatial distribution of pairs of fragments

    a) double hammers

    b) all fragments (Leningrad curve).

Spectre d'énergie du ^{8}Li produit par l'interaction des
mésons π^- à l'arrêt sur les noyaux de $^{42}_{6}C, ^{14}_{7}N, ^{16}_{8}O$

$$\pi^- + ^{42}_{6}C \longrightarrow ^{4}_{1}H + ^{4}_{0}n + ^{40}_{4}Be^*$$
$$\hookrightarrow ^{8}_{3}Li + ^{2}_{1}H$$

$$\pi^- + ^{14}_{7}N \longrightarrow ^{4}_{1}H + ^{4}_{0}n + ^{42}_{5}B^*$$
$$\hookrightarrow ^{8}_{3}Li + ^{4}_{2}He$$

$$\pi^- + ^{46}_{8}O \longrightarrow ^{4}_{1}H + ^{4}_{2}He + ^{4}_{0}n + ^{2}_{1}H + ^{8}_{3}Li$$

$$T = 2 \text{ MeV } ; \ V = 0 \ ; \ v = 0,02 \ c$$
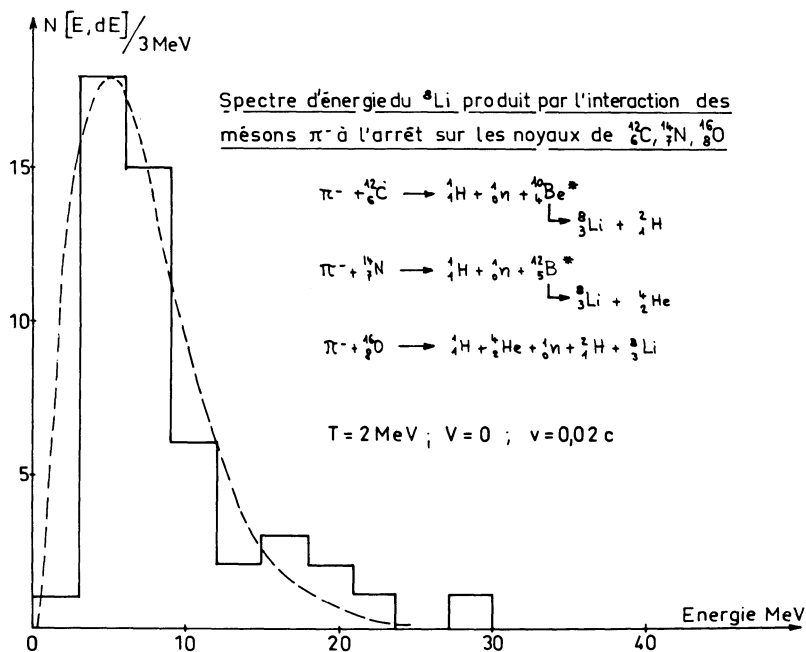
Fig. 19. - Energy spectrum of Li^8 fragments produced by the interaction of π^--mesons at
rest with the nuclei of $^{12}_{6}C$, $^{14}_{7}N$, and $^{16}_{8}O$.

PRODUCTION OF FRAGMENTS WITH CHARGE NUMBER Z = 4 - 9 IN THE INTERACTIONS OF PROTONS WITH HEAVY NUCLEI

O.V. Lozhkin and N.A. Perfilov,
V.G. Khlopin Radium Institute of the Academy of
Sciences of the USSR, Leningrad.

I. INTRODUCTION

It is hardly possible to give a detailed account of all the investigations of the fragmentation process done in the Radium Institute of the Academy of Sciences of the USSR. We restrict ourselves to the presentation of those features of the fragmentation which are essential for the mechanism of the process and are related simultaneously with hyperfragments. The main emphasis will be on the experimental part of the investigations. Moreover, we consider here mainly the emission of fragments with charge number $Z \geqq 4$ and energy $E \geqq 2$ MeV per nucleon.

II. CROSS-SECTIONS OF THE PRODUCTION OF FRAGMENTS

One of the characteristic features of fragmentation is the dependence of the yield of fragments on the energy of the incident particles. As typical for high-energy reactions, Fig. 1 shows the cross-sections for the emission of fragments with $Z \geqq 4$ and Li^8 in the interactions with heavy nuclei Ag and Br in the incident particle energy interval 100 MeV - 9 GeV $^{1-8)}$. One sees that the cross-section for fragmentation increases strongly with increasing energy of protons, the growth being particularly steep in the energy interval ~ 1 GeV. Beginning at about 100 MeV with the value of the cross-section for $Z \geqq 4$ fragments less than 0.1% of the total inelastic cross-section up to the energy $E_p \approx 2$ GeV, the cross-section for fragmentation increases

by three orders of magnitude. A further increase of the incident particle energy does not lead to a strong increase of the cross-section. It is interesting that the total cross-section for fragmentation, including the fragments with the charge number $Z = 3$ in the energy interval of several GeV of the incident protons, is equal to about 25% of the total inelastic cross-section; thus fragmentation plays an essential role in the process of the disintegration of nuclei.

An analysis of nuclear disintegrations leading to fragment emission has shown that these disintegrations take place for a much higher energy transfer to the target nuclei as compared with usual disintegrations. The energy transfer to the target nucleus was characterized by the number of heavily ionizing charged particles $n_{\alpha p}$ (black and grey tracks). From the point of view of the cascade-evaporation model, the number is determined by the degree of the development of the intranuclear cascade and by the excitation energy of the residual nucleus as well.

Figure 2 shows the $n_{\alpha p}$-spectrum for normal disintegrations and for the disintegrations with fragment emission in the interactions of 9 GeV and 660 MeV protons with Ag and Br nuclei[1,8]. The average number of charged particles in stars with fragment emission is greater by a factor 1.8 than the average $n_{\alpha p}$-number in normal disintegrations, the relation being the same in the wide energy interval of the incident particles: from 460 MeV to 9 GeV. From the analysis of the spectrum one finds that the probability of fragment emission in a disintegration increases strongly with the increase of the number of particles emitted. This can be seen in Fig. 3 which shows the dependence of fragment emission

$$W_\rho = \frac{N_\rho}{N_\rho + N_{norm}}$$

on the $n_{\alpha p}$-number for different energies of the incident protons[3,5,6-8]. The curves in Fig. 3 also show interesting features of fragment emission: the high probability of disintegration with fragment emission for a given

$n_{\alpha p}$ -number and a more steep increase of the probability with the increase of $n_{\alpha p}$ for higher energies of the incident protons. As in the paper by Ostroumov[9], it has been shown that a given $n_{\alpha p}$ -number is related to the smaller excitation energy of the residual nucleus for higher energy of an incident proton, the last observation shows the connection between the probability of fragment emission with the total number of cascade particles, i.e. with the development of the intranuclear cascade. This is supported by the observation that after exclusion of black tracks, which according to the cascade-evaporation model are evaporated, one gets the increase of the emission probability of fragments with an increase of the number of cascade particles (grey tracks)[6,8]. One does not observe, on the other hand, any dependence of the probability W_ρ on the number of shower particles (thin tracks) in the incident proton energy interval of several GeV. This indicates that the character of the first collisions in the target nucleus is irrelevant for the fragmentation process.

The above-described specific feature of the fragmentation process, the necessity of a high-energy transfer to the nucleus for the appearance of the fragment emission, is connected with the observation that the emission of fragments not accompanied by other charged particles is a very rare phenomenon. Consequently we concluded that the increase of the fragmentation cross-section is related with the increase of the fraction of high-energy transfers with the increase of the energy of the incident protons[3,21]. The last statement follows from observations of the track distributions for different energies of the incident protons. The strong increase of the fragmentation cross-section in the energy interval 600 - 1,000 MeV can probably be related to the appearance of the additional mechanism of high-energy transfer, namely to the production and re-absorption of pions in the nuclei[5]. In the energy interval above 1 GeV the increase of the fraction of high-energy transfers is relatively weaker. Also the fragmentation cross-section changes little in this energy region. The energy transfers to the nuclei are

characterized by the total number of charged particles created
in the disintegrations and with the increase of the proton energy
E_p the number of cascade particles in the total $n_{\alpha p}$-number increases.
Thus the increase of the fragmentation cross-section with the
increase of the energy E_p can again be attributed to the degree of
the development of the intranuclear cascade in the nucleus.

The dependence of the fragmentation cross-section on the
mass number of the target nucleus is an essential feature of the
fragmentation. This dependence has not at present been sufficiently
investigated. Up until now the measurements of the cross-sections
for the emission of fragments with $Z \gtrsim 4$ and energy $E \gtrsim 2$ MeV per
nucleon have been done for the C,N,O nuclei in emulsion, for Bi and U
in loaded emulsions, and for C,Al,Cd and Pb in the experiments with
thin foils in emulsions[2, 10-13].

The measurements at $E_p = 660$ MeV have shown that the
fragmentation cross-section increases with the mass number of the
target nuclei roughly proportional to the geometrical cross-section
of the nuclei: the cross-sections for C,Ag,Br,Bi and U are equal to
1,4,10,25 and 22 mb respectively [errors about 30%][4].

However, this relation is probably accidental as it was shown
that the fragmentation cross-section of light nuclei changes only little
with energy[2-4, 22] whereas the cross-section for heavy nuclei increases
strongly in the energy interval ~ 1 GeV.

III. NATURE OF FRAGMENTS

The mass and charge distribution of fragments emitted in nuclear
disintegrations has not at present been thoroughly investigated. By means
of emulsion we have investigated the charge distribution of fragments
for disintegrations of silver and bromine nuclei at the proton energies
100, 660, 930 and 9,000 MeV[1, 3, 6-8]. The main conclusion is the lack of
any marked dependence of the form of the charge distribution on the proton

energy. Figure 4 shows the charge distribution of fragments at $E_p = 9$ GeV [14]. Analogous charge distributions are observed at other proton energies. The majority of fragments observed in disintegrations are the stable isotopes of light nuclei. An investigation of the β radioactivity of fragments with $Z \geq 4$ in electron-sensitive emulsion has shown that 90% or more of fragments are stable against the β decay with $\tau_{1/2} \lesssim$ five hours. This is supported by the data on the relative yield of the Li^8 and B^8 among the fragments with $Z = 3$ and 5. The ratio of the cross-sections for Li^8 to $Li^{6,7}$ is 0.012 for $E_p = 930$ MeV and for B^8 to $B^{10,11,12}$ is $\simeq 0.025$ for $E_p = 9$ GeV. Analogous relative cross-sections are found [5] by comparison of the data on the emission of fragments with charge numbers 4, 6 and 9 with the cross-sections for Be^7, C^{11}, F^{18} obtained in investigations using radiochemical methods.

In the analysis of the nature of fragments some conclusions were reached concerning the excitation state of the emitted fragments and concerning the most probable n/p ratio in the emitted fragments. The presence among the fragments of the rather unlikely (for a given Z) isotopes of light nuclei with a sole state stable against the emission of nucleons (such as Li^8, Li^9 and B^8) show that the conditions of fragment emission are of such a kind that fragments do not get high excitations and can be emitted in ground states. The analysis of events of the emission of Be^8 fragments decaying into two α particles also indicates the strong likelihood of emission in the ground state. A comparison of the cross-section of the Be^8 emission in the ground state with the cross-sections for the Li^8 and B^8 emission has indicated a more frequent emission of the Be^8 isobar in spite of the fact that the total cross-section for fragments with $Z = 4$ is smaller than that for $Z = 3$ [3].

Considering these observations one could conclude that the high probability of the emission of fragments in low excited states and the preference for some definite ratios (near unity) in the fragments emitted are characteristic for the fragmentation process. However, it is clear that problems of this kind require a further experimental investigation.

As already mentioned no marked dependence in the charge distribution on the incident proton energy has been found. This is somewhat surprising as we know that many essential features of the fragmentation process (cross-section, multiplicity, angular distribution) depend on the energy of incident particles. In connection with this the investigation of the charge distribution of fragments was done for the disintegrations at the same incident proton energy but for the following different conditions of the emission of fragments:

i) for large and small energy transfers to the target nuclei;

ii) for different emission angles of fragments;

iii) for different numbers of fragments emitted in one disintegration.

The investigation, done at $E_p = 9$ GeV, has shown that in all cases the charge distributions were practically the same[14].

Investigation of the fragment emission in the disintegrations of the Bi and U nuclei at $E_p = 660$ MeV[10-12], lead to the conclusion that even for such heavy nuclei the charge distribution of fragments probably does not differ markedly to that observed for Ag and Br nuclei. The small statistics of the observations did not permit the determination of the charge distribution of the fragment emission from Bi and U nuclei; one can only say that the average charge number for fragments with $Z \geq 4$ is 5 and 6 for Bi and U respectively. The data obtained are too scanty, however, to reach a definite conclusion.

IV. ANGULAR AND ENERGY DISTRIBUTION OF FRAGMENTS

The angular distribution of fragments investigated in the energy interval of the incident protons from 100 MeV to 9 GeV[1,3-8] is characterized by a marked anisotropy in the laboratory system with respect to the direction of flight of the incident protons. Figures 5 and 6 show the angular distributions of fragments with $Z \geq 4$ at $E_p = 660$ MeV and 9 GeV and the dependence of the forward to backward ratio F/B on the proton energy. One sees that the anisotropy of the angular distribution decreases

strongly with the increase of the energy of the incident protons.
It is also found that the anisotropy of the angular distribution is
greater for faster fragments, the relative number of them increasing
with the increase of the incident proton energy. However, the
anisotropy of the fast fragments probably also decreases with the
increase of incident proton energy. This could explain the dependence
of the F/B ratio on the incident proton energy as seen in Fig. 6. This
follows from the results of measurements of angles of long range
fragments: the F/B ratio at E = 660 MeV for fragments with range R > 80 μm
is 5.6 whereas at E_p = 9 GeV for fragments with R > 100 μm it is 3.6.
It is necessary to note that no significant dependence of the angular
distribution of fragments on the magnitude of the energy transfer to
the nuclei has been found for a given E_p [3].

An interesting problem is the dependence of the angular
distribution of fragments on the mass number of the target nucleus.
The available data on the emission of fragments from Bi and U nuclei
at E_p = 660 MeV show that the anisotropy of the angular distribution
increases when passing from Ag and Br nuclei to the heavy nuclei
(F/B ratio being $\cong$ 3 and $\cong$ 5 respectively). It is possible that in
this case the same effect is operating which leads to the increase of
the anisotropy of the angular distribution in the case of Ag and Br
nuclei when the incident proton energy is decreasing.

A more marked increase of the anisotropy of the angular
distribution of fragments is seen in the case of light nuclei. The
forward to backward ratio for fragments with Z $\geq$ 4 and range R > 20 μm
in the disintegrations of carbon nuclei at E_p = 660 MeV is $\gtrsim$ 15 [13].
An investigation of the energy distribution of fragments emitted in the
disintegrations of nuclei like Ag with different Z numbers and at
different E_p-values, shows that the most probable value of the energy
of fragments is near to the nominal value of the Coulomb barrier. A
specific feature of the distributions is their broadness and a long tail
in the energy part much higher than the energies of the Coulomb repulsion,
the tail being present also in the part of the fragments emitted in the

backward hemisphere[3]. It is interesting that among the fragments with $E \gg E_{Coul.}$ in Ag and Br disintegrations at $E_p = 660$ MeV events have been observed with momentum comparable or even exceeding that of the primary protons $p_0 = 1,290$ MeV/c. Their relative frequency with respect to all fragments with $Z \geq 4$ is about 1%[15]. On the low-energy part, the energy spectrum contains a considerable fraction of fragments with energies smaller than the nominal values of the Coulomb barrier. For large variation of the incident proton energy, the most probable value of the energy of fragments hardly changes. A change in the spectrum is mainly due to the increase of the relative fraction of the fragments with $E \gg E_{Coul.}$[8]. Figure 7 shows the range distributions of fragments for different energy values of incident protons. Taking into account that the charge spectra are conserved for this E_p-interval, one can see well the above-described features of the energy distribution of fragments.

An investigation of fragment emission from Bi and U nuclei has shown that the relative fraction of "sub-barrier" fragments is greater as compared with Ag and Br disintegrations[12].

V. MULTIPLICITY OF FRAGMENTATION

An interesting feature of the fragmentation process is the emission of two or more fragments from a single disintegration. The existence of this phenomenon leads by itself directly to the conclusion that the conditions necessary for fragment emission can often be realized in the development of a process of interaction of an incident particle with a nucleus. An investigation of the specific features of disintegrations of this kind and an analysis of the relative correlations of charges, energies and emission angles in the multiple fragment emission, give additional information on the mechanism of fragment emission.

The multiplicity of fragment emission was investigated in the energy interval of incident protons ranging from 660 to 9,000 MeV[1,3,5,8,16,17]. The excitation function of the Ag and Br disintegrations, accompanied by the emission of two or more fragments, in shown in Fig. 8. It has an analogous

dependence on the incident proton energy as in the case of single fragment emission. The cross-section for the emission of two or more fragments is about 4% of the total fragmentation cross-section at E_p = 660 MeV and about 16% at E_p = 9,000 MeV.

Figure 9 shows the frequency distribution of multiplicities of fragment emission at E_p = 660 MeV and E_p = 9 GeV. One sees the steep decrease of the cross-section for an increasing number of fragments emitted in a single disintegration.

An analysis of disintegrations, leading to the emission of two or more fragments, has shown that the size of the disintegrations is still more shifted towards a large number of prongs in the stars as compared with single fragment emission events. Thus they are related to still higher energy transfers to the target nuclei. The average $n_{\alpha p}$-number (excluding fragments) in such disintegrations is more than twice the corresponding number for usual disintegrations. An investigation of the charge and energy distributions in the disintegrations with the emission of two or more fragments[16] leads to the result that the distributions are analogous in the case of single fragment emission. The analysis of the relative probabilities of different multiplicities of fragment emission (Fig. 9) and of the relative probabilities of different charges, Z_1 and Z_2, in the events with two fragment emission (Fig. 10), supports the hypothesis that fragments are independently emitted[16].

In an apparent contradiction with this assumption is the observation of a strong angular correlation of fragments in the two and three fragment events[3,8,16,17]. Figure 11 shows the observed distribution of angle between two fragments compared with that obtained from the assumption of an independent emission. A marked angular correlation is clearly seen: the fragments are emitted preferentially with an angle greater than 120° between them. An analogous correlation (a preference for large angles) has been found for disintegrations with three fragments[16]. It is interesting that no connection between the angular correlation of fragments and the magnitude of their charges has been observed: for different values of the sum of the charges of fragments the average value of the angle between fragments has the same value.

The explanation of the angular correlation in multiple emission of fragments, without rejecting the assumption of the independent emission, requires **definite** models to be invoked related either to the structure of nuclei or to the mechanism of formation of fragments in the disintegration[16].

VI. FEATURES OF THE FRAGMENTATION CAUSED BY HIGH-ENERGY PIONS

An investigation of the fragmentation process in the case of the incident particles being pions is particularly interesting as, contrary to the proton case, a small momentum is transferred to the target nucleus, fast nucleons being formed in the nucleus as a result of interactions (scattering and absorption) of pions with nucleons. This enables us to check some considerations arising in the study of fragmentation.

In the investigations of the fragmentation caused by 80 and 280 MeV positive pions[18-20,31] the following features of the process have been found.

i) The cross-section of the production of fragments with $Z \geq 4$ in the disintegrations of Ag and Br nuclei is 1.2 ± 0.5 mb at $E_\pi = 80$ and 1.4 ± 0.5 mb at $E_\pi = 280$ MeV.

ii) The energy distributions of fragments are approximately the same for both values of E_π and are similar to those obtained in the case of protons.

iii) The angular distribution of fragments is more anisotropic at $E_\pi = 280$ MeV ($F/B = 2.8 \pm 0.6$) than at $E_\pi = 80$ MeV ($F/B = 1.3 \pm 0.3$).

iv) An angular correlation between the directions of emission of a fragment and a fast proton ($E > 50$ MeV) has been observed: preferential emission occurs for angles of $120° - 180°$ between the particles.

v) Similar to the disintegrations induced by protons, the disintegrations with fragment emission are characterized by higher numbers of prongs when compared with usual disintegrations.

The results obtained were interpreted from the point of view of fragment production exclusively by fast protons generated in elastic collisions of pions and their absorption by nucleon pairs in the nuclei. The angular distribution of fragments calculated on that basis (using the angular distribution of protons in the reaction $\pi^+ + d \rightarrow p + p$ and the angular distribution of fragments produced in emulsion nuclei by protons with energy about 200 MeV) shows a good agreement with the observed distribution for both values of energy of the π^+ mesons (Fig. 12). In the case of the higher energy of pions, nucleons from the elastic scattering of pions in the nucleus were also taken into account. The nucleons have a strong forward collimation, therefore they contribute largely to the difference of angular distributions of fragments at E_π = 280 MeV and E_π = 80 MeV.

VII. CONCLUSIONS

Considering the fragmentation process as a whole, one can see that many features of the nuclear disintegrations accompanied by the emission of multicharged particles (angular and energy distributions of protons and α particles, their relative yield, angular and energy distributions of residual nuclei) do not contradict the basic assumptions of the cascade-evaporation model[3]. The analysis of the specific features of the production of fragments with Z $\geq$ 4 from the point of view of this model[5-7,24] leads us to the conclusion that the concept of the emission of fragments at the first stage of an interaction of a fast particle with a nucleus (i.e. during the development of the intranuclear cascade) enables us to give a more complete explanation of the characteristic features of fragmentation known from experiment.

A comparison of the characteristic features of fragmentation with that of the production of α particles with energies greater than 30 MeV for disintegrations of Ag and Br nuclei supports this point of view. As has been shown[25-27] the angular and energy distributions of α particles with energy above 30 MeV can be explained by the process of quasi-elastic

knock-on of α clusters from the nucleus by the cascade nucleons. It was also shown that the specific features of the disintegrations with emission of fast α particles and the angular distribution of α particles are analogous to that concerning the production of fragments with $Z \geq 4$ [28].

Therefore, retaining the point of view of the cascade excitation of nuclei, we should consider the mechanism of fragmentation as some kind of direct nuclear reaction leading to the ejection of rather large aggregates of nucleons (of the order of ten) with high energies which are sometimes even higher than the binding energy of the nucleons constituting the clusters. Independently of the mechanism of the energy transfer to the nucleon aggregates, it is necessary in this picture to assume the existence of nucleon clusters correlated in space in the nucleus [29].

At present we cannot completely reject a possibility of some contribution to the production of fragments from the process of de-excitation of a highly excited nucleus. Although in its present form the evaporation theory leads to contradiction with experimental data, if one takes into account, however, the indirect evaporation mechanism (evaporation of single particles accompanied by their association inside a nucleus), the agreement with experiment can be improved. The calculations of the indirect evaporation of the H^3 nuclei, carried out in our laboratory [30], give rise to some hope concerning this problem.

In conclusion, a few words about the connection of the processes of production of fragments and hyperfragments. To us it seems reasonable not to invoke any specific mechanism of hyperfragment production differing from that of the ordinary fragments. Conditions for fragment production do exist for relatively low energies of the incident protons (of the order of 100 MeV) and with the increase of the proton energy the mechanism of the fragment production probably remains the same; only the relative contributions of several possible mechanisms change.

At proton energies high enough for the production of
strange particles, some fraction (a very small one, of the order of
0.5% at E_p = 9 GeV) of fragments is emitted with a Λ° particle,
accidentally coming into the given aggregate of nucleons. This point
of view is convincingly verified by comparison of the charge, angle
and energy distributions of fragments and hyperfragments.

* * *

REFERENCES

1) O.V. Lozhkin and N.A. Perfilov, ZHETF 31, 913 (1956).

2) O.V. Lozhkin, ZHETF 33, 354 (1957).

3) O.V. Lozhkin, Thesis, published by G.P.U., Leningrad (1957).

4) N.A. Perfilov, Documents relating to the meeting on the application
   of radiochemical methods to the study of nuclear reactions and on
   β and γ ray spectroscopy of neutron-deficient atoms, Vol. I,
   p. 84, UINR (1958).

5) N.A. Perfilov, O.V. Lozhkin and V.P. Shamov, UFN 60, 3 (1960).

6) O.V. Lozhkin, N.A. Perfilov and A.A. Rimskij Korsakov, Dzh.Dremlin,
   ZHETF 38, 1388 (1960).

7) U.R. Arifkhanov, M.M. Makarov, N.A. Perfilov and V.P. Shamov,
   ZHETF 38, 1115 (1960).

8) N.A. Perfilov, N.S. Ivanova, O.V. Lozhkin, M.M. Makarov, V.I. Ostroumov,
   Z.I. Soloveva and V.P. Shamov, ZHETF 38, 345 (1960).

9) V.I. Ostroumov, ZHETF 32, 3 (1957).

10) N.A. Perfilov and G.F. Denisenko, ZHETF 35, 631 (1958).

11) G.F. Denisenko, N.S. Ivanova, N.R. Novikova, N.A. Perfilov,
    E.I. Prokofeva and V.P. Shamov, Phys.Rev. 109, 1779 (1958).

12) V.F. Darovskikh, H.P. Kocherov and N.A. Perfilov, ZHETF 37, 1292 (1959).

13) V.I. Ostroumov and Yu.P. Yakovlev, ZHETF 35, 1358 (1958).

14) P.A. Gorichev, O.V. Lozhkin and N.A. Perfilov, ZHETF 41, 35 (1961).

15) O.V. Lozhkin, Documents relating to the meeting on the application of radiochemical methods to the study of nuclear reactions, Vol. I, p. 117, UINR (1958).

16) P.A. Gorichev, O.V. Lozhkin, N.A. Perfilov and Yu.P. Yakovlev, ZHETF 41, 327 (1961).

17) O.V. Lozhkin, Documents relating to the meeting on the application of radiochemical methods to the study of nuclear reactions, Vol. I, p. 116, UINR (1958).

18) N.S. Ivanova, ZHETF 34, 1381 (1958).

19) N.S. Ivanova, V.I. Ostroumov and Yu.V. Pavlov, ZHETF 37, 1604 (1959).

20) A.S. Assovskaya and N.S. Ivanova, ZHETF 39, 1511 (1960).

21) N.A. Perfilov, Collection "Physics of the fission of atomic nuclei", Atomizdat, Moscow, p. 98 (1957).

22) M.M. Makarov and N.A. Perfilov, DAN 138, 579 (1961).

23) P.A. Gorichev, V.F. Darovskikh, O.V. Lozhkin, N.A. Perfilov, A.I. Obukhov and Yu.P. Yadovlev, Phys.Rev. 126, 2196 (1962).

24) N.A. Perfilov, O.V. Lozhkin and V.I. Ostroumov, Nuclear reactions due to high-energy particles, published by AN USSR Leningrad (1962).

25) P.A. Vaganov and V.I. Ostroumov, ZHETF 33, 1131 (1957).

26) V.I. Ostroumov and R.A. Filov, ZHETF 37, 643 (1959).

27) V.I. Ostroumov, N.A. Perfilov and R.A. Filov, ZHETF 39, 105 (1960).

28) V.I. Ostroumov, N.A. Perfilov and R.A. Filov, ZHETF 36, 367 (1959).

29) P.A. Gorichev, O.V. Lozhkin and N.A. Perfilov, published by AN USSR 26, 1190 (1962).

30) I.I. Pianov and S.V. Izmajlov, ZHETF 41, 118 (1961).

31) N.S. Ivanova, V.I. Ostroumov and R.A. Filov, Publications concerning the International Conference on the peaceful uses of atomic energy, Vol. I, p. 452, Atomizdat, Moscow (1959).

* * *

Figure Captions

Fig. 1   Dependence of the cross-section for the production of
         fragments with $Z \geq 4$, and of Li^8 fragments, on the
         incident proton energy.

Fig. 2   Distributions of the number of charged particles $n_{\alpha p}$
         (without fragments) in the usual disintegrations
         (dotted line) and disintegrations with fragment emission
         (continuous line).

Fig. 3   Dependence of the probability of disintegrations with
         fragment emission for a given $n_{\alpha p}$-number on the $n_{\alpha p}$-number.

Fig. 4   Charge distribution of fragments in the disintegrations of
         Ag and Br nuclei by 9 GeV protons.

Fig. 5   Angular distribution of fragments with $Z \geq 4$ emitted in
         Ag and Br disintegrations by protons at: 0 - 100 MeV;
         0 - 660 MeV;   0 - 9 GeV.

Fig. 6   Dependence of the F/B ratio on the proton energy for
         production of fragments with $Z \geq 4$ in Ag and Br nuclei.

Fig. 7   Range distribution of fragments with $Z \geq 4$ in emulsions for
         different incident proton energies.

Fig. 8   Dependence on the incident proton energy of the cross-section
         for disintegrations with two and more fragments emitted.

Fig. 9   Frequency distribution of multiplicities of fragment
         emission in a disintegration.

Fig. 10   Dependence of the relative probabilities of the occurrence
         of the given pairs of charges, Z_1 and Z_2, for disintegrations
         with two fragment emission. Continuous line corresponds to
         the distribution calculated from the assumption of an independent
         emission of fragments.

Fig. 11   Distribution of space angles between fragments. Continuous
         line corresponds to the assumption of the independent
         emission.

Fig. 12   Angular distributions of fragments with $Z \geq 4$ for the
         disintegrations of Ag and Br nuclei by positive pions. The
         continuous line corresponds to the calculated distribution.
         (See text.)

Fig. 1. Dependence of the cross-section for the production of fragments with $Z \gtrless 4$, and of Li^8 fragments, on the incident proton energy.

Fig. 2. Distributions of the number of charged particles $n_{\alpha p}$ (without fragments) in the usual disintegrations (dotted line) and disintegrations with fragment emission (continuous line).
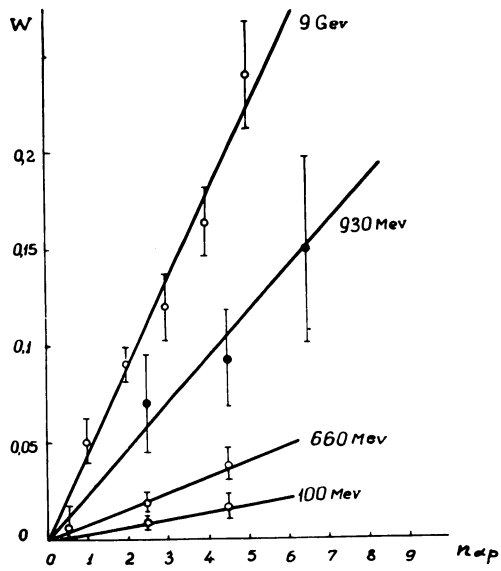
Fig. 3. Dependence of the probability of disintegrations
with fragment emission for a given $n_{\alpha p}$ -number
on the $n_{\alpha p}$ -number.

Fig. 4. - Charge distribution
of fragments in the
disintegrations of
Ag and Br nuclei
by 9 GeV protons.

Fig. 5. - Angular distribution
of fragments with Z ≥ 4
emitted in Ag and Br
disintegrations by pro-
tons of : 0-100 MeV;
0-660 MeV; 0-9 GeV.

Fig. 6. Dependence of the F/B ratio on the proton energy
for production of fragments with Z ≥ 4 in Ag and
Br nuclei.

Fig. 7. Range distribution of fragments with $Z \geq 4$ in emulsions for different incident proton energies.

Fig. 8. Dependence on the incident proton energy of the cross-section for disintegrations with two and more fragments emitted.

Fig. 9.   Frequency distribution of multiplicities of
          fragment emission in a disintegration.

Fig. 10. Dependence of the relative pro-
          babilities of the occurence of
          the given pairs of charges Z_1
          and Z_2 for disintegrations
          with two fragment emission.
          Continuous line corresponds
          to the distribution calculated
          from the assumption of an
          independent emission of frag-
          ments.

Fig. 11. Distribution of space angles between
          fragments. Continuous line corres-
          ponds to the assumption of the inde-
          pendent emission.

Fig. 12. Angular distributions of fragments with $Z \geq 4$
          for the disintegrations of Ag and Br nuclei by
          positive pions. The continuous line corres-
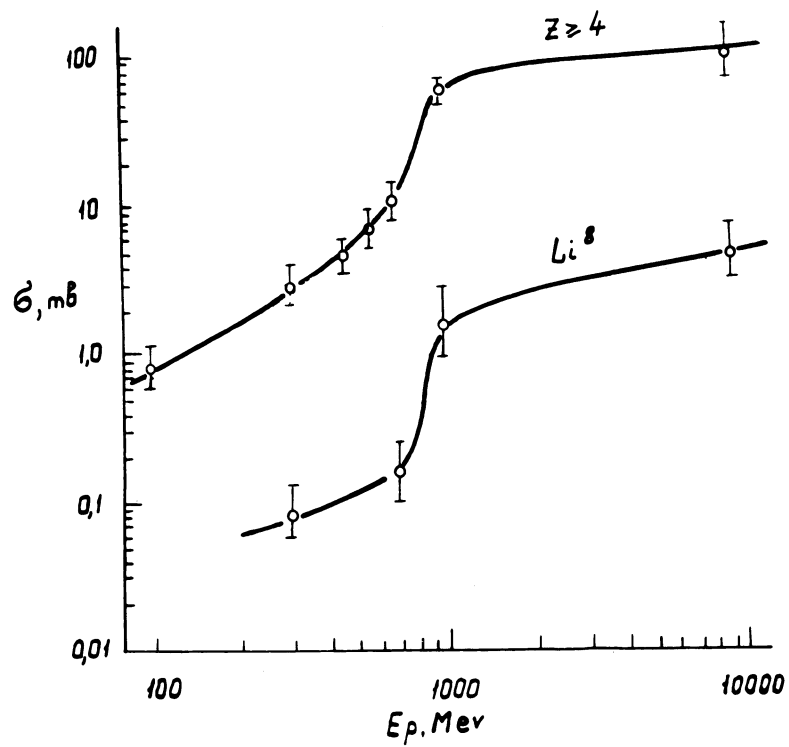   ponds to the calculated distribution. (see
          text)

VI. THEORY

THE STRONG AND WEAK INTERACTIONS OF BOUND Λ PARTICLES[*]

R.H. Dalitz,

The Enrico Fermi Institute for Nuclear Studies and
Department of Physics, The University of Chicago,
Chicago, Illinois.

I. THE NUCLEAR INTERACTIONS OF THE Λ PARTICLE

1. The s-wave Λ-N interaction

The binding of Λ particles to the s-shell nuclei H^2, H^3, He^3 and He^4 is due dominantly to the s-wave Λ-N interactions V_S for the singlet (S = 0) and triplet (S = 1) configurations. From the spin determinations for $_\Lambda H^3$(J = $\frac{1}{2}$) and for $_\Lambda H^4$ (J = 0), we know that the singlet interaction V_0 is more attractive than the triplet interaction V_1. Our knowledge of their strengths depends on quantitative calculations on the structure of these light hypernuclei, as discussed below. However, the conclusion that the triplet interaction V_1 is attractive depends on rather qualitative considerations. The mean Λ-N attraction in $_\Lambda H^3$ is given by $\frac{1}{4}(3V_0 + V_1)$, dominated by the singlet interaction; hence calculations on $_\Lambda H^3$ alone provide a lower limit on the strength of V_0. In $_\Lambda He^5$, on the other hand, the mean Λ-N attraction $\frac{1}{4}(3V_1 + V_0)$ arises dominantly from the triplet interaction; owing to its small weighting, the singlet interaction cannot provide sufficient attraction to account for the $_\Lambda He^5$ binding and we must conclude that V_1 is also attractive.

In order to estimate the strength of the Λ-N interaction, we must make a definite assumption about its range. We shall assume that this interaction has the same intrinsic range (1.5 f) as a Yukawa potential of range parameter $(2m_\pi)^{-1}$. This corresponds to the assumption that the

---

Λ-N potential arises dominantly from the exchange of pions; charge symmetry for the Λ particle (which has isospin I = 0) forbids one pion exchange, but the two-pion-exchange potential is allowed and is expected to be strong, in view of our current belief (based on the existence of a $p_{3/2}$ π-Λ resonance analogous to the π-N resonance, for example) that the $\pi\Sigma\Lambda$ coupling has strength comparable with that of the pion-nucleon coupling. This value for the intrinsic range is quite close to the values obtained for the Yukawa potentials which are equivalent (in the sense of having the same zero-energy scattering length a_s and effective range r_s) to the meson-theoretic Λ-N potentials calculated recently by de Swart and Iddings[1]. In fact, in view of the low binding energies of the light hypernuclei, it is reasonable to expect that these will not be greatly sensitive to the details of the potentials V_0 and V_1, but that they will be determined primarily by the low-energy scattering parameters, (a_0, r_0) and (a_1, r_1), of these potentials. As we shall see, the detailed calculations which have been made to date (but always with central potentials) do bear out this expectation.

$_\Lambda$H^3 is the lightest hypernucleus, with Λ-d separation energy $B_\Lambda = 0.21 \pm 0.2$ MeV, and is known to be a singlet state, with isospin I = 0 and spin J = $\frac{1}{2}$. This npΛ system is sufficiently simple to allow quite detailed and accurate variational calculations, even with hard-core potentials. For its space wave-function, Downs, Smith and Truong[2] have recently used a ten-parameter trial function,

$$\psi = f(r_{\Lambda n}) \, f(r_{\Lambda p}) \, g(r_{np}),$$ (1)

where f,g both have the general form,

$$\left\{ \left[\exp[-\alpha(r-d)] - \exp[-\beta(r-d)] \right] + x\left[\exp[-\mu(r-d)] - \exp[-\nu(r-d)] \right] \right\}.$$ (2)

This calculation used a Λ-N potential of the exponential form

$$V_{\Lambda N}(r) = \bar{U} \exp[-3.54(r-d)/(b-2d)], \qquad r \geq d$$ (3)

outside the hard core radius d. The intrinsic range is given by
b = 1.5 f. For d = 0.4 f, their result was $\bar{U}$ = 1144 MeV, which
corresponds to a mean well-depth parameter $\bar{s}$ = 0.810. The scattering
length which corresponds to this mean Λ-N potential is $\bar{a}$ = - 1.82 f.
Calculations were also made for d = 0.2 f and 0.6 f, leading to
scattering lengths $\bar{a}$ = - 1.75 f and - 2.11 f, respectively. It is also
of interest to compare these results with the value $\bar{a}$ = - 1.55 f which
was obtained in an earlier calculation[3] of comparable complexity,
for Yukawa potentials of the same intrinsic range, without hard cores.
These results illustrate the insensitivity of the low-energy parameters
obtained (for fixed intrinsic range) for the mean potential to the shape
assumed for this potential. We may also compare this result of Downs
et al. with that from their earlier calculation[2] using a four-parameter
trial function of the form (1), with f,g of the form (2) with x = 0,
which gave $\bar{U}$ = 1202 MeV. The more elaborate trial function led only to
4.8% improvement in the value obtained for $\bar{U}$, so that we may assume their
final value to be rather close (better than 1%) to the true value.

Muller[4] has also made calculations on $_\Lambda H^3$ for exponential
hard-core potentials, using an eight-parameter trial function of the
form (1). He assumed a potential of greater intrinsic range, of the
form $\bar{U}$ exp[- 2.38(r-d)] outside hard-core radius d, and obtained
$\bar{U}$ = 228.2 MeV. The corresponding calculation of Downs et al.[2], for
potential shape $\bar{U}$ exp[- 2.36(r-d)], gave $\bar{U}$ = 226.1 MeV, so that their
results are in good agreement. The scattering length for this potential
is $\bar{a}$ = - 2.7 f; we note that the scattering length obtained does
increase with the potential range assumed, as is reasonable.

For $_\Lambda He^5$, it is a reasonable assumption to neglect the
distortion of the He^4 core by the presence of the Λ particle, in view
of the tight binding of He^4. Since the form of He^4 is known from
electron-scattering experiments, the strength of the mean Λ-N potential
in $_\Lambda He^5$ may be deduced directly, for an assumed Λ-N potential shape
without hard core. This calculation was done quite early[5] for Λ-N
potentials of Gaussian form, and was combined with the results of
calculations for $_\Lambda H^3$ to give the results shown in the first column

of Table 1. For later reference, we quote here the volume integrals of the singlet and triplet potentials obtained by this way:
$\bar{V}_0$ = 386 MeV f³, $\bar{V}_1$ = 170 MeV f³. The errors quoted in the Table are those derived from the uncertainties in the B_Λ values and in the radius of He⁴.

With hard-core potential shapes, calculations have been made for $_\Lambda$He⁵ and $_\Lambda$H⁴ (with charge symmetry, $_\Lambda$He⁴ is the mirror hypernucleus to $_\Lambda$H⁴, with the same structure and the same B_Λ value, as is consistent with the data) by Dietrich et al.[6] and by Gutsch[7], using a method proposed by Mang and Wild[8] for light nuclei. This method takes into account accurately the two-body correlations in these light nuclei, rather in the spirit of the Brueckner method as developed for the discussion of nuclear matter, although the detailed justification of the method for these light nuclei depends on quite different physical factors (essentially on the large spacing of the one-particle states for the oscillator potential determined self-consistently) than does its justification (the Pauli principle and the high Fermi momentum) for the problem of nuclear matter. To date, these calculations have used square-well potentials of width (b-2d) outside hard-core radius d; the results available for d = 0.2 f and d = 0.4 f, with intrinsic range b = 1.484 f, are given in Table 1. It is of interest to note the insensitivity of the conclusion to the hard-core radius assumed; for orientation, we remark that, for d = 0, the increase from a_0 = 2.4 f to a_0 = 4.2 f requires an increase by only 10% in the potential strength of V_0. For d = 0.4 f, the scattering length a_0 corresponds to a well-depth parameter s = 0.8 for the ¹S₀ potential, so that there is no reason to expect a bound state for the Λ-N system.

Dietrich et al.[6] and Gutsch[7] have also made calculations for $_\Lambda$H³, using the same method. For d = 0.4 f, Gutsch finds that the observed B_Λ requires a mean well-depth $\bar{V}_3$ = 170 MeV for the outer square-well potential; the value $\frac{1}{4}(3V_0 + V_1)$ given by the potentials V_0 and V_1 obtained from the discussion of $_\Lambda$H⁴ and $_\Lambda$He⁵ is 168.0 MeV. The scattering length corresponding to this value $\bar{V}_3$ is $\bar{a}$ = 2.5 f. This is appreciably larger than the value (2.0 f) found from the variational calculations mentioned

above, and corresponds to a well-depth parameter about 12% too large; this is probably due to the fact that the Mang-Wild method is least accurate for small binding energies, as it does not give a correct account of the asymptotic region (which is of particular importance for small B_Λ). However, the internal comparisions between all of these calculations for the s-shell hypernuclei are rather satisfactory, in view of their approximate nature and the range of potential forms which have been used.

Finally, we consider whether there exists a J = 1 particle-stable state for the hypernuclei $_\Lambda H^{4*}$ and $_\Lambda He^{4*}$. This question is of great interest in view of its bearing on the interpretation of the $_\Lambda H^4$ and $_\Lambda He^4$ hypernuclei observed following $K^- - He^4$ capture events, whether these are produced directly (which would imply that the KΛ parity is odd) or whether they result from γ decay of such directly-produced excited states, with direct production of the ground state hypernuclei being forbidden. The situation is summarized in Table 1. The calculations[3,15] for d = 0 (corrected to the He^3 r.m.s. radius recently measured by Hofstadter and Collard) do indicate the existence of a bound state with $B_\Lambda^* \approx 1.3$ MeV, corresponding to a well-depth parameter of about 1.25 for the J = 1 configuration. The more recent calculations[6,7] carried out for hard-core potentials do not allow the existence of a J = 1 bound state. The attraction predicted for the J = 1 configuration actually decreases with increasing hard-core radius, the well-depth parameter of the $\Lambda - He^3$ attraction being only 0.83 in this state for d = 0.4 F. Further calculations along these lines for outer potential shapes more realistic than the square well, and which can be compared directly with the more accurate variational calculations on the $_\Lambda H^3$ system, would be rather desirable at this point.

The interpretation of these potentials V_0 and V_1, together with the data available on the ratio R = $(\Sigma^0 n)/(\Lambda n)$ for $\Sigma^- p$ capture from rest, has been extensively discussed in terms of the pion-hyperon interactions $\Sigma\Sigma\pi$ and $\Sigma\Lambda\pi$ by de Swart and Iddings[1]. Their calculations are based on a two-channel approach, in which the ΛN and ΣN channels are treated on the same footing in view of the relatively small mass difference $(m_\Sigma - m_\Lambda) \approx 80$ MeV. We confine our attention here to their essential conclusions for the case of

even $\Sigma\Lambda$ parity. The $^1S_0$ potential deponds primarily on the coupling $f_{\Sigma\Lambda}$ and its strength requires that $f_{\Sigma\Lambda}$ be comparable in magnitude with the pion-nucleon coupling f_{NN}. The $^3S_1$ potential strength and the ratio R both depend quite strongly on $f_{\Sigma\Sigma}$ and an adequate fit to all three data requires $f_{\Sigma\Sigma} \approx 0.1$, taking the hard-core radius to be d = 0.5 f, as required for the corresponding NN potentials.

For small $f_{\Sigma\Sigma}$, the coupling between the ΛN and ΣN channels is not of major importance in the $^1S_0$ state, and the dominant interaction is the two-pion exchange potential in the ΛN channel, which depends only on the $\Sigma\Lambda\pi$ coupling. In the $^2S_1$ state, the one-pion exchange potential linking ΛN and ΣN channels is very strong and of the tensor form; there is a strong $f_{\Sigma\Sigma}$ dependence both because of the importance of the $\Sigma\Sigma\pi$ coupling in the ΣN channel and because $f_{\Sigma\Sigma}$ contributes to the fourth-order potential $V(\Lambda N, \Sigma N)$ which interferes with the strong one-pion exchange term in this potential. However, the low-energy ΛN scattering wave-function does not have a large D-state, so that the tensor component of the effective ΛN potential is expected to be of relatively minor importance, in contrast with the situation for the NN system.

2. The s-wave Λ-Λ interaction

Very recently Danysz et al.[9] have reported the first example of a double Λ hypernucleus, for which the most probable interpretation is $_{\Lambda\Lambda}Be^{10}$, with separation energy $B_{\Lambda\Lambda} = 17.5 \pm 0.5$ MeV relative to $\Lambda + \Lambda + Be^8(g.s.)$. Since $B_\Lambda = 6.5 \pm 0.15$ MeV $_\Lambda Be^9$, $B_{\Lambda\Lambda}$ exceeds $2B_\Lambda(Be^9)$ by 4.5 ± 0.6 MeV, so that we conclude that the Λ-Λ interaction is attractive. Since both particles are in the ground s-orbit relative to the nuclear core, the Pauli principle requires that their spins be coupled in the singlet configuration, so that $B_{\Lambda\Lambda}$ is determined predominantly by the $^1S_0$ Λ-Λ potential.

An estimate of the Λ-Λ potential strength may be obtained using a simple product wave-function[10],

$$\psi = \varphi(|\underline{r}_1 - \underline{R}|)\,\varphi(|\underline{r}_2 - \underline{R}|)\,(u_1 v_2 - v_1 u_2)/\sqrt{2}, \qquad (4)$$

where $\underline{R}$ denotes the c.m. position of the Be^8 core. If $E_\Lambda(\varphi)$ denotes the separation energy of $_\Lambda Be^9$ [relative to $\Lambda + Be^8(g.s.)$] calculated for the wave-function φ, then

$$- B_{\Lambda\Lambda} \geq - 2E_\Lambda(\varphi) + <V_{\Lambda\Lambda}> . \tag{5}$$

We take the potential $V_{\Lambda\Lambda}$ to be of Gaussian form $- \bar{v}_{\Lambda\Lambda}(\lambda/\pi)^{3/2} \times \exp(-\lambda r^2)$, with $\lambda = 2.0604/b^2$ and intrinsic range $b = 1.5$ f corresponding to the process of two-pion exchange. If φ is taken to be the wave-function for $_\Lambda Be^9$, then $-<V_{\Lambda\Lambda}>$ can be identified with $(B_{\Lambda\Lambda} - 2B_\Lambda) = 4.5 \pm 0.6$ MeV, which leads to a first estimate 520 ± 70 MeV f^3 for the volume integral $\bar{v}_{\Lambda\Lambda}$ of the $^1S_0$ Λ-Λ potential. However, this estimate is considerably too large, since, owing to the additional binding energy, the wave-function φ appropriate to $_{\Lambda\Lambda}Be^{10}$ will actually fall off much more rapidly with r than φ for $_\Lambda Be^9$. To allow for this, we vary the form of φ, using the inequality (5) as a variational principle for $\bar{v}_{\Lambda\Lambda}$. The form

$$\varphi(r) = N [\exp(-ar^2) + y \exp(-cr^2)] \tag{6}$$

provides a good fit to the $_\Lambda Be^9$ wave-function for $a = 0.25$ f^{-2}, $c = 0.07$ f^{-2} and $y = 0.33$, the Λ-Be^8 potential being represented by a shell-model form with strength adjusted to fit the observed B_Λ value. The effect of interest is roughly represented by decreasing y; the minimum occurs for $y = 0.15$, leading to the improved estimate,

$$\bar{v}_{\Lambda\Lambda} = 440 \pm 60 \text{ MeV } f^3 . \tag{7}$$

Further improvements to this estimate are still necessary, with improved wave-functions which take into account:

i) the possibility of strong spatial correlations between the two Λ particles;

ii) the distortion of the nuclear core by the presence of two strongly bound Λ particles.

The inclusion of these effects may be expected to lower our estimate for $\bar{v}_{\Lambda\Lambda}$ further, but certainly not by more than the error quoted in Eq. (7).

As pointed out by Danysz et al.[9], there is possibly an alternative interpretation for this event as $_{\Lambda\Lambda}\text{Be}^{11}$ with separation energy 19.0 ± 0.6 MeV relative to $\Lambda + \Lambda + \text{Be}^9$. For $_{\Lambda}\text{Be}^{10}$, $B_{\Lambda} = 7.9 \pm 0.4$ MeV, but only the spin-average $\Lambda - \text{Be}^9$ interaction is effective in $_{\Lambda\Lambda}\text{Be}^{11}$, since the Λ spins are in the singlet configuration. Using intermediate coupling wave-functions for Be^9, the spin dependent term in B_{Λ} is $0.32<\Delta>$, where $<\Delta>$ is an appropriate expectation value of the spin-dependent part of the $\Lambda - N$ interaction which has the value 1.8 ± 0.4 MeV for neighbouring hypernuclei, as discussed in Section III. Hence the quantity $(B_{\Lambda\Lambda} - 2\bar{B}_{\Lambda})$ has the value $[19.0 - 2(7.9 - 0.6)] = 4.4 \pm 1.0$ MeV, quite comparable with the value used above for $_{\Lambda\Lambda}\text{Be}^{10}$, so that our estimate (7) of $\bar{v}_{\Lambda\Lambda}$ would not be appreciably modified if the alternative interpretation $_{\Lambda\Lambda}\text{Be}^{11}$ were adopted.

As for the $\Lambda - N$ potential, the long-range part of the $\Lambda - \Lambda$ potential arises from two pion exchange. For even $\Sigma\Lambda$ parity, the $^1S_0$ $\Lambda - \Lambda$ interaction arises dominantly from the two-pion exchange potential in the $\Lambda\Lambda$ channel, since the potential coupling the $\Lambda\Lambda$ and $\Sigma\Sigma$ channels is relatively weak. The reason for this is essentially the same as for the $\Lambda - N$ case, namely:

a) for pseudoscalar mesons, the one-pion exchange potential is known to be quite weak;

b) the two-pion contribution to $V(\Lambda\Lambda - \Sigma\Sigma)$ is necessarily proportional to $f_{\Sigma\Sigma}^2$, which appears to be a relatively small coupling parameter.

The structure of the two-pion contribution to $V(\Lambda\Lambda,\Lambda\Lambda)$ is the same as that for $V(\Lambda N,\Lambda N)$, except for the additional factor $f_{\Sigma\Lambda}^2/f_{NN}^2$. Hence, if the same hard-core radius is assumed for the $\Lambda - \Lambda$ and $\Lambda - N$ interactions, the comparison of the values $\bar{v}_{\Lambda\Lambda} = 440$ MeV f^3 indicates that $f_{\Sigma\Lambda} \approx f_{NN}$ quite closely.

3. Binding energies for the p-shell hypernuclei

On the basis of a shell-model representation for the core nuclei, Lawson and Rotenberg[11] and Iwao[12] have proposed the following expression:

$$B_\Lambda = C + N_p <\bar{V}> + \alpha_N <\Delta> \qquad (8)$$

for the binding energies of hypernuclei with nuclear cores belonging to the lp shell. In this expression N_p denotes the number of p-shell nucleons, and $<\bar{V}>$, $<\Delta>$ denote the expectation values of $\frac{1}{4}(3V_1 + V_0)$ and $(V_0 - V_1)$ respectively between the Λ-particle wave-function and the wave-function of a p-shell nucleon. The coefficient α_N depends on the spin of the hypernuclear state and on the details of the structure of the core nucleus; values of α_N have been calculated by Dalitz and Soper[13] using intermediate coupling wave-functions for the core nuclei and including the admixture of excited nuclear states where these are of significance. Generally speaking, the values of α_N are close to those for L-S coupling at the beginning of the p-shell, for A < 9, and close to those for j-j coupling for A > 9. For j-j coupling, the value of α_N is

$$\alpha_N = -\frac{1}{4}\left[1 - \frac{\ell(\ell+1) - \frac{3}{4}}{j(j+1)}\right]\left[J(J+1) - J_N(J_N+1) - \frac{3}{4}\right]. \qquad (9)$$

We note here that the result established empirically for $_\Lambda H^3$, $_\Lambda H^4$ and $_\Lambda Li^8$ [14] that the ground-state hypernuclear spin value is $|(J_N - \frac{1}{2})|$ is not expected to be a general rule. For example, C^{13} belongs to the $p_{1/2}$ shell, so that $j = \frac{1}{2}$, $\ell = 1$, $J_N = \frac{1}{2}$, and the coefficient α_N has the values $+\frac{1}{12}$ for J = 1, $-\frac{1}{4}$ for J = 0. Hence spin J = 1 is expected to hold for the ground state of $_\Lambda C^{14}$ and $_\Lambda N^{14}$, contrary to the above rule. With J = 1, the two-body decays $_\Lambda C^{14} \rightarrow \pi^- + N^{14}(J = 1+)$ and $_\Lambda N^{14} \rightarrow \pi^- + O^{14}(J = 0+)$ are both allowed through the dominant s-interaction. However, if J = 0 held for the $(_\Lambda C^{14}, _\Lambda N^{14})$ doublet, the two-body decay $_\Lambda N^{14} \rightarrow \pi^- + O^{14}$ would be forbidden for the s-interaction, although still allowed through the p-interaction (about 10 times weaker). Since O^{14} has

no known particle-stable excited states, this means that there can be no confusion from $(\pi^- + O^{14*})$ modes, and the two-body decay of $_\Lambda N^{14}$ would be quite rare; for $J = 0$, the two-body decay $_\Lambda C^{14} \to \pi^- + N^{14}$ is allowed through the s-interaction.

The derivation of expression (8) is based essentially on a variational estimate for B_Λ, in which the same trial function is used to describe the Λ-nucleus relative motion for all the p-shell hypernuclei. The wave-functions directly calculated do not deviate far from such a mean wave-function, for as the B_Λ value increases and the tail of the wave-function falls off more rapidly, so also does the radius of the Λ-nucleus potential increase, partly compensating this effect. The constant term C then results from the kinetic energy terms and the interaction of the Λ particle with the s-shell nucleons.

For hypernuclei whose core nuclei are spinless, expression (8) gives a linear relation between B_Λ and N_p. For the systems $_\Lambda He^5 (B_\Lambda = 3.1 \pm 0.05$ MeV$)$, $_\Lambda Be^7 (B_\Lambda = 4.9 \pm 0.5$ MeV$)$, $_\Lambda Be^9 (B_\Lambda = 6.5 \pm 0.15$ MeV$)$ and $_\Lambda C^{13} = 10.6 \pm 0.4$ MeV$)$, this linear relation is well satisfied, with $C = 3.1 \pm 0.05$ MeV and $<\bar{V}> = 0.90 \pm 0.04$ MeV. This value of $<\bar{V}>$ is in good agreement with the value directly calculated[15] from the s-wave Λ-N potentials (without hard core) discussed in Section I.

The spin-dependent term $<\Delta>$ can be estimated in four reliable cases, from $_\Lambda Li^7 (B_\Lambda = 5.52 \pm 0.45$ MeV$)$, $_\Lambda Li^8$ and $_\Lambda Be^8 (\bar{B}_\Lambda = 6.50 \pm 0.25$ MeV$)$, $_\Lambda Li^9 (B_\Lambda = 8.0 \pm 0.3$ MeV$)$, and $_\Lambda B^{12} (B_\Lambda = 10.5 \pm 0.2$ MeV$)$. The comparison with the expression (8) is given in Table 2. In the $_\Lambda Be^7 - _\Lambda Li^7$ comparison, it is clear that $\Delta B_\Lambda = <\Delta>$ cannot exceed $0.9(\pm 0.1)$ MeV, otherwise $_\Lambda Be^7$ would not be particle-stable. The value expected for $<\Delta>$ on the basis of our knowledge of the Λ-N s-wave potentials is about 0.85 MeV, not incompatible with this value for $A = 7$, especially when the mean wave-function assumed in (8) is replaced by the more diffuse wave-function appropriate to the low B_Λ values for these systems. On the other hand, the large difference $\Delta B_\Lambda = 1.5$ MeV between $_\Lambda Be^9$ and $_\Lambda Li^9$ requires a correspondingly large value for $<\Delta>$, not really consistent with this estimate for $<\Delta>$. Indeed, the values of $<\Delta>$ given in Table 2 show a

steady increase as N_p increases through the p-shell, roughly in proportion with N_p. The reason for this behaviour of the B_Λ values is not yet known. Possibly it reflects the inadequacies of the approximations made in the derivation of the expression (8), or perhaps it reflects properties of the Λ-N forces (for example, the effect of a spin-orbit term) which have not yet been taken into account here.

At this point, accurate and reliable B_Λ values for further hypernuclear species in this p-shell region would be of great interest, to explore further the dependence of B_Λ on the spin and structure of the core nucleus. In order for such events to represent a useful addition to the present data, it is essential that they allow a unique and reliable identification of the species, either from analysis of its production process or from its decay process, or both.

II. THE DECAY INTERACTIONS OF THE Λ PARTICLE

1. The mesic decay processes

It is well known that, owing to the low momentum (100 MeV/c) of the proton resulting from Λ decay at rest, the rate of π^- decay of a Λ particle in nuclear matter is generally reduced as a result of the Pauli principle, since a large fraction of the final states which can be reached by the final proton are already occupied. This effect is already quite large in $_\Lambda He^5$, where the π^- decay rate is reduced by a factor of about 0.37; in $_\Lambda C^{13}$, the calculated reduction factor is about 0.14.

It is perhaps less well known that in the lightest hypernuclei, the effect of the Pauli principle can lead to an enhancement of the decay rate in suitable circumstances, namely if the spin configuration and the decay interaction are such that the final proton is necessarily emitted into a final state which satisfies the symmetry requirements of the Pauli principle. For example, in $_\Lambda H^4 \rightarrow \pi^- + He^4$ decay with $J = 0$ for

$_\Lambda H^4$, the s-interaction for Λ decay is spin-independent, so that the final proton is necessarily s-wave and in the spin configuration appropriate to He^4, and the decay rate for this transition is enhanced by almost a factor 2 (the space wave-functions do not overlap precisely) as a result of the antisymmetrization appropriate for a final state with two protons.

These same effects hold also for the π^0 decay modes, of course. Thus, with $J = 0$ for $_\Lambda He^4$, the rate for π^0 decay through the s_0 inter-action is enhanced, whereas the rate for π^0 decay through the p_0 inter-action is strongly suppressed; the rate for π^- decay of $_\Lambda He^4$ is also strongly suppressed, by a factor about 0.35, since there are already two s-wave protons present in the initial state. Hence the π^0/π^- ratio in $_\Lambda He^4$ decay is strongly sensitive to the p_0/s_0 ratio in $\Lambda \to n + \pi^0$ decay. For free Λ decay, the π^0/π^- ratio is very close to 0.5; for $_\Lambda He^4$ decay Block et al.[16] have observed the π^0/π^- ratio to be 2.0 ± 0.3. From this striking result, Block et al. have been able to deduce that the π^0 mode of Λ decay is dominantly through the s_0-channel, with $p_0^2/(p_0^2 + s_0^2) = 0.23 \pm 0.16$, in agreement with expectation (0.12 ± 0.03) from the $\Delta I = \frac{1}{2}$ rule.

2. The non-mesic de-excitation of the Λ particle

For bound Λ particles, the presence of nucleons allows the weak interactions

$$\Lambda + p \to n + p \tag{10a}$$

$$\Lambda + n \to n + n \tag{10b}$$

to become effective, releasing the full energy difference of about 176 MeV between the Λ particle and nucleon. This weak interaction can scarcely be investigated without appeal to studies of Λ-hypernuclear decay, and rather little is known of its detailed properties at this time.

These processes (10) represent the only strangeness-changing weak interaction which is readily accessible to observation and which involves four strongly-interacting fermions[*]. With our present views on the nature of weak interactions, it is natural to expect the existence of a primary four-fermion interaction (10a). The validity of the $\Delta I = \frac{1}{2}$ rule for strangeness-changing weak interactions then requires also the existence of a primary interaction of the form (10b), although there is no direct evidence for a neutral weak interaction current (in fact, there is very strong evidence against neutral leptonic currents of strength comparable with the charged currents for leptons). In this view, it is natural to regard the $\Lambda \to N + \pi$ decay interactions as secondary in character since they can occur as a consequence of these four-fermion interactions; this connection is illustrated explicitly in Fig. 1, which depicts one sequence of processes by which the interaction (10a) can give rise to $\Lambda \to p + \pi^-$ decay. Since this four-fermion interaction involves four strongly-interacting particles, mesonic corrections may be expected to distort the form of the interaction quite strongly from the (V-A) form which the current-current theory would predict. This is illustrated in Fig. 2, which shows a series of processes contributing to the physically-observed interaction (10a). The terms (a) and (b) show the primary interactions (10a) derived from the charged and neutral currents, in turn, the vertices shown being distorted from their primary forms by the usual vertex corrections. The remaining graphs (c) - (f) show corrections which involve the exchange of various mesonic systems between the strangeness-changing and strangeness-conserving currents; the relation between these graphs and the primary interaction may be seen by analysing each ($\Lambda \to N + \text{meson}$) vertex in the manner of Fig. 1. The terms (c) and (d) are well known, from their discussion by Karplus and Ruderman[24] who recognized the importance of their contribution if the Λ spin were large and used its comparison with the experimental data to argue against

---

[*] The strangeness-conserving weak interaction $n + p \to n + p$ is expected to exist if the current-current hypothesis of Feynman and Gell-Mann [Phys.Rev. 109, 193 (1958)] holds valid. This weak interaction is expected to produce parity-violating effects of very small amplitude in nuclear forces and the properties of nuclear states, some of which have been quantitatively estimated by Blin-Stoyle and co-workers.

the possibility of spin $\geq \frac{3}{2}$ for the Λ particle. Now that $j_\Lambda = \frac{1}{2}$ is well established and the $\Lambda \to N + \pi$ interaction is known to be dominantly s-wave, there is no reason to believe that these Karplus-Ruderman terms contribute dominantly to the observed process $\Lambda + N \to N + N$; these terms must be taken together with a large number of other mesonic correction terms, of which several are given explicitly in Fig. 2.

Rather little is known at present concerning the properties of this weak interaction:

$$\Lambda + N \to N + N . \tag{11}$$

The simplest properties of interest are its charge-dependence and its spin-dependence. For bound Λ particles this interaction will dominantly occur for ΛN s-states, in view of the relatively low Λ-N relative momenta to be expected in hypernuclei. The final nucleon momentum for ΛN de-excitation at rest is about $q = 400$ MeV/c, so we shall simplify the discussion by using the non-relativistic form for the matrix-elements. For Λp capture from an s-state configuration the general form of the matrix-element is

$$M(\Lambda p \to np) = a_p P_0 + b_p P_1 + \frac{3}{\sqrt{8}} c_p (\underline{\sigma}_Y \cdot \underline{q}\underline{\sigma}_N \cdot \underline{q} - \frac{1}{3}\underline{\sigma}_Y \cdot \underline{\sigma}_N q^2)/M^2$$

$$+ \sqrt{\frac{3}{8}} d_p (\underline{\sigma}_Y + \underline{\sigma}_N) \cdot \underline{q}/M + e_p (\underline{\sigma}_Y - \underline{\sigma}_N) \cdot \underline{q} P_0/2M \tag{12}$$

$$+ \sqrt{3} f_p (\underline{\sigma}_Y - \underline{\sigma}_N) \cdot \underline{q} P_1/M ,$$

where $P_0 = (3 + \underline{\sigma}_Y \cdot \underline{\sigma}_N)/4$ and $P_1 = (1 - \underline{\sigma}_Y \cdot \underline{\sigma}_N)/4$ denote the singlet and triplet spin projection operators, $\underline{\sigma}_Y$ denotes the Λ or n spin and $\underline{\sigma}_N$ here denotes the proton spin. In this expression the terms a_p and e_p denote the $^1S_0$ transition amplitudes leading to the $^1S_0$ and $^3P_0$ final states, respectively, and the terms b_p, c_p, d_p and f_p denote the $^3S_1$ transition amplitudes leading to the $^3S_1, ^3D_1, ^3P_1$ and $^1P_1$ final states. For Λn capture the corresponding form is

$$M(\Lambda n \to nn) = a_n P_0 + \sqrt{\frac{3}{8}} d_n (\underline{\sigma}_Y + \underline{\sigma}_N) \cdot \underline{q}/M + e_n (\underline{\sigma}_Y - \underline{\sigma}_N) \cdot \underline{q} P_0/2M \tag{13}$$

where $\underline{\sigma}_Y$ here denotes the spin of the Λ particle and either of the final neutrons and $\underline{\sigma}_N$ denotes the spin of the other neutron. Terms of the form b, c and f are absent here, as they lead to final states which are forbidden for the n-n system. If the $\Delta I = \frac{1}{2}$ rule holds then we have in addition the following equalities:

$$a_n = \sqrt{2}\, a_p, \quad d_n = \sqrt{2}\, d_p, \quad e_n = \sqrt{2}\, e_p. \tag{14}$$

We note that the transitions a, b and c conserve parity, whereas the transitions d, e and f reverse the parity of the state. If time-reversal invariance holds then the phases of each of these amplitudes may be determined from the known NN scattering phases by the use of Watson's theorem. Obviously the determination of all these parameters, and the test of the equalities (14), will require polarization experiments involving the measurement of the longitudinal polarization of the fast n and p emitted from unpolarized hypernuclei (or the angular distribution of the fast nucleons from non-mesic decay of polarized hypernuclei), and of the polarization correlation coefficients for the fast (np) and (nn) pairs emitted in non-mesic decay of hypernuclei. These polarization coefficients could also be measured for initial ΛN states of definite spin by selecting the appropriate light hypernuclei (cf. below). Such experiments will be difficult to carry out and to interpret and lie far in the future.

In principle, for the calculation of non-mesic decay rates for hypernuclei, matrix-elements of the forms (12) and (13) should be used for each of the nucleons and evaluated between the initial hypernuclear wave-function and the final nuclear states. Here, we shall consider instead a simplified calculation for the non-mesic decay rates which treats the Λ de-excitation by different nucleons as incoherent. This approximation is not strictly valid, because, owing to the identity of the neutrons and of the protons, the same final state can generally be reached through capture on any one of the nucleons; however, because of the large energy release, it is rather likely that these interference effects will generally be small and will tend to cancel out in the total de-excitation rates, summed over all final states.

Let us denote by R_{NS} the $\Lambda N \to NN$ transition rate, when the ΛN system is in an s-state of total spin S, for unit density of nucleons of type N at the Λ position. The non-mesic decay rate for a given hypernucleus is then given by the expression

$$R_{n.m.} = \bar{R}(_{\Lambda}Z^{A+1}) \, \rho_A ,$$

$$= \bar{R}(_{\Lambda}Z^{A+1}) \, A \int \psi_{\Lambda}^2 \, \rho_N(\underline{r}) d_3 r , \qquad (15)$$

where ρ_A is the mean density of nucleons at the Λ position, $\rho_N(\underline{r})$ being the nucleon density at position $\underline{r}$ and ψ_{Λ} the wave-function for the Λ nucleus relative motion and $\bar{R}$ is the spin and charge average of the R_{NS} which is appropriate to the hypernucleus considered. In terms of the amplitudes (12) and (13), these quantities R_{NS} are given by

$$R_{po} = |a_p|^2 + |e_p|^2 (q/M)^2 , \qquad (16a)$$

$$R_{p1} = |b_p|^2 + |c_p|^2 (q/m)^4 + |d_p|^2 (q/M)^2 + |f_p|^2 (q/M)^2 , \qquad (16b)$$

$$R_{no} = [\,|a_n|^2 + |e_n|^2 (q/M)^2\,] , \qquad (16c)$$

$$R_{n1} = |d_n|^2 (q/M)^2 . \qquad (16d)$$

In the last expressions R_{nS}, we have taken into account the symmetry requirements of the final state and the identity of the two final neutrons. If the $\Delta I = \frac{1}{2}$ rule holds, the equalities (14) lead to the predictions

$$R_{po} = \frac{1}{2} R_{no} , \qquad (17a)$$

$$R_{p1} \geq \frac{1}{2} R_{n1} . \qquad (17b)$$

The quantity most readily measured is the ratio $Q = (\text{non-mesic}/\pi^- - \text{mesic})$. Here, we shall not include π^0- mesonic decay events[25] among the non-mesic decay rate, for the π^0-mesonic events normally give an exceedingly small star with a visible energy release of at most several

MeV and would very frequently be overlooked, whereas the non-mesic decay events involve a large energy release. For $_\Lambda$He hypernuclei in emulsion, estimates of this ratio have been reported as follows: $Q = 2.3 \pm 1.0$ by Fry[17], $1.5(\pm 0.4) \le Q \le 2.8$ by Silverstein[18] and $Q \ge 1.1 \pm 0.5$ by Schlein[19], whose non-mesic decay rate includes only two-prong events. For $_\Lambda$He^4, Block et al.[16] have obtained a rather accurate value, $Q = 0.52 \pm 0.10$. About 80% of the π^- decays of $_\Lambda$He in emulsion are due to $_\Lambda$He^5 decay; adopting the value $Q = 1.5$ for $_\Lambda$He, the correction for admixture of $_\Lambda$He^4 non-mesic decay events leads to the estimate $Q = 1.8$ for $_\Lambda$He^5. On this basis, it is then possible to estimate Q for some of the heavier hypernuclei. This involves an estimate of $R_{n.m.}$ from Eq. (15), using the value $\rho_4 = 0.038$ f^{-3} for $_\Lambda$He^5 and corresponding calculated values ρ_Λ for the hypernuclei of interest, together with an estimate of the π^- decay rate $R(\pi^-)$ using the completeness-relation method[20]. For example, for $_\Lambda$He^5, the calculated value of $R(\pi^-)$ is 0.25 Γ_Λ, where $1/\Gamma_\Lambda$ denotes the free Λ lifetime, so that our estimate of Q and the above value for ρ_4 lead to the estimate

$$\bar{R}(_\Lambda He^5) = \tfrac{1}{8}(3R_{p1} + R_{po} + 3R_n + R_{no})$$

$$= (1.8) \ (0.25) \ \Gamma_\Lambda/(0.038) = 12(\pm 3) \ \Gamma_\Lambda,$$

(18)

where the error quoted represents only the statistical uncertainty on Q. With this value for $\bar{R}$, estimates have been made for Q for $_\Lambda$Li^7 (neglecting the spin-dependence of R_{NS}), $_\Lambda$Be^9 and $_\Lambda$C^{13}, as given in Table 3. The rapid rise in Q with increasing A is due primarily to the rapidly increasing suppression of the π^- decay process by the Pauli principle. However, the non-mesic decay rate does increase from 0.45 Γ_Λ for $_\Lambda$He^5, through 1.5 Γ_Λ for $_\Lambda$C^{13}, to a value of 2.0 Γ_Λ for a very heavy hypernucleus (say $A \approx 100$). Several independent estimates of $R(\pi^-)$ we have made for a hypernucleus of mass number $A \approx 100$, including pion re-absorption effects, lead to values about 0.015 Γ_Λ, and therefore to a large value $Q \approx 130$. We conclude that the decay lifetime of a heavy hypernucleus ($A \approx 100$) may be expected to be essentially independent of A, with the value $\approx 1.2 \times 10^{-10}$ sec.

The evidence on the charge dependence of the non-mesic process appears somewhat contradictory at first sight. For $_\Lambda He^4$, Block et al.[16] have classified non-mesic decay events with a recoil proton of momentum exceeding 250 MeV/c as due to Λp capture, leading to the estimate $(\Lambda p)/(\Lambda n) = 2.2 \pm 0.8$. Since $_\Lambda He^4$ has $J = 0$, this corresponds to the ratio

$$\frac{(3R_{p1} + R_{po})/2}{R_{no}} = 2.2(\pm 0.8). \tag{19}$$

On the other hand, for spallation hyperfragments following high-energy K^- interactions in emulsion, for which typically $A \approx 70$, Beniston[21] and Lagnaux[22] have compared the observed proton spectrum with those predicted by a Monte Carlo calculation for (Λp) and (Λn) capture processes, and have concluded that, in these heavy hypernuclei, the (Λn) capture process is the dominant non-mesic decay process. The ratio $(\Lambda n)/[(\Lambda n) + (\Lambda p)]$ obtained by Beniston was $\gamma = 0.8 \pm 0.1$, and by Lagnaux $\gamma = 0.65 \pm 0.1$, the difference between these values being due, at least in part, to the differing assumptions made about the spatial distribution of the Λ particle. To continue, we shall adopt the value $\gamma = 0.7$, so that

$$\frac{3R_{p1} + R_{po}}{3R_{n1} + R_{no}} = \left(\frac{1}{\gamma} - 1\right) \approx 0.4. \tag{20}$$

From this ratio and the value of Eq. (19), we can conclude the value $3R_{n1} + R_{no} = 69(\pm 20) \Gamma_\Lambda$ to be used below. The striking difference between the $(\Lambda p)/(\Lambda n)$ ratios observed for $_\Lambda He^4$ and for heavy hypernuclei can be understood quite simply if the (Λn) de-excitation process has a strong spin-dependence, with

$$R_{no}/R_{n1} \approx 0.3, \tag{21}$$

the non-mesic (Λn) decay interaction being significantly weaker in the singlet configuration.

The remaining information to be discussed consists of the non-mesic rates for $_\Lambda He^4$ and $_\Lambda H^4$, for which the nucleon density ρ_3 is 0.019 f^{-3}.

For $_\Lambda\text{He}^4$, the calculated suppression[20] of $R(\pi^-)$ to $0.26\ \Gamma_\Lambda$, and the above value $Q = 0.52 \pm 0.10$, lead to

$$3R_{pl} + R_{po} + 2R_{no} = 41(\pm 10)\ \Gamma_\Lambda.\qquad(22)$$

From Eqs. (18), (21) and (22) we conclude that $R_{nl} = 21(\pm 7)\ \Gamma_\Lambda$, $R_{no} = 6(\pm 2)\ \Gamma_\Lambda$ and $(3R_{pl} + R_{po}) = 28(\pm 8)\ \Gamma_\Lambda$. For $_\Lambda\text{H}^4$, the π^- decay rate $R(\pi^-)$ has been calculated[20] to be $0.74\ \Gamma_\Lambda$, and the non-mesic rate is given by

$$0.31(\pm 0.06) \geq (0.019)\ (R_{po} + 3R_{nl} + R_{no})/6 \geq 0.22(\pm 0.06),\qquad(23)$$

using the above values for $(3R_{nl} + R_{no})$ and the requirement $0 \leq R_{po} \leq 28(\pm 8)\ \Gamma_\Lambda$. On this basis, the ratio Q for $_\Lambda\text{H}^4$ is expected to lie between $0.29(\pm 0.08)$ and $0.42(\pm 0.08)$. In the experiment of Block et al.[16], $120(\pm 11)\ _\Lambda\text{H}^4 \to \pi^-$ events were seen. From the number of $_\Lambda\text{He}^4$ production events and from charge independence, it was concluded that the total number of $_\Lambda\text{H}^4$ production events was 163 ± 10. From the π^0/π^- ratio (2.5 ± 0.5) observed for $_\Lambda\text{He}^4$ decay, and from the prediction of the $\Delta I = \frac{1}{2}$ rule that[20]

$$\frac{\pi^0}{\pi^-}\ (_\Lambda\text{He}^4) \times \frac{\pi^0}{\pi^-}\ (_\Lambda\text{H}^4) = \frac{1}{4},\qquad(24)$$

we may estimate the number of $_\Lambda\text{H}^4 \to \pi^0$ events as 12 ± 1. The remainder of the events, amounting to 31 ± 15, must be attributed to non-mesic decay processes; this leads to the ratio $Q = 0.26 \pm 0.13$, which is not at all in disagreement with the value predicted above.

This small fraction of $_\Lambda\text{H}^4$ decay events which proceed through the non-mesic mode may not be easy to identify in the helium bubble chamber experiment, especially because of the confusion possible with slow Σ^- hyperons following $K^- - \text{He}^4$ capture which come to rest and interact to give

a one-prong star. If we assume [for lack of other knowledge[*]] that the Λp capture interaction is spin independent, i.e. $R_{po} = R_{p1}$, then R_{po} has the value $7(\pm 2)$ Γ_{Λ} and the $(\Lambda p)/(\Lambda n)$ ratio predicted for $_{\Lambda}H^4$ has the value $2R_{po}/(3R_{n1} + R_{no}) = 14(\pm 2)/69$ $(\pm 20) = 0.2(\pm 0.06)$, so that only six non-mesic $_{\Lambda}H^4$ decay events are expected to occur with a fast proton (say $\gtrsim 250$ MeV/c) in the experiment of Block et al.[16]. However, the majority of the (Λn) capture events are expected to give a visible prong. Some indication on this can be obtained from the $\pi^- + He^4$ interaction studies of Bortolani et al.[23], which also proceeds through two-nucleon emission with a comparable energy release (≈ 140 MeV). Of 356 π^- interactions at rest in a helium chamber, only 23 gave no visible track; since the primary capture interaction $\pi^- + p + n \to n + n$ is believed to account for at least $3/4$ of these capture events (the remainder being due to the $\pi^- + p + p \to n + p$ interaction), we may estimate[**] that not more than 9% of the (Λn) de-excitation events for $_{\Lambda}H^4$ will give no visible track. Although the separation of the $_{\Lambda}H^4$ non-mesic decay events is a difficult task, a value of the $(\Lambda p)/(\pi^- -mesic)$ ratio for $_{\Lambda}H^4$, or even an upper limit on this would be very valuable in providing a limit on R_{po}, and therefore a direct indication of the spin dependence for the (Λp) de-excitation process.

---

[*] With the $\Delta I = 1/2$ rule for the $\Lambda N \to NN$ process, the value $R_{no} = 6(\pm 2)$ Γ_{Λ} and Eq. (17a) would require $R_{po} = 3.0(\pm 1.0$ $\Gamma_{\Lambda})$, an appreciably smaller value than that assumed here. With this value the $(\Lambda p)/(\Lambda n)$ ratio for $_{\Lambda}H^4$ would be $0.08(\pm 0.04)$, which would predict only two non-mesic $_{\Lambda}H^4$ with a fast proton in this experiment. We may note here that these spin-dependences for the Λn and Λp processes are quite at variance with a simple (V-A) form for the $\Lambda N \to NN$ interaction; in the non-relativistic limit, the first term (a_p) of (5.4) would be dominant, and the ratio R_{po}/R_{p1} would be predicted to be exceedingly large.

[**] We should emphasize here that the $\Lambda n \to nn$ interaction may have quite different spin dependence from the $\pi^- pn \to nn$ interaction, in which case this proportion might well turn out to be larger than this estimate. For example, H^3 production is found to occur in 22% of $\pi^- - He^4$ capture events; this appears to be a particular feature of the $(\pi^- pn)$ and $(\pi^- pp)$ capture amplitudes. There is certainly no reason to expect the (Λn) and (Λp) capture amplitudes to have a similar spin and charge dependence, and it is quite unlikely that the mode $H^3 + n$ will prove to be as abundant in $_{\Lambda}H^4$ non-mesic decay.

REFERENCES

1. J. de Swart and C. Iddings, Phys.Rev. 128, 2810 (1962); Phys.Rev. 130, 319 (1963).

2. B. Downs, D. Smith and T. Truong, Phys.Rev. 129, 2730 (1963); also private communications (1963).

3. B. Downs and R. Dalitz, Phys.Rev. 114, 593 (1959).

4. D. Muller, Untersuchunger zum Dreikorperproblem der Kernphysik, (Heidelberg, 1962).

5. R. Dalitz and B. Downs, Phys.Rev. 111, 967 (1958).

6. K. Dietrich, R. Folk and H. Mang, Proc.Rutherford Jubilee Int.Conf. (Heywood, London, 1961), p. 165.

7. U. Gutsch, University of Frankfurt (private communication, 1963).

8. H. Mang and W. Wild. Z.Phys. 154, 182 (1959).

9. M. Danysz, K. Garbowska, J. Pniewski, T. Pniewski, J. Zakrewski, E. Fletcher, J. Lemonne, P. Renard J. Sacton, D. O'Sullivan, T.P. Shah, A. Thompson, P. Allen, Sr. M. Heeran, A. Montwill, J.E. Allen, M.J. Beniston, D.H. Davis, D.A. Garbutt, V.A. Bull, R.C. Kumar and P.V. March, Phys.Rev.Letters, to be published (1963).

10. R.H. Dalitz, Phys.Letters, to be published (1963).

11. R.D. Lawson and M. Rotenberg, Nuovo Cimento 17, 449 (1960).

12. S. Iwao, Nuovo Cimento 17, 491 (1961).

13. R.H. Dalitz and J. Soper, report in preparation (1963).

14. R.H. Dalitz, Nucl.Phys. 41, 78 (1963).

15. R.H. Dalitz, Proc.Rutherford Jubilee Int.Conf. (Heywood, London, 1962); p. 103.

16. M.M. Block, R. Gessaroli, J. Kopelman, S. Ratti, M. Schneeberger, L. Grimellini, T. Kikuchi, L. Lendinara, L. Monari, W. Becker and E. Harth, Hyperfragment studies in the helium bubble chamber, Proc.Int.Con.on Hyperfragments (CERN, 1963).

17. W.F. Fry, Ann.Revs.Nucl.Sci.

18. E. Silverstein, Suppl.Nuovo Cimento 10, 41 (1959).

19. P. Schlein, Phys.Rev.Letters 2, 220 (1959).

20. R.H. Dalitz and L.S. Liu, Phys.Rev. 116, 1312 (1959).

21. M.J. Beniston, University of Chicago, private communication (1963).

22. J.P. Lagnaux, Université Libre de Bruxelles, Brussels (1963).

23. M.V. Bortolani, L. Lendinara and L. Monari, Nuovo Cimento
    25, 603 (1962).

24. M. Ruderman and R. Karplus, Phys.Rev. 76, 1458 (1949); see also
    F. Cerulus, Nuovo Cimento 5, 1685 (1957) and R.H. Dalitz,
    Rev.Mod.Phys. 31, 823 (1959).

25. R. Ammar, Nuovo Cimento 14, 1226 (1959).

* * *

Table 1

Hard core radius d	d = 0.0 f (Gaussian shape)	d = 0.2 f (square well)	d = 0.4 f (square well)
a_0 (f)	$-2.4 {}^{+1.2}_{-0.6}$	$-4.2 {}^{+3.0}_{-1.3}$	-4.5
a_1 (f)	-0.5 ± 0.1	-0.55 ± 0.05	-0.6
Notes	obtained from $_\Lambda H^3$ and $_\Lambda He^5$ (Refs. 3,5)	obtained from $_\Lambda H^4$ and $_\Lambda He^5$ (Ref. 6)	obtained from $_\Lambda H^4$ and $_\Lambda He^5$ (Ref. 7)
Existence of J = 1 excited state $_\Lambda H^{4*}$?	$B_\Lambda^* \approx 1.3$ MeV ($s^* = 1.25$)	Not bound ($s^* = 0.90$)	Not bound ($s^* = 0.83$)

Table 2

Hypernuclei compared	ΔB_Λ (MeV)	Estimate from Eq. (8)[†]	Value of $\langle\Delta\rangle$
$_\Lambda Be^7 - _\Lambda Li^7$	0.6 ± 0.5 (≤ 0.9)	$0.98 \langle\Delta\rangle$	$\langle\Delta\rangle = 0.6 \pm 0.5$ MeV
$_\Lambda Be^8 - _\Lambda Be^9$	0.0 ± 0.3	$0.59 \langle\Delta\rangle - \langle\bar{V}\rangle$	$\langle\Delta\rangle = 1.5 \pm 0.5$ MeV
$_\Lambda Be^9 - _\Lambda Li^9$	1.50 ± 0.3	$0.70 \langle\Delta\rangle$	$\langle\Delta\rangle = 2.1 \pm 0.4$ MeV
$_\Lambda B^{12} - _\Lambda C^{13}$	-0.10 ± 0.4	$0.28 \langle\Delta\rangle - \langle\bar{V}\rangle$	$\langle\Delta\rangle = 2.7 \pm 1.3$ MeV

[†] The coefficients α_N used here are those computed from intermediate coupling nuclear wave-functions constructed by J. Soper.

Table 3

$$Q = (\text{non-mesic})/(\pi^- \text{-mesic})$$

Hypernucleus	$_\Lambda H^4$	$_\Lambda He^4$	$_\Lambda He^5$	$_\Lambda Li^7$	$_\Lambda Be^9$	$_\Lambda C^{13}$	$_\Lambda Ag^{109}$
$Q =$	0.15	0.5	1.8	2.7	6.2	11.3	130

The underlined entries represent the empirical values for Q; the other entries are calculated values based on the entry for $_\Lambda He^5$.
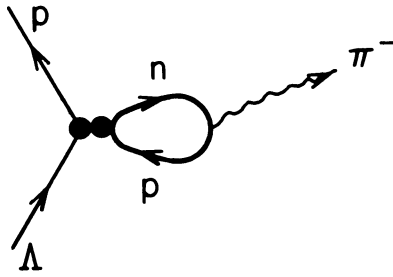
Fig. 1.   The Decay $\Lambda \rightarrow p + \pi^-$ as a consequence of the Four-fermion Weak Interaction. (5.1a)
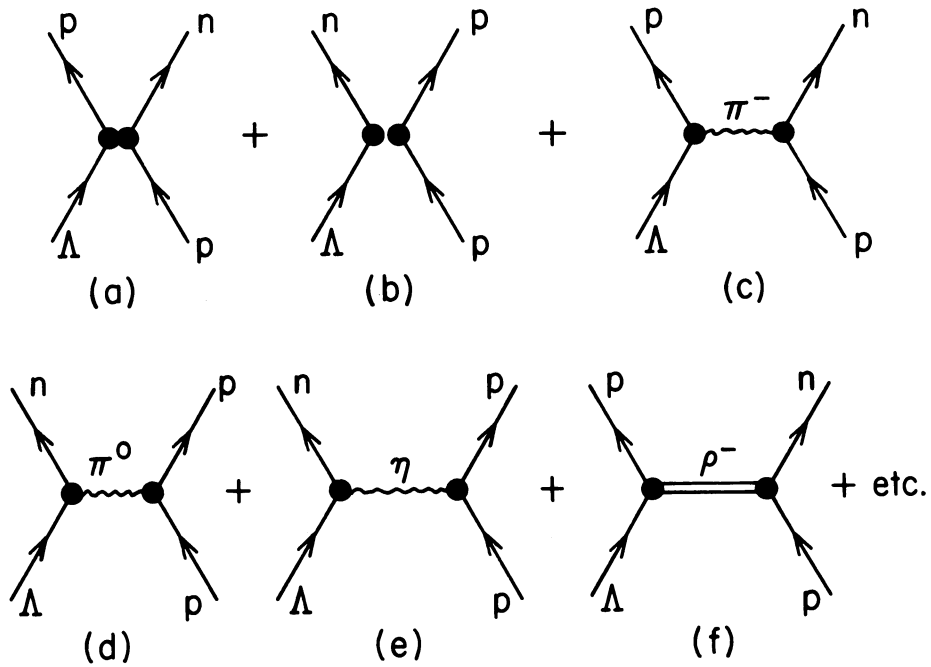
Fig. 2.   Contributions to the Process $\Lambda + p \rightarrow n + p$.

THE NUCLEAR WELL-DEPTH FOR Λ PARTICLES

B.W. Downs,
University of Colorado, Boulder, Colorado.

I.   INTRODUCTION

The binding energy of a Λ particle in its ground state in nuclear matter is a quantity of some interest in the study of the Λ-nucleon interaction.   This binding energy is equal to the well-depth D seen by a Λ particle whose ground state is a state of zero momentum with respect to the bottom of the well.   The well-depth D will, presumably, also be very nearly the central depth seen by a Λ particle bound in its ground state in a heavy nucleus on account of the expectation that the potential well seen by a Λ particle in nuclear matter will be only slightly momentum-dependent[1,2].   This expectation also suggests that the well-depth D may give a good indication of the central depth of the real part of the optical potential for scattering of low-energy Λ particles by heavy nuclei.

Several attempts have been made to deduce the well-depth D from the observed binding energies of the light hypernuclei[2-5].   These have resulted in estimates in the range

$$D \approx 22 - 30 \text{ MeV}. \tag{1}$$

The lower values in Eq. (1) have been obtained from the trend of the binding energies of the observed hypernuclei with $3 \leq A \leq 12$[2-4];   the higher, from an analysis of the binding energy of $_{\Lambda}C^{13}$[5].   The former are suspect because the binding energies of the light hypernuclei are strongly influenced by the density and spin structure of the nucleon cores, both of which fluctuate and differ, in most cases, from their values in nuclear matter, which is taken to be a spin-saturated collection of an equal number of protons and neutrons with a nucleon density equal to the central density observed in the heaviest nuclei[6].   The higher estimates, based on $_{\Lambda}C^{13}$,

would seem to be more reliable because the nucleon core comes very close to matching the conditions of nuclear matter at its centre[6]; even in this case, however, the finite radius of the core and uncertainties concerning its structure leave the estimated values of D open to some question.

The well-depth D is determined, in part, by aspects of the Λ-nucleon interaction which play a quantitatively different role in determining the binding energies of the light hypernuclei[2,3,5] and it is principally from the analyses of these binding energies that the phenomenological Λ-nucleon interaction potential has been deduced[2,5,7,8]. It is the purpose of this paper to discuss those aspects of the Λ-nucleon interaction which play a role in determining D. In Section II the calculations of D by Bodmer and Sampanthar[2] in terms of two-body and three-body Λ-nucleon potentials without hard cores are briefly reviewed. Calculations of D in terms of two-body Λ-nucleon potentials with hard cores are discussed in Section III. The final Section IV contains a summary of the results of these calculations and an indication of the relation between D and the properties which the optical potential for scattering of low-energy Λ-particles by heavy nuclei might be expected to have.

II. THE WELL-DEPTH D CORRESPONDING TO Λ-NUCLEON POTENTIALS WITHOUT HARD CORES

Bodmer and Sampanthar[2] have used Λ-nucleon potentials without hard cores to calculate D in perturbation theory, nuclear matter being treated as a Fermi gas. The first-order contribution to D from central two-body direct (non-exchange) Λ-nucleon interactions is[9]

$$D_{direct}^{(1)} = \rho\Omega, \qquad (2)$$

where ρ is the density of nuclear matter and Ω is the volume integral of the spin-average Λ-nucleon potential. The first-order contribution

from two-body exchange potentials of Yukawa form

$$V(r) = - V_0 \, R \, e^{-r/R}/r \tag{3}$$

is

$$D^{(1)}_{exchange} = \rho\Omega\{3/(k_F R)^2 - [3/(k_F R)^3] \tan^{-1} k_F R\}, \tag{4}$$

where the Fermi momentum k_F is related to the density of nuclear matter by

$$\rho = 2k_F^3/3\pi^2 . \tag{5}$$

The exchange contribution (4) is smaller than the direct (2) and reduces to it in the limit $(k_F R) \to 0$ [10]. The calculations of Bodmer and Sampanthar indicate that the second-order contributions to both D_{direct} and $D_{exchange}$ are less than or about 10% of the first-order contributions [and have the same sign as $D^{(1)}$] for relevant values of k_F and R.

Analysis of the binding energy of $_\Lambda He^5$ in terms of two-body Λ-nucleon potentials without hard cores, leads directly to a determination of Ω [5,7]:

$$\Omega = \begin{Bmatrix} 230 \pm 10 \\ 175 \pm 5 \end{Bmatrix} \text{MeV f}^3 \text{ for } b = \begin{Bmatrix} 1.5 & \text{f} & (R = \hbar/2M_\pi) \\ 0.85 & \text{f} & (R = \hbar/M_K) \end{Bmatrix} . \quad \begin{matrix} (6a) \\ (6b) \end{matrix}$$

The volume integrals (6) thus deduced are nearly shape-independent for two-body potentials having the same intrinsic range b [11]. The range parameters used to obtain (6) were chosen as being representative of the two simplest meson-exchange mechanisms which can give rise to a charge-independent Λ-nucleon interaction [7]. There is, of course, no assurance that either of these range parameters is the correct one; extensive scattering data, from which the range of the nucleon-nucleon interaction was determined, are not available for the Λ-nucleon system. If the range parameter $(\hbar/2M_\pi)$ is the correct one, and if the Λ-nucleon

interaction arises primarily from the exchange of two pions as such
a range would indicate, then that interaction would be primarily a
direct interaction. If, on the other hand, $R = (\hbar/M_K)$ and the Λ-nucleon
interaction arises primarily from the exchange of a single kaon, that
interaction would be primarily an exchange interaction. On this
account, Bodmer and Sampanthar[2] restricted attention to direct
interactions of range $(\hbar/2M_\pi)$ and to exchange interactions of range
$(\hbar/M_K)$.

For the values

$$\rho = 0.172 \text{ nucleons/f}^3 \tag{7a}$$

and

$$k_F = 1.366 \text{ f}^{-1}, \tag{7b}$$

appropriate to the central density in heavy nuclei[6], the calculations
of Bodmer and Sampanthar lead to the values given in Table 1 for the
first-order contributions to D corresponding to the central values of
Ω given in (6).

Table 1

First-order contributions to D in MeV. The total
value $D^{(1)}$ and the contributions $D^{(1) \cdot \ell}$ from
interactions in s- and p-states are given. The
missing values of $D^{(1) \cdot \ell}$ correspond to situations
not considered by Bodmer and Sampanthar.

b	$D^{(1) \cdot \ell}_{\text{direct}}$ $\ell = 0$	$\ell = 1$	$D^{(1)}_{\text{direct}}$	$D^{(1) \cdot \ell}_{\text{exchange}}$ $\ell = 0$	$\ell = 1$	$D^{(1)}_{\text{exchange}}$
1.5 f	33	6	40	-	-	26
0.85 f	-	-	30	27.4	- 1.8	25.6

These values indicate that $D_{exchange}$ is in reasonably good agreement with the empirical estimates (1) for either range considered, but that agreement with D_{direct} can be obtained only for a range which would be expected to correspond to an exchange interaction. Bodmer and Sampanthar have pointed out that, on the basis of this comparison alone, it would appear that exchange interactions of range $(\hbar/M_K)$ may play a significant role in the Λ-nucleon interaction. It should be noted that the range-dependence of D_{direct}, which follows directly from (6), may play a role in determining D if the actual range turns out to be intermediate between $(\hbar/2M_\pi)$ and $(\hbar/M_K)$. The dependence of $D^{(1)}$ on the density of nuclear matter follows from Eq. (2) exactly for direct interactions and approximately for exchange interactions of range as short as $(\hbar/M_K)$. The relative importance of the contributions $D^{(1) \cdot e}$ depends slightly on the density, the p-wave contributions being relatively larger for greater densities[12].

Bodmer and Sampanthar[2] have also analysed the binding-energy data of the light hypernuclei considering the possible presence of three-body Λ-nucleon interactions, potentials without hard cores being taken for both two-body and three-body interactions. Analyses of the binding energies of $_\Lambda H^3$ and $_\Lambda He^5$ including attractive three-body Λ-nucleon potentials lead to a reduction of the two-body contributions to D from those given by Eqs. (2) and (4). Bodmer and Sampanthar have calculated the values of D which result from these reduced two-body contributions and the additional contribution which arises from the corresponding three-body potentials. They found that consideration of three-body potentials can bring D into agreement with the empirical estimates for a variety of situations. In particular, agreement can be obtained for direct two-body interactions of range $(\hbar/2M_\pi)$ and a relatively strong three-body interaction; this could be a consistent combination because both interactions presumably arise predominantly from two-pion-exchange mechanisms.

III. THE WELL-DEPTH D CORRESPONDING TO Λ-NUCLEON POTENTIALS WITH HARD CORES

The potentials without hard cores used by Bodmer and Sampanthar[2] to estimate D may not provide an adequate representation of the Λ-nucleon interaction. The presence of a hard core in the nucleon-nucleon interaction[13] suggests that a hard core may also be characteristic of the Λ-nucleon interaction. In particular, the assumption of the existence of a universal pion-baryon interaction leads to a pion-exchange contribution to the Λ-nucleon potential which is a linear combination of nucleon-nucleon potentials[14]; in this case, the hard core in the nucleon-nucleon interaction implies a hard core in the Λ-nucleon interaction. If the Λ-nucleon interaction does have a hard core, the perturbation technique of Bodmer and Sampanthar[2] cannot be used to calculate D; but many-body techniques developed for use with hard-core potentials can be used. Typical of these are the independent-pair approximation of Gomes, Walecka and Weisskopf[15] and the potential-separation technique of Moszkowski and Scott[16]. The former has been applied by Walecka[17] to the calculation of D; the later, by Moszkowski et al.[18] to the calculation of the s-wave contribution to D.

The more transparent of the methods which have been used for the calculation of D in terms of hard-core potentials is that of Walecka[17]. In this method the relative motion of the Λ particle and a nucleon in nuclear matter is described by a self-consistent Bethe-Goldstone equation in which the particle masses are replaced by appropriate effective masses[19]. The well-depth D is then given by

$$D = -D_C + D_A = \frac{-4}{(2\pi)^3} (M_N^*/\mu^*)^3 \int_0^{\mu^* k_F/M_N^*} d^3K \int e^{-i\vec{K}\cdot\vec{r}} [V_C(r) + V_A(r)] \psi_{BG}(\vec{r}) d^3r, \quad (8)$$

where V_C is the hard-core part of the Λ-nucleon potential (assumed to be the same for both spin states) and V_A is the spin-average of the attractive parts of the singlet and triplet potentials. These two parts

of the potential give rise to the two contributions D_C and D_A to the depth D. A superscript * on a mass indicates an effective mass, and $\mu^* = M_N^* M_\Lambda^* / (M_N^* + M_\Lambda^*)$. In Eq. (8) $\vec{K}$ is the relative momentum of a Λ-nucleon pair, the Λ particle being at rest; the maximum momentum which a nucleon can have is the Fermi momentum k_F. The integral over $\vec{r}$ in Eq. (8) represents the effect of the interaction of a Λ-nucleon pair with relative momentum $\vec{K}$; the integral over $\vec{K}$ is essentially a summation over the possible relative momenta. The wave function $\psi_{BG}(\vec{r})$ is the solution to the Bethe-Goldstone equation for the relative motion with the reduced effective mass μ^* [19]. Although this function vanishes for $r \leq c$, the hard-core radius, the radial part $R^\ell(r)$ of each partial-wave component of $\psi_{BG}(\vec{r})$ has a discontinuous derivative at $r = c$, which leads to the partial-wave contributions D_C^ℓ to D_C through [20,21]

$$V_C(r) \, R^\ell(r) \approx \lim_{\epsilon \to 0} \frac{\hbar^2}{2\mu^*} \left[\frac{d}{dr} R^\ell(r) \right]_{r=c+\epsilon} \delta(r-c) . \qquad (9)$$

The core contributions D_C^ℓ essentially take account of the fact that the core forces the radial functions to zero at the core radius, thereby increasing the curvature of the functions in the neighbourhood of the core (over that which they would have in the absence of the interaction), which corresponds to an increase in the kinetic energy of the interacting pair.

Only s-wave solutions of the Bethe-Goldstone equation have so far been obtained [15,20]. For the case of the interaction between the nucleons in nuclear matter, Gomes et al. [15] found that the s-wave solution with the potential $(V_C + V_A)$ is nearly the same as that with the hard-core interaction V_C alone. An analytic expression for the latter can be obtained, and this has been used in calculations of interaction energies in nuclear matter [15,17]. The characteristic features of the s-wave solution to the Bethe-Goldstone equation are that:

    i)   it vanishes at the hard-core radius c;

    ii) it is very nearly equal to the free-pair (with the reduced mass μ^* appropriate to nuclear matter) solution for $(r - c) > 4/k_F$;

iii) its amplitude exceeds that of the free-pair solution

for $(r - c) \lesssim 4/k_F$ (the last property is a necessary

consequence of the first two).

These properties of the s-wave Bethe-Goldstone function have prompted
the use of several simple approximate functions which incorporate
these features[17,22]. The one which will be used for the present
discussion is

$$R^0(r) \approx B[1 - e^{-2(r-c)/a}] \, j_0(Kr) \tag{10}$$

with

$$B = 1.08 \tag{11a}$$

and

$$a = 1/k_F \, . \tag{11b}$$

This function gives a very good representation of $R_{BG}^0(r)$ for all
values of K which contribute to Eq. (8) and for all values of r which
are important with the short-ranged potentials appropriate to the
Λ-nucleon interaction[23]. If it is further assumed that the same cut-
off factor is appropriate to all partial waves[24], then the corresponding
approximation to the full Bethe-Goldstone function is

$$\psi(\vec{r}) \approx B[1 - e^{-2(r-c)/a}]e^{i\vec{K}\cdot\vec{r}} \, . \tag{12}$$

The approximate functions (10) and [with somewhat less
certainty[24]] (12) are appropriate for the evaluation of the contribution
D_A of the attractive well. With Eqs. (12) and (8), the contribution of
the (central) attractive well is of the form

$$D_A = \rho\Omega_A \, B(1 - x) \, . \tag{13}$$

where Ω_A is the volume integral of the attractive well, and x contains
the effect of the cut-off term $\exp[-2(r-c)/a]$. The partial-wave
contributions D_A^ℓ to D_A can, of course, be obtained from a partial-wave

expansion of (12). The volume integral Ω_A can be expressed in the form

$$\Omega_A = \Omega_A^0 \, f(c/b^0) , \tag{14}$$

where Ω_A^0 is the volume integral the attractive well would have if it were translated to the origin and b^0 is the intrinsic range of the translated well. For a given b^0 and a given value of the well-depth parameter[25], the value of Ω_A^0 is essentially shape-independent; the factor $f(c/b^0)$, however, is very far from being shape-independent, being smaller for short-tailed wells such as a square well than it is for longer-tailed wells such as an exponential. In order to investigate the possible effects of this shape-dependence on the value of D_A, Λ-nucleon potentials with both exponential and square attractive wells are considered here. The cut-off term x in Eq. (13) also has a shape-dependence, which tends to compensate that of $f(c/b^0)$.

If the approximate function (12) is used with Eq. (9) to obtain the core contribution, one obtains from Eq. (8)

$$D_C = \frac{\hbar^2}{2\mu^*} k_F^2 \, \frac{8 \, k_F \, c}{3\pi} \, 2Bc/a, \tag{15}$$

the partial-wave contributions D_C^ℓ being obtained in a similar manner. The parameters (11) were chosen to give the best match of Eq. (10) to $R_{BG}^0(r)$ over the range $c \le r \le 3/k_F$ [23]. Consequently, Eq. (10) with the parameters (11) has a smaller slope at $r = c$ than the correct function $R_{BG}^0(r)$. Since the values of D_C^ℓ depend entirely on the slope of the radial function at $r = c$ [see Eq. (9)], the value of $2Bc/a$ used in calculations of D_C should be adjusted to reproduce this slope exactly. Since an analytic solution to the Bethe-Goldstone equation can be obtained for $\ell = 0$ with $V(r) = V_C$, D_C^0 can be obtained from this and used to determine the appropriate value of $2Bc/a$ to be used in Eq. (15). For c = 0.4 f, and the value of k_F given in Eq. (7b), this procedure leads to $2Bc/a = 1.4$, in contrast to the value 1.2 which follows from Eq. (11). Since the core contributions D_C^ℓ depend so critically on the form of $R^\ell(r)$ in the

neighbourhood of $r = c$, the expression (15) is relatively less reliable than expression (13) for D_A. On this account, approximate expressions for $D_C^{\ell > 0}$, obtained by consideration of the actual radial solutions of the Bethe-Goldstone equation in the neighbourhood of the hard-core radius[21], were used to obtain the values reported in this section; the values of D_C^0 were obtained from the exact solution for $V(r) = V_C$. The expression (15) exhibits the qualitative features of D_C[17]; it has been included primarily for that reason.

The spin-average Λ-nucleon potentials used for this discussion were assumed to have the following characteristics:

i) a hard core of radius $c = 0.4$ f or 0.6 f;

ii) a zero-energy scattering length equal to that of a potential without a hard core having an intrinsic range $b = 1.5$ f, corresponding to a Yukawa range parameter $R = (\hbar/2M_\pi)$, and the volume integral $\Omega_\Lambda = 230$ MeV f^3 given in Eq. (6a)[26].

Several values of the intrinsic range b^0 of the (translated) attractive well were used with

$$b - 2c \leq b^0 \leq b . \tag{16}$$

The minimum value of b^0 given in Eq. (16) is appropriate to a hard-core potential which has a bound state at zero energy[27], and the maximum is the largest possible consistent with an interaction which arises from the two-pion-exchange mechanism[7].

The results of calculations of D for two hard-core radii and several intrinsic ranges b^0 for potentials with exponential and square attractive wells are reported below. The values of Eq. (7) were used for the density of nuclear matter and the Fermi momentum. The effective mass M^* of the Λ particle was taken to be equal to the real mass M_Λ[1,17]; the effective mass of the nucleon $M_N^* = 0.735 \, M_N$ was determined in the manner described in Ref. 15 with the (Serber mixture) nucleon-nucleon interaction used there and the value of k_F given in Eq. (7b)[1]. The attractive contributions were evaluated with the approximate function (12);

the core contributions, in the manner described at the end of the paragraph containing Eq. (15).

1. Hard-core radius c = 0.4 f. In this case

$$D_C^0 = 55 \text{ MeV} \tag{17a}$$

$$D_C^1 = 3 \text{ MeV} \tag{17b}$$

$$D_C^2 \approx 0 \text{ MeV}. \tag{17c}$$

i) Potentials with exponential attractive wells.

Table 2

Values of D and the partial-wave contributions D^ℓ in MeV for potentials with exponential attractive wells and hard-core radius c = 0.4 f.

	D^ℓ			
b^0	$\ell = 0$	$\ell = 1$	$\ell = 2$	D
0.7 f	26	7	< 1	33
1.1 f	24	15	2	41
1.5 f	18	22	4	44

ii) Potentials with square attractive wells.

Table 3

Values of D and the partial-wave contributions D^ℓ in MeV for potentials with square attractive wells and hard-core radius c = 0.4 f.

	D^ℓ			
b^0	$\ell = 0$	$\ell = 1$	$\ell = 2$	D
0.7 f	21	7	< 1	27
1.1 f	21	15	1	36

potentials have rather longer tails than one would expect from consideration of the two-pion-exchange mechanism. The exponential well with $c = 0.4$ f and $b^0 = 1.5$ f is the one previously considered by Walecka[17] and by Moszkowski et al.[18]. The value $D^0 = 18$ MeV obtained here for this well is remarkably close to the value 16 MeV obtained by Moszkowski et al.[18] by a rather different method with a slightly larger value of the Fermi momentum ($k_F = 1.4$ f^{-1}). For the even larger Fermi momentum ($k_F = 1.48$) used by Walecka[17], the calculations described here led to $D = 52$ MeV with $D^0 = 13$ MeV, $D^1 = 31$ MeV and $D^2 = 7$ MeV[28]. A comparison of these results with the corresponding values in Table 2 gives an indication of the dependence of D on the value of the Fermi momentum. An estimate of this dependence on k_F can be made from Eqs. (13) and (15) which show that, in first approximation[23], D_A is proportional to k_F^3 and that D_C is proportional to k_F^4 ($a = 1/k_F$); and the values of D_A are about 50% greater than the value of D_C.

The calculations leading to Table 4 were made to investigate the dependence of D on the value of the hard-core radius c. The dependence of D_C on the core radius is apparent in Eq. (15)[29], but the dependence of D_A on c is hidden in the factors $(1 - x)$ and $f(c/b^0)$ in Eqs. (13) and (14). Comparison of Tables 2 and 4 indicates that D decreases with increasing hard-core radius, but not nearly so much as one would expect from Eq. (15) alone.

The effective masses play an obvious role in D_C [see Eq. (15)] and in all the partial-wave contributions D_C^ℓ. Whereas the effective masses do not play a role in D_A [see Eq. (13)], they do determine the relative contributions of D_A^ℓ: the smaller the value of the reduced mass M_N^* of the nucleon, the smaller is the s-wave contribution D_A^0.

Finally, it should be remarked that the method used in the calculations reported in this section has not been completely justified; it has, in fact, been the subject of some criticism[16].

IV. CONCLUDING REMARKS

The results reported in Tables 2 - 4 indicate that a value of D in the range 30 - 40 MeV might be expected; and these values are consistent with the values reported in Table 1 for a direct Λ-nucleon interaction. Values of D much larger than 30 MeV are, however, inconsistent with the empirical estimates given in Eq. (1). It remains to be seen whether the value of D will be found to lie in the range (1) or will fall in the higher range 30 - 40 MeV.

Attempts by Bodmer and Sampanthar[2] to bring theoretical estimates into agreement with Eq. (1) by invoking an exchange and/or a three-body component in the Λ-nucleon interaction have been discussed in Section II.

On the basis of a calculation mentioned near the end of Section III, Walecka[17] suggested that agreement between Eq. (1) and calculated values of D could be obtained if the strength of the Λ-nucleon interaction is reduced in odd-parity states. The large p-wave contributions to D reported in Tables 2 - 4 confirm that this suggestion is a possibility.

The two potentials with $b^o = 0.7$ f, for which results are reported in Tables 2 and 3, lead to values of D which are pretty close to the largest empirical estimates given in Eq. (1). These potentials, of course, are the ones which lead to relatively small p-wave contributions to D. They may be as unreasonably narrow as those with $b^o = 1.5$ f are wide. In any case, the relatively small values of D obtained with these potentials indicate that a value of D in reasonably good agreement with Eq. (1) might be obtained with a hard-core potential having a narrow, deep body and a longer, weak tail whose parameters would presumably be dictated by the two-pion exchange mechanism.

That the potential which is seen by a Λ particle imbedded in nuclear matter is expected to be only slightly momentum-dependent[1,2] was mentioned in Section I. This suggests that the central depth of the real part of the optical potential for scattering of low-energy Λ particles

of heavy nuclei may be very close to D. If this is true, Λ-nucleus scattering data (when this becomes available) may provide a method for determining D. Preliminary estimates of some of the properties of the Λ-nucleus optical potential which might be expected have been made by Ram[30]. He assumed the optical potential to have a central depth of 30 MeV, consistent with the values of D discussed here. A trapezoidal shape appropriate to the nucleon distributions in heavy nuclei[6] was assumed for computational convenience; a half-density radius $c = 1.1 \ A^{1/3}$f and a skin-thickness $t = 2.4$ f were used[6]. Ram found that, for $A \geq 64$, the low-energy s-wave scattering parameters (zero-energy scattering length and effective range) of these trapezoidal optical potentials can be reproduced with considerable accuracy by square wells having a depth of 25 MeV and a radius of $1.26 \ A^{1/3}$ f. Assuming that the same square wells are appropriate to low-energy scattering in states with higher angular momenta, the values of A for which abnormally large cross-sections (resonances) can be expected are easy to determine. For the square well just mentioned, s-wave resonances will occur for target nuclei with mass numbers $A = 31$ and 144, and p-wave resonances will occur for $A = 73$ and 248. These mass numbers are, of course, only suggestive of those which one might hope to be able to establish.

The calculations reported in Section III were made by the author in collaboration with Dr. W.E. Ware of the University of Colorado and the U.S. Air Force Academy. The partial-wave contributions D_A^ℓ and the core contribution D_C^0 were evaluated numerically on the IBM 1620 computer at the University of Colorado with the aid of a grant from the National Science Foundation. The author is indebted to Professor S.C. Miller for his assistance with these computations.

REFERENCES AND NOTES

1) W.E. Ware, Thesis (University of Colorado, 1962).

2) A.R. Bodmer and S. Sampanthar, Nucl.Phys. $\underline{31}$, 251 (1962).

3) J.D. Walecka, Nuovo Cimento $\underline{16}$, 342 (1960).

4) V.A. Filimonov, Soviet Phys. JETP $\underline{9}$, 1113 (1959).

5) R.H. Dalitz, Proceedings of the Rutherford Jubilee Int.Conf., Manchester, 1961, J.B. Birks, Editor, p. 103 (Heywood and Co. Ltd., London, 1961).

6) R. Hofstadter, Revs.Mod.Phys. $\underline{28}$, 214 (1956).

7) R.H. Dalitz and B.W. Downs, Phys.Rev. $\underline{111}$, 967 (1958).

8) B.W. Downs and R.H. Dalitz, Phys.Rev. $\underline{114}$, 593 (1959) and other references cited there.

9) An equivalent derivation of Eq. (2) is given, for example, in Ref. 7.

10) This property of $D_{exchange}$ is, of course, independent of the shape of the Λ-nucleon potential. See also Appendix C of Ref. 7.

11) See the corresponding calculations for $_\Lambda H^3$ by R.H. Dalitz and B.W. Downs, Phys.Rev. $\underline{110}$, 958 (1958). The relation between b and R for a Yukawa potential is b = 2.1196 R; see, for example, Ref. 25.

12) For example, Bodmer and Sampanthar found the p-wave contribution to $D_{direct}^{(1)}$ for R = $(\hbar/2M_\pi)$ to be 14% for k_F = 1.3 f^{-1} and 18% for k_F = 1.5 f^{-1}.

13) See, for example, M.J. Moravcsik and H.P. Noyes, Ann.Rev.Nucl.Sci. $\underline{11}$, 95 (1961).

14) See, for example, D.B. Lichtenberg and M. Ross, Phys.Rev. $\underline{107}$, 1714 (1957).

15) L.C. Gomes, J.D. Walecka and V.F. Weisskopf, Ann.Phys. $\underline{3}$, 241 (1958).

16) S.A. Moszkowski and B.L. Scott, Ann.Phys. $\underline{11}$, 65 (1960).

17) J.D. Walecka, Nuovo Cimento $\underline{16}$, 342 (1960).

18) M. Taherzadeh, S.A. Moszkowski and P.C. Sood, Nuovo Cimento $\underline{23}$, 168 (1962).

19) The Bethe-Goldstone equation for the relative motion of a Λ-nucleon pair is the same as that for a nucleon-nucleon pair only when the momentum $\vec{P}$ of the centre-of-mass of each pair is zero; see Refs. 1 and 17. The solution of the Bethe-Goldstone equation is not expected to depend very much on the value of $\vec{P}$; see Ref. 15.

20) H.A. Bethe and J. Goldstone, Proc.Roy.Soc. (London) A238, 551 (1957).

21) J.D. Walecka, Thesis (Massachusetts Institute of Technology, 1958).

22) T. Tagami, Progr.Theoret.Phys. (Kyoto) 21, 465 (1959).

23) The parameters (11) were obtained by matching the function (10) to the s-wave solutions of the Bethe-Goldstone equation for a nucleon-nucleon pair with the interaction $(V_C + V_A)$ for $K = 0$, $0.3 \, k_F$ and $0.6 \, k_F$ given in Refs. 15 and 21. The match was made for $k_F c \leq k_F r \leq 3$; for $k_F r > 3$, the approximate function begins to deviate appreciably from the Bethe-Goldstone function because the amplitude factor B prevents Eq. (10) from approaching the free pair solution. In order to investigate the consequences of an incorrect choice of the cut-off parameter a of Eq. (11b), the cut-off factor $(1 - x)$, which appears in Eq. (13), was evaluated with several values of a for the exponential potentials reported in Table 2. A 20% change in a on either side of the value given in Eq. (11b) produced changes of 10%, 7% and 5% in $(1 - x)$, the larger changes corresponding to the smaller values of b°.

24) Since the Bethe-Goldstone equation has not been solved for $\ell > 0$, there is no real basis for this assumption. The effect of the cut-off term in Eq. (12) on $D_A^{\ell > 0}$ is, however, negligible except for attractive wells of very short range. For example, use of the Born approximation to evaluate D_A^1 for the exponential potentials reported in Table 2 leads to an increase in D_A^1 over the values reported there by 3.5 MeV, 1.6 MeV and 0.3 MeV, respectively; the corresponding increases for the potentials reported in Table 4 are 7.9 MeV and 2.4 MeV. The effect on D_A^2 is completely negligible.

25) See, for example, J.M. Blatt and J.D. Jackson, Phys.Rev. 76, 18 (1949).

26) That the zero-energy scattering length of the effective Λ-nucleon potential in light hypernuclei is insensitive to the value of the hard-core radius is suggested by a recent analysis of the hypertriton by B.W. Downs, D.R. Smith and T.N. Truong, Phys.Rev. (to be published). The scattering length of a wholly-attractive exponential well with the range and volume integral given here is $- 0.76 \, f$; for a square well, the scattering length is $- 0.78 \, f$. The prescription used here for obtaining the parameters of potentials with hard cores leads to a spin-average potential 4% less deep than that deduced by Dietrich, Folk and Mang (Proceedings of the Rutherford Jubilee Int.Conf., Manchester, 1961) from an analysis of the binding energy of $_{\Lambda}\text{He}^5$

in terms of Λ-nucleon potentials with a hard-core radius
c = 0.2 f and an attractive square well. This prescription
also leads to hard-core potentials with exponential attractive
wells whose depths differ by less than 1% from those used in
Refs. 17 and 18.

27) See, for example, T. Ohmura (Kikuta), M. Morita and M. Yamada,
Progr.Theoret.Phys. (Kyoto) 15, 222 (1956).

28) These calculations indicate that Walecka underestimated D_C^0 by
about 9 MeV in Ref. 17.

29) See also Ref. 17.

30) Budh Ram, private communication.

*   *   *

MESON THEORY OF HYPERON-NUCLEON FORCES

J.J. de Swart[*],

Theory Division, CERN.

I. INTRODUCTION

We will assume that the interaction between a hyperon and a nucleon can be described by a local potential. For low energy Λ-nucleon scattering in the $^1S_0$ state we have to solve the Schrödinger equation

$$- \frac{\hbar^2}{2m_\Lambda} \chi'' + (V_1 - E)\, \chi = 0 \, . \tag{1}$$

To simplify equations we will consider only $^1S_0$ states; no essential features will be lost, however.

From the existence of the reaction

$$\Lambda + N \to \Sigma + N$$
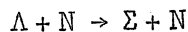
we know that the Λ-nucleon channel is strongly coupled to the Σ-N channel. A description like Eq. (1), taking into account only the Λ-nucleon channel, has to break down if E > 77 MeV. In fact it is reasonable to assume that it breaks down much earlier.

A better way to describe the Λ-nucleon interaction is to take also explicitly account of the Σ-nucleon channel. Therefore, we need to consider potentials

$$V_2 = \begin{pmatrix} V_{\Lambda\Lambda} & V_{\Lambda\Sigma} \\ V_{\Sigma\Lambda} & V_{\Sigma\Sigma} \end{pmatrix} \tag{2}$$

---

[*] On leave from the University of Nijmegen, Nijmegen, Netherlands.

with the coupled Schrödinger equations

$$- \frac{\hbar^2}{2m_\Lambda} u_\Lambda'' + V_{\Lambda\Lambda} u_\Lambda + V_{\Lambda\Sigma} u_\Sigma = E \, u_\Lambda$$

$$- \frac{\hbar^2}{2m_\Sigma} u_\Sigma'' + V_{\Sigma\Lambda} u_\Lambda + V_{\Sigma\Sigma} u_\Sigma = (E - \Delta Mc^2) \, u_\Sigma \, .$$

(3)

Here m_Λ and m_Σ are the reduced masses in the different channels, and $\Delta M = M_\Sigma - M_\Lambda$ is the difference between the rest masses. In solving Eq. (3) for low-energy Λ-nucleon scattering we have to impose the boundary conditions:

$$\text{if } r = 0 \text{ or } r = r_c \text{ then } \begin{cases} u_\Lambda = 0 \\ u_\Sigma = 0 \end{cases}$$

and

$$\text{if } r \to \infty \text{ then } \begin{cases} u_\Lambda \to \sin(k_\Lambda r + \delta) \\ u_\Sigma \to a \, e^{-Kr} \end{cases}$$

where

$$E = \frac{\hbar^2 k_\Lambda^2}{2m_\Lambda} = \Delta Mc^2 - \frac{\hbar^2 K^2}{2m_\Sigma} \, .$$

It is hoped that with a potential like Eq. (2) one can describe the Λ-nucleon scattering up to about 300 MeV, like the nucleon-nucleon scattering can be done. Our task is to determine V.

We will restrict ourselves to the case of even relative parity, which seems to be firmly established by now[1,2].

II. MESON THEORETICAL POTENTIALS

At this moment there are many mesons available, each of which could be responsible for a significant part of the hyperon-nucleon forces. We have, for example, the $Y = 0$ mesons like π, η, ρ, ω, and ABC particle, and the $Y = \pm 1$ mesons like K and K*. The relevant experimental data

are unfortunately still so scarce that from them almost no indication about the importance of the different mesons can be obtained.

To make any progress in understanding these forces one has to rely therefore heavily upon theoretical arguments and upon the experience obtained in the similar problem of the nucleon-nucleon forces.

The theory in the nucleon-nucleon problem is at this moment in a transition phase; the transition being from considering only the pions[3] as the agent of the force, to including in the calculation of the potentials also the recently discovered mesons as ρ, ω, η, ABC, etc.[4]. This transition is surely not completed but one is only at the beginning.

We will base our arguments on the older theories [to be specific we will use the Brueckner-Watson prescription[5]] and we will totally neglect the existence of these new mesons. The main justification for considering only pions lies in the fact that a very satisfactory description can be found employing only the pions.

Because of charge independence the interaction Hamiltonian, between the pions and the baryons, in isospace is

$$H_{int} = f_{NN}(N^+ \underline{\tau} N) \cdot \underline{\pi} + f_{\Lambda\Sigma}(\Lambda^+ \underline{\Sigma} + \underline{\Sigma}^+ \Lambda) \cdot \underline{\pi} - if_{\Sigma\Sigma}(\underline{\Sigma}^+ \times \underline{\Sigma}) \cdot \underline{\pi}. \tag{4}$$

For the dependence on the space and spin we will always take the form

$$\frac{f}{\mu}(\psi^+ \sigma \tau) \cdot \underline{\nabla} \varphi. \tag{5}$$

The different kind of diagrams that contribute are given in Fig. 1. For completeness we give in Fig. 2 the most important diagrams which are neglected.

Using the prescription of Brueckner and Watson[5] we can then calculate the potentials due to the exchange of one and two pions[6,7]. The complete potential is then characterized by four constants; the coupling constants $f_{\Lambda\Sigma}$ and $f_{\Sigma\Sigma}$, and the cores x_0 and x_1 in the singlet and triplet states respectively.

We will try to determine these different constants.

III. LOW-ENERGY Λ-NUCLEON SCATTERING[7]

From the different analysis[8] of the light hyperfragments one can estimate the Λ-nucleon scattering lengths. We take[9]

$$a_0 = - (3.6^{+3.6}_{-1.8}) \text{ fm}$$

$$a_1 = - (0.53 \pm 0.12) \text{ fm}.$$

Using the meson theoretical potentials in Eq. (2) we can, for a fixed x_0 and $f_{\Sigma\Sigma}$, determine the value of $f_{\Lambda\Sigma}$ which will give the correct scattering length a_0. This can be done for every value of $f_{\Sigma\Sigma}$, still keeping the core radius x_0 fixed. For a fixed core we obtain therefore a line in the $(f_{\Lambda\Sigma}, f_{\Sigma\Sigma})$ diagram (Fig. 3); every point on this line giving the correct a_0. The same procedure can be repeated for different values of the core and also for the triplet case. We notice then that every combination $(f_{\Lambda\Sigma}, f_{\Sigma\Sigma})$ can reproduce the scattering lengths a_0 and a_1 provided we choose the right cores x_0 and x_1.

To be able to make any conclusion we have to place restrictions on the possible values of the cores. We will assume that the cores are of the same order of magnitude as the cores in the nucleon-nucleon problem, therefore

$$0.30 \lesssim x_c \lesssim 0.40 \ \mu^{-1}.$$

Despite the fact that this drastically limits the possible values for $f_{\Lambda\Sigma}$ and $f_{\Sigma\Sigma}$, it still leaves us with quite a large choice (see Fig. 3).

IV. LOW-ENERGY Σ^--p AND Σ^--d INTERACTIONS[10]

When Σ^- hyperons come to rest in hydrogen they form Σ^-p atoms, which decay due to the reactions

$$\Sigma^- + p \rightarrow \Sigma^0 + n + 3.16 \text{ MeV}$$
$$\rightarrow \Lambda^0 + n + 79.30 \text{ MeV}.$$
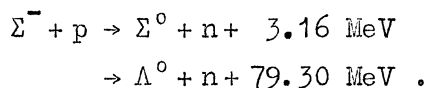
The measured ratio[11] is $r_R(H) = \Sigma^0/\Sigma^0 + \Lambda^0 = 0.33 \pm 0.05$. Using the cores, x_0 and x_1, which give the correct scattering lengths, this ratio $r_R(H)$ is calculated for different combinations $(f_{\Lambda\Sigma}, f_{\Sigma\Sigma})$. This gives a limitation on $f_{\Sigma\Sigma}$. Only those values of $f_{\Sigma\Sigma}$ are allowed which lie to the left of the line H in Fig. 3. This allowable region extends to slightly negative values of $f_{\Sigma\Sigma}$.

An analogous reaction is

$$\Sigma^- + d \to \Sigma^0 + 2n + 0.94 \text{ MeV}$$

$$\to \Lambda + 2n + 77.08 \text{ MeV}.$$
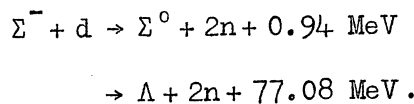
The measured ratio at rest is[12] $r_R(D) = 0.037 \pm 0.022$. Also this ratio is calculated[10,13]. This restricts $f_{\Sigma\Sigma}$ to lie to the left of the line D in Fig. 3.

V. UNITARY SYMMETRY

The unitary symmetry model[14] (octet model) of strong interactions predicts the relation

$$\sqrt{3}\, f_{\Lambda\Sigma} + f_{\Sigma\Sigma} = 2f_{NN} \tag{6}$$

if we assume that the basic couplings are pseudovector[7]. This is described by the straight line in Fig. 3. If the basic couplings are pseudoscalar[7] then the relation is:

$$\frac{\sqrt{3}}{2} (M_\Lambda + M_\Sigma) f_{\Lambda\Sigma} + M_\Sigma\, f_{\Sigma\Sigma} = 2M_N\, f_{NN}.$$

However, in the latter case a restriction to only pion couplings is perhaps not justified and kaon exchange potentials should be included in the analysis.

Λ-Λ POTENTIAL

We can, of course, consider the low-energy Λ-Λ interactions. Due to the recent discovery[15] of a double hyperfragment this becomes quite interesting. If we restrict ourselves again to only pion forces, then we have again a set of coupled equations like Eq. (2). We can calculate the Brueckner-Watson potentials and determine the scattering length as a function of the core and the coupling constants. Using the relation[9]

$$\bar{V} = \frac{\hbar^2}{M_\Lambda} \frac{4\pi a}{1 - 1.23\, a/b} \tag{7}$$

we can translate the scattering lengths into volume integrals $\bar{V}$ of the potential. The range parameter is $b = 1.4843$ f corresponding to a two-pion range.

The volume integral as a function of the coupling constant $f_{\Sigma\Sigma}$ is given in Fig. 4. The constant $f_{\Lambda\Sigma}$ is determined by unitary P.V. symmetry [Eq. (6)].

VII. EQUIVALENT POTENTIAL

Finally, we want to consider potentials like V_1 [see Eq. (1)] anyway. How can we deduce a reasonable V_1 from the knowledge of the potential V_2 [Eq. (2)]?

To obtain the correct phase shift we need a solution χ of Eq. (1) such that if $r \to \infty$, then $\chi \to u_\Lambda$. The choice $\chi(r) = u_\Lambda(r)$ everywhere would give us the correct scattering length at the energy considered. However, it will not give the same effective range in both cases.

The effective range is given by

$$r_0 = 2 \int_0^\infty (v^2 - \chi^2)\, dr \tag{8}$$

for the one-channel Eq. (1), where $v = \sin(k_\Lambda r + \delta)/\sin \delta$ and by

$$r_0 = 2 \int_0^\infty (v^2 - u_\Lambda^2 - u_\Sigma^2)\, dr \tag{9}$$

for the two-channel Eq. (3).

To obtain thus the same scattering length and the same effective range in both cases, we have to take

$$\chi = u_\Lambda \sqrt{1 + \left(\frac{u_\Sigma}{u_\Lambda}\right)^2}. \tag{10}$$

For $E = 0$ scattering u_Λ has no zero's (a = negative) and Eq. (10) is a good wave function. This χ is a solution of Eq. (1), if

$$V_1 = \frac{\hbar^2}{2m_\Lambda} \left(\frac{\chi''}{\chi}\right)$$

$$= \frac{u_\Lambda^2}{u_\Lambda^2 + u_\Sigma^2} V_{\Lambda\Lambda} + \frac{2u_\Lambda u_\Sigma}{u_\Lambda^2 + u_\Sigma^2} \left(\frac{m_\Lambda + m_\Sigma}{2m_\Lambda}\right) V_{\Lambda\Sigma}$$

$$+ \frac{u_\Sigma^2}{u_\Lambda^2 + u_\Sigma^2} \frac{m_\Sigma}{m_\Lambda} \left[V_{\Sigma\Sigma} + (M_\Sigma - M_\Lambda) c^2\right] + \frac{\hbar^2}{2m_\Lambda} \left(\frac{u_\Lambda u_\Sigma' - u_\Sigma u_\Lambda'}{u_\Lambda^2 + u_\Sigma^2}\right)^2.$$

Therefore, if we solve the system of Eq. (3) for $E = 0$, then we can construct readily the potential V_1, which will give the correct a_0 and r_0. Important is this for the triplet case, because the same procedure is applicable there and we can construct therefore easily a potential with the correct amount of tensor force, etc., to describe the low energe Λ-nucleon scattering.

VIII. CONCLUSION

Any conclusion is dependent on our answer to: "what is a reasonable core?" As long as we do not have a satisfactory way of treating the cores, our conclusions have to be viewed with the proper caution.

The following conclusions can then be made. If we neglect the K mesons, a rather satisfactory way of describing the hyperon-nucleon interaction can be found. The coupling constant $f_{\Lambda\Sigma}$ is of the same order as f_{NN}, but $f_{\Sigma\Sigma}$ is much smaller,

$$\left(\alpha = \frac{f_{\Sigma\Sigma}}{2f_{NN}} \le \frac{1}{5}\right).$$

ACKNOWLEDGEMENTS

* * *

REFERENCES

1) R.H. Dalitz, Proc.of 1962 Int.Conf.on High-Energy Phys.at CERN, p. 391.

2) R. Burnstein, T.B. Day, F. Herz, B. Kehoe, M. Sakitt, N. Seeman, G.A. Snow, B. Zorn, R. Adair, H. Courant, H. Filthuth, P. Franzini, R.G. Glasser, A. Minguzzi-Ranzi, A. Segar and W. Willis, Bull.Am. Phys.Soc. 8, 349 (1963).

3) For a rather complete review of the different methods, see M.J. Moravcsik and H.P. Noyes, Ann.Rev.Nucl.Sci. 11, 95 (1961) and R.J.N. Phillips, Reports on Progress in Physics 22, 562 (1959).

4) R. Bryan, C. Dismukes and W. Ramsay (to be published); A. Scotti and D.Y. Wong, Phys.Rev.Letters 10, 142 (1963).

5) K.A. Bureckner and K.M. Watson, Phys.Rev. 92, 1023 (1953).

6) D.B. Lichtenberg and M.H. Ross, Phys.Rev. 107, 1714 (1957).

7) J.J. de Swart and C.K. Iddings, Phys.Rev. 128, 2810 (1962).

8) R.H. Dalitz and B.W. Downs, Phys.Rev. 110, 958 (1958); Phys.Rev. 111, 967 (1958); Phys.Rev. 114, 593 (1959). K. Dietrich, R. Folk and H.J. Mang, Rutherford Jubilee Int.Conf., Manchester 1961.

9) J.J. de Swart and C. Dullemond, Ann.Phys. (N.Y.) 19, 458 (1962).

10) J.J. de Swart and C.K. Iddings, Phys.Rev. 130, 319 (1963).

11) R.R. Ross, Bull.Am.Phys.Soc. 3, 336 (1958).

12) O. Dahl, N. Horowitz, D. Miller and J. Murray, Phys.Rev.Letters 4, 77 (1960).

13) D.E. Neville, Ph.D. Thesis, University of Chicago (1962), Phys.Rev. 130, 327 (1963).

14) M. Gell-Mann, "The eightfold way; a theory of strong interaction symmetry", California Institute of Technology, Report CTSL-20, .March 1961. Phys.Rev. 125, 1067 (1962). Y. Ne'eman, Nucl.Phys. 26, 222 (1961).

15) M. Danysz, K. Garbowska, J. Pniewski, T. Pniewski, J. Zakrzewski, E.R. Fletcher, J. Lemonne, P. Renard, J. Sacton, W.T. Toner, D.O'Sullivan, T.P. Shah, A. Thompson, P. Allen, Sr. M. Heeran, A. Montwill, J.E. Allen, M.J. Beniston, D.H. Davis, D.A. Garbutt, V.A. Bull, R.C. Kumar and P.V. March, Phys.Rev.Letters 11, 29 (1963).

*   *   *
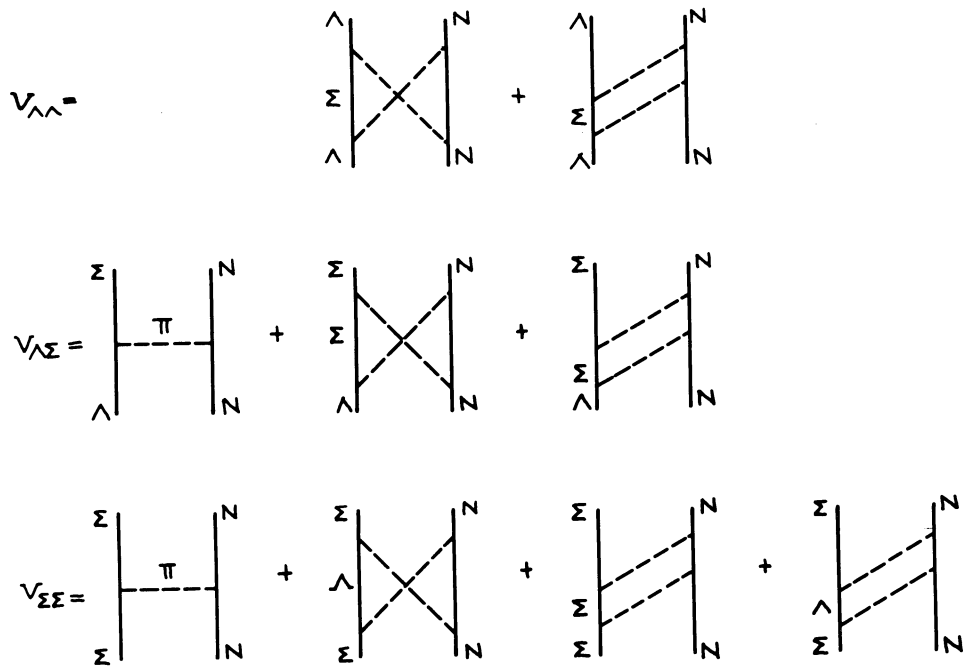
Fig. 1. - The one and two-pion exchange diagrams which contribute to the different hyperon-nucleon potentials.
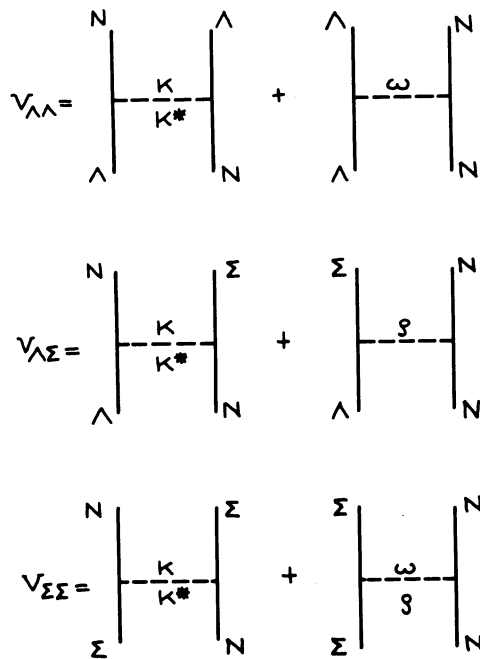
Fig. 2. - The most important one-meson exchange diagrams which are neglected in the calculation of the hyperon-nucleon potentials.
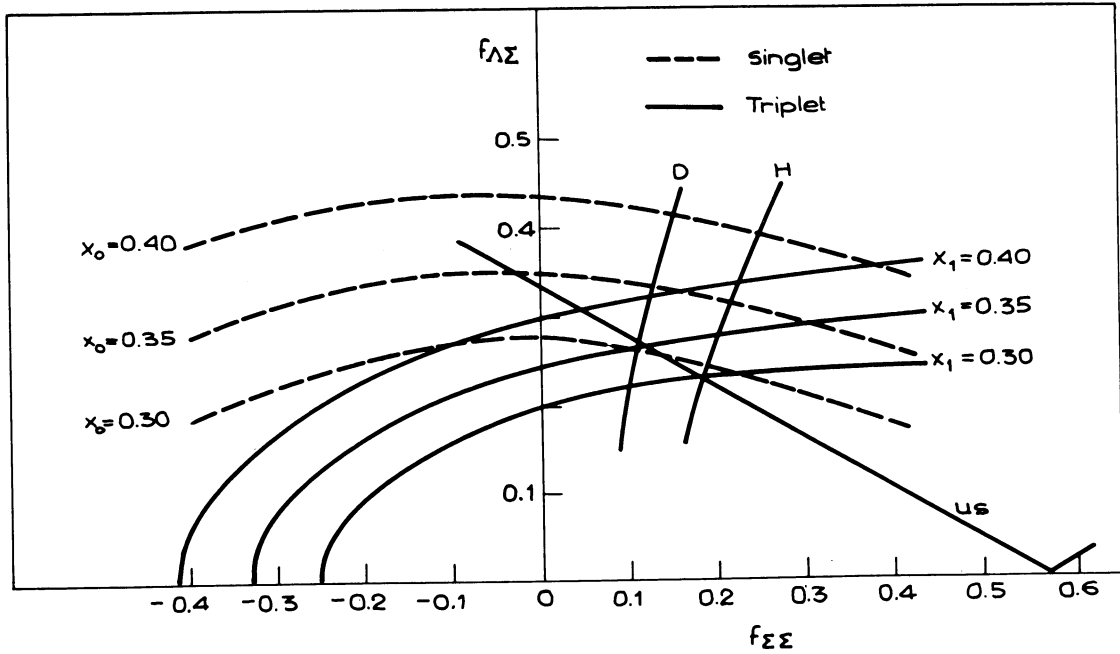
Fig. 3. - The $f_{\Lambda\Sigma}$ - $f_{\Sigma\Sigma}$ diagram.

The dashed lines represent the values of $(f_{\Lambda\Sigma}$, $f_{\Sigma\Sigma}$) which give the correct scattering length a_0 for a fixed core x_0.

The solid lines represent the values of $(f_{\Lambda\Sigma}$, $f_{\Sigma\Sigma}$) which give the correct scattering length a_1 for a fixed core x_1.

The line marked H are those points where $r_R(H) = 0.33 + 0.05$.

The points to the left of this line give $r_R(H)$ within the experimental limits. The line marked D are those points where $r_R(D) = 0.037 + 0.022$. The points to the left of this line give $r_R(D)$ within the experimental limits.

The line US gives the combinations $(f_{\Lambda\Sigma}$, $f_{\Sigma\Sigma}$) which are required by unitary symmetry (pseudovector coupling).
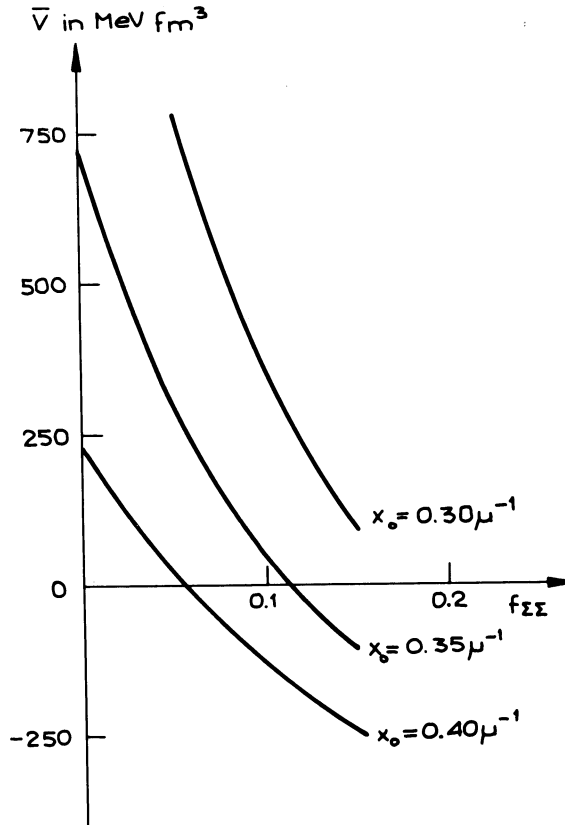
Fig. 4. - The volume integral of the Λ-Λ potential as a function of $f_{\Sigma\Sigma}$

The corresponding $f_{\Lambda\Sigma}$ is chosen to be consistent with unitary P.V. symmetry (6). The results for different core radii are given. $\bar{V} \geq 530$ MeV fm^3 corresponds to a bound state.

VII. THE OUTLOOK IN HYPERNUCLEAR PHYSICS

THE OUTLOOK IN HYPERNUCLEAR PHYSICS*)

R.H. Dalitz,
The Enrico Fermi Institute for Nuclear Studies and
Department of Physics, The University of Chicago, Chicago.

I. INTRODUCTION

A reasonable classification of the information obtained in the study of hypernuclei may be made according to its bearing on the following three areas of physical problems:

  i) the properties of the nuclear interactions of the hyperons;

 ii) the weak interactions of the Λ hyperon;

iii) the properties of nuclei.

Here we shall survey briefly some of the questions of current or future interest in these areas, as well as some of the experiments which appear feasible in the near future and which will bear directly on these questions.

II. THE NUCLEAR INTERACTIONS OF THE HYPERONS

From the study of binding energies of Λ hypernuclei, we have already learned a great deal about the qualitative properties of the Λ-N interaction in the $^1S_0$ and $^3S_1$ states, and this information has been given an interpretation by de Swart and Iddings[1] in terms of the properties of the pion-hyperon couplings $\Sigma\Lambda\pi$ and $\Sigma\Sigma\pi$. However, there are still many questions of detail about the Λ-N forces about which we know little.

---

i) The exchange character of the Λ-N interaction.

The exchange of a K or K* meson between Λ and N will give rise to an exchange term in the Λ-N potential. There are theoretical reasons to believe that this will not be a significantly large term but this needs to be checked directly.

ii) The tensor potential contribution to the Λ-N interaction.

Meson-theoretical calculations suggest that there is no reason to expect this to be a large term for the Λ-N system, in contrast with the N-N situation.

iii) The nature of the hard core interaction in the Λ-N interaction.

This information would be enlightening on the origin of the hard core in baryon-baryon interactions. At present, the most attractive hypothesis is that this hard core repulsion arises primarily from a universal and very strong coupling of the baryon with a neutral vector meson field (possibly the ω meson). This hypothesis would require the Λ-N hard core to have radius comparable with that for the N-N system, apart from small modifications due to the exchange of other vector mesons such as the ρ, K* and φ, which appear to be less strongly coupled to baryons and which have different couplings for different baryon multiplets.

iv) The spin-orbit coupling for the Λ-N system.

The most natural origin for strong spin-orbit forces in a baryon-baryon system is the exchange of vector mesons, so that this question may have quite direct relationship with (iii). In this view it is natural to expect a strong spin-orbit interaction in the Λ-N system, just as is known for the N-N system, and it will be very informative to learn about its sign and strength.

Probably it will be quite difficult to learn about these questions from Λ hypernuclei. In p-shell hypernuclei, the s-wave Λ particle interacts with p-shell nucleons and so the magnitudes of the exchange component and especially of the spin-orbit interaction are relevant to the B_Λ value and the pattern of excited levels in these nuclei. More accurate and reliable

B_Λ values for a wide range of Λ hypernuclei are very desirable to allow a more detailed study of their systematics in this region. Another parameter directly relevant to these questions is the well depth D_Λ of nuclear matter for a Λ particle; D_Λ depends quite strongly on the properties of the p-wave Λ-N interaction.

Experiments on Λp scattering would naturally give much more direct information about the Λ-N interaction, but these are generally rather difficult experiments, in view of the short lifetime of the Λ particle. One possibility is the use of Λ particles from the reaction $K^- + p \to \Lambda + \pi^0$ for K^- coming to rest in liquid hydrogen; this provides a copious source of Λ particles of 32 MeV kinetic energy (there are also lower energy Λ particles from the $\Sigma^0 + \pi^0$, $\Sigma^0 \to \Lambda + \gamma$ sequence) and a search for the rare Λp scattering events near these K^- stops can be carried out rather quickly and efficiently. In this way it should be possible to obtain a good value for $\sigma_{tot}(\Lambda p)$ for Λp c.m. energies in the s-wave region, which should provide an interesting check on the Λ-N potentials deduced from hypernuclear B_Λ values. These Λ particles are necessarily unpolarized; a source of strongly polarized Λ particles would allow much more informative experiments. For π^- momenta in the range 1,000-1,500 MeV/c at least, the reaction $\pi^- + p \to \Lambda + K^0$ leads to strongly polarized Λ particles with an angular distribution strongly peaked in the backward direction, thus giving quite strong production of relatively slow Λ particles with strong polarization. In due course it may be possible to make use of these particles to study some polarization properties of Λp scattering; already a number of Λp scattering events have been observed in this way[2,3] and used to estimate an average value $\bar\sigma_{tot}(\Lambda p)$ = 25 ± 10 mb over the laboratory momentum range 400-640 MeV/c (c.m. kinetic energy range 60-76 MeV). The simplest polarization property to measure is the mean depolarization of the Λ particles due to Λp scattering; this parameter is directly related to the relative strengths of the singlet and the triplet Λ-N scattering. Possibly experiments of this kind will prove possible with spark chambers, using a hydrogen target inside the chamber; this would allow the collection of events at a much

more reasonable rate. Another possibility would be the study of secondary Λ-N collisions for Λ particles which are produced on one nucleon in π-d or K^--d collisions and then collide with the other nucleon of the same nucleus. These events could be selected by requiring the presence of both a Λ particle and a fast nucleon in the final state, confining attention to nucleon momenta well above the momentum distribution which is known for "by-stander nucleons" (and which is well fitted by the distribution claculated with the impulse approximation and with a simple deuteron wavefunction) in high-energy processes involving deuterium as target. The simplest such situation to interpret would be the study of π-d reactions for pion energy well below the threshold for Σ production, since this would ensure that the intermediate hyperon was predominantly a Λ particle.

Similar studies of Σ^--p and Σ^+-p cross-sections, using hydrogen chambers or spark chamber methods, would also be of great value in providing new parameters to relate to the primary mechanisms giving rise to hyperon-nucleon forces.

The study of hyperfragment production rates in specific hyperon reactions should also prove quite informative on the detailed character of the primary hyperon-nucleon interactions. For example, whereas $_\Lambda H^4$ and $_\Lambda He^4$ are produced in about 20% of K^--He^4 reactions which lead to a primary Λ particle (identified by the characteristic momentum of the associated π^- meson), not more than one example of $_\Lambda H^4$ has been observed in 300 examples of $\Sigma^- + He^4$ capture at rest[4]. This low rate of $_\Lambda H^4$ formation (which involves about the same momentum transfer as occurs in the $K^- + He^4 \rightarrow _\Lambda He^4 + \pi^-$ reaction) is probably related with the detailed spin character of the interaction $\Sigma^- + p \rightarrow \Lambda + n$.

The recent and remarkable observation of a $\Lambda\Lambda$ hypernucleus by the Warsaw group[5] as part of a large European collaborative effort has opened up a large new field of research. When suitable methods are developed to increase the yield of slow Ξ^- mesons which can be stopped in emulsion, the study of the $\Lambda\Lambda$ hypernuclei formed will quickly lead to a rather accurate value for the Λ-Λ interaction in the $^1S_0$ state. For this

determination observations on the system $_{\Lambda\Lambda}He^6$ will be of particular
interest since this is the system for which the most reliable calculations
can be made at present. From the study of the heavier systems, we may
expect to learn further about the spin-dependent term in the Λ-nucleus
interaction (about which we have some indications from Λ-hypernuclear
B_Λ values) and about the distortion of the core nuclei by the presence
of several Λ particles. The study of specific capture reactions of
particular simplicity will also be important; to illustrate this we may
mention the reaction $\Xi^- + Li^7 \rightarrow {}_\Lambda H^4 + {}_\Lambda H^4$, whose interest [as pointed out by
Wilkinson[6])] lies in the fact that the final state consists of two identical
spinless particles. It will also be of interest to study the angular
correlations between the two successive Λ decays of the $\Lambda\Lambda$ hypernuclei,
for example in the sequence $_{\Lambda\Lambda}He^8 \rightarrow \pi^- + {}_\Lambda Li^8 \rightarrow \pi^- + Be^{8*}$ (J = 2+), which
provide a direct check on the spin value for $_\Lambda Li^8$. Probably studies of
this kind should not be made in emulsion since the atomic fields probably
suffice to destroy the alignment of the $_\Lambda Li^8$ during the relatively long
time ($\sim 10^{-10}$ sec) it remains at rest awaiting the second Λ decay. The
study of the branching ratios for the various decay modes of $\Lambda\Lambda$ hypernuclei
would also provide a check on many of our present beliefs about the decay
of bound Λ particles. To provide an example, we may consider $_{\Lambda\Lambda}H^4$ and its
two-body decay mode $_{\Lambda\Lambda}H^4 \rightarrow \pi^- + {}_\Lambda He^4$. With J = 1 expected for $_{\Lambda\Lambda}H^4$, and
J = 0 for $_\Lambda He^4$, this decay requires $\ell = 1$ for the pion and can therefore
occur only through the relatively weak p interaction for Λ decay: hence
the two-body decay modes for $_{\Lambda\Lambda}H^4$ may be expected to be relatively rare,
in contrast with the situation for $_\Lambda H^4$.

Now that an example of the $\Lambda\Lambda$ hypernucleus has been established,
it appears reasonable to mention the possibility of forming hypernuclei
containing three Λ particles. The systematics of the $p_{3/2}$ meson-baryon
resonances, the $N_{3/2}^*$ (1238 MeV), the Y_1^* (1385 MeV), strongly suggest the
existence of a further state, the Ω^- baryon with mass about 1680 MeV[7,8]).
This object has not yet been established, although there was an event
reported by Eisenberg[9]) in 1954 which may have been an example of Ω^- decay.
The point is that this Ω^- baryon is predicted to be long-lived, with decay

modes $\pi + \Xi$, $K^- + \Lambda$ and $\bar{K} + \Sigma$ due to the weak interactions, and to have strangeness $s = -3$. When the Ω^- particle comes to rest in emulsion and interacts with a nucleus, the following one- and two-nucleon capture processes are possible:

$$\Omega^- + p \to \Xi^- + \Lambda \tag{1}$$

$$\Omega^- + p + n \to \Lambda + \Lambda + \Lambda \, . \tag{2}$$

In Eq. (1), if the Ξ^- hyperon undergoes a second interaction in the same nucleus, or in Eq. (2), the effect of the capture process would be to release three Λ particles within the nucleus. Even though the net energy release is quite high [~ 110 MeV for reaction (2)], there is a finite probability that all three Λ particles may be trapped to form a $\Lambda\Lambda\Lambda$ hypernucleus. In such a system the lowest state available to the third Λ particle is a p-state, in consequence of the Pauli principle. This condition will forbid the binding of the three Λ particles to the lightest nuclei, since the p-level of the Λ-nucleus interaction is bound only for sufficiently large core nuclei. The simplest estimates suggest that $_{\Lambda\Lambda\Lambda}Be^{11}$ should certainly be stable; this system could be formed in reactions such as

$$\Omega^- + C^{12} \to {}_{\Lambda\Lambda\Lambda}Be^{11} + n + p \, . \tag{3}$$

III. THE WEAK INTERACTIONS OF THE Λ HYPERON

The study of the β decay processes for hypernuclei could usefully complement studies of the properties of Λ-β decay carried out for free Λ particles. Processes of particular interest which may be studied in a helium bubble chamber are

$$_{\Lambda}H^4 \to e^- + \bar{\nu} + He^4 \tag{4a}$$

$$_{\Lambda}H^4 \to \mu^- + \bar{\nu} + He^4 \, . \tag{4b}$$

With $J = 0$ for $_{\Lambda}H^4$, these processes represent zero-zero transitions which are allowed only through the Fermi part of the Λ_e and Λ_μ interactions so that a knowledge of their rate would allow a direct separation between the

Fermi and Gamow-Teller terms in these interactions. This information may also be obtained from studies of the β decay of free polarized Λ particles. The greatest difficulty in the study of processes (4) will be the problem of low statistics; the branching ratio for these processes in $_\Lambda H^4$ is expected to be of the order of 10^{-3} so that there is no advantage in this respect over the study of free Λ decay.

The lifetimes of the light hypernuclei form a subject of great interest, especially in view of the short lifetimes which have recently been found for $_\Lambda H^3$ by two different investigations[10,11]. This result is very much of a surprise, in view of the light binding in $_\Lambda H^3$; it is difficult to obtain a lifetime much shorter than 1.8×10^{-10} sec from the theoretical calculations which have given a good account of the branching ratios observed for $_\Lambda H^3$ and other light hypernuclei. Until this short lifetime is understood, there is reason for some scepticism about our progress in the quantitative understanding of the weak interaction processes in hypernuclei, so that it is of importance to confirm this result and to establish more accurate lifetimes for the other light hypernuclei $_\Lambda H^4$, $_\Lambda He^4$ and $_\Lambda He^5$.

Observations on hypernuclei offer the only means available for the study of the weak interaction

$$\Lambda + N \to N + N \tag{5}$$

giving rise to non-mesic de-excitation of the Λ particle. There has already been a great clarification in our knowledge of the charge and spin dependence of this interaction, due to the data available on $_\Lambda He^4$ studies in the helium chamber[10]. Direct studies of the non-mesic rates for $_\Lambda H^4$ and $_\Lambda He^5$ (and also for $_\Lambda H^3$, although here the rate expected is quite small, due to the low Λ binding) would be very valuable at this point, both of the total rates and of the $(\Lambda p)/(\Lambda n)$ ratio. Data on the rates (or branching ratios) for specific modes of decay, such as

$$_\Lambda He^4 \to n + He^3 \tag{6a}$$

$$\to p + H^3 \tag{6b}$$

$$\to p + n + H^2 , \tag{6c}$$

would also provide valuable information. The decay rates for specific modes would also allow further tests of the $\Delta I = \frac{1}{2}$ rule for interaction (5); at present the only test available involves the inequality $\Gamma_{nm}(_{\Lambda}H^4) \leq 2 \Gamma_{nm}(He^4)$, which appears to be just satisfied. The comparison of the absolute rates for the modes (6a), (6b) and for

$$_{\Lambda}H^4 \rightarrow n + H^3 \tag{7}$$

provide another inequality, $R(nHe^3) + R(pH^3) \geq \frac{1}{2}R(nH^3)$, which can give a further test of the $\Delta I = \frac{1}{2}$ rule in this process (5).

The spin dependence of the interaction (5) may be investigated to some extent by comparing the $_{\Lambda}H^4$, $_{\Lambda}He^4$ and $_{\Lambda}He^5$ rates, especially the rates for the individual two-body modes. However, there will be both parity-conserving and parity-reversing terms in this interaction and these can be separated only by polarization studies. These require observations on the angular distribution of non-mesic decay, relative to the polarization direction for the initial hypernucleus, for example for $_{\Lambda}He^5$ decay, or on the longitudinal polarization of the high-energy nucleons emitted from each of the light hypernuclei. The study of polarization correlations between the two fast nucleons emerging from non-mesic decay will probably also be necessary before a complete analysis of the spin dependence of the non-mesic interactions can be made.

There is the possibility that multinucleon contributions to the non-mesic Λ decay rate may complicate the situation. It appears difficult to separate these processes from the process (5) on a purely empirical basis, since there can always be final state interactions which involve further nucleons. In light hypernuclei, complicated final states, involving the emission of a fast deuteron or a roughly equal sharing of the energy between three final particles, can occur even without invoking secondary interactions, as has been shown for the case of $\pi^- + He^4$ capture by the calculations of Eckstein[12]. The identification of multinucleon terms will require the observation of detailed deviations from the results of calculation based on the two-body interaction (5). Probably the proper procedure is to assume that the de-excitation process is dominantly of the type (5), until data turns up which cannot be reconciled with this hypothesis.

The absolute strength of the interaction (5) is of particular interest. One parameter directly relevant to this is the lifetime for a large hypernucleus (say A ~ 100-200). This lifetime could probably be measured by electronic techniques, by studying the occurrence of large energy releases following K^- capture in heavy nuclei with delay times of the order of 10^{-10} sec. The present data suggests that this interaction (5) is intrinsically weaker than that of the nuclear β decay interaction by about an order of magnitude; however, it is difficult to make this comparison meaningful until more is known about the form of the interaction (5).

IV. NUCLEAR PHYSICS AND HYPERNUCLEI

1. Nuclei away from the stability valley

Very little is know about the properties of many nuclear species with excess neutrons or protons relative to the normal species, such as H^5, He^7, He^8, C^9, etc. In most cases it is not even known empirically whether these systems have particle stable ground states. These systems are generally quite difficult to form in the kind of nuclear reactions which have been most convenient for experiment in the past, since they usually involve the transfer of at least two neutrons or two protons to (or from) the stable target nucleus. When these systems are formed (at a low rate), it is often difficult to establish their identity conclusively with the usual techniques. For example, the emulsion technique is very convenient for the detailed study of individual rare events; there have been reported in the literature several events following high-energy nuclear disintegrations[13], which may represent $C^9 \xrightarrow{\beta^+} B^9 \xrightarrow{\beta^+} Be^{9*} \to n + 2\alpha$, but even with this striking sequence of phenomena, it has been difficult to establish conclusively even the existence of bound C^9. Similarly, there have recently been reports[14] of the observation of the β decay of H^5, following $\gamma + Li^7$ reactions at high energy, but here again the arguments are sufficiently indirect as to allow question concerning this interpretation of the observations.

Any of these "exotic nuclei" which are particle stable will certainly form a Λ hypernucleus, and this will even be the case for many nuclear systems for which there is no stable ground state since a bound Λ particle generally adds at least an additional MeV to the stability of the system with respect to removal of the least strongly-bound nucleon[15]. $_{\Lambda}Be^7$ provides a well-known example of this situation, for there is no bound state Be^6; from an accurate knowledge of B_{Λ} for $_{\Lambda}Be^7$ it would be possible to deduce (after some necessary corrections) the position of the lowest level of Be^{6*}. In these "exotic hypernuclei", it is the last nucleon which has the least binding; in $_{\Lambda}Be^7$ the last proton has binding $B_p = 0.4 \pm 0.5$ MeV, compared with $B_{\Lambda} = 3.5$ MeV (relative to $He^4 + 2p$). The formation rate for these lightly-bound hypernuclei may be expected to be quite appreciable; $_{\Lambda}H^3$, with $B_{\Lambda} = 0.2$ MeV, is a well-known system and the formation rate for $_{\Lambda}Be^7$ must also be quite appreciable [since the two identified events represent only the (strongly suppressed) π^- mode]. Then, in the $\Lambda \to p + \pi^-$ decay for the bound Λ particle, the relatively large energy release gives rise to fragments whose tracks are frequently long enough to allow identification and accurate measurement; the interpretation of the hypernucleus may be checked by the requirements that the momenta balance and that the B_{Λ} value obtained agrees with the known pattern of B_{Λ} values for neighbouring hypernuclei. For example, the systems $_{\Lambda}H^6$, $_{\Lambda}He^8$, $_{\Lambda}He^9$, $_{\Lambda}Li^{10}$, $_{\Lambda}C^{10}$, etc. are all to be expected, and perhaps even neutral systems such as $_{\Lambda}n^5$ (following a recent report[16]) that n^4 may have a bound state at -4 MeV) may be observed in work with propane chambers.

Little is known about the existence and properties of light nuclei with high isospin, $I \geq 3/2$, and it is quite possible that observations on "exotic Λ hypernuclei" may allow some more convenient and conclusive eivdence to be obtained concerning such nuclei. We should emphasize that the process of K^- capture with π^+ emission, or of Σ^- capture with proton emission, can readily lead to the charge changes necessary to reach the neutron-rich systems; the proton-rich systems may be less readily accessible, although it is relatively easy to emit several neutrons in these formation reactions, in view of the large kinetic energy released.

2. Excited states of hypernuclei

Λ hypernuclei will generally possess excited states, some of which may be particle stable. Some of these states may even be metastable, i.e. they may undergo Λ decay preferentially, rather than γ decay. For example, Danysz and Pniewski[17] have suggested that the first excited state of $_\Lambda\text{He}^{7*}$ (which will have $J = \frac{3}{2}+$) may be metastable, a possibility which may account for unusual spread in the B_Λ value reported for $_\Lambda\text{He}^7$ events; Pniewski[17] has also pointed out that $_\Lambda\text{O}^{17*}$ ($\frac{1}{2}+$) at 6 MeV would also be metastable, at least that the Λ decay and (e^+e^-) decay modes would be competitive for this system. However, generally, these excited states will decay by γ emission; for example, the second excited state of $_\Lambda\text{He}^{7*}$ (which will have $J = \frac{5}{2}+$) may be expected to decay by an M1 transition to the $J = \frac{3}{2}+$ excited state of $_\Lambda\text{He}^{7*}$.

Questions of interest in connection with these γ transitions are as follows.

i) The energies of the excited states.

It is conceivable that these may be observed from the study of production reactions, in favourable cases where the levels are widely spaced. For example, the first level of $_\Lambda\text{C}^{13*}$ may be expected at an excitation energy of about 4 MeV, and its formation might be distinguished from ground state formation in the reaction

$$K^- + N^{14} \rightarrow {}_\Lambda\text{C}^{13*} + p + \pi^- . \tag{8}$$
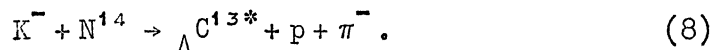
On the other hand, it may be feasible to observe the γ rays directly (which would generally be a more satisfactory procedure) with the use of counter techniques. Mesic X-rays have been observed at Berkeley for K^- stopping in various light materials[18], and the possibility of observing the γ rays emitted from the resulting Λ hypernuclei has been considered by Ashmore and Falla in a communication to this conference. Observations on the locations of these excited states would give additional evidence on the spin dependence of the Λ-nucleon interaction; for example, the attachment of a Λ particle to Li^6 forms two levels, the ground level

with spin $\frac{1}{2}+$ and an excited level with spin $\frac{3}{2}+$, their splitting being due directly to the spin dependent term in the Λ-N potential. Also, such information could frequently give an informative test of current theories of nuclear structure. For example, in $_{\Lambda}\text{Be}^{9*}$ the J = 2+ level Be^{8*} at 3 MeV gives rise to two excited levels with spins $\frac{3}{2}+$ and $\frac{5}{2}+$. If L-S coupling holds, or if the α particle model were valid for Be^{8*}, the splitting between these levels should vanish, whereas their splitting should be quite large for nuclear j-j coupling; the magnitude of this splitting actually gives a measure of the degree of intermediate coupling appropriate to Be^{8*}.

ii) (γ,γ) and (γ,π) angular correlation studies can be made between the hypernuclear γ rays and with the final decay pion. These could provide direct tests of the spin values predicted for these excited states.

iii) The measurement of γ lifetimes for selected transitions. These lifetimes will provide tests of theoretical calculations of the structure of the hypernuclear wavefunctions in selected cases; for M1 transitions they will depend on the Λ magnetic moment (which will probably have been determined by experiments on the free Λ particle, by the time hypernuclear γ lifetimes can be determined).

3. **Branching ratios for mesic decay of hypernuclei**

For the transitions

$$(_{\Lambda}Z^A) \to \pi^- + (Z+1)^{A*}, \tag{9}$$

the relative transition rates to various final states will provide tests of the structure of the wavefunctions for the hypernucleus $_{\Lambda}Z^A$ and for the nuclear states $(Z+1)^{A*}$. For example, the rate for the decay mode $_{\Lambda}\text{Li}^8 \to \pi^- + \text{Be}^{8*}$ (J = 2+, I = 1) depends quite strongly on the nuclear coupling scheme[20], being forbidden through the s-interaction of Λ decay for L-S coupling (since the transition is then $^1P_1 \to {}^3P_2$, which requires spin-flip) and being quite strong for j-j coupling.

REFERENCES

1) J. de Swart and C. Iddings, Phys.Rev. 128, 2810 (1962);
   Phys.Rev. 130, 319 (1963).

2) G. Alexander, J. Anderson, F. Crawford, N. Laskar and L. Lloyd,
   Phys.Rev.Letters 7, 348 (1961).

3) T.H. Groves, Phys.Rev. 129, 1372 (1963).

4) W. Bugg, Oak Ridge National Laboratory (private communication 1963).

5) M. Danysz, K. Garbowska, J. Pniewski, T. Pniewski, J. Zakrzewski,
   E. Fletcher, J. Lemonne, P. Renard, J. Sacton, D. O'Sullivan,
   T.P. Shah, A. Thompson, P. Allen, Sr. M. Heeran, A. Montwill,
   J.E. Allen, M.J. Beniston, D.H. Davis, D.A. Garbutt, V.A. Bull,
   R.C. Kumar and P.V. March, Phys.Rev.Letters 11, 29 (1963).

6) D.H. Wilkinson, S. St. Lorant, D. Robinson and S. Lokanathan,
   Phys.Rev.Letters 3, 347 (1959).

7) M. Gell-Mann, Proc.Int.Conf.on High-Energy Phys., CERN, Geneva, 1962,
   p. 805.

8) S.L. Glashow and J. Sakurai, Nuovo Cimento 26, 622 (1962).

9) Y. Eisenberg, Phys.Rev. 96, 541 (1956).

10) M.M. Block, R. Gessaroli, J. Kopelman, S. Ratti, M. Schneeberger,
    L. Grimellini, T. Kikuchi, L. Lendinara, L. Monari, W. Becker
    and E. Harth, Hyperfragment Studies in the Helium Bubble Chamber,
    Proc.Int.Conf.on Hyperfragments, CERN, 1963.

11) W.F. Fry, report to the Int.Conf.on Hyperfragments at St. Cergue,
    March, 1963.

12) S. Eckstein, Phys.Rev. 129, 413 (1963).

13) See F. Ajzenberg-Selove and T. Lauritsen, Nucl.Phys. 11, 1 (1957).

14) B. Nefkens, Phys.Rev.Letters 10, 55 (1962).

15) R.H. Dalitz and R. Levi-Setti, Some possibilities for unusual light
    hypernuclei, Nuovo Cimento, to be published (1963).

16) P.E. Argan, G. Bendiscirli, A. Piazzole, V. Bisi, M.I. Ferrero and
    G. Piraguro, report at CERN Conf.on High-Energy Phys.and Nucl.Structure,
    February, 1963. See also P.E. Argan and A. Piazzole, Some possible
    consequences of the existence of the states H^4 and H^5, to be published
    (1963).

17) M. Danysz and J. Pniewski, Phys.Letters 1, 142 (1962); also J. Pniewski, private communication (1963).

18) J.J. Murray, Lawrence Radiation Laboratory, private communication (1958).

19) A. Ashmore and D. Falla, Queen Mary College, London, Possible experiments on hypernuclear excited states, communication to the Int.Conf.on Hyperfragments at St. Cergue, March, 1963.

20) R.H. Dalitz, Nucl.Phys. 41, 78 (1962).

* * *

VIII. AFTER-DINNER TALK

AFTER-DINNER TALK GIVEN BY PROFESSOR C.F. POWELL

H.H. Wills Physics Laboratory, Royal Fort, Bristol.

Let me say how much we have all enjoyed the Conference
which has been organized here under the auspices of CERN; and how
deeply, certainly we in Europe, appreciate the existence and the
continuing success of CERN. I would like to think, too, that our
many friends here from the United States of America, Poland, India
and Latin America, appreciate the advantages created by this Institution.
It really would be a poor world, for our friends in America for example,
if they did not have some people to keep them on their toes; and surely
it is a function of CERN to provide them also with valid excuses for
frequent agreeable visits to this most delectable Continent of Europe.

Of course, to speak more seriously, the CERN Organization
greatly benefits from the fact that it can attract to its Conferences
and to the work in the Laboratory, people from all over the world for
long and for short periods. Long may it continue.

This Conference was of particular interest to me because it
transported me, in a vivid way, back in time through about 15 years.
This afternoon our Polish colleagues described their remarkable observation
which establishes the existence of nuclei with two Λ particles in them
and tells us something about the Λ-Λ interaction. We asked: "How long
must it be before we can expect to get a second one?" The answer was:
"Well maybe in two years, maybe in six months." The factor is impossible
to predict on the statistics of one. I was reminded of a situation 15 years
ago, when some of us in Bristol found an event which we called a τ meson.
The analysis looked convincing, but we said, "Yes, one is all very well,
but we would like two. How long will it take to get another one?" Those

of you who are hoping for a great extension in the library of Λ-Λ particles may be heartened to learn that it took us two years before we got our second τ.

This Λ-Λ event reminded me also that 20 years ago we were being told that the photographic method was really dead, only it would not lie down. Of course no technique can remain pre-eminent and the field of activity with emulsions has become much more restricted than it was; but it is very remarkable how frequently the method has allowed decisive conclusions to be drawn from a single observation. With this Λ-Λ event we have another illustration. I am reminded of a famous remark of Napoleon. Whenever he was presented with a young man for military advancement, he invariably asked the question: "Is he lucky?" This was by no means a casual inquiry. The important quality for which he was seeking was - does this man put himself in a situation where he can be lucky? If you fail to put yourself in a situation where it is possible to have good fortune then you cannot have any success; if you do, you may. So I hope that in that field of experiment we are going to discuss tomorrow, which Professor Dalitz is going to review, and which is so well-adapted to work with emulsions, we shall all be vigorous and energetic in the future.

One final remark that Professor Weisskopf asked me to make about our present situation in physics. We, of course, are the heirs of all the ages. We sometimes think, and in a certain sense it is true, that our experience is unique. However, men in the past have also been through the kind of excitement, the delight in investigation, which we so much enjoy, and this enthusiasm is well illustrated by a remark of Clerk Maxwell's made nearly one hundred years ago. I mentioned it to Weisskopf and he asked me to repeat it to you. If I remember it right it runs: "The mind of man is not like Fourier's heated body, continually settling down to a state of quiet uniformity, the character of which we can already predict. It is rather like a tree, shooting out branches which adapt themselves to the new aspects of the air towards which they climb, or roots which contort themselves among the strange strata of the earth into which they delve. For us who breathe only the spirit of our own age, and who know only the

characteristics of contemporary thought, it is as difficult to anticipate the general tone of the science of the future as it is to predict the particular discoveries it will make. Experimental science is continually revealing to us new features of natural processes and we are thus compelled to search for new forms of thought appropriate for their description." He goes on to refer to the importance of a close study of the relations between mathematical theories and physical reality, so that we may see when it is safe to import mathematical conceptions into one branch of physics from another.

You will see that these remarks from 90 or 100 years ago breathe very much the spirit of our own times and closely anticipate the nature of our own activity. A delight in colours and textures, enquiry into the nature of things, appears very early in human life and it can be encouraged or frustrated in the child or in the man. In our times it is more important than ever before that it should flourish at all levels. Both for the health of natural philosophy in Europe, and indeed throughout the whole world, the progress and support of CERN is of very great importance. I therefore come back to my old friend Weisskopf, and want to propose a toast: "To the Institution of CERN and its Director-General."

*   *   *

APPENDIX A

COLLECTION OF HYPERFRAGMENT DATA

COLLECTION OF HYPERFRAGMENT DATA

The following partial report of the discussion following Levi Setti's talk on 27 March, 1963, explains the situation.

Danysz : Following upon what Dr. Levi Setti said earlier, I would like to propose that it would be of interest for experimentalists to have a library of raw experimental data concerning hyperfragments. In publications, final results only are given, and I think it would be most interesting for those who work in the field and for the others to be able to obtain raw experimental data of analysed hyperfragments from a library where this material will be available to anybody who asks for it. And I think I will propose a place for it: the Chicago Laboratory would be the most suitable if they would like to take up the hard work of organizing such a library.

Levi Setti : I think that the suggestion is excellent in matter of principle, and as a matter of fact I would very much like to see this library start building up at CERN. On my side, I have already contributed a tabulation of all the mesic decays that have been analysed in Chicago, and have obtained assurance from Dr. Ammar that he also would be glad to contribute the information available at Northwestern University on mesic decays, so that I think this will be, if agreeable, certainly an excellent solution.

Powell : In connection with this suggestion of Danysz about making a library, I wondered would it not be a good plan to make sure that you specify on this occasion, here and now,

Powell
(cont.)
: precisely what information you want. All the interested
parties are here, and if the specification of the informa-
tion could be laid down here, I think it would be a very
timely and useful statement towards such a library.

Levi Setti : The best thing is perhaps simply to give raw data: namely
the ranges of the hyperfragment, of the decay products,
and their dip angles and projected angles. When there
is a possibility of analysing the primary star, one would
like to have the same information for all prongs origina-
ting from the capture star. Even if it is impossible to
analyse such a star, one would like to know at least if a
pion was emitted and the number of other prongs.

Powell : It would be worth while to achieve some form of standardi-
zation.

Levi Setti : I would say that the standardization is essentially
achieved when the density of the emulsion is given in a
way or an order, by giving, for example, the range of
protons from Σ^+ decay in the stack. I would believe
that one has already achieved a substantial standardiza-
tion of the methods of measurement, which in this case are
so simple, that perhaps there is no need to go any further,
but try to collect the angles and ranges as they come.

Burhop : I wonder if following up Prof. Danysz' suggestion, there
shouldn't be appointed a small subcommittee at this
meeting, here and now, to prepare the instructions of the
type of data which is required for such a hyperfragment
bank and also to go to the question of where it could be
situated. I feel that it is such a valuable suggestion
that this is the time to act on it.

Block   : In the interests of keeping the discussion short, I
would like to suggest that Professors Danysz, Burhop,
Levi Setti and Lock get together after the meeting
and talk this over in private.

The work of this subcommittee resulted in the following
letter, which has been sent to all the participants at the Conference.

*   *   *

NP/855/894   14.6.1963

Dear Colleague,

At the Hyperfragment Conference held at St. Cergue,
Switzerland, in March 1963, it was widely felt that it would be
useful to establish a central collection of data on hyperfragments.
This could be distributed periodically to all interested groups.
The collection of data should include sufficient detail to facilitate
world compilation of data on various aspects of hyperfragment pro-
duction and decay processes. It would be quite impracticable of
course to include complete detail but in those cases where more
information about particular events is needed it should serve to
promote exchanges by correspondence between the interested labora-
tories.

On behalf of the CERN emulsion group I offered to provide
facilities for the collection of this data. You will appreciate
that a collection of this kind can only be valuable if the informa-
tion provided by each laboratory is presented in a standard form.
A small subcommittee has therefore drawn up the enclosed form for
the tabulation of the data.

You are therefore invited to send me data on hyperfragment
events which your group finds and analyses from this date onwards
tabulated in conformity with the enclosed form. If you were able to
provided data on events already found and analysed, this would be very
useful but I realise that this may require an undue expenditure of
effort.

Yours sincerely,

W.O. Lock

on behalf of
    E.H.S. Burhop (London)
    M. Danysz (Warsaw)
    R. Levi-Setti (Chicago)

787/p

Suggested form for the tabulation of hyperfragment data:

Event	Track	Range (μm) [d]	Dip Angle [g] (degrees)	Azimuth (degrees)
Code No. [a]	HF	.....	.....	.....
	π^-	.....	.....	.....
References [b]	.....	.....	.....	.....
	.....	.....	.....	.....
Identity [c]	Rec. [e]	.....	.....	.....
	n [f]			

(a)   The code number for the event may be followed by the letter
      P or D to indicate production or decay star. E.g. 3-58-4-P.
      40001-D. The particle producing the hyperfragment, its energy
      and the production reaction, if known, should be given.

(b)   Published work in which the event has been first reported
      but also subsequent work in which the event might have been
      included.

(c)   The standard notation for events at rest in flight should be
      used. Example : $F_{\Lambda}H^4$, $R_{\Lambda}He^5$, etc.

(d)   Indicate when the range is measured from grid coordinates with
      (grid). Tabulate measured ranges, uncorrected for density
      effects. The information on the density of the emulsion should
      be given as measured density, or range of protons from Σ-p decay
      at rest, or range of muons from $\pi^-\mu$ decay.

(e)   Indicate the observation of a decay electron (β) or recoil
      disintegration (Hammer) etc.

(f)   n among the decay products indicates that the analysis requires
      the emission of a neutron.

(g)   Sign convention : positive to surface, negative to glass.

APPENDIX B

LIST OF PARTICIPANTS

LIST OF PARTICIPANTS

Country	Name	Institute/Laboratory
BELGIUM	Lemonne, J.	Université libre, Brussels.
	Renard, P.	Université libre, Brussels.
BRAZIL	de Carvalho, H.G.	Centro Brasileiro de Pesquisas Fisicas, Rio de Janeiro.
EIRE	Heeran, M. Sr.	University College, Dublin.
	O'Ceallaigh, C.	Institute for Advanced Studies, Dublin.
	Thompson, A.	Institute for Advanced Studies, Dublin.
FRANCE	Baumann, G.	Centre d'Etudes nucléaires, Strasbourg.
	Braun, H.	Centre d'Etudes nucléaires, Strasbourg.
	Burdet, A. Mrs.	Institut de Physique nucléaire, Lyon.
	Cuer, P.	Centre d'Etudes nucléaires, Strasbourg.
	Philbert, G.	Institut de Physique nucléaire, Lyon.
GERMAN FEDERAL REPUBLIC	Diaz, J.	Institut für Experimentalphysik, Hamburg II.
	Harmsen, D.	Institut für Experimentalphysik, Hamburg II.
	Muller, D.	Institut für Theoretische Physik, Heidelberg
	Tietge, I.	Max-Planck Institut für Physik und Astrophysik, Munich.
INDIA	Pal, Y.	Tata Institute of Fundamental Research, Bombay.
	Rao, N.K.	Tata Institute of Fundamental Research, Bombay.
ISRAEL	Perlmutter, A.	The Weizmann Institute of Science, Rehovoth.
ITALY	Bizzari, R.	Istituto di Fisica, Rome.
	Della Corte, M.	Istituto di Fisica, Florence.
	Iwao, S.	Istituto di Fisica, Genoa.

Country	Name	Institute/Laboratory
ITALY (cont.)	Quareni, G.	Istituto di Fisica, Bologna.
	Ratti, S.	Istituto di Fisica, Milan.
	Rosati, S.	Istituto di Fisica, Pisa.
	Sassi, E. Miss	Istituto di Fisica, Naples.
	Tomasini, G. Miss	Istituto di Fisica, Genoa.
	Vignudelli-Quareni, A. Mrs.	Istituto di Fisica, Bologna.
JUGOSLAVIA	Adamovic, O. Miss	Institute of Physics, Belgrade.
	Boskovic, B.	Institute of Physics, Belgrade.
NETHERLANDS	Kluyver, J.C.	Zeeman Laboratorium, Amsterdam.
	Tenner, A.G.	Zeeman Laboratorium, Amsterdam.
NORWAY	Sorensen, S.O.	Institute of Physics, Blindern.
POLAND	Danysz, M.	Institute of Physics, Warsaw.
	Gajewski, W.	Institute of Physics, Warsaw.
	Pniewski, J.	Institute of Physics, Warsaw.
	Zakrzewski, J.	Institute of Physics, Warsaw.
UNITED KINGDOM	Allen, J.E.	University College, London.
	Ashmore, A.	Queen Mary College, London.
	Bodmer, A.	Manchester University, Manchester.
	Davis, D.H.	University College, London.
	Elton, L.R.B.	Battersea College of Technology, London.
	Falla, D.	Queen Mary College, London.
	Fletcher, E. Miss	H.H. Wills Physics Laboratory, Bristol.
	Fowler, P.H.	H.H. Wills Physics Laboratory, Bristol.
	Garbutt, D.A.	University College, London.
	Ismail, A.Z.M.	Nuclear Physics Laboratory, Oxford.
	Lawson, R.D.	Atomic Energy Research Establishment, Harwell.
	Lokanathan, S.	Nuclear Physics Laboratory, Oxford.

Country	Name	Institute/Laboratory
UNITED KINGDOM (cont.)	Major, J.	Durham University, Durham.
	March, P.V.	Westfield College, London.
	Murphy, J.W.	Manchester University, Manchester.
	Prakash, Y.	Nuclear Physics Laboratory, Oxford.
	Powell, C.F.	H.H. Wills Physics Laboratory, Bristol.
	Stannard, F.R.	University College, London.
U.S.A.	Ammar, R.G.	Northwestern University, Evanston.
	Block, M.M.	Northwestern University, Evanston.
	Byers, N. Miss	University of California, Los Angeles.
	Dalitz, R.	The Enrico Fermi Institute for Nuclear Studies, Chicago.
	Downs, B.W.	University of Colorado, Boulder.
	Dyer, J.N.	Naval Postgraduate School, Monterey.
	Fry, W.F.	Wisconsin University, Wisconsin.
	Harth, E.M.	Syracuse University, Syracuse.
	Levi-Setti, R.	The Enrico Fermi Institute for Nuclear Studies, Chicago.
	Lomon, E.L.	Institute of Technology, Massachusetts.
	Nickols, N.A.	Lockheed-California Company, Los Angeles.
	Prowse, D.J.	University of California, Los Angeles.
	Schneps, J.	Tufts University, Medford.
	Steinberg, P.H.	Maryland University, Maryland.

* * *